COMPOSITE ACTION OF BRICKWALLS ON THIN REINFORCED CONCRETE BEAMS

A Thesis Submitted
In Partial Fulfilment of the Requirements
for the Degree of
DOCTOR OF PHILOSOPHY

By

JAI PRAKASH

to the

DEPARTMENT OF CIVIL ENGINEERING

INDIAN INSTITUTE OF TECHNOLOGY KANPUR

DECEMBER, 1979

CE-1979-D-PRA-COM

TO

My Parents and Wife

CERTIFICATE

This is to certify that the work presented in this thesis entitled 'COMPOSITE ACTION OF BRICKWALLS ON THIN R.C. BEAMS' by Jai Prakash has been carried out under my supervision and it has not been submitted elsewhere for a degree.

Kapoor
31/12/79

December, 1979

(M.P. KAPOOR)
Professor
Department of Civil Engineering
Indian Institute of Technology,Kanpur

ACKNOWLEDGEMENTS

The author expresses his deep gratitude and indebtedness to Dr. M.P. Kapoor, Professor, Department of Civil Engineering for his constant guidance and encouragement and help through out the course of this work.

The author is grateful to Dr. P. Dayaratnam, Professor, Dr. Ashwini Kumar, Assistant Professor, and Dr. A.S.R. Sai, Assistant Professor, Department of Civil Engineering for fruitful discussions and suggestions from time to time. Thanks are also due to Dr. Y.C. Das, Professor, Department of Civil Engineering, Dr. N.G.R. Iyengar, Professor, Department of Aeronautical Engineering for their excellent courses.

Special thanks are due to Mr. S.C. Goel, Senior Foreman, Structures lab, without whose continuous help, it would have not be possible to complete the experimental work in time.

The author would like to thank Mr. A.K. Jain for helping in the development of computer programme, Mr. R.C. Gupta Ph.D. student in Mechanical Engineering, Mr. J. Selvanathan, for their assistance at various stages during the preparation of this thesis.

The author is also grateful to Board of Governors of M.N.R. Engineering College, Allahabad, for granting leave of absence for carrying out the work.

Thanks are also due to Mr. G.S. Trivedi for efficient typing, Mr. J.C. Verma for preparing tracings and Mr.R.S. Dwivedi for neat cyclostyling and blue prints.

Last but not the least, a special thank goes to my wife, Rajesh and daughter, Damini, for their patience in putting up with my irregular routine during the period of this work.

Jai Prakash

CONTENTS

			Page
		LIST OF TABLES	
		LIST OF FIGURES	
		NOTATION	
		SYNOPSIS	
		INTRODUCTION	1
CHAPTER I		REVIEW OF EXISTING LITERATURE	5
	1.1	Experimental Studies	5
	1.1.1	Studies on Brickwork	5
	1.1.2	Studies on Walls Supported on Beams	7
	1.1.3	Review of I.S. Code of Practice	10
	1.2	Analytical Studies	10
	1.2.1	Finite Element Study of Reinforced Concrete Structures and Brick Wall on Concrete Beams	12
	1.3	Object and Scope of Present Investigation	20
CHAPTER II		MATERIAL PROPERTIES	23
	2.1	Introduction	23
	2.2	Experimental Determination of Mechanical Properties of Brick work	24
	2.2.1	Bricks	24
	2.2.1.1	Dimensional Tolerences	25
	2.2.1.2	Density and Water Absorbtion Test	25
	2.2.1.3	Compressive Strength	26
	2.2.2	Cement Sand Mortar	26
	2.2.3	Compressive Strength and Modulus of Elasticity of Brickwork	27
	2.2.3.1	Preparation of Specimen	27
	2.2.3.2	Testing Arrangement	27
	2.2.3.3	Test Results	29
	2.2.4	Resistance to Diagonal Tension of Reinforced Brick Masonry	30

Page

	2.2.4.1	Preparation of Specimen	30
	2.2.4.2	Testing Arrangement	31
	2.2.4.3	Test Results	31
	2.3	Constitutive Relations for Brickwork	32
	2.3.1	Brickwork in Elastic Range	32
	2.3.2	Yielding of Brickwork	34
	2.3.3	Cracking of Brickwork	38
	2.4	Mechanical Properties of Concrete	41
	2.4.1	Compressive and Tensile Strength of Concrete	41
	2.4.2	Stress-Strain Curve for Concrete	41
	2.5	Constitutive Relations for Concrete	44
	2.5.1	Concrete in Elastic Range	44
	2.5.2	Yielding of Concrete	46
	2.5.3	Crushing of Concrete	50
	2.5.4	Cracking of Concrete	51
	2.6	Properties of Steel Reinforcement	53
	2.7	Constitutive Relations for Steel Reinforcement	54
CHAPTER III		EXPERIMENTAL INVESTIGATION	90
	3.1	Preparation of Test Specimen	91
	3.1.1	Reinforced Concrete Beams	91
	3.1.2	Brick Masonry Walls	92
	3.1.3	Loading	93
	3.1.4	Instrumentation	94
	3.1.4.1	Dial Gauges	94
	3.1.4.2	Strain Measuring Device	95
	3.2	Parametric Studies	95
	3.2.1	Variation in Cement Sand Ratio in Mortar	96
	3.2.2	Variation in Height to Span Ratio	96
	3.2.3	Variation in Size and Location of Openings	98
	3.3	Test Results	99
	3.3.1	Effect of Variation in Cement Sand Mortar For Brickwork	99
	3.3.2	Effect of Variation in Height to Span Ratio	103
	3.3.3	Effect of Variation in Size and Location of Openings in Brickwork	108

		Page
CHAPTER IV	ANALYTICAL INVESTIGATION	195
4.1	Introduction	195
4.2	Displacement Formulation	196
4.3	The Linearly Varying Strain Triangular (L.S.T.) Element	199
4.3.1	Element Stiffness Matrix	199
4.3.2	Consistent Load Vector	206
4.4	The Linearly Varying Strain Bar Element (L.S.B.)	208
4.5	Pseudo Load Due to Cracking or Yielding	211
4.5.1	Computation of Pseudo Loads on Concrete Brickwork Element	214
4.5.2	Computation of Pseudo Load Vector on Steel Reinforcement	215
4.6	Nonlinear Analysis	217
4.6.1	Incremental-Iterative Methods	218
4.6.1.1	Incremental Tangent Stiffness Methods	219
4.6.1.2	Initial Stress Method	222
4.7	Convergence Criteria	224
4.8	Results of Finite Element Analysis	225
4.8.1	Effect of Variation in Cement Sand Mortar for Brickwork	227
4.8.2	Effect of Variation in Height to Span Ratio	233
4.8.3	Effect of Variation in Size and Location of Openings	237
CHAPTER V	SUMMARY, CONCLUSIONS AND RECOMMENDATIONS	308
5.1	Summary	308
5.2	Conclusions	309
5.3	Design Methodology for Composite Element	313
5.4	Proposal for Further Extension of Present Work	314
REFERENCES		317
APPENDIX		323

LIST OF TABLES

Table No.	Title	Page
2.1	Variation in Dimension of Bricks Used in Experimental Work	55
2.2	Variation in Area, Volume, Dry Density and Percentage Water Absorbtion of Bricks Used in Experimental Work	58
2.3	Compressive Strength of Bricks	59
2.4	Compression Test on 7 cm Mortar Cubes Proportion 1:3 by Weight	60
2.5	Compression Test on 7 cm Mortar Cubes Proportion 1:4 by Weight	61
2.6	Compression Test on 7 cm Mortar Cubes Proportion 1:5 by Weight	62
2.7	Compression Test on 7 cm Mortar Cubes Preparation 1:6 by Weight	63
2.8	Compression Test on 7 cm Mortar Cube Proportion 1:8 by Weight	64
2.9	Calculation of Stress and Strain for One Prism Specimen of Type H in 1:3 Mortar	65
2.10	Compressive Strength of Brick Prism Type H	66
2.11	Compressive Strength of Brick Prism Type V	66
2.12	Modulus of Elasticity of Brick Prism Type H	67
2.13	Modulus of Elasticity of Brick Prisms Type V	69
2.14	Maximum Resistance to Diagonal Tension in Reinforced Brick Beams	71

Table No.	Title	Page
3.14	Strains: H/L =0.33, Mortar 1:5, Tensile Loading	127
3.15	Strains: H/L =0.33, Mortar 1:6, Tensile Loading	129
3.16	First Crack and Failure Load :H/L=0.33, Compressive Loading	131
3.17	First Crack and Failure Load: H/L =0.33, Tensile Loading	132
3.18	Deflections: H/L=0.25, Mortar 1:6 , Compressive Load	133
3.19	Deflections: H/L=0.4, Mortar 1:6, Compressive Loading	134
3.20	Deflections: H/L =0.5 , Mortar 1:6, Compressive Loading	135
3.21	Deflections: H/L =0.8, Mortar 1:6, Compressive Loading	137
3.22	Deflections: H/L =0.25, Mortar 1:3, Tensile Loading	138
3.23	Deflections: H/L =0.4, Mortar 1:3, Tensile Loading	139
3.24	Deflections: H/L =0.5 , Mortar 1:3, Tensile Loading	140
3.25	Deflections: H/L =0.8, Mortar 1:3, Tensile Loading	141
3.26	Strains: H/L =0.25, Mortar 1:6, Compressive Loading	142
3.27	Strains: H/L = 0.4 , Mortar 1:6, Compressive Loading	144
3.28	Strains: H/L = 0.5 , Mortar 1:6, Compressive Loading	146
3.29	Strains: H/L =0.8 , Mortar 1:6, Compressive Loading	148

Table No.	Title	Page
3.30	Strains: H/L =0.25 , Mortar 1:3, Tensile Loading	150
3.31	Strains: H/L =0.4 , Mortar 1:3, Tensile Loading	152
3.32	Strains: H/L =0.5 , Mortar 1:3, Tensile Loading	154
3.33	First Crack and Failure Load: Mortar 1:6, Compressive Loading	156
3.34	First crack and Failure Load: Mortar 1:3, Tensile Loading	157
3.35	Deflections: H/L =0.25 , Mortar 1:3, Tensile Loading	158
3.36	Deflections: H/L=0.33, Mortar 1:3, Tensile Loading	159
3.37	Deflections: H/L =0.33, Mortar 1:3, Tensile Loading	160
3.38	First Crack and Failure Load: H/L=0.33, Mortar 1:3, Tensile Loading	161
3.39	Deflections: H/L =0.8 , Mortar 1:6, Compressive Loading, Symmetric Window Opening	162
3.40	Deflections: H/L=0.8, Mortar 1:6, Compressive Loading , Symmetric Door Opening	163
3.41	Deflections: H/L =0.8 , Mortar 1:6, Compressive Loading, Unsymmetric Window Opening	164
3.42	Deflections : H/L =0.8, Mortar 1:6, Compressive Loading, Unsymmetric Door Opening	165
3.43	Deflections: H/L=0.8, Mortar 1:3, Tensile Loading, Symmetric Window Opening	166

Table No.	Title	Page
3.44	Deflections: H/L=0.8, Mortar 1:3, Tensile Loading, Symmetric Door Opening	167
3.45	Deflections: H/L =0.8, Mortar 1:3, Tensile Loading, Symmetric Door Opening	168
3.46	Deflections: H/L =0.8, Mortar 1:3, Tensile Loading, Unsymmetric Window Opening	169
3.47	First Crack and Failure Load: H/L=0.8, Mortar 1:6, Compressive Loading	170
3.48	First Crack and Failure Load: H/L=0.8, Mortar 1:3, Tensile Loading	171
4.1	First Crack and Failure Load: H/L=0.33 Compressive Loading	243
4.2	Imminent Failure Loads: H/L=0.33, Compressive Loading	243
4.3	Computer Time: H/L=0.33, Compressive Loading	244
4.4	First Crack and Failure Load:Mortar 1:6, Compressive Loading	245
4.5	Computer Time: Mortar 1:6, Compressive Loading	246
4.6	First Crack and Failure Load: H/L=0.8, Mortar 1:6, Compressive Loading	247

LIST OF FIGURES

Figure No.	Title	Page No.
2.1	Arrangement of Brick Layers in Brick Prisms	76
2.2	Stress-Strain Curve for Brick Prisms in 1:6 Mortar	77
2.3	Stress-Strain Curve of Brickwork for Type H Prisms	78
2.4	Stress-Strain Curve of Brickwork for Type V Prism	79
2.5	Idealised Stress-Strain Curves of Brickwork for Type H prisms	80
2.6	Idealised Stress-Strain Curves of Brickwork for Type V Prisms	81
2.7	Loading Arrangement and Failure Pattern of R.B.M. Beams	82
2.8	Load Versus Deflection Curves: R.B.M. Beams	83
2.9	Brickwork Element in Global Coordinate System	84
2.10	Cracked Brickwork Element	84
2.11	Bilinear Stress-Strain Curve for Concrete	85
2.12	Parabola Rectangle Stress-Strain Curve for Concrete	85
2.13	Biaxial Strength Envelope of Concrete	86
2.14	Crush Surface of Concrete	87
2.15	Cracked Concrete Element	87
2.16	Stress-Strain Curve for Steel	88

Figure No.	Title	Page
2.17	Idealised Stress-Strain Curve for Steel	89
2.18	Local and Global Coordinate for Framing Constitutive Matrix for Reinforcing Steel	89
3.1(a)	Mould for Casting R.C. Beams (Compressive Loading)	172
3.1(b)	Mould for Casting R.C. Beams (Tensile Loading)	172
3.2(a)	Details of R.C. Beam (Compressive Loading)	173
3.2(b)	Details of R.C. Beam (Tensile Loading)	173
3.3	Loading Arrangement (Compressive Loading)	174
3.4	Loading Arrangement (Tensile Loading)	175
3.5	A Typical Specimen	176
3.6	Details of Specimens with Openings	177
3.7	Load Versus Vertical Deflection Curves to Study the Effect of Mortar Ratio on Specimens Tested Under Compressive Loading	178
3.8	Load Versus Vertical Deflection Curves to Study the Effect of Mortar Ratio on Specimens Tested Under Tensile Loading	179
3.9	Variation in Longitudinal Strain at Mid Span to Study the Effect of Mortar Ratio Under Both Type of Loading	180
3.10	Crack Pattern to Study the Effect of Variation in Mortar Ratio	181
3.11	Load Versus Deflection Curves to Study the Effect of Height to Span Ration on Specimens Tested Under Compressive Loading	182

Figure No.	Title	Page
3.12	Load Versus Deflection Curves to Study the Effect of Height to Span Ratio on Specimens Tested Under Tensile Loading	183
3.13	Variation of Longitudinal Strains to Study the Effect of Height to Span Ratio on Specimens Tested Under Tensile Loading	184
3.14	Crack Pattern at Failure for Specimens 11 to 14 and 15 to 18 Tested Under Compressive and Tensile Loading Respectively	185
3.15	Photographs Showing Failure Pattern of Specimens Number 13 and 14, Having Height to Span Ratio of 0.5 and 0.8 Respectively and Tested Under Compressive Loading	186
3.16	Load Versus Deflection Curves for Specimen Having 24 Number, 6 mm Dia Connectors, Cast in 1:3 Mortar and Tested Under Tensile Loading (H/L=0.25)	187
3.17	Crack Pattern at Failure for Specimen Having 24 Numbers, 6 mm Dia Connectors, Cast in 1:3 Mortar and Tested Under Tensile Loading (H/L=0.25)	187
3.18	Load Versus Deflection Curves to Study the Effect of Variation in Size and Number of Vertical Connectors and Tested Under Tensile Loading	188
3.19	Load Versus Deflection Curves to Study the Effect of Variation in Size and Location of Openings on Specimens Tested Under Compressive Loading	189
3.20	Load Versus Deflection Curves to Study the Effect of Variation in Size and Location of Openings on Specimens Tested Under Tensile Loading	190
3.21	Crack Pattern at Failure to Study the Effect of Variation in Location and Size of Openings on Specimen Tested Under Compressive Loading	191

Figure No.	Title	Page
3.22	Crack Pattern at Failure to Study the Effect of Variation in Location and Size of Openings on Specimens Tested Under Tensi e Loading	192
3.23(a)	Photographs Showing Failure Patterns of Specimens Having Unsymmetric Window and Door Openings and Tested Under Compre-ssive Loading	193
3.23(b)	Photographs Showing Failure Patterns of Specimens Having Symmetric Door Openings and Tested Under Tensile Loading	194
4.1	Linear Strain Triangular Element (a) Local Coordinate System (b) Natural Coordinate System	248
4.2	Linearly Varying Bar Element (a) Global Coordinate System (b) Local Coordinate System (c) Natural Coordinate System	249
4.3	Sub-regioning of Triangular Element	250
4.4	Sub-regioning of Bar Element	250
4.5	Incremental Iterative Tangent Stiffness Meth d	251
4.6	Incremental Iterative Initial Stress Method	252
4.7	Finite Element Idealisation of a Typical Element	253
4.8	Figure Showing Analytical Results for Specimen Cast in 1:3 Mortar, Having a Height to Span Ratio of 0.33 and Tested Under Compressive Loading	
	(a) Longitudinal Stress Distribution at Various Cross Sections	254
	(b) Vertical Stress Distribution Along Span at Various Heights	254
	(c) Shear Stress Distribution at Various Cross Sections	255

Figure No.	Title	Page
4.8	(d) Variation of Stress in Bending Reinforcement Along Span at Various Load	255
	(e) Vertical Deflection Along Span at Various Loads	256
	(f) Crack Pattern at Failure	256
4.9	Figure Showing Analytical Results for Specimen Cast in 1:4 Mortar, Having Height to Span Ratio of 0.33, and Tested Under Compressive Loading	
	(a) Longitudinal Stress Distribution at Various Cross Sections	257
	(b) Vertical Stress Distribution Along Span at Various Heights	257
	(c) Shear Stress Distribution at Various Cross Sections	257
	(d) Variation of Stress in Bending Reinforcement Along Span at Various Load	257
	(e) Vertical Deflection Along Span at Various Loads	258
	(f) Crack Pattern at Failure	258
4.10	Figure Showing Analytical Results for Specimen Cast in 1:5 Mortar Having Height to Span Ratio of 0.33 and Tested Under Compressive Loading	
	(a)Longitudinal Stress Distribution at Various Cross Sections	259
	(b) Vertical Stress Distribution Along Span at Various Heights	259
	(c) Shear Stress Distribution at Various Cross Sections	260
	(d) Variation of Stress in Bending Reinforcement Along Span at Various Load	260
	(e) Vertical Deflection Along Span at Various Loads	261
	(f) Crack Pattern at Failure	261
4.11	Figure Showing Analytical Investigation Results for Specimen Cast in 1:6 Mortar Having Height to Span Ratio of 0.33 and Tested Under Compressive Loading	
	(a) Longitudinal Stress Distribution at Various Cross Sections	262

Figure No.	Title	Page
	(b) Vertical Stress Distribution Along Span at Various Heights	262
	(c) Shear Stress Distribution at Various Cross Sections	263
	(d) Variation of Stress in Bending Reinforcement Along Span at Various Load	263
	(e) Vertical Deflection Along Span at Various Loads	264
	(f) Crack Pattern at Failure	264
4.12	Figure Showing Analytical Investigation Results for Specimens Cast in Mortar 1:8 Having Height to Span Ratio of 0.33	
	(a) Longitudinal Stress Distribution at Various Cross Section	265
	(b) Vertical Stress Distribution Along Span at Various Heights	265
	(c) Shear Stress Distribution at Various Cross Sections	266
	(d) Variation of Stress in Bending Reinforcement Along Span at Various Load	266
	(e) Vertical Deflection Along Span at Various Loads	267
	(f) Crack Pattern at Failure	267
4.13	Load Versus Deflection Curves: To Study the Effect of Variation in Mortar Ratio on Specimens Having a Height to Span Ratio of 0.33 and Tested Under Compressive Loading	268
4.14	Variation of Longitudinal Strains at Mid Span: To Study the Effect of Variation in Mortar Ratio on Specimens Having Height to Span Ratio of 0.33 and Tested Under Compressive Loading	269
4.15	Load Versus Deflection Curves: To Study the Effect of Variation in Mortar Ratio Having Height to Span Ratio of 0.33 and Tested Under Tensile Loading	270

Figure No.	Title	Page
4.16	Figure Showing Analytical Investigation Results for Specimens Cast in Mortar 1:6 Having a Height to Span Ratio of 0.25 and Tested Under Compressive Loading	
	(a) Longitudinal Stress Distribution at Various Cross Sections	271
	(b) Vertical Stress Distribution Along Span at Various Heights	271
	(c) Shear Stress Distribution at Various Cross Sections	272
	(d) Variation of Stress in Bending Reinforcement Along Span at Various Load	272
	(e) Vertical Deflection Along Span at Various Loads	273
	(f) Crack Pattern at Failure	273
4.17	Figure Showing Analytical Results for Specimen Cast in Mortar 1:6, Having a Height to Span Ratio of 0.4 and Tested Under Compressive Loading	
	(a) Longitudinal Stress Distribution at Various Cross Sections	274
	(b) Vertical Stress Distribution Along Span at Various Heights	274
	(c) Shear Stress Distribution at Various Cross Sections	275
	(d) Variation of Stress in Bending Reinforcement Along Span at Various Load	275
	(e) Vertical Deflection Along Span at Various Loads	276
	(f) Crack Pattern at Failure	276
4.18	Figure Showing Analytical Results for Specimen Cast in Mortar 1:6, Having a Height to Span Ratio of 0.5 and Tested Under Compressive Loading	
	(a) Longitudinal Stress Distribution at Various Cross Sections	277
	(b) Vertical Stress Distribution Along Span at Various Heights	278
	(c) Shear Stress Distribution at Various Cross Sections	278
	(d) Variation of Stress in Bending Reinforcement Along Span at Various Load	279

Figure No.	Title	Page
4.18	(e) Vertical Deflection Along Span at Various Loads	279
	(f) Crack Patern at Failure	280
4.19	Figure Showing Analytical Results for Specimen Cast in Mortar 1:6, Having a Height to Span Ratio of 0.8 and Tested Under Compressive Loading	
	(a) Longitudinal Stress Distribution at Various Cross Sections	281
	(b) Vertical Stress Distribution Along Span at Various Heights	282
	(c) Shear Stress Distribution at Various Cross Sections	283
	(d) Variation of Stress in Bending Reinforcement Along Span at Various Load	284
	(e) Vertical Deflection Along Span at Various Loads	284
	(f) Crack Pattern at Failure	285
4.20	Load Versus Deflection Curves at Mid Span: To Study the Effect of Height to Span Ratio of Specimens Cast in Mortar 1:6 and Tested Under Tensile Loading	286
4.21	Figure Showing Analytical Results for Specimen Cast in 1:6 Mortar Having a Symmetric Window Opening and Tested Under Compressive Loading	
	(a) Longitudinal Stress Distribution at Various Cross Sections	287
	(b) Vertical Stress Distribution Along Span at Various Heights	288
	(c) Shear Stress Distribution at Various Cross Sections	289
	(d) Variation of Stress in Bending Reinforcement Along Span at Various Load	290
	(e) Vertical Deflection Along Span at Various Loads	290
	(f) Crack Pattern at Failure	291

Figure No.	Title	Page
4.22	Figure Showing Analytical Results for Specimen Cast in 1:6 Mortar Having a Symmetric Door pening and Tested Under Compressive Loading	
	(a) Longitudinal Stress Distribution at Various Cross Sections	292
	(b) Vertical Stress Distribution Along Span at Various Heights	293
	(c) Shear Stress Distribution at Various Cross Sections	294
	(d) Variation of Stress in Bending Reinforcement Along Span at Various Load	295
	(e) Vertical Deflection Along Span at Various Loads	295
	(f) Crack Pattern at Failure	296
4.23	Figure Showing Analytical Results for Specimen Cast in 1:6 Mortar Having an Unsymmetric Window Opening and Tested Under Compressive Loading	
	(a) Longitudinal Stress Distribution at Various Cross Sections	297
	(b) Vertical Stress Distribution Along Span at Various Heights	298
	(c) Shear Stress Distribution at Various Cross Sections	299
	(d) Variation of Stress in Bending Reinforcement Along Span at Various Load	300
	(e) Vertical Deflection Along Span at Various Loads	300
	(f) Crack Pattern at Failure	301
4.24	Figure Showing Analytical Results for Specimen Cast in 1:6 Mortar Having an Unsymmetric Door Opening and Tested Under Compressive Loading	
	(a) Longitudinal Stress Distribution at Various Cross Section	302
	(b) Vertical Stress Distribution Along Span at Various Heights	303
	(c) Shear Stress Distribution at Various Cross Sections	304
	(d) Variation of Stress in Bending Reinforcement Along Span at Various Load	305

Figure No.	Title	Page
4.24	(e) Vertical Deflection Along Span at Various Loads	305
	(f) Crack Pattern at Failure	306
4.25	Load Versus Deflection Curves: To Study the Effect of Variation in Location and Size of Openings	307

NOTATIONS

A	Area
$[B]$	Strain-displacement transformation matrix
$[B_n]$	Nodal-strain displacement transformation matrix
$[C]$	Material constitutive matrix
$[C_{cr}]$	Constitutive matrix for cracked element
$[C_{ep}]$	Elasto-plastic matrix
E	Modulus of elasticity
E_x	Modulus of elasticity of brickwork in the direction of mortar beds
E_y	Modulus of elasticity of brickwork in the direction perpendicular to mortar beds
$F(\sigma)$	Yield surface
$F_c(\epsilon)$	Crush surface
G	Shear modulus
H	Height of composite element
I	Moment of inertia
$[k]$	Element stiffness matrix
$[K]$	Global stiffness matrix
L	Span of composite element
L, L_1, L_2, L_3	Natural co-ordinates
$[N]$	Shape function matrix
$\{P\}$	Total load vector
$\{P_{cc}\}$	Pseudo load vector due to cracking

$\{P_{cy}\}$	Pseudo load vector due to yielding of triangular element
$\{P_{sy}\}$	Pseudo load vector due to yielding of reinforcement
$\{\delta\}$	Element nodal displacement vector
$\{Q\}$	Global nodal displacement vector
$[T]$	Transformation matrix
$\{u\}$	Displacement vector in local co-ordinate system
U	Strain energy
U_{cc}, U_{cy}, U_{sy}	Strain energy released due to cracking and yielding
W	Potential energy due to external loads
$\bar{X}$	Body force vector
α_B	Shear retention factor for brickwork
α_C	Shear retention factor for concrete
α_i's	Generalized co-ordinates
α_{ij}'s	Anisotropic parameters
γ_{xy}	Shear strain
$\{\varepsilon\}$	Strain vector
ε_{cu}	Ultimate strain of concrete
ε_{oct}	Octahedral strain
ν	Poisson's ratio
ν_x, ν_y	Poisson's ratio of brick masonry
ξ	Local cartesian co-ordinate for bar element
$\{\sigma\}$	Stress vector

σ_{0x}	Yield stress of brickwork in the direction of mortar beds
σ_{0y}	Yield stress of brickwork in the direction perpendicular to mortar beds
σ_x', σ_y'	Deviotoric stresses
π	Potential energy
τ	Shear stress
τ_{oct}	Octahedral shear stress

SYNOPSIS

COMPOSITE ACTION OF BRICKWALLS ON THIN R.C. BEAMS
A thesis
submitted in partial fulfilment of the requirements
for the degree of
DOCTOR OF PHILOSOPHY
BY JAI PRAKASH
to the
Department of Civil Engineering
Indian Institute of Technology Kanpur
December, 1979
Thesis supervisor: Dr. M.P. Kapoor

The brick masonry work over beams and lintels in buildings has been considered only as an overburden in conventional method of design. However, with the increased understanding of reinforced brick masonry, it has been established that reinforced brick masonry on reinforced concrete beams gives additional strength to the latter. Earlier investigators have established that composite action between the beam and the masonry over it is possible i.e. additional strength is available only if height of brick masonry above the beam is more than half the span and load is applied at the top of brick work. Therefore, no change in design procedure has been recommended for situations where height to span ratio is below 0.5 and also in situations where the load is applied at the junction of the beam and masonry wall.

The present work addresses itself to the study of the extent of interaction between the concrete beam and the masonry above it by considering two types of loading (i) system loaded at the top of brick work (2) system loaded at the junction of concrete beam and masonry wall which is of common occurrence in multistoreyed framed construction. Through out the experimental investigation, the supporting beam was a precast concrete member, 8.0 cm thick, in 1:2:4 nominal mix except in two samples where thickness was increased to 16 cm . Single legged Z shaped shear cum tensile connectors were provided through out the span at a uniform spacing to make the concrete beam and the brick panel act as a composite structure. Parametric study has been made to study the effect of following parameters on the ultimate load-carrying capacity of composite structure.

(1) Variation of cement sand ratio in mortar for brick work.

(2) Variation of height to span ratio.

(3) Location and size of symmetric and non-symmetric openings in the brick masonry.

In order to conduct the above study, 30 full scale load tests have been conducted in the laboratory at I.I.T. Kanpur using local materials. Mechanical properties of brick work, concrete and reinforcing steel

has been established and reported in the present work. Some of the wall-beam interaction tests have been conducted, loaded from top of brick masonry while others loaded at the junction of concrete beam and brick masonry. The experimental results obtained have been verified by analytical study. For the purpose of analytical study, the composite structure has been idealised as a plane stress problem and solved by finite element method. A linear strain triangular element has been used for concrete and brick work while linear strain bar element has been used for reinforcement. The sub-regioning of linear strain triangular element and linear strain bar elements have been carried for the purposes of accuracy of results and economy in computations. The ultimate load carrying capacity of the composite structure has been obtained by analysing cracking of concrete and/or brick work and yielding of concrete, brick work and steel. The uniaxial stress strain law for concrete is represented by an idealised bilinear curve. Brick work is assumed to be elastic and orthotropic upto yield point beyond which its behaviour is assumed to be perfectly plastic. The steel is idealised as an elasto-plastic material. Maximum stress theory is used to check for cracking. Vonmises yield criterion is used for yielding of concrete and Hill's anisotropic yield criterion is used for brick work.

A computer programme has been developed, making use of criteria described above to trace the load deflection response and crack propagation from zero load to ultimate load. The salient conclusions from the present study are:

(1) Single legged Z shaped shear cum tensile connectors have been found adequate to make the structure behave as a composite structure.

(2) The entire structure behaves as an under-reinforced beam.

(3) Cement sand mortar of 1:6 ratio has been found adequate incase the load is applied at the top of brick work, while a rich mortar of 1:3 cement sand ratio is necessary when the load is applied at the junction of concrete beam and the brick panel above it.

(4) Openings at the centre of wall do not affect the load carrying capacity of the structure but an opening near the support affects the load carrying capacity adversely for the case of the load applied at the top of the system. However, if the load is applied at the junction of concrete beam and the wall, both types of openings affect the load carrying capacity.

(5) Finite element model used in the present work predicts deflection, ultimate load capacity and crack propagation quite accurately for the case of load applied at the top of brick work. On the other hand this model predicts accurately ultimate load but fails to predict the deflection and crack propagation accurately in case when the load is applied at the junction of concrete beam and brick masonry wall.

INTRODUCTION

Beams and lintels are important structural components of buildings. They contribute appreciably towards the cost of building. This is more so in case of framed construction. The lintels above all the doors and windows, the verandah beams and the grade beams support the masonry upto the ceiling level. In framed structures, this masonry work serves as partition walls. The brick masonry work over beams and lintels in buildings has been considered only as an over-burden in the conventional method of design. However, with the increased understanding it has been established that brick masonry on reinforced concrete beams behaves differently and gives additional strength to the composite system.

Earlier investigators observed that composite action between beams and masonry is possible i.e. additional strength is available only if the height of brick masonry above the beam is more than half of the span and load is applied at the top of brickwork. Therefore, no change in design procedure is recommended for situations where height to span ratio is less than 0.5.

The present work addresses itself to the study of interaction between the concrete beam and the masonry above it, using single legged Z-shaped vertical connectors of mild

steel bars embedded along the length of the composite construction. Two types of loads have been considered in the present study both being inplane loads applied at (1) the top of brickwork henceforth called the compressive loading and (2) the junction of concrete beam and masonry wall henceforth called the tensile loading. The ultimate load carrying capacity of the composite structure is obtained experimentally and verified analytically. The crack propagation with increased load is also studied.

Existing work on brick-masonry and brick-masonry supported on R.C. beams has been reviewed and presented in Chapter I section 1.1. The work on analytical tools to study the behaviour of such composite systems is also briefly reviewed in this chapter in section 1.2. The scope of present investigation is described in section 1.3 of this very chapter.

In any investigation of this kind the importance of material properties can not be over emphasized, while the material properties of reinforced concrete are by and large well-known and can be easily established for a given situation, the same is not true for brickwork. The material properties of brick-masonry depend upon the quality of bricks, the mortar used and, the last but not the least, the workmanship. Quantifying the mechanical material properties for

brickwork and establishing suitable constitutive laws for brickwork, concrete and reinforcing steel is the subject of discussion of Chapter II.

Experimental studies have been conducted on about 30 specimens to study the effect of following parameters on the ultimate load carrying capacity of the composite structure.

(1) Variation of cement sand ratio in mortar for brickwork.

(2) Variation of height to span ratio.

(3) Location and size of symmetric and non-symmetric openings in the brick masonry.

Full scale load tests have been conducted in the Structural Engineering laboratory at IIT Kanpur. The experimental details, loading arrangements and results of experimental studies form the subject matter of Chapter III.

The experimental results obtained in the present work have been verified by analytical study. For the purposes of analytical study, the composite structure has been idealised as a plane stress problem and solved by finite element method. A linear strain triangular element has been used for concrete and brickwork while linear strain bar element has been used for reinforcement. The sub-regioning of linear strain triangular elements and linear strain bar elements have been carried out for purposes of

accuracy in identifying the cracked region. The ultimate load carrying capacity of the composite structure has been obtained by analysing cracking of concrete and/or brickwork and yielding of concrete, brickwork and steel. The uniaxial stress-strain law for concrete is represented by an idealised bilinear curve. Brickwork is assumed to be elastic and orthotropic upto yield point beyond which its behaviour is assumed to be perfectly plastic. The steel is idealised as an elastoplastic material. Maximum stress theory is used to check for cracking. Von Mises yield criterion is used for yielding of concrete and Hill's anisotropic yield criterion is used for brickwork. These are discussed in Chapter IV. A computer programme in Fortran IV has been developed making use of the model developed and criteria described in order to trace the load deflection response and crack propagation from initial load to failure load. The analytical results of various experimental specimens have been obtained using the developed programme which are presented in this Chapter. There is a good agreement between the experimental and analytical results obtained. Differences, if any, are discussed herein.

The conclusions drawn on the basis of experimental and analytical work are summarised in Chapter V. A design methodology for such composite systems based on the experience of present work is described herein. Some suggestions for future developmental work in this regard are also indicated in this Chapter.

CHAPTER I

REVIEW OF EXISTING LITERATURE

1.1 EXPERIMENTAL STUDIES

1.1.1 Studies on Brickwork

Brick masonry has been in use for times immemorial. However, use of reinforced brick masonry (R.B.M.) dates back to about one and half century. Sir Mark Isambard Brunel a Chief Engineer of Newyork was probably the first man to introduce R.B.M. in the year 1813. In 1836, he tested some structures to determine the strength contribution of reinforcement in brick masonry. In 1837, Colonel Pasley conducted a series of tests on R.B.M.beams. In 1851, several tests on R.B.M. beams were done in London using portland cement. Corsion in 1872 computed allowable stresses for use in masonry lintels and discussed relation of tensile strength of masonry to that of mortar. Hugofillipi in 1853 and Mench in 1919 made some tests on R.B.M. beams. Government of India in 1923 published a technical paper No.38 with various test results of R.B.M. beams, columns, arches etc. This work done by Brener is a hall mark towards the development of R.B.M. in India. Pearson, Stang and Mc Burney (1) in 1932 reported the test results on R.B.M. beams. Withey (2,3) also carried out some tests on R.B.M. beams and

columns. During the period 1922 to 1950 research was conducted on both plain and reinforced brickwork at National Bureau of standards and practically all Engineering Institutions of U.S.A. It has been established some 45 years ago that height/thickness ratio of compression specimens of brickwork is important. In order to obtain data on the effect of varying the strength of brick and mortar, very large number of tests have been conducted in Building Research Station England by Thomas, F.G. (4) on brick piers, 9 inches squares and 36 inches high. He showed that strength of brickwork is a function of both i.e. the strength of bricks and of mortar used. Results obtained by him further indicate that the effect of increasing mortar strength, in terms of the resulting brickwork, is not proportional. In 1973 Purshothaman (5) carried out some tests at I.I.T. Kanpur on brick masonry and also determined the properties of brickwork, analytically using finite element method. There is vast difference between the experimental and analytical results obtained by him. The Structural Clay Products Institute (SCPI) (6), has recommended that brickwork prism tests be conducted on specimen not less than 12 inches in height and shall have a height/thickness ratio of not less than 2 and not more than 5. The Institute recommends that modulus of elasticity, E, for brickwork be taken as 1000 f'm

where f'm is the 28 day compressive strength of brick prisms of h/t ratio of 5. The shear modulus is predicted to be 400 f'm.

1.1.2 Studies on Walls Supported on Beams

Wood R.H. (7) was the first to conduct a series of experiments on walls supported on beams. Tests on 9'' brick walls without supporting beams showed that even these unsupported walls can resist large vertical loads. When reinforced concrete beams were used with brick walls, tension concentration in supporting beams was noticed. Walls with door and window openings were also tested. Wood found that deep girder action did not apply to loading at the junction of concrete beam and masonry wall, unless tensile connectors could be placed between wall and beam. He suggested that some light reinforcement may be necessary in the walls to take care of shrinkage and also continuity in case of continuous walls. Ultimate load could not be reached in these tests.

Rosenhaupt and his associates (8,9,10,11,12) studied the behaviour of walls on continuous beams, effect of various types of openings with and with out stiffening concrete frames surrounding the openings and the effect of prestressing the brickwork, besides the effect of foundation settlement. They found that reinforcement in supporting beams had secondary

effect, except when flexure controlled the failure as in the case of shallow walls or strong brickwork. On the other hand shear, bond and vertical compressive stresses in deep walls controlled failure. Inclusion of horizontal and vertical concrete ties in the beam wall system had significant effect on the internal stress distribution. The openings definitely weakened the structure but they showed that strength could be compensated by prestressing or by the introduction of vertical concrete ties. While testing continuous composite walls, it was found that positive moments existed even over the middle supports. The failure modes peculiar to such walls and beams are the crushing of masonry over the supports and effects of shear in masonry panel.

Burhouse (13) used concrete beams and encased joists as supporting beams. He introduced a building paper joint at the mid span as previous investigators had found the separation of supporting beam from the masonry wall. Crushing of brickwork was found to be the predominant mode of failure and strong brickwork is advocated if the beneficial arching action in walls on beams is to be fully utilised. In shallow beams, progressive slipping of walls on beams was noticed, showing the need for an adequate connection between the walls and the beams.

Purshothaman (5) conducted a series of experiments at IIT Kanpur. He studied the effect of mortar ratio in brickwork, effect of height to span ratio and effect of openings. He concludes that the beneficial interaction is available only if the load is applied at top of brickwork with symmetric door and window openings. It is further concluded that the interaction exists only if rich mortar of 1:3 cement sand ratio is used. No interaction exists if the opening is eccentric or if the load is applied at the junction of beam and the wall. It is further recommended that for design purposes, the benefit of interaction should be used only if the height to span ratio is more than 0.5.

Prasad Rao and Mallick (14) conducted tests on walls-on-beams giving particular attention to their ultimate strength.

Ramesh et al (15) also tested the wall on beams. They provided tensile connectors in the form of two legged stirrups, close near the supports and wide apart at the midspan. It is concluded that by this arrangement, the load carrying capacity of the composite structure is increased and claimed a saving of 20 percent in reinforcement.

Smith B. Stafford (16) conducted a series of experiments to study the collapse of masonry walls on steel beams and reinforced concrete beams. Six tests were conducted on

wall beams 6 ft span and 4 ft high. They concluded that the behaviour of two types of wall beam structure differ to the extent that modifications to the design method are necessary. They also proposed the recommendation for changes in design method.

1.1.3 Review of I.S. Code of Practice

Actually speaking there are no codes of practice which deal specifically with the problem of wall on beams. National Building Code of India 1970 has made an indirect use of the arch action for the design of capping beams over under reamed piles. It has suggested the use of maximum bending moment of $\frac{WL^2}{50}$ where W is the uniformly distributed load per cm run and L is the effective span in cm provided the beams are supported during construction. If it is not supported during construction, an increased value of $\frac{WL^2}{30}$ for the maximum bending moment has been recommended. The minimum depth of capping beams recommended is 15 cm.

1.2 ANALYTICAL STUDIES

Earlier investigators have carried out analytical investigations on the interaction between brick walls and their supporting beams by classical theory of elasticity, latice analogy, beam truss and virendel girder analogy. The first simplification for the state of stress in a wall on beam was given by Wood (7). Based on the observation that

most of the compressive load was transferred to the supports through arch action, he suggested that the beams be designed for a reduced bending moment of $\frac{WL}{50}$ to $\frac{WL}{100}$ depending upon the position of openings. An equivalent moment arm of 2/3 of depth subject to a maximum of 0.7 times the span was also suggested to determine the area of reinforcement. He further suggested that the limiting moment arm method be used in walls without openings. For smaller depths, arch action may be absent and hence no change in design moments was suggested. Rosenhaupt (9) also suggested the equivalent moment arm method using 0.6 times the height of wall. Rosenhaup suggested the uses of truss analogy to deal with openings in wall.

Prasad Rao and Mallick (14) have discussed several simple methods of computing the ultimate strength of walls on beams without opening. The simplest is to use an equivalent lever arm of 0.75 to 0.85 times of the depth and multiply the same by the area of reinforcement and yield stress of steel to obtain the ultimate moment. This approach is valid for tension failure. For compression failure Whitney's theory could be used.

Chandrashekharan, K. and Abraham Jacob, K. (17) carried out two dimensional photo elastic analysis to study the composite action of walls supported on beams. They

constructed the photoelastic composite model of two different materials which gave the required ratio of elastic constants of wall and beam at an elevated temperature of 115°C. The two materials used by them were Columbia resin CR 39 and Araldite CY 230. CR-39 was used to represent the beam and CY-230 represented the wall portion. The ratio of modulus of elasticity obtained at room temperature for CR 39-Araldite composite was 1.32 while at elevated temperature (115°c) this ratio was 23.5. They have shown that the inter face stresses can be obtained directly using the photoelastic data along with continuity conditions at the interface. The stresses at the interior of wall portion were obtained by using numerical technique which requires only the boundary stresses to be known. They considered walls with and without openings. Their results compared well with those of Rosenhaupt(9).

1.2.1 Finite Element Study of Reinforced Concrete Structures and Brick Wall on Concrete Beams

In recent years, the finite element technique has successfully been applied to perform the non-linear analysis of reinforced concrete structures. However, its use for brick masonry structures has been very limited.

Scordelis (18) in his state of art report has reviewed the present status of research and application of

finite element method to the analysis of reinforced concrete structures. The application of finite element technique to reinforced concrete was first reported by Nago and Scordelis(19). They preformed linear elastic analysis on simple beams with predefined crack patterns to determine the principal stresses in concrete, stresses in steel reinforcement and bond stresses. They also took into account bond slip by use of finite spring elements designed as bond links between steel and concrete spaced along the bar length. Ngo, Scordelis and Franklin (20) used the same approach to study the shear in beams with diagonal tension cracks considering the effect of stirrups, dowel shear, aggregate interlock and horizontal splitting along reinforcement near the support. Nilson (21) extended the technique further by adding non-linear material and non-linear bond slip relationships. He modelled the cracking of concrete by separation of nodes. Thus propagation of cracks in the structure was constrained and cracks developed only along the inter element boundries. Moreover, nodal separation amounted to a continuous change in the structural topology and nodal connectivity of finite element mesh.

Rashid (22) and Franklin (23) incorporated the cracking of concrete and non-linear material properties in the analytical model by altering the elasticity matrices of individual elements. Incremental loading, with iterations

within each increment, were used to account for cracking of the elements and non-linear properties of materials. Franklin made use of special frame type elements, quadrilateral plane stress elements, axial bar elements. He analysed the frames with and without infils. Zienkiewicz et al (24) carried out the analysis of rock as'no tension' material by finite element method. A linear elastic analysis was conducted to determine the stresses in the elements. Since the rock was assumed as a no tension material, tensile stresses from the elements were released and equivalent nodal forces due to stress release were computed. The structure was reanalysed for these nodal forces and the process was repeated until convergence was obtained. Valliappan and Nath (25) assumed the concrete to initially exhibit a limited tensile strength which was reduced to zero once cracking occurred. An incremental loading procedure was employed and redistribution of stress due to cracking of concrete was achieved by iterative 'stress transfer approach'. Zienkiewicz et al (26) presented on 'initial stress' finite element approach for the solution of elastoplastic problems. The pseudo load vector due to change in material properties was computed and material non-linearity was included by applying and iterating these pseudo loads. Valliappan and Doolan (27) applied in 'initial stress' finite element method to study the behaviour of reinforced concrete

structures which included tensile cracking and yielding of concrete and steel. They made use of constant strain triangular elements for concrete and bar elements for reinforcement.

Mufti et al (28) studied the non-linear behaviour of structural concrete. Plane stress triangular and rectangular elements were used. The superiority of rectangular elements over triangular elements for nonlinear analysis of reinforced concrete structures was shown. Concrete was assumed to be linear elastic in tension and nonlinear stress strain relationship was used in compression. Steel elements were connected to concrete elements through bond linkage elements.

Purshothaman (5) developed a finite element model to predict the behaviour of brick masonry walls over reinforced concrete beams. In this model, brickwork was idealised as a linearly elastic orthotropic material and concrete and steel as elastic perfectly plastic material. Von Mises criterion was used for all the three materials. Bond slip was neglected. No slip between brick wall and concrete beam was assumed. Elastic, post cracking and failure stages were incorporated in the model. Constant strain triangular elements for brickwork and concrete and beam elements for steel were used. Incremental iterative method modifying the stiffness of critical elements, was used to trace the

progressive cracking, local compression failure and yielding of steel. Suidan and Schnorbrich (29) performed the three dimensional finite element analysis of reinforced concrete beams. Three dimensional 20 noded isoparametric elements were used in the analysis. Elastoplastic behaviour of concrete and reinforcing steel and cracking of concrete were accomodated in the finite element model. The results obtained compared well with those obtained experimentally.

Colville and Abbasi (30) presented a finite element approach for nonlinear analysis of reinforced concrete plane stress problems where in the reinforcing steel was included in the stiffness formulation of element . Constant strain triangular elements and rectangular elements with linear edge displacements were used in the analysis. Nonhomogeneity and anisotropy due to reinforcement and effect of tension cracking were considered in the model. The initial stress approach was used to predict the extent and location of tension cracks. Houde (31) has proposed nonlinear bond slip, aggregate interlock and dowel action relationships, and has used these to study the propagation of cracks in simple beams. Mirza and mufti (32) have employed these relationships to analyse a reinforced concrete bracket and a beam column joint. Nam, Chung-Hyum and Salmon (33) studied the nonlinear behaviour of reinforced concrete beams under short term loading. They

used combination of incompatable isoparameteric quadrilateral element and a linear bas element. Effects of progressive cracking and yielding of both steel and concrete were included in the analysis. Incremental iterative method with constant and variable stiffness was used to study in nonlinear behaviour. Incorrectness of constant stiffness method in the evaluation of nonlinear behaviour of reinforced concrete due to cracking was shown.

Failure of brittle materials due to crack propagation was studied by Majid and Hashimi (34) using finite element method. An incremental finite element method was used to detect the origin of initial crack and to trace the formation and propagation of subsequent cracks upto failure. Two types of elements, simple constant strain triangular elements and eight noded isoparametric quadrilateral elements, were used. Cracking was accounted for by separating the nodes when an element indicated the tensile failure. To avoid termination of analysis and renumbering of nodes after cracking and to allow for automatic continuation of analysis after cracking, a multiple numbering was adopted in the solution procedure. Failure loads obtained by using this method were found to be higher than those obtained experimentally

Cedolin and Poli (35) conducted finite element studies of shear critical reinforced concrete beams. A nonlinear

model was developed to trace the history of strains, stresses and crack propagation in reinforced concrete beams subjected to plane state of stress for a monotonic increase of external load. Concrete was assumed to be an orthotropic material in the direction of existing principal stresses. The stress transfer between steel and concrete was achieved through experimentally determined nonlinear bond slip relationship. Cracks in concrete were assumed capable of transmitting some shear parallel to crack it self. Analysis was performed using constant strain triangular element and an incremental iterative procedure based on tangent stiffness approach. Cedolin et al (36,37) presented a finite element analysis of deep beams and prestressed concrete beams. The analysis included nonlinear constitutive relation of concrete, presence of main and web reinforcement, their relative movement with respect to concrete and crack propagation in concrete along with other related phenomena such as aggregate interlocking and dowel action. Constant strain triangular elements were used to idealize concrete. One dimensional linkage elements, parallel to steel bars, with nonlinear bond slip characteristic, were used to connect the steel and concrete elements. An incremental iterative method was used to predict the history of stresses, deflections and crack propagation upto failure.

Paneerselvam (38) presented a nonlinear finite element analysis of reinforced concrete framed structures.

A reinforced concrete element using 4 noded isoparameteric quadrilateral with incompatable modes wad developed. This element included reinforcement in any orientation. Sub-regioning of elements was carried out for the computation of pseudo loads due to nonlinearities. The uniaxial curve for concrete was idealised by parabola-rectangle. Octahedral shear stress and shear strain criteria were used for biaxial yielding and crushing of concrete. Nonlinearities due to nonlindar stress strain law for concrete, cracking, yielding and crushing of concrete and yielding of steel were included in the analysis. 'Initial stress' approach for incremental iterative procedure was used. A.B. Agarwal (39) studied the nonlinear analysis of reinforced concrete planar structures subjected to monotonic reversed cyclic and dynamic loads. He idealised the concrete and steel as elastoplastic material. The finite element model used accounted for material non-linearities developed due to cracking, yielding and crushing of concrete and plasticity of steel reinforcement. Rectangular plane stress element, with three degrees of freedom at each node was used. Steel reinforcemenr was assumed as a uni-axially stressed material, and smeared or uniformly distributed over the concrete in an element. The results obtained using this model compared well with experimental results.

1.3 OBJECT AND SCOPE OF PRESENT INVESTIGATION

The preceding literature survey reveals that experimentation on masonry walls supported on concrete beams shows interaction between them only when the height of masonry wall supported on R.C. beam is more than half the span and the load is applied at the top of brickwork. This interaction is basically due to arch action which helps to reduce the dimensions of concrete beam and the reinforcement provided therein. There is no accepted guideline for this reduction as experimental results of various investigators show different reduction coefficients. The reason for this variation is that the extent of arch action depends upon the properties of brickwork used for masonry wall. All the investigators have agreed that little or no interaction is there in case of height to span ratio below 0.5. Furthermore, when the load is applied at the junction of concrete beam and the masonry wall, it is reported that no interaction exists for any height to span ratio. To achieve interaction in such situations Wood (7) has suggested the use of some suitable shear connectors.

The present work has been motivated to study the interaction between brick walls on R.C. beams using single legged Z shaped vertical connectors of mild steel bars embedded along the length of composite construction. In the

event of such an interaction, the thickness of R.C. beam can be reduced to bare minimum (sufficient only to provide cover to tensile reinforcement). Moreover, composite action shall tend to reduce the requirement of tensile reinforcement thereby reducing the cost of construction as compared to conventional practice. Therefore full load tests on 30 specimens of brick masonry walls supported on thin reinforced concrete beams having a constant span of 3.25 metres have been conducted upto failure and their load response characteristics, crack propagation and ultimate load carrying capacity have been recorded. The studies have been made by loading the specimen either at (1) the top of brick masonry or (2) the junction of concrete beam and masonry wall. In any effort of this kind, determination of mechanical properties of brickwork using local material is inevitable. The same has been carried out in the present work in order to achieve rational results. To study the variation of interaction of such composite construction parametric study has been conducted by varying the following parameters,

(1) Cement sand ratio in the mortar used for brick work,

(2) Height of brick masonry,

(3) Location and size of symmetric and nonsymmetric openings in brick masonry.

The experimental results obtained have been verified by analytical study. For the purpose of analytical study, the

composite structure has been idealised as a plane stress problem and solved by finite element method. A linear strain triangular element has been used for concrete and brickwork while linear strain bar element has been used for reinforcement. The sub-regioning of linear strain triangular element and linear strain bar elements have been carried for the purposes of accuracy of results and economy in computations. The ultimate load carrying capacity of the composite structure has been obtained by analysing cracking of concrete and/or brickwork and yielding of concrete, brickwork and steel. The uniaxial stress strain law for concrete is represented by an idealised bilinear curve. Brickwork is assumed to be elastic and orthotropic upto yield point beyond which its behaviour is assumed to be perfectly plastic. The steel is idealised as an elasto-plastic material. Maximum stress theory is used to check for cracking. Von Mises yield criterion is used for yielding of concrete and Hill's anisotropic yield criterion is used for brickwork.

A computer programme in fortran IV has been developed, making use of the model developed and criteria described above to trace the load deflection response and crack propagation from initial load to failure load.

CHAPTER II

MATERIAL PROPERTIES

2.1 INTRODUCTION

Brick walls supported on R.C. beams consists of three main materials i.e. concrete, brickwork and steel reinforcement. Properties of steel reinforcement are generally well defined as it is comparatively close to ideal material. It is the hetrogeneity of concrete and brickwork which makes the determination of the constitutive relations for these materials a difficult task. The structural response of reinforced concrete and brickwork is a function of the properties of component materials apart from other parameters. The realistic determination of the response of reinforced concrete and brickwork structures requires the knowledge of the inelastic behaviour of the component materials as well the ability to incorporate these into the rational analysis of real life structures. The properties of reinforced concrete are also by now well documented. However it is the brickwork whose properties are not so readily available, primarily because they vary widely from place to place. This chapter deals with the determination of mechanical properties of brickwork. The material

constitutive relations used to carry out nonlinear finite element analysis of composite system are also described herein.

2.2 EXPERIMENTAL DETERMINATION OF MECHANICAL PROPERTIES OF BRICKWORK

Mechanical properties of brickwork, for example, compressive strength, modulus of elasticity and resistance to diagonal tension vary greatly, depending upon the properties of constituent material, the arrangement of brick layers, thickness of mortar beds, workmanship and direction of loading etcetra. The properties of bricks change from country to country. Furthermore, in a vast country like India, the properties of bricks vary even from place to place. Therefore mechanical properties of brickwork have been determined experimentally in the present work and are reported in the following section.

Before embarking on the determination of mechanical properties of brickwork, it is imperative to determine the physical and mechanical properties of bricks and mortar used. This is the subject matter of study which follows.

2.2.1 Bricks

Bricks available at Kanpur, India are hand moulded, sun dried and burnt in country kiln with coal or fire wood. A consignment of 30,000 bricks was commercially procured for the present investigation. Out of each stack of five

thousand bricks, five bricks were picked up in a random manner. Thus a total of thirty bricks were tested to get the physical and mechanical properties of bricks through the following tests.

2.2.1.1 Dimensional tolerences

Length, breadth and depth of each of thirty bricks was measured at four cross-sections to get the idea of average dimensions of the bricks. The results are given in Table 2.1. Simple statistical analysis showed that the length, breadth and depth of bricks had coefficient of variation of 0.88 percent, 1.43 percent and 1.43 percent respectively. The coefficient of variation in area and volume turns out to be 1.74 percent and 2.12 percent respectively as given in Table 2.2.

2.2.1.2 Density and water absorbtion test

All the specimen bricks were weighted to get the dry density of bricks. These were subsequently soaked in water for 24 hours, wiped and weighed again to get the water absorbtion. The results are shown in Table 2.2. Analysis of these results gives the coefficient of variation of dry density and percentage water absorbtion as 3.89 percent and 30.1 percent respectively.

2.2.1.3 Compressive strength

After conducting the water absorbtion test, frog of all the thirty bricks was filled with 1:3 cement sand mortar and both surfaces top and bottom levelled with this very mortar. The bricks, cured for 24 hours as per I.S. code, were finally subjected to compression test on a universal testing machine. The results are shown in Table 2.3. The average compressive strength of bricks is 270.55 kg/cm^2 and the coefficient of variation is 11.74 percent which shows that strength of bricks even in same consignment vary greatly.

2.2.2 Cement Sand Mortar

7 cm cubes of cement sand mortar were prepared for each of the five cement sand ratio i.e. 1:3, 1:4, 1:5, 1:6 and 1:8. The mortar for the preparation of these cubes was taken either from the mortar prepared for making the brick prisms or that used for the masonry work over the concrete beams. After curing for about 28 days, these specimens were tested in compression testing machine. The results are shown in Tables 2.4, 2.5, 2.6, 2.7 and 2.8 respectively. The mean compressive strength for five mortars are 228.37, 183.77, 66.44, 54.92 and 23.55 kg/cm^2 respectively.

2.2.3 Compressive Strength and Modulus of Elasticity of Brickwork

Since brickwork is an orthotropic material, its compressive strength and modulus of elasticity is required along two mutually perpendicular directions. Hence two types of masonry prisms have been tested (1) cast with horizontal mortar layers Fig. (2.1a) and (2) cast with vertical mortar layers Fig. (2.1b). Henceforth, the brick masonry prisms with horizontal mortar layers are termed as type H and those with vertical mortar layers as type V.

2.2.3.1 Preparation of specimen

A total of sixty brick masonry prisms, six each of type H and V for each of 1:8 and ranging from 1:6 to 1:3 cement sand mortar were prepared. All the specimens were cast by two skilled masons under supervision. The time taken in casting each prism was two mason hours. The dimension of prism for type H and type V respectively turned out to be 35.5 cm x 35.5 cm x 143 cm high and 35 cm x 36 cm x 135 cm high. The thickness of joints was kept constant at 1 cm through out the present work.

2.2.3.2 Testing arrangement

Compressive strength test was carried out on a 200 tonnes universal testing machine. A 12 mm thick rubber sheet was placed at the top and the bottom of every prism. A mild

steel plate of 40cm x 40cm x 8cm thick was placed at the top over the rubber sheet. This plate projected equally on all the four sides beyond column edges. At the top of steel plate, load was applied through a circular compression tool of 25cm diameter. For measurement of strains, a mechanical dial gauge of 0.01 mm least count was fixed between the two platforms of universal testing machine. The load was applied gradually in interval of 2.5 or 5.0 tonnes depending upon the total load. In order to account for the compression of rubber sheet, a separate load deflection measurement was made by keeping the two rubber sheets one over the other covered by the same mild steel plate. The load was again applied by the same compression tool and the same dial gauge was used to note the deflections. Finally, a curve was drawn between stress versus deflection for the combination of rubber sheet and mild steel plate. This deflection was subtracted from the deflections obtained for the assembly of brick prisms with rubber sheet and mild steel plate to obtain the net deflection of the brick masonry prism. From these deflections strains were calculated. To get the mean stress strain curve, stresses were interpolated at unit interval of strains. It is assumed that strains go on increasing without any increase of stress beyond the failure of prism due to splitting. Table 2.9

shows a specimen detailed computation of strains and stresses from the observed data for a brick prism of 1:3 cement sand mortar.

2.3.3.3 Test results

(i) Compressive strength: The maximum compressive strength obtained for thirty samples of each of type H and type V are given in Tables 2.10 and 2.11 respectively.

(ii) Modulus of elasticity: The secant modulus of elasticity has been calculated for each brick prism separately at ten, twenty, forty, sixty and eighty percent of mean compressive strength. These values are given in Table 2.12 for type H and Table 2.13 for type V brick masonry prisms.

(iii) Stress strain curve: For an assumed value of strain, a set of three to six values of stresses were available (refer Table 2.10 and Table 2.11). The value of mean stress corresponding to a strain was obtained from this data for 1:6 mix using (1) arithmetic mean (2) root mean square. These stress strain curves are shown in Fig. 2.2. From this plot it is seen that the two averaging techniques do not give any appreciable difference. Therefore, only the arithmetic mean was considered for the plot of stress strain curves for the remaining specimen. These are shown in Fig. 2.3 for type H and in Fig. 2.4 for type V brick masonry prisms cast in different mortar mix. For

finite element analysis these curves have been idealised as linearly elastic upto yield limit and perfectly plastic afterwards. The idealised stress strain curves are shown in Fig. 2.5 for type H and in Fig. 2.6 for type V brick masonry prisms.

2.2.4 Resistance to Diagonal Tension of Reinforced Brick Masonry

In order to carryout the analysis of reinforced brick masonry it is necessary to obtain the tensile strength of brickwork in bending and its resistance to diagonal tension. Since the actual failure in both cases takes place due to tensile stress being more than the tensile strength, the value determined in the present work, as discussed subsequently, has been used for both.

2.2.4.1 Preparation of specimen

A total of 15 reinforced brick beams, three for each mortar defined earlier were prepared as per the arrangement shown in photograph affixed as Fig. 2.7. Each of these specimens was reinforced with three bars of sixteen millimetre diameter tor steel on tension side two bars of twelve millimetre diameter tor steel on compression side. The dimensions of all beam specimens were 57.5 cm wide , 26 cm deep and 150 cm long.

2.2.4.2 Testing arrangement

The specimens were tested as simply supported beams. Centre to centre distance between the supports was kept as 120 cm. Two point loads were applied with the help of 24000 lbs hydraulic jack as shown in Fig. 2.7. Both the load points were kept at 30 cm from centre of supports. Deflections were measured at three points, at the centre and quarter spans, by the help of mechanical dial gauges.

2.2.4.3 Test results

All the specimen failed near the supports in diagonal tension. Though the test specimen and loading was symmetrical, the diagonal tension crack developed on either the left or right support. The maximum shear stress taken as a measure of diagonal tension is calculated using the expression $q = \frac{S}{bjd}$ where S is the maximum shear force, b is the width of beam and jd is the lever arm. The lever arm is computed assuming the section to be uncracked i.e. brickwork is assumed to offer resistance to tensile force. The value of modulus of elasticity of steel reinforcement is taken as 2.1×10^6 kg/cm^2 and for brickwork the average of the corresponding value determined in previous section at 10 percent of average compressive stress is considered. Thus the value of modular ratio m varies with mortar mix used. However, the value of modular ratio m was kept limited to a maximum

of 200, because with the increase in this value, the stress in compression steel exceeds the yield stress.

The load at failure due to diagonal tension, the maximum deflection at mid point and the strength in diagonal tension for each specimen are shown in Table 2.14. The mean load versus mid point deflection curves are shown in Fig. 2.8 which are more or less linear.

2.3 CONSTITUTIVE RELATIONS FOR BRICKWORK

2.3.1 Brickwork in Elastic Range

Brickwork in elastic range in compression as well as in tension is assumed as linear orthotropic material. Therefore orthotropic constitutive law given by Darwin et.al. (40) has been used for the present work.

$$\begin{Bmatrix} \sigma_x \\ \sigma_y \\ \tau_{xy} \end{Bmatrix} = \frac{1}{1-\nu_x\nu_y} \begin{bmatrix} E_x & \nu_y E_x & 0 \\ \nu_x E_y & E_y & 0 \\ 0 & 0 & (1-\nu_x\nu_y)G \end{bmatrix} \begin{Bmatrix} \epsilon_x \\ \epsilon_y \\ \gamma_{xy} \end{Bmatrix} \quad (2.1)$$

$$\text{where } \nu_x E_y = \nu_y E_x \quad (2.2)$$

E_x, E_y are the modulus of elasticity in two directions and

ν_x, ν_y the poisson's ratio in two directions

G is the shear modulus

Equivalent poisson's ratio ν is defined as

$$\nu^2 = \nu_x \nu_y \tag{2.3}$$

From equations (2.1) to (2.3) , we get,

$$\begin{Bmatrix} \sigma_x \\ \sigma_y \\ \tau_{xy} \end{Bmatrix} = \frac{1}{1-\nu^2} \begin{bmatrix} E_x & \nu\sqrt{E_x E_y} & 0 \\ \nu\sqrt{E_x E_y} & E_y & 0 \\ 0 & 0 & (1-\nu^2)G \end{bmatrix} \begin{Bmatrix} \varepsilon_x \\ \varepsilon_y \\ \gamma_{xy} \end{Bmatrix} \tag{2.4}$$

There are four independent material constants in the above equations. While modulus of elasticity E_x and E_y can be obtained from the stress strain curves, it has not been possible to determine the value of the Poissons ratio, ν , experimentally. The value of ν in the present work has been taken as 0.1435 and 0.1 as used by Jain A.K.(41),referring(42).It is also difficult to determine experimentally the shear modulus,G, for brickwork. Grimm (42) suggested that shear modulus for brickwork is about half of the modulus of elasticity in compression. Darwon and Pecknold (40) while developing orthotropic nonlinear model for plain concrete derived the following expression for shear modulus in terms of modulus of elasticity and poisson's ratio

$$G = \frac{1}{4(\ 1-\nu_x\nu_y\ )}[\ E_x+E_y\ -2\sqrt{\nu_x\nu_y E_x E_y}\ ] \tag{2.5}$$

This expression has been derived on the assumption

that it is independent of the orientation of axis. The value of G derived from this expression has been used in the present work.

2.3.2 Yielding of Brickwork

There is no evidence in the literature regarding strength envelope for brickwork in the state of combined stresses. Purshothaman (5) used Von Mises criterion to check for biaxial compression yielding of brickwork, though this criterion is valid for isotropic materials only. Therefore in the present work Hill's anisotropic yield criterion has been used as brickwork is orthotropic in nature before cracking. Hill's anisotropic yield criterion is written as

$$F(\sigma) = \frac{1}{\sqrt{2}}\Big[\alpha_{12}(\sigma_{11}-\sigma_{22})^2+ \alpha_{23}(\sigma_{22}-\sigma_{33})^2+\alpha_{31}(\sigma_{33}-\sigma_{11})^2$$

$$+6(\alpha_{44}\tau_{12}^2+\alpha_{55}\tau_{23}^2+\alpha_{66}\tau_{31}^2)\Big]^{1/2} - \bar{\sigma}_0 \qquad (2.6)$$

where σ_0 is the effective stress: α_{ij}'s are anisotropic parameters, σ_{11}, σ_{22}, σ_{33} are normal stresses in the direction of anisotropic axes 1,2,3 and τ_{12}, τ_{23}, τ_{31} are shear stresses in planes 12, 23 and 31.

Now for plane stress problems, $\sigma_{11}=\sigma_x$, $\sigma_{22}=\sigma_y$, $\tau_{12}=\tau_{xy}$ and all other components are zero, therefore the yield criterion given by equation (2.6) reduces to

$$F(\sigma) = \left[\frac{\alpha_{11}}{2}\sigma_x^2 + \frac{\alpha_{22}}{2}\sigma_y^2 - \alpha_{12}\sigma_x\sigma_y + 3\alpha_{44}\tau_{xy}^2 \right]^{1/2} - \bar{\sigma}_o \qquad (2.7)$$

where $\alpha_{11} = \alpha_{12} + \alpha_{31}$

$\alpha_{22} = \alpha_{23} + \alpha_{12}$

The anisotropic parameters are determined from yield stresses in various directions obtained from independent tests. The initial anisotropic parameters α_{11}, α_{22}, α_{33} and α_{44} are obtained successively letting all stress components in yield criterion equal to zero except the one under consideration. Therefore from yield criterion and from an uniaxial test in X direction, we get

$$\alpha_{12} + \alpha_{31} = \alpha_{11} = 2\left(\frac{\bar{\sigma}_o}{\sigma_{ox}}\right)^2 \qquad (2.8)$$

similarly, from an uniaxial test in Y direction, we obtain

$$\alpha_{12} + \alpha_{23} = \alpha_{22} = 2\left(\frac{\bar{\sigma}_o}{\sigma_{oy}}\right)^2 \qquad (2.9)$$

and from an uniaxial test in Z direction, we get

$$\alpha_{23} + \alpha_{31} = \alpha_{33} = 2\left(\frac{\bar{\sigma}_o}{\sigma_{oz}}\right)^2 \qquad (2.10)$$

similarly from a shear test, we obtain

$$\alpha_{44} = \frac{1}{3}\left(\frac{\bar{\sigma}_o}{\tau_{oxy}}\right)^2 \qquad (2.11)$$

where σ_{ox}, σ_{oy}, σ_{oz} and τ_{oxy} are initial yield stresses

obtained from the uniaxial tests and $\bar{\sigma}_o$ is the initial effective stress adopted from one of the above four uniaxial test values.

The three unknown parameters α_{12}, α_{23} and α_{31} can be obtained by solving equations (2.8) to (2.10) and thus

$$\alpha_{12} = \left(\frac{\bar{\sigma}_o}{\sigma_{ox}}\right)^2 + \left(\frac{\bar{\sigma}_o}{\sigma_{oy}}\right)^2 - \left(\frac{\bar{\sigma}_o}{\sigma_{oz}}\right)^2 \qquad (2.12)$$

$$\alpha_{23} = -\left(\frac{\bar{\sigma}_o}{\sigma_{ox}}\right)^2 + \left(\frac{\bar{\sigma}_o}{\sigma_{oy}}\right)^2 + \left(\frac{\bar{\sigma}_o}{\sigma_{oz}}\right)^2 \qquad (2.13)$$

$$\alpha_{31} = \left(\frac{\bar{\sigma}_o}{\sigma_{ox}}\right)^2 - \left(\frac{\bar{\sigma}_o}{\sigma_{oy}}\right)^2 + \left(\frac{\bar{\sigma}_o}{\sigma_{oz}}\right)^2 \qquad (2.14)$$

For brick element shown in Fig. 2.9, it is assumed that $\sigma_{oz} = \sigma_{ox}$. If effective stress is adopted from the uniaxial test in X direction, the yield criterion given by equation (2.7) takes the following form on simplification (43)

$$F(\sigma) = \left[\left(\frac{\sigma_x}{\sigma_{oy}}\right)^2 + \left(\frac{\sigma_y}{\sigma_{oy}}\right)^2 - \frac{1}{r}\left(\frac{\sigma_x}{\sigma_{ox}}\right)\left(\frac{\sigma_y}{\sigma_{oy}}\right) + \left(\frac{\tau_{xy}}{\tau_{oxy}}\right)^2\right]^{1/2} - 1 \qquad (2.15)$$

where $r = \dfrac{\sigma_{oy}}{\sigma_{ox}}$

In the finite element increment analysis the constitutive relation for material under going plastic deformation can be expressed as

$$\{d\sigma\} = [\,C_{ep}\,]\,\{d\varepsilon\} \qquad (2.16)$$

where $[C_{ep}]$ is the elastoplastic matrix which is derived using flow rule of plasticity. The elastoplastic matrix is given by (26)

$$[C_{ep}] = [C] - \left[\frac{[C] \left\{ \frac{\partial F}{\partial \sigma} \right\} \left\{ \frac{\partial F}{\partial \sigma} \right\}^T [C]}{H' + \left\{ \frac{\partial F}{\partial \sigma} \right\}^T [C] \left\{ \frac{\partial F}{\partial \sigma} \right\}} \right] \tag{2.17}$$

where C is the elasticity matrix and H' is the slope of uniaxial stress versus plastic strain curve at a particular value of $\bar{\sigma}_0$. The yielding of brickwork is not caused by actual plastic flow. Infact it is the cumulative effect of microcrack propagation which is responsible for onset of yielding in brickwork (44). Moreover, the yielding of brickwork does not affect the overall behaviour of the structure to the extent the cracking of concrete, brickwork and yielding of steel does. Therefore, in the present work, an 'unconstrained flow rule' suggested and used by Lin et al. (44) has been used. This flow rule assumes that the flow of plastic strains is not constrained but stresses are fixed at the initial yield points on the yield surface. The stress strain relation for the unconstrained flow rule in incremental form is expressed as follows.

$$\{d\sigma\} = [0] \{d\varepsilon\} \tag{2.18}$$

where $[0]$ is a null matrix.

2.3.3 Cracking of Brickwork

Much of literature is not available on failure criterion for cracking of brickwork. Purshothaman (5) has used maximum stress theory to predict cracks in brick masonry and the same has been used in the present work. According to maximum normal stress criterion, when one of the principal stress exceeds the tensile strength of brickwork, brickwork is assumed to have cracked perpendicular to that principal stress. After cracking, normal stress at crack drops to zero and shear modulus also gets reduced.

Fig. 2.10 shows a cracked brickwork element in global coordinate system x y. X' Y' is a local coordinate system having the coordinate axis coinciding with the direction of principal stresses at the time of cracking. Material constitutive matrix in local coordinate system X'Y' is obtained by transforming the initial constitutive matrix from global coordinate system through the following transformation.

$$[C'] = [T_2]^T \; [C] \; [T_2] \qquad (2.19)$$

where C is the initial constitutive matrix given by equation (2.4) and T_2 the transformation matrix given by

$$[T_2] = \begin{bmatrix} \cos^2\beta & \sin^2\beta & -\cos\beta\,\sin\beta \\ \sin^2\beta & \cos^2\beta & \cos\beta\,\sin\beta \\ 2\,\sin\beta\cos\beta & -2\cos\beta\sin\beta & \cos^2\beta-\sin^2\beta \end{bmatrix} \qquad (2.20)$$

Since brickwork is orthotropic in nature in global coordinate system XY it becomes anisotropic in any other coordinate system. Therefore material constitutive matrix of brickwork in X'Y' coordinate system given by equation (2.19) can be written as

$$[C'] = \begin{bmatrix} C'_{11} & C'_{12} & C'_{13} \\ C'_{12} & C'_{22} & C'_{23} \\ C'_{13} & C'_{23} & C'_{33} \end{bmatrix} \tag{2.21}$$

where C'_{ij}'s are the elements of matrix $[C']$. The stress strain relations for brickwork in X'Y' coordinate system are written as

$$\begin{Bmatrix} \sigma'_x \\ \sigma'_y \\ \tau'_{xy} \end{Bmatrix} = \begin{bmatrix} C'_{11} & C'_{12} & C'_{13} \\ C'_{12} & C'_{22} & C'_{23} \\ C'_{13} & C'_{23} & C'_{33} \end{bmatrix} \begin{Bmatrix} \varepsilon'_x \\ \varepsilon'_y \\ \gamma'_{xy} \end{Bmatrix} \tag{2.22}$$

Since element has cracked along Y' axis, stress perpendicular to crack would be zero for all values of strains. This requires that first row of $[C']$ matrix should be zero and hence for symmetry of constitutive matrix first column should also be zero. Thus material constitutive matrix for cracked brickwork can be written as

$$[C'_{cr}] = \begin{bmatrix} 0 & 0 & 0 \\ 0 & C'_{22} & C'_{23} \\ 0 & C'_{23} & \alpha_B C'_{33} \end{bmatrix} \qquad (2.23)$$

where α_B is the shear retention factor. The shear retention factor α_B has an upper and lower bound values of unity and zero. In case of brickwork the cracks are more uneven and due to the presence of shear cum tensile connectors in brickwork, value of α_B should be quite high. Therefore, in the present work, the upper bound value of unity has been used. The material constitutive matrix in transformed from local coordinate system to global coordinate system through following transformation.

$$[C_{cr}] = [T_2]^T [C'_{cr}][T_2] \qquad (2.24)$$

where $[C_{cr}]$ is the constitutive matrix of the cracked element in global coordinate system and $[C'_{cr}]$ is the constitutive matrix of cracked brickwork in local coordinate system.

If both the principal stresses in an uncracked brick work element exceeds the tensile strength capacity of brick work it is assumed to have cracked in both principal stress directions. However, brickwork cracked in one direction can further crack along a second direction when the tensile stress perpendicular to that direction exceeds the tensile strength capacity. The brickwork cracked in two directions

is assumed not to transfer any load in tension. Therefore, brickwork cracked in two directions is assumed to have zero stiffness. The constitutive matrix for such a situation is given by

$$[C_{cr}] = \begin{bmatrix} 0 & 0 & 0 \\ 0 & 0 & 0 \\ 0 & 0 & 0 \end{bmatrix} \qquad (2.25)$$

2.4 MECHANICAL PROPERTIES OF CONCRETE

2.4.1 Compressive and Tensile Strength of Concrete

The experimental investigation carried out on concrete was the control tests conducted during the fabrication of concrete beams. 15 cm concrete cubes were cast to determine the compressive strength and 30 cm long, 15 cm diameter cylinders were prepared to determine the tensile strength of concrete. Concrete mix used was 1:2:4 by weight and a constant water cement ratio of 0.65 was maintained. The results of control tests are shown in Table 2.15 and 2.16.

2.4.2 Stress Strain Curve for Concrete

The uniaxial stress-strain curve for concrete is affected by numerous factors, such as shrinkage, creep and microcracking. In compression, its early deviation from a linear elastic path has mainly been attributed to

the microcracking which develops at the aggregate mortar interface. Further disintigration and ultimate failure of concrete occurs due to propagation of these cracks through the mortar. For the quantitative description of the stress strain relationship of plain concrete, several emperical formulae are available in the literature. A good review of this area has been presented by Popovics (45).

To study the behaviour of plane concrete under biaxial stress fields, Kupfer, Hilsdorf and Rusch (46) have conducted extensive experimental work. They have presented their experimental results in the form of a failure envelope. Their findings have also indicated that the strength of concrete under biaxial compression, $\sigma_1 = \sigma_2$, is only 16 percent larger than under uniaxial compression but the biaxial tensile strength of concrete is approximately equal to its uniaxial tensile strength. Liu, Nilson and Slate (47) have also studied the behaviour of plane concrete in biaxial compression state.

Kupfer and Gerstile (48) have used the experimental data of Kupfer et. al. (46), and have derived empirical expressions to describe the failure envelope of concrete. Romstad, Taylor and Herrmann (49) have also developed an elaborate multilinear biaxial constitutive material model for plain concrete. They have divided the principal stress

space in four damage zones. In each zone the damage level is assumed to be constant and the material properties are treated as being linear, isotropic and constant. Each isotropic state is described by an appropriate value of modulus of elasticity and the Poisson's ratio based on experimental evidence of Kupfer et al. (46).

In early applications (19,27) plane concrete has been idealised as an isotropic and linear elastic or elastoplastic material. This is shown in Fig. (2.11) Panneerselvam (38), adopted a nonlinear stress strain curve proposed by Rusch (50). This stress strain law shown in Fig. 2.12 is a second degree parabola-rectangle and is given by

$$\begin{aligned} \sigma &= K_3 f_c' \left(\epsilon \times 10^3 - \frac{\epsilon^2}{4} \times 10^6\right) && 0 < \epsilon < 0.002 \\ &= K_3 f_c' && 0.002 < \epsilon < 0.0035 \qquad (2.26) \\ &= 0 && \epsilon \geq 0.0035 \end{aligned}$$

The overall nonlinear behaviour of reinforced concrete and brickwork structures in the elastic stage is primarily due to tensile cracking. Hence the nonlinear portion (Fig. 2.12) can be idealized as a linear curve as shown in Fig. 2.11. This means that material non-linearity in the elastic range due to stress strain relationship can be neglected as compared to nonlinearity due to tensile

cracking. The computer programme developed can be used to accomodate any of the two stress strain laws. However, in the present work nonlinear stress strain law has been used.

The stress strain relationship for concrete in tension is a curve corresponding to linearly elastic brittle material.

2.5 CONSTITUTIVE RELATIONS FOR CONCRETE

Concrete, in general, is in a state of biaxial stress condition and for a rational analysis, the behaviour and constitutive law under biaxial stress-state must be known.

2.5.1 Concrete in Elastic Range

Case 1: Concrete in biaxial tension

Under this condition, concrete is assumed to be an isotropic homogeneous material. Thus material constitutive matrix is given by

$$[C] = \frac{E_c}{1-\nu^2} \begin{bmatrix} 1 & \nu & 0 \\ \nu & 1 & 0 \\ 0 & 0 & \frac{1-\nu}{2} \end{bmatrix} \qquad (2.27)$$

where E_c is the modulus of elasticity and ν is the Poisson's ratio for concrete.

Case 2: Concrete in biaxial compression

In case it is assumed that concrete follows a linear

stress strain relationship, the constitutive law given by equation (2.27) still holds good for the biaxial compression state of stress. If nonlinear stress strain relationship is used as in present work then determination of modulus of elasticity for concrete in biaxial compression is difficult, since little is known about the interrelationship between biaxial modulii and associated Poisson's effect. Kupfer and Gerstle (48) studied the nonlinear response of concrete under biaxial compression and proposed a biaxial constitutive law in terms of bulk and shear modulii. Darwin et al (40) considered the concrete in biaxial compression state to be orthotropic and proposed a biaxial stress strain law. Panneerselvam (38) determined the two elastic modulii corresponding to two principal strains and used the minimum of two to define the constitutive law in biaxial compression. This approach though simple, is not accurate. In the present work, the constitutive matrix in biaxial compression is obtained as follows.

A simple modulus of elasticity in biaxial compression is found out using the concept of equivalent strain given in (51). An equivalent one dimensional effective strain ϵ^* is defined as

$$\epsilon^* = \frac{\sqrt{2}}{2(1+\nu)} \left[(\epsilon_x-\epsilon_y)^2 + (\epsilon_y-\epsilon_z)^2 + (\epsilon_z-\epsilon_x)^2 + \frac{3}{2}\left(\gamma_{xy}^2 + \gamma_{yz}^2 + \gamma_{zx}^2\right)\right]^{1/2} \tag{2.28}$$

Now for plane stress condition $\gamma_{yz}=\gamma_{zx}=0$ and $\varepsilon_z = \frac{-\nu}{1-\nu}(\varepsilon_x + \varepsilon_y)$.
Therefore equivalent strain for a plane stress case will be

$$\varepsilon^* = \frac{\sqrt{2}}{2(1+\nu)}\left[(\varepsilon_x-\varepsilon_y)^2 + (\varepsilon_y-\varepsilon_z)^2 + (\varepsilon_z-\varepsilon_x)^2 + \frac{3}{2}\gamma_{xy}^2\right]^{1/2} \quad (2.29)$$

Single modulus of elasticity E_n is found out at equivalent strain ε^* from the assumed uniaxial stress strain curve. Hence for elastic concrete in biaxial compression, the constitutive matrix [C] is given by

$$[C] = \frac{E_n}{1-\nu^2}\begin{bmatrix} 1 & \nu & 0 \\ \nu & 1 & 0 \\ 0 & 0 & \frac{1-\nu}{2} \end{bmatrix} \quad (2.30)$$

2.5.2 Yielding of Concrete

The failure criterion for concrete in a biaxial stress state was proposed by Kupfer et al. (46,48) based on their experimental investigation. The yield failure surface proposed by them is shown in Fig. 2.13. This yield-failure surface was modified by Wanchoo and May (52) as shown by solid lines in the same figure. The modified surface assumes that compressive yielding is governed by Von Mises criterion and associated flow rule and is slightly more conservative than Kuffer's surface in the biaxial compression zone. It is less conservative in tension compression zone but since it

simplifies the computational procedure it is used in the present work.

The Von Mises yield criterion in terms of octahedral shear stress is given by

$$F(\sigma) = \frac{3}{\sqrt{2}} \tau_{oct} - \bar{\sigma}_o = 0 \qquad (2.31)$$

where $\bar{\sigma}_o$ is the yield stress of concrete in uniaxial case and

$$\tau_{oct} = \frac{1}{3} [(\sigma_x-\sigma_y)^2 + (\sigma_y-\sigma_z)^2 + (\sigma_z-\sigma_x)^2 + 6(\tau_{xy}^2 + \tau_{yz}^2 + \tau_{zx}^2)]^{1/2}$$

If the value of τ_{oct} is substituted in the above equation, the yield criterion would be

$$F(\sigma) = \frac{1}{\sqrt{2}} [(\sigma_x-\sigma_y)^2 + (\sigma_y-\sigma_z)^2 + (\sigma_z-\sigma_x)^2 + 6(\tau_{xy}^2 + \tau_{yz}^2 + \tau_{zx}^2)]^{1/2} - \bar{\sigma}_o = 0 \qquad (2.32)$$

For a plane stress case $\tau_{yz} = \tau_{zx} = \sigma_z = 0$, so the above criterion becomes

$$F(\sigma) = (\sigma_x^2 + \sigma_y^2 - \sigma_x \sigma_y + 3\tau_{xy}^2)^{1/2} - \bar{\sigma}_o = 0 \qquad (2.33)$$

In finite element incremental analysis the constitutive relation for a material undergoing plastic deformation can be expressed as follows (26)

$$\{d\sigma\} = [C_{ep}] \{d\varepsilon\} \qquad (2.34)$$

where $[C_{ep}]$ is the elastoplastic matrix which is derived using the flow rule of plasticity. The elastoplastic matrix is given by (26)

$$[C_{ep}] = [C] - \left[\frac{[C]\left\{\frac{\partial F}{\partial \sigma}\right\}\left\{\frac{\partial F}{\partial \sigma}\right\}^T [C]}{H' + \left\{\frac{\partial F}{\partial \sigma}\right\}^T [C]\left\{\frac{\partial F}{\partial \sigma}\right\}} \right] \tag{2.35}$$

where $[C]$ is the elasticity matrix and H' is the slope of uniaxial stress versus plastic strain curve at a particular value of σ_o. The elastoplastic matrix for Von Mises criterion and plane stress is obtained by simplifying the above equation as (51)

$$[C_{ep}] = \frac{E_c}{Q}\begin{bmatrix} \sigma_y'\sigma_y' + 2P & (-\sigma_x'\sigma_x' + 2\nu P) & \left(-\frac{\sigma_x' + \nu\sigma_y'}{1+\nu}\right)\tau_{xy} \\ -(\sigma_x'\sigma_x' + 2\nu P) & (\sigma_x'\sigma_x' + 2P) & \left(\frac{-\sigma_y' + \nu\sigma_x'}{1+\nu}\right)\tau_{xy} \\ \left(-\frac{\sigma_x' + \nu\sigma_y'}{1+\nu}\right)\tau_{xy} & \left(\frac{-\sigma_y' + \nu\sigma_x'}{1+\nu}\right)\tau_{xy} & \left(\frac{R}{2(1+\nu)} + \frac{2H'}{9E_c}(1-\nu)\bar{\sigma}_o^2\right) \end{bmatrix} \tag{2.36}$$

where $P = \left[\frac{2H'\bar{\sigma}_o}{9E_c} + \frac{\tau_{xy}^2}{1+\nu}\right]$

$R = [\sigma_x'^2 + \sigma_y'^2 + 2\nu\sigma_x'\sigma_y']$

$Q = [R + 2(1-\nu^2)P]$

and σ_x', σ_y' are the deviotric stresses i.e.

$$\sigma_x' = \sigma_x - \frac{\sigma_x + \sigma_y + \sigma_z}{3}$$

$$\sigma_y' = \sigma_y - \frac{\sigma_x + \sigma_y + \sigma_z}{3}$$

Most of the finite element investigators have used normality law of flow rule valid for yielding of concrete. The physical meaning of this flow rule, is that the increment of plastic strain has to be normal to yield surface. This rule has been shown to be applicable to most of the ductile metals. However, for concrete, the flow rule with respect to yield surface is not well established. The apparent plastic yielding of concrete is caused, not by actual plastic flow, but by cumulative effect of microcrack propagation (44). Moreover, the yielding of concrete does not affect the overall behaviour of the structure to the extent the cracking of concrete, brickwork and yielding of steel does. Therefore, in the present work, an 'unconstrained flow rule' suggested and used by Lin et al (44) has been used. This rule assumes that the flow of plastic strains is not constrained but stresses are fixed at the initial yield points on the yield surface. The stress strain relationship for the 'unconstrained flow rule' in incremental form is expressed as follows

$$\{d\sigma\} = [0]\ \{d\varepsilon\} \tag{2.37}$$

where $[0]$ is a null matrix

2.5.3 Crushing of Concrete

A crush surface, analogous to yield surface but interms of strains, is postulated to define the complete collapse (or crush) for the yielded concrete (44,53). The crush surface in terms of octahedral shear strain is expressed as

$$F_c(\varepsilon) = \sqrt{2}\ \varepsilon_{oct} - \varepsilon_{cu} = 0 \qquad (2.38)$$

where ε_{cu} is the ultimate strain in uniaxial case and

$$\varepsilon_{oct} = \frac{1}{3}\left[(\varepsilon_x-\varepsilon_y)^2+(\varepsilon_y-\varepsilon_z)^2+(\varepsilon_z-\varepsilon_x)^2 + \frac{3}{2}(\gamma_{xy}^2 + \gamma_{yz}^2 + \gamma_{zx})\right]^{1/2}$$

Now for plane stress condition $\gamma_{yz} = \gamma_{zx} = 0$ and $\varepsilon_z = -\varepsilon_x - \varepsilon_y$

therefore,

$$F_c(\varepsilon) = \frac{\sqrt{2}}{3}\left[(\varepsilon_x-\varepsilon_y)^2 + (\varepsilon_y-\varepsilon_z)^2+(\varepsilon_z-\varepsilon_x)^2 + \frac{3}{2}\gamma_{xy}^2\right]^{1/2} - \varepsilon_{cu} \qquad (2.39)$$

The crush surface as shown in Fig. 2.14 is the principal strain plane. The boundary between crushed and noncrushed region defined by equation (2.39) is valid only for biaxial compression state . If one or both principal strains are positive i.e. tensile, no such boundary is defined. In such a condition, concrete will crack much before crushing strain is reached. Therefore, it is to sufficient to define the failure envelope only for the case of biaxial compression (38, 53).

Once concrete is crushed, it is assumed to have lost all its stiffness. Thus, crushed concrete is assumed to have zero stiffness and therefore, its material constitutive matrix is given by

$$[C] = \begin{bmatrix} 0 & 0 & 0 \\ 0 & 0 & 0 \\ 0 & 0 & 0 \end{bmatrix} \tag{2.40}$$

2.5.4 Cracking of Concrete

When one of the principal stresses exceeds the tensile strength of concrete, concrete is considered to have cracked in a direction perpendicular to that of principal stress. The normal stress at crack drops to zero and shear modulus gets reduced due to cracking.

Referring to Fig. 2.15, the stress strain relation for cracked concrete in X'Y' coordinate is given by

$$\begin{Bmatrix} \sigma'_x \\ \sigma'_y \\ \tau'_{xy} \end{Bmatrix} = \begin{bmatrix} 0 & 0 & 0 \\ 0 & E & 0 \\ 0 & 0 & \alpha_c G \end{bmatrix} \begin{Bmatrix} \epsilon_{x'} \\ \epsilon_{y'} \\ \gamma'_{xy} \end{Bmatrix} \tag{2.41}$$

where G is the uncracked shear modulus, α_c is a factor to account for aggregate interlock, dowel action etc. that may be present (α_c is always less than unity). X'Y' is the coordinate system having the coordinate axis coinciding with the principal stress directions at the time of cracking.

The above equation can be written as

$$\{\sigma'\} = [C'] \{\epsilon'\} \tag{2.42}$$

α_c the shear retention factor retains certain amount of shear stress in the cracked concrete. Since shear strength along the cracks is a function of crack width, the possible upper and lower bound values for α_c are unity and zero. A value of zero will mean that the cracked element behaves as a bundle of uniaxial fibres capable of sustaining tensile or compressive loads only parallel to the direction of crack. This is not true as cracks in concrete are not smooth, parallel and frictionless slippage planes. Instead they are irregular rough planes at unequal distance apart. Based upon the numerical experimentation done by Jain A.K. (41) as value of 0.4 for α_c has been used in the present work.

The constitutive relations of equation (2.42) are transformed to global coordinate system using the following transformation.

$$[C_{cr}] = [T_2]^T [C'] [T_2] \tag{2.43}$$

where $[C']$ is the constitutive matrix of cracked element in local coordinate system X'Y', $[C_{cr}]$ is the constitutive matrix of cracked element in global coordinate system and

$$[T_2] = \begin{bmatrix} \cos^2\beta & \sin^2\beta & \sin\beta\,\cos\beta \\ \sin^2\beta & \cos^2\beta & -\sin\beta\,\cos\beta \\ -2\sin\beta\cos\beta & 2\sin\beta\cos\beta & \cos^2\beta-\sin^2\beta \end{bmatrix} \qquad (2.44)$$

where β is the inclination of principal stress measured positive in anticlockwise direction from X axis in global coordinate system.

If both principal stresses in an uncracked concrete element exceeds the tensile strength of concrete, concrete will crack in both principal stress directions. However , concrete cracked along one direction can further crack along a second direction when tensile stress in that direction exceeds the tensile strength of concrete. Like the first one ,this crack is also assumed to develope perpendicular to the direction of principal tensile stress. The concrete cracked along two directions is assumed to be unable to transfer any load in tension. Therefore, concrete cracked along two directions is assumed to have zero stiffness. The constitutive matrix for such a case is given by

$$[C_{cr}] = \begin{bmatrix} 0 & 0 & 0 \\ 0 & 0 & 0 \\ 0 & 0 & 0 \end{bmatrix} \qquad (2.45)$$

2.6 PROPERTIES OF STEEL REINFORCEMENT

Mild steel plain rounds have been as reinforcement in bending and as single legged Z shaped vertical connectors.

Mild steel bars of all diameters used i.e. 6 to 16 mm were subjected to control tests. The yield stress, ultimate stress and the percentage elongation were determined. Table 2.17 gives the details of results obtained from control test. Fig. 2.16 shows the stress strain curve obtained for the steel used.

2.7 CONSTITUTIVE RELATIONS FOR STEEL REINFORCEMENT

The steel reinforcement has been idealised as an elastoplastic material in the present investigation with yield stress $\pm\ \sigma_y$ and Modulus of Elasticity E_s. The idealised stress-strain curve is shown in Fig. 2.17. It is further assumed that the reinforcing bars carry only axial stresses. When stresses in steel are in elastic range, the stress strain relation with respect to X'Y' coordinate system Fig. 2.18 are

$$\begin{Bmatrix} \sigma'_x \\ \sigma'_y \\ \tau'_{xy} \end{Bmatrix} = \begin{bmatrix} E_s & 0 & 0 \\ 0 & 0 & 0 \\ 0 & 0 & 0 \end{bmatrix} \begin{Bmatrix} \epsilon_{x'} \\ \epsilon_{y'} \\ \gamma'_{xy} \end{Bmatrix} \qquad (2.46)$$

Equation 2.44 can be used to transform the above relation is global coordinate system.

When reinforcing steel has yielded it is assumed to have zero incremental stiffness. The constitutive relations in such cases are as follows.

$$\{d\sigma\} = [\,0\,]\ \{d\epsilon\} \qquad (2.47)$$

where $[0]$ is a null matrix

Sl. No.	Length in cm				
	L_1	L_2	L_3	L_4	$L = \Sigma L_1/4$
1	23.10	23.30	23.35	23.10	23.21
2	23.00	22.90	23.15	22.95	23.00
3	22.96	22.70	22.75	23.00	22.85
4	22.90	23.10	22.95	23.05	23.00
5	22.85	23.50	23.00	22.85	23.05
6	23.35	23.30	23.35	23.35	23.34
7	23.35	22.75	22.80	23.40	23.08
8	23.30	23.10	23.00	23.35	23.19
9	22.85	23.10	23.10	22.95	22.96
10	23.10	23.50	23.40	23.15	23.29
11	22.75	22.40	22.50	22.70	22.59
12.	23.30	23.15	23.50	23.35	23.33
13	22.95	23.15	23.20	22.95	23.05
14	23.21	23.30	23.35	23.30	23.29
15	22.60	22.65	22.65	22.70	22.65
16	23.20	23.30	23.30	23.25	23.26
17	22.85	23.05	23.05	22.95	22.98
18	23.10	22.95	23.00	23.05	23.03
19	23.30	23.10	23.05	23.25	23.16
20	23.20	23.15	23.15	23.15	23.16
21	23.25	23.35	23.40	23.40	23.35
22	23.15	23.25	23.20	23.30	23.23
23	22.95	23.05	23.00	22.95	22.99
24	22.90	23.00	22.95	22.85	22.93
25	22.95	23.10	23.20	23.15	22.85
26	23.10	23.15	23.05	23.10	23.11
27	23.15	23.05	23.20	23.10	23.24
28	22.90	23.10	23.10	22.95	23.01
29	23.30	23.20	23.35	23.40	23.31
30	22.80	22.75	22.65	22.70	22.73

Arithmetic mean $= \dfrac{\text{Sum}}{30} = \bar{L} = 23.07$

Coefficient of variation =0.88 percent

Standard deviation $\sigma_{n-1} = \sqrt{\Sigma \dfrac{(L-\bar{L})^2}{n-1}}$ = 0.203

Table contd..on page 56

Table 2.1 contd...

Sl.No.	Breadth in cm				
	B_1	B_2	B_3	B_4	$B=\Sigma B_i/4$
1	11.10	11.15	11.50	11.50	11.31
2	11.05	11.10	10.95	11.00	11.14
3	10.85	10.75	10.75	10.85	10.85
4	10.95	11.00	10.90	11.05	11.09
5	10.95	11.15	11.15	11.15	11.10
6	11.25	11.20	11.15	11.25	11.21
7	10.70	11.10	11.50	10.80	11.03
8	10.90	11.25	11.40	10.95	11.13
9	10.80	10.95	11.50	10.90	11.04
10	10.85	10.85	10.85	10.95	10.88
11	11.00	11.15	11.15	11.15	11.11
12	10.65	10.95	11.50	10.70	10.95
13	11.20	11.20	11.15	11.15	11.18
14	11.35	11.50	11.55	11.30	11.43
15	10.75	11.00	10.80	11.00	10.89
16	10.65	10.95	10.95	10.70	10.81
17	11.05	11.30	11.30	11.05	11.18
18	10.95	10.70	10.75	10.85	10.81
19	10.90	10.90	10.95	11.00	10.94
20	10.95	10.85	10.85	10.90	10.89
21	11.10	11.05	11.15	11.00	11.08
22	11.05	10.85	10.95	11.00	10.96
23	11.25	11.30	11.15	11.20	11.23
24	11.00	11.15	11.25	11.15	11.13
25	11.10	10.95	10.95	11.00	11.00
26	11.15	11.35	11.35	11.25	11.28
27	10.75	11.00	10.95	10.90	10.90
28	10.85	10.95	11.20	10.95	10.99
29	10.65	10.95	11.00	10.95	10.89
30	10.80	11.00	10.95	10.90	10.91

Arithmetic mean $= \frac{\text{Sum}}{30} = \bar{B} = 11.045$ Coefficient variation $=1.43$ percent

Standard deviation $\sigma_{n-1} = \sqrt{\Sigma \frac{(B-\bar{B})^2}{n-1}} = 0.158$

Table contd..on page 57

Table 2.1 contd...

Sl.No.	Depth in cm				
	D_1	D_2	D_3	D_4	$D=\Sigma D_i/4$
1	6.65	6.25	6.10	6.50	6.38
2	6.60	6.40	6.35	6.25	6.40
3	6.50	6.35	6.65	6.45	6.49
4	6.40	6.55	6.45	6.40	6.45
5	6.10	6.35	6.45	6.25	6.29
6	6.55	6.64	6.45	6.54	6.54
7	6.45	6.60	6.50	6.70	6.56
8	6.50	6.45	6.35	6.30	6.40
9	6.75	6.50	6.55	6.70	6.63
10	6.35	6.25	6.50	6.41	6.38
11	6.30	6.55	6.30	6.20	6.34
12	6.65	6.30	6.10	6.30	6.34
13	6.65	6.70	6.65	6.55	6.64
14	6.60	6.45	6.50	6.30	6.46
15	6.60	6.65	6.60	6.25	6.53
16	6.65	6.40	6.45	6.60	6.53
17	6.75	6.70	6.35	6.60	6.60
18	6.75	6.35	6.40	6.50	6.50
19	6.55	6.50	6.45	6.60	6.53
20	6.55	6.60	6.60	6.65	6.60
21	6.60	6.45	6.50	6.50	6.51
22	6.55	6.45	6.40	6.60	6.50
23	6.45	6.60	6.55	6.50	6.53
24	6.35	6.65	6.50	6.40	6.48
25	6.30	6.55	6.35	6.45	6.41
26	6.45	6.55	6.60	6.50	6.53
27	6.60	6.45	6.50	6.35	6.48
28	6.70	6.55	6.60	6.70	6.64
29	6.65	6.45	6.20	6.50	6.45
30	6.55	6.60	6.65	6.45	6.55

Arithmetic mean = $\frac{\text{Sum}}{30} = \bar{D} = 6.42$ Coefficient of variation =1.43 percent

Standard deviation $\sigma_{n-1} = \sqrt{\Sigma\frac{(D-\bar{D})^2}{n-1}} = 0.092$

PERCENTAGE WATER ABSORBTION OF BRICKS USED IN EXPERIMENTAL WORK

Sl. No.	Area A=LxB	Volume V=LxBxD	Dry weight in kg	Wet weight in kg	Dry density in gm/cm^3	Percentage absorbtion
1	262.51	1674.78	2.646	2.863	1.580	8.20
2	256.22	1639.81	2.615	2.860	1.595	9.37
3	247.92	1609.02	2.534	2.859	1.575	12.83
4	255.07	1645.20	2.545	2.880	1.547	13.16
5	255.86	1609.33	2.615	2,910	1.625	11.28
6	261.64	1711.13	2.498	2.821	1.460	12.93
7	254.37	1669.98	2.687	3.082	1.609	14.70
8	258.10	1651.84	2.631	2.968	1.593	12.81
9	253.48	1680.57	2.544	2.887	1.514	13.48
10	253.40	1616.69	2.519	2.908	1.558	15,44
11	250.97	1591.15	2.531	2.848	1.591	12.52
12	255.46	1619.62	2.554	2.866	1.577	12.22
13	257.70	1711.13	2.722	2.842	1.591	4.41
14	266.20	1719.65	2.607	3.109	1.516	19.26
15	246.66	1610.68	2.682	2.976	1.665	10.63
16	251.44	1641.90	2.772	3.021	1.688	8.98
17	256.92	1695.67	2.651	3.034	1.563	14.44
18	248.95	1618.18	2.633	3.056	1.627	16.07
19	253.37	1654.57	2.447	2.903	1.479	18.64
20	252.21	1664.59	2.691	2.773	1.617	3.05
21	258.72	1684.27	2.770	3.015	1.645	8.84
22	254.60	1654.90	2.765	3.120	1.671	12.84
23	257.41	1681.41	2.575	2.981	1.531	15.77
24	255.21	1653.77	2.642	3,010	1.598	13.93
25	251.35	1611.15	2.775	3.100	1.722	11.71
26	260.68	1702.24	2.615	2.910	1.536	11.28
27	253.32	1641.51	2.687	2.990	1.637	11.28
28	252.88	1679.12	2.631	2.972	1.567	12.96
29	253.85	1637.33	2.605	3.109	1.591	19.35
30	247.98	1631.74	2.770	3.025	1.698	9.20
A.M	254.830	1653.762			1.592	12.386
S.D	4.446	35.038			0.062	3.728
C_v	1.740	2.119			3.890	30.102

TABLE 2.5: COMPRESSIVE STRENGTH OF BRICKS

Sl. No.	Area	Failure load in kg.	Compressive strength in kg/cm^2
1	262.51	77750	296.179
2	256.22	72000	281.008
3	247.92	70000	282.370
4	255.07	71050	278.551
5	255.86	74000	289.221
6	261.64	64750	246.480
7	254.37	57250	225.066
8	258.10	77000	298.334
9	253.48	66500	262.348
10	253.40	54750	216.060
11	250.97	70250	279.914
12	255.46	77000	301.417
13	257.70	80500	312.379
14	266.20	58500	219.760
15	246.66	56500	229.116
16	251.44	72500	288.339
17	256.92	72000	280.265
18	248.95	63250	254.067
19	253.37	83500	329.558
20	252.21	83000	329.090
21	258.72	64500	249.309
22	254.60	68000	267.086
23	257.41	71500	277.770
24	255.21	69500	272.325
25	251.35	59500	236.722
26	260.68	63250	242.635
27	253.32	70250	277.317
28	252.88	57750	228.369
29	253.85	62500	246.208
30	247.98	78500	316.558
A.M.			270.550
S.D			31.778
C_V			11.745

TABLE 2 4 : COMPRESSION TEST ON 7 CM MORTAR CUBES PROPORTION 1:3 BY WEIGHT

Sl.No.	No. of Days of Curing	Failure Load in Kg.	Compressive Stress in kg/cm^2
1	29	12900	258
2	29	12100	242
3	29	11500	230
4	28	12200	244
5	28	11100	222
6	28	12700	254
7	30	10800	216
8	30	10200	204
9	30	11100	222
10	28	11300	226
11	28	13500	270
12	28	12000	240
13	29	10200	204
14	29	10400	208
15	29	11000	220
16	30	11500	230
17	30	11400	228
18	30	12100	242
19	30	12100	242
20	30	10800	216
21	30	11300	226
22	27	12100	242
23	27	10700	214
24	27	11000	220
25	28	11300	226
26	28	10200	204
27	28	10800	216
	Mean		228.37

TABLE 2.5: COMPRESSION TEST ON 7 CM MORTAR CUBES

PROPORTION 1:4 BY WEIGHT

Sl.No.	No. of days of curing	Failure load in kg.	Compressive strength in kg/cm^2
1	29	10100	202.0
2	29	9100	182.0
3	29	9000	180.0
4	30	9500	190.0
5	30	9200	184.0
6	30	8700	174.0
7	28	8500	170.0
8	28	8800	176.0
9	28	9800	196.0
	Mean		183.77

TABLE 2.6 : COMPRESSION TEST ON 7 CM MORTAR CUBES

PROPORTION 1:5 BY WEIGHT

Sl.No.	No. of days of curing	Failure load in Kg.	Compressive strength in kg/cm^2
1	28	3700	74.0
2	28	3200	64.0
3	28	3500	70.0
4	30	4000	80.0
5	30	3100	62.0
6	30	3400	68.0
7	31	3000	60.0
8	31	3100	62.0
9	31	2900	58.0
	Mean		66.444

TABLE 2.7 : COMPRESSION TEST ON 7 CM CUBES

PROPORTION 1:6 BY WEIGHT

Sl.No.	No. of days of curing	Failure load kg.	Compressive stress in kg/cm^2
1	29	2800	56.0
2	29	2700	54.0
3	29	2400	48.0
4	29	2900	58.0
5	29	2750	55.0
6	29	2800	56.0
7	28	2500	50.0
8	28	2200	44.0
9	28	2800	56.0
10	30	2900	58.0
11	30	3100	62.0
12	30	2800	56.0
13	31	2600	52.0
14	31	2800	56.0
15	31	3200	64.0
16	29	2750	55.0
17	28	2400	48.0
18	28	2600	52.0
19	30	2500	50.0
20	30	2700	54.0
21	30	2900	58.0
22	30	3200	64.0
23	30	3000	60.0
24	30	2600	52.0
	Mean		54.916

TABLE 2 8 : COMPRESSION TEST ON 7 CM MORTAR CUBE
PROPORTION 1:8 BY WEIGHT

Sl.No.	No. of days of curing	Failure load in kg.	Compressive strength in kg/cm^2
1	29	1250	25.0
2	29	1400	28.0
3	29	1100	22.0
4	29	1000	20.0
5	29	1150	23.0
6	29	1300	26.0
7	30	1200	24.0
8	30	1150	23.0
9	30	1050	21.0
	Mean		23.555

TABLE 2.9: CALCULATION OF STRESS AND STRAIN FOR ONE PRISM SPECIMEN OF TYPE H IN 1:3 MORTAR

Sl. No.	Load in tonnes	Stress in kg/cm²	Deflection of rubber sheet corresponding to stress in col.(3) in mm	Reading of dial gauge for test assembly in mm	Deflection of test assembly in mm	Net deflection of prism in mm (6)-(4)	Strains x 10^{-4} corresponding to stress in Col.(3)	Assumed strains x10-4	Interpolated stress in kg/cm² for strain in(9)
(1)	(2)	(3)	(4)	(5)	(6)	(7)	(8)	(9)	(10)
1	0.00	0.000	0.00	6.39	0.00	0.00	0.00	1	1.289
2	1.00	0.794	0.10	6.58	0.19	0.09	0.63	2	2.629
3	5.00	3.968	0.50	7.32	0.93	0.43	3.00	3	3.968
4	10.00	7.936	0.97	8.14	1.75	0.78	5.45	4	5.588
5	15.00	11.905	1.30	8.72	2.33	1.03	7.20	5	7.208
6	20.00	15.873	1.56	9.13	2.74	1.18	8.25	6	9.183
7	25.00	19.841	1.75	9.47	3.08	1.33	9.30	7	11.452
8	27.50	21.825	1.82	9.63	3.24	1.42	9.94	8	14.929
9	30.00	23.809	1.92	9.79	3.40	1.48	10.35	9	18.706
10	32.50	25.994	2.00	9.97	3.58	1.58	11.05	10	22.116
11	35.00	27.777	2.07	10.30	3.91	1.84	12.87	11	25.651
12	37.50	29.762	2.14	10.62	4.23	2.09	14.60	12	26.829
13	40.00	31.746	2.20	11.03	4.64	2.44	17.05	14	29.074
14	42.50	33.730	2.26	11.22	4.83	2.57	18.00	16	30.810
15	45.00	35.714	2.33	-	-	-	-	18	33.730
16	47.50	37.698	2.39	-	-	-	-	20	33.730
17	50.00	39.683	2.45	-	-	-	-	25	33.730

TABLE 2.10: COMPRESSIVE STRENGTH OF BRICK PRISM TYPE H

Sl. No.	Mortar mix	Compressive Strength in kg/cm^2 Sample No.						Mean value
		1	2	3	4	5	6	
1	1:3	35.714	42.857	41.667	42.857	37.698	*	40.159
2	1:4	27.778	32.738	31.746	30.357	31.746	34.524	31.482
3	1:5	25.794	27.778	29.762	29.762	27.778	30.952	28.638
4	1:6	26.825	21.429	26.587	26.190	26.984	*	25.603
5	1:8	20.238	27.222	16.508	22.222	*	*	21.548

TABLE 2.11: COMPRESSIVE STRENGTH OF BRICK PRISM TYPE V

Sl. No.	Mortar Mix	Compressive Strength in kg/cm^2 Sample No.						Mean Value
		1	2	3	4	5	6	
1	1:3	31.746	33.730	29.762	42.460	35.714	39.683	35.516
2	1:4	22.222	29.762	29.762	30.555	21.826	32.540	27.778
3	1:5	14.286	14.683	17.659	16.071	17.063	18.650	16.402
4	1:6	13.492	15.159	18.651	10.714	16.270	*	14.857
5	1:8	6.825	8.730	9.127	*	*	*	8.227

* Broken during handling i.e. transporting from curing site to the Universal Testing Machine.

TABLE ?.12: MODULUS OF ELASTICITY OF BRICK PRISMS TYPE H

Specimen number	Secent Modulus in $kg/cm^2 \times 10^4$ at percentage of mean compressive stress				
	10	20	40	60	80
Mortar mix 1:3					
1	1.323	1.457	1.924	2.300	1.862
2	1.418	1.536	2.736	3.662	4.372
3	1.418	1.383	1.783	2.267	2.685
4	1.418	1.554	2.248	2.861	3.488
5	1.383	1.367	1.907	2.467	2.701
Mortar mix 1:4					
1	0.908	1.007	1.645	1.855	1.543
2	1.091	1.143	1.756	1.654	1.482
3	1.342	1.408	1.855	2.006	1.492
4	1.124	1.176	1.657	1.757	1.613
5	1.115	1.134	1.543	1.578	1.575
6	0.966	0.990	1.478	1.514	1.249
Mortar mix 1:5					
1	0.823	1.042	1.514	1.342	1.167
2	0.912	0.934	1.146	1.267	1.085
3	0.857	0.914	1.312	1.214	0.986
4	0.842	0.872	1.356	1.425	1.384
5	0.861	0.965	1.524	1.617	0.727
6	0.868	0.811	0.914	0.695	**

** Strain measuring dial gauge was removed before reaching 80 percent average stress.

Table contd...on page 68

Table 2.12 contd...

Specimen number	Secant modulus in kg/cm^2 x 10^4 at percentage of mean compressive stress				
	10	20	40	60	80
Mortar mix 1:6					
1	0.798	0.806	0.902	0.938	0.855
2	0.699	0.759	1.210	1.493	0.755
3	0.521	0.600	0.702	0.632	**
4	0.846	0.852	1.027	1.229	1.246
5	0.747	0.772	1.037	1.112	0.845
Mortar mix 1:8					
1	0.510	0.523	0.732	0.625	**
2	0.516	0.571	0.766	0.815	0.727
3	0.726	0.731	0.841	0.855	0.820
4	0.732	0.782	0.829	0.873	0.805

** Strain measuring dial gauge was removed before reaching 80 percent average stress.

TABLE 2.13: MODULUS OF ELASTICITY OF BRICK PRISMS TYPE V

Specimen number	Secent modulus in kg/cm^2 x 10^4 percentage of mean compressive stress				
	10	20	40	60	80
Mortar mix 1:3					
1	1.526	1.373	1.575	1.580	1.197
2	1.628	2.377	3.691	3.674	2.081
3	3.055	3.060	3.752	3.065	**
4	1.952	3.153	4.372	4.694	2.621
5	3.296	3.817	5.357	3.763	2.621
6	4.278	3.693	3.246	3.829	4.085
Mortar mix 1:4					
1	1.914	1.981	1.869	1.406	**
2	0.956	1.236	1.674	1.435	1.112
3	0.878	0.980	1.295	1.314	1.005
4	0.765	1.036	1.411	1.173	1.044
5	2.816	2.724	2.549	1.098	**
6	1.627	1.806	2.201	2.153	2.101
Mortar mix 1:5					
1	1.713	1.752	1.801	1.811	1.924
2	1.514	1.601	1.623	1.610	1.426
3	1.362	1.371	1.412	1.394	1.012
4	1.028	1.029	1.124	1.216	1.314
5	1.276	1.314	1.213	1.189	0.784
6	1.107	1.100	1.217	1.312	**

** Strain measuring dial gauge was removed before reaching 80 percent average stress.

Table contd..on page 70

Table 2.13 contd...

Specimen number	Secant modulus in $kg/cm^2 \times 10^4$ at percentage of mean compressive stress				
	10	20	40	60	80
Mortar mix 1:6					
1	0.558	0.662	0.643	0.675	0.637
2	1.067	1.277	1.237	0.977	0.882
3	1.408	1.374	1.640	1.800	1.984
4	1.487	0.575	0.401	0.339	**
5	1.073	1.050	1.317	1.858	1.846
Mortar mix 1:8					
1	0.269	0.268	0.325	0.298	**
2	0.260	0.260	0.306	0.263	0.233
3	0.265	0.265	0.301	0.263	0.216

** Strain measuring dial gauge was removed before reaching 80 percent average stress.

TABLE 2.14: MAXIMUM RESISTANCE TO DIAGONAL TENSION IN REINFORCED BRICK BEAMS

Specimen Number	Maximum total load in kg.	Maximum deflection at mid point in mm	Maximum shear stress as diagonal tension kg/cm^2
	Mortar Mix 1:3	Modular ratio 80	
1	7292.516	1.81	5.567
2	8625.850	1.70	6.584
3	9306.122	1.98	7.104
Mean	8408.163	1.83	6.418
	Mortar mix 1:4	Modular ratio 100	
1	6893.424	2.10	5.261
2	8163.265	1.70	6.230
3	8163.265	1.78	6.230
Mean	7739.985	1.86	5.907
	Mortar mix 1:5	Modular ratio 160	
1	4136.054	0.910	3.145
2	4952.381	1.290	3.766
3	3918.367	1.050	2.980
Mean	4335.601	1.083	3.297
	Mortar mix 1:6	Modular ratio 200	
1	2802.721	1.340	2.124
2	3401.360	1.200	2.577
3	2993.197	1.460	2.268
Mean	3065.759	1.333	2.323
	Mortar mix 1:8	Modular ratio 200	
1	2476.190	1.65	1.876
2	2721.088	1.60	2.062
2	2938.775	1.70	2.227
Mean	2712.018	1.65	2.055

TABLE 2.15: COMPRESSION TEST ON 15CM CONCRETE CUBE

Sl.No.	Number of days of curing	Failure load in kg.	Compressive strength in kg/cm^2
1	30	46500	206.667
2	30	45500	202.222
3	30	48500	215.555
4	28	47000	208.889
5	28	47500	211.111
6	28	47000	208.889
7	28	47500	211.111
8	28	45500	202.222
9	28	46500	206.667
10	27	46000	204.440
11	27	48000	213.330
12	27	47500	211.111
13	29	47500	211.111
14	29	45000	200.000
15	29	45500	202.222
16	29	46000	204.444
17	29	47000	208.889
18	29	45500	202.222
19	23	47000	208.889
20	28	46500	206.667
21	28	44500	197.778
22	30	47500	211.111
23	30	45000	200.000
24	30	45500	202.222
25	27	44500	197.778
26	27	47000	208.889
27	27	47500	211.111
28	29	45000	200.000
29	29	44000	195.556
30	29	44500	197.778

Table contd... on page

Table 2.15 contd...

Sl.No.	Number of days of curing	Failure load in kg.	Compressive strength in kg/cm^2
31	29	46000	204.444
32	29	45000	200.000
33	29	47000	208.889
34	28	44500	197.778
35	28	46000	204.444
36	28	47000	208.889
37	30	46500	206.667
38	30	47500	211.111
39	30	46000	204.444
40	28	47000	208.889
41	28	45500	202.222
42	28	47500	211.111
43	28	46000	204.444
44	28	46500	206.667
45	28	45000	200.000
46	29	47500	211.111
47	29	48000	213.333
48	29	46000	204.444
49	27	45500	202.222
50	27	46000	204.444
51	27	46500	206.667

Mean = 205.621 kg/cm^2

TABLE 2.16: SPLIT TEST ON C NCRETE CYLINDERS FOR TENSILE STRENGTH OF CONCRETE

Size of cylinder = 15 cm dia and 30 cm long

Sl.No.	No.of days of curing	Failure load P in kg.	Tensile strength in $kg/cm^2 = \frac{2P}{\pi d l}$
1	28	18000	25.465
2	28	19500	27.587
3	28	17500	24.757
4	28	18500	26.172
5	28	17000	24.050
6	28	18500	26.172
7	28	17500	24.757
8	28	18000	25.465
9	28	19000	26.880
10	28	19000	26.880
11	28	17000	24.050
12	28	17500	24.757
Mean			25.582

TABLE 2.17: TENSILE STRENGTH TEST RESULTS OF REINFORCEMENT

Sl. No.	Nominal diameter of bar in mm	Actual mean dia of bar in mm	Actual area of bar in mm^2	Yield load in kg.	Yield stress in kg/mm^2	Ultimate load in kg.	Ultimate tensile strength in kg/mm^2	Percentage Elongation
1	6	5.94	27.712	800	28.87	1200	43.300	36.7
2	6	5.91	27.432	840	30.62	1210	44.110	35.4
3	6	6.00	28.274	830	29.35	1210	42.795	22.9
Mean					29.615		43.40	31.66
4	8	8.10	51.530	1550	30.080	2415	46.860	19.5
5	8	8.08	51.276	1650	32.179	2480	48.366	24.6
6	8	8.08	51.276	1550	30.229	2470	48.170	22.3
Mean					30.829		48.465	22.13
7	10	9.26	67.346	2050	30.440	2950	43.80	29.4
8	10	9.64	72.987	2150	29.457	3150	43.16	31.3
9	10	9.60	72.382	2200	30.392	3100	42.83	32.4
Mean					30.096		43.262	31.03
10	12	12.12	115.371	3400	29.470	5150	44.64	28.5
11	12	12.14	115.752	3300	28.509	5300	45.79	27.3
12	12	12.10	114.990	3150	27.393	5400	46.96	29.8
Mean					28.457		45.796	28.53
13	16	15.84	197.061	5750	29.179	9500	48.21	24.6
14	16	15.92	199.056	5800	29.137	9200	46.22	25.3
15	16	15.92	199.056	5700	28.635	9400	47.22	27.5
Mean					29.187		47.22	25.8
				Mean	29.637	Mean	45.628	

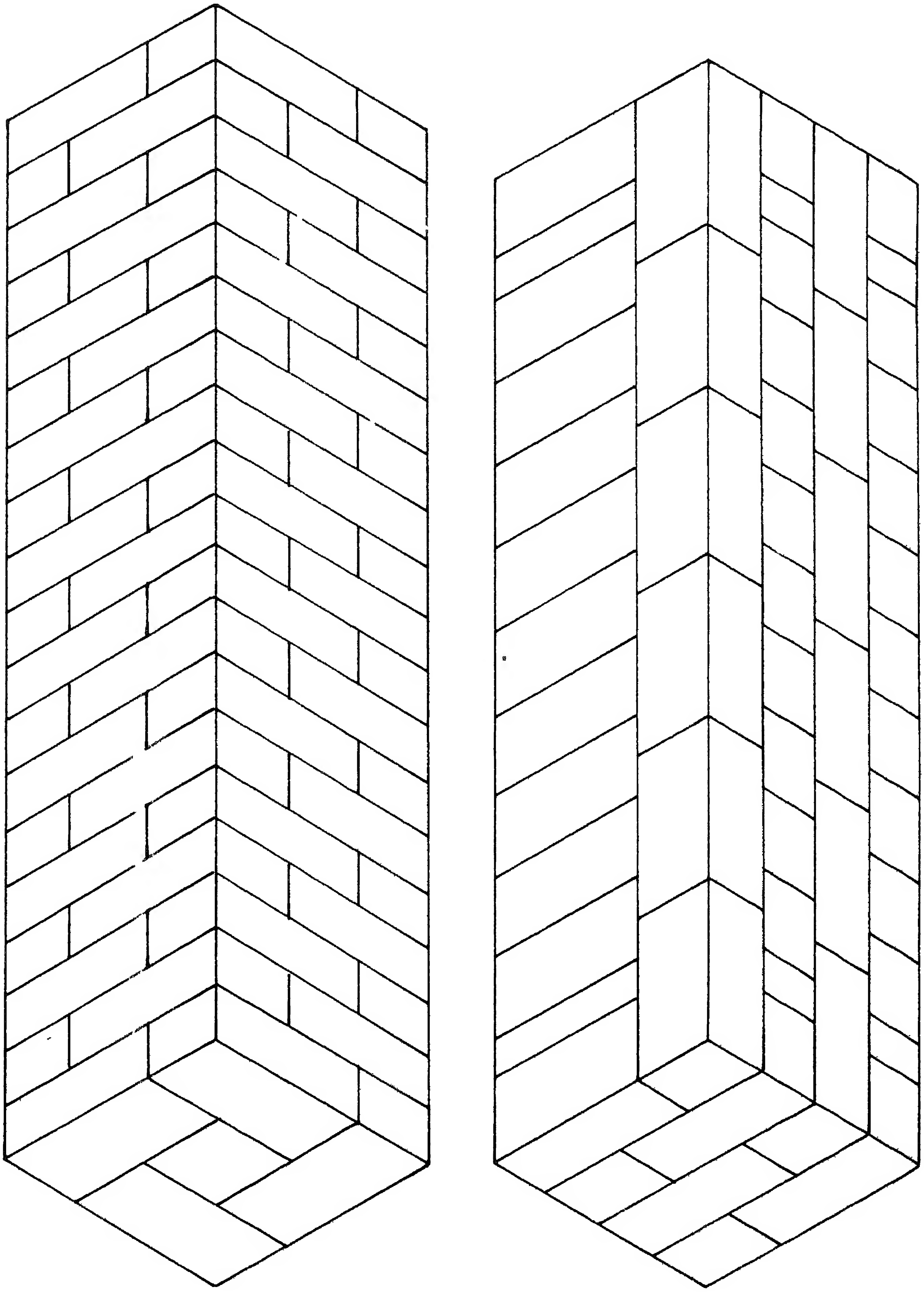

Fig. 2·1 Arrangement of brick layers in brick prisms

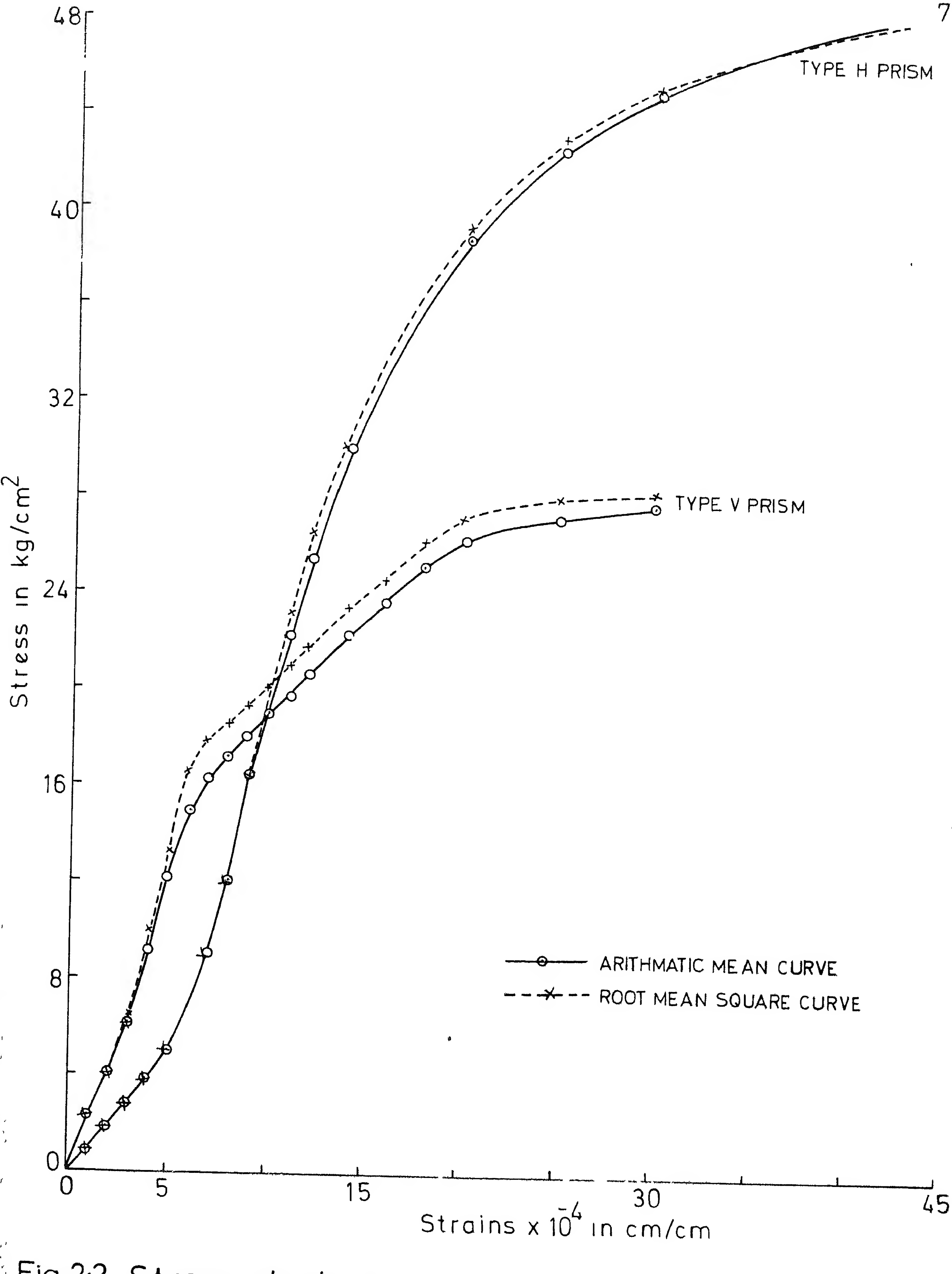

Fig.2·2 Stress-strain curve for brick prisms in 1:6 mortar

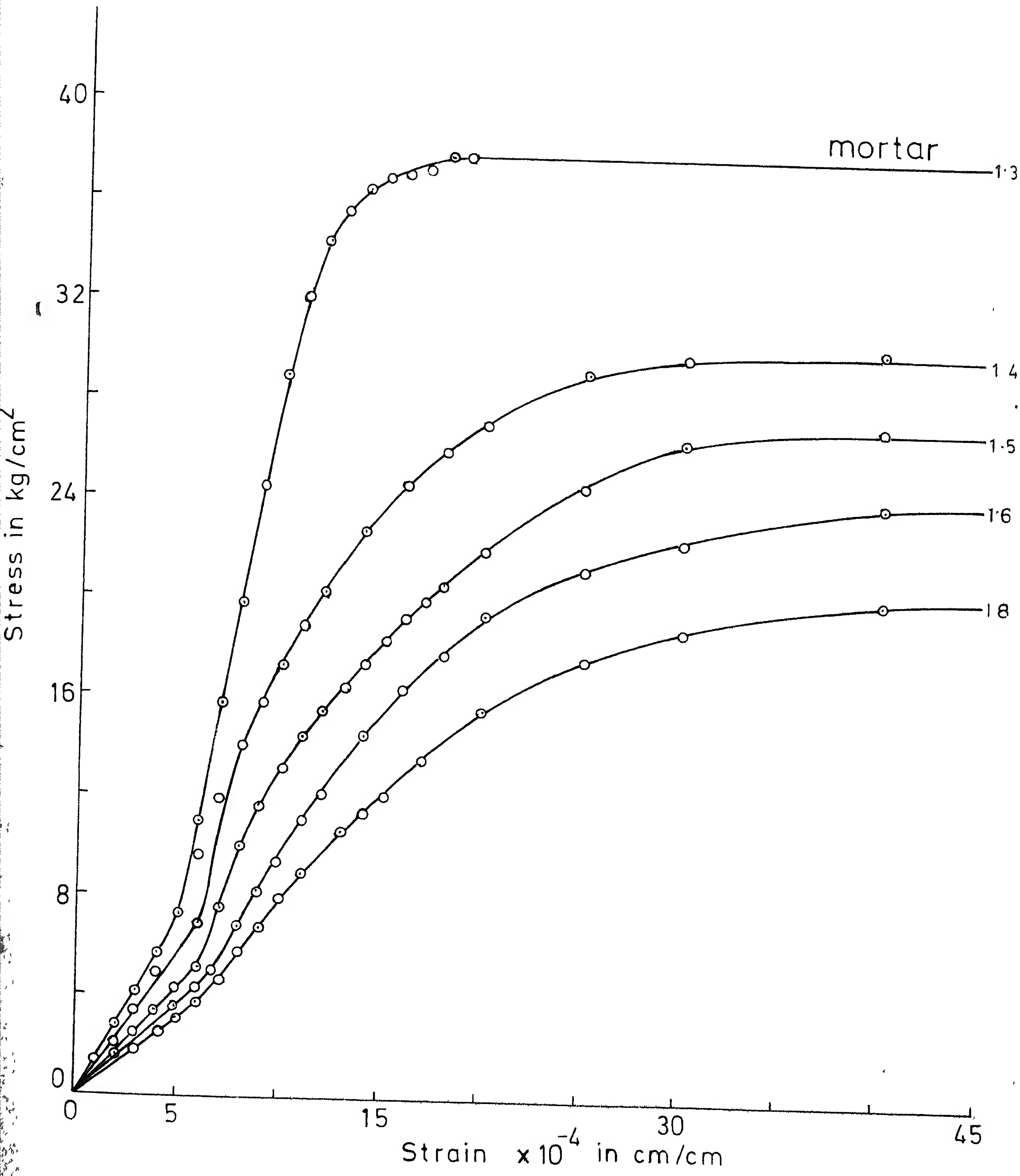

Fig. 2·3 Stress-strain curve of brick work for type H prism

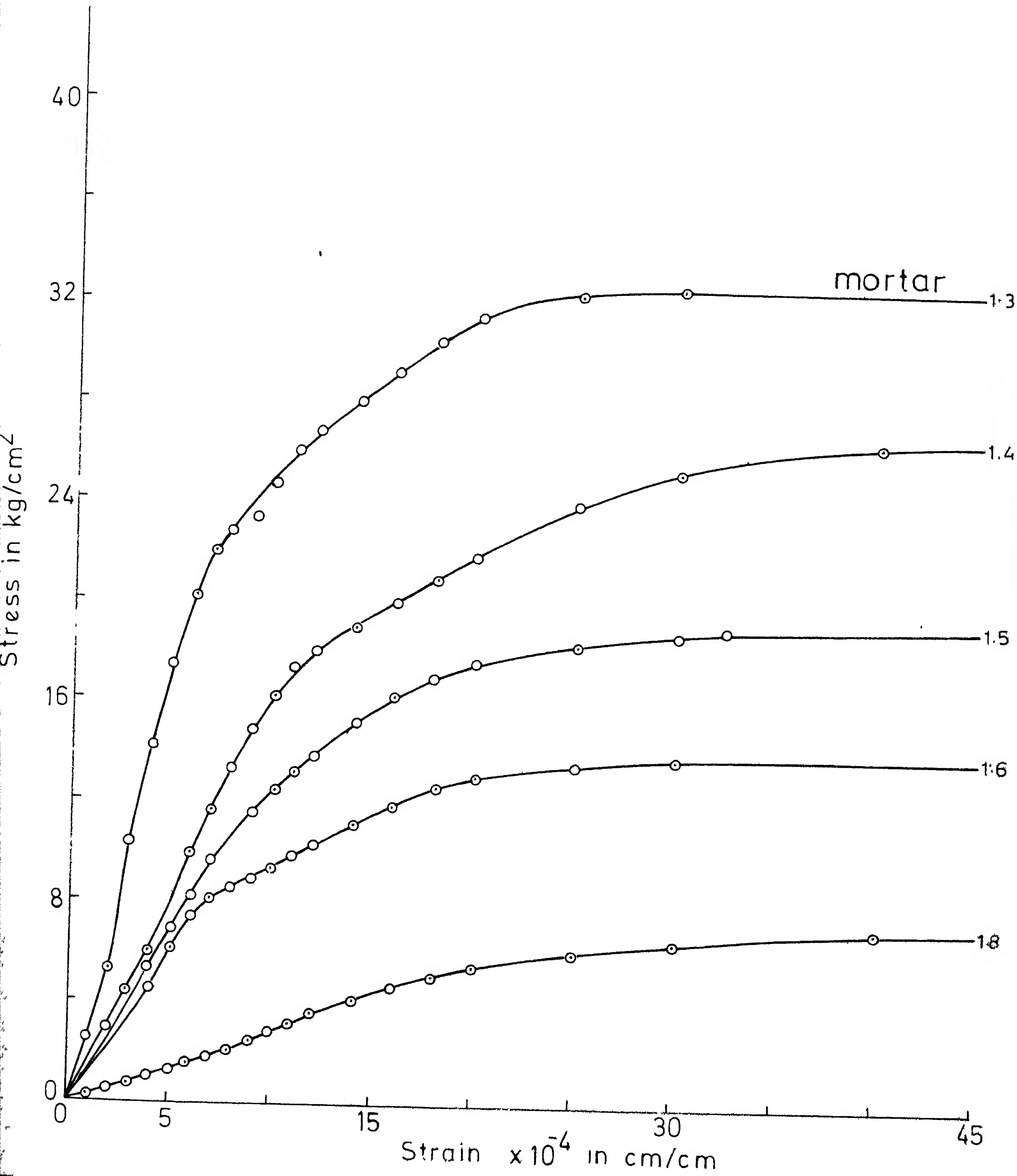

Fig 2·4 Stress-strain curve of brick work for type V prism

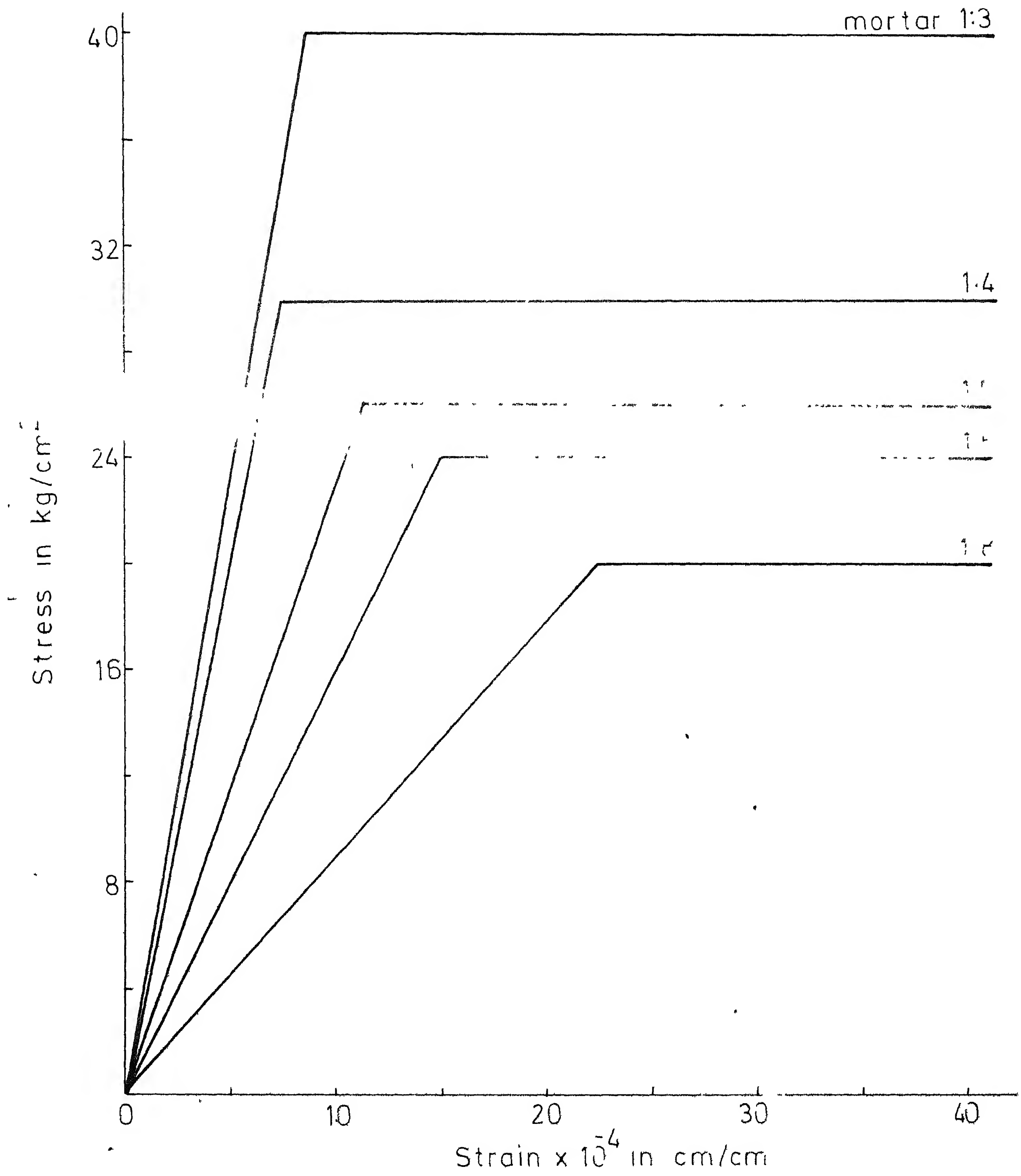

Fig. 2·5 Idealised stress-strain curves of brickwork for type H prisms

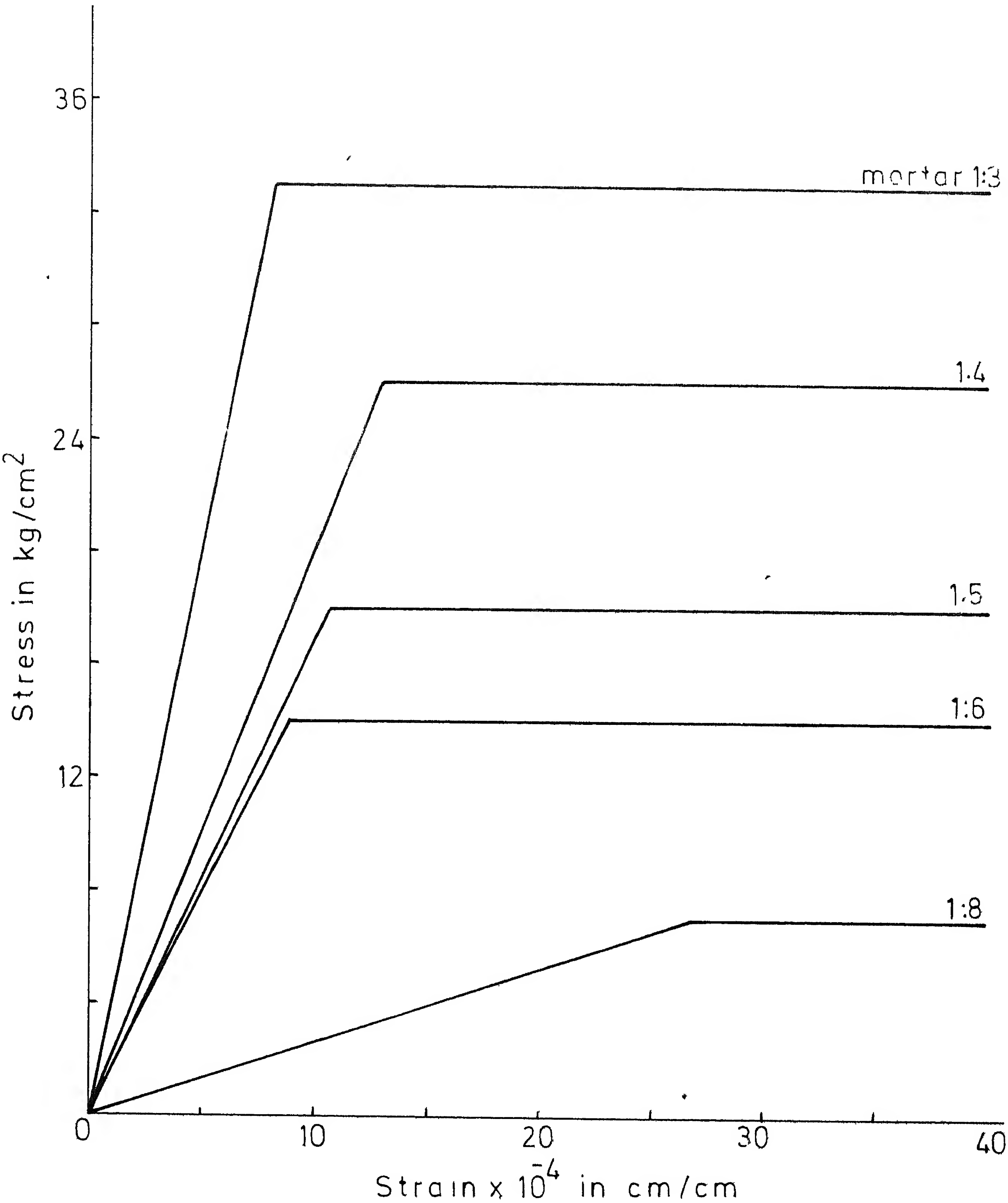

Fig. 2·6 Idealised stress-strain curves of brickwork for type V prisms

Fig. 27 Loading arrangement and failure pattern

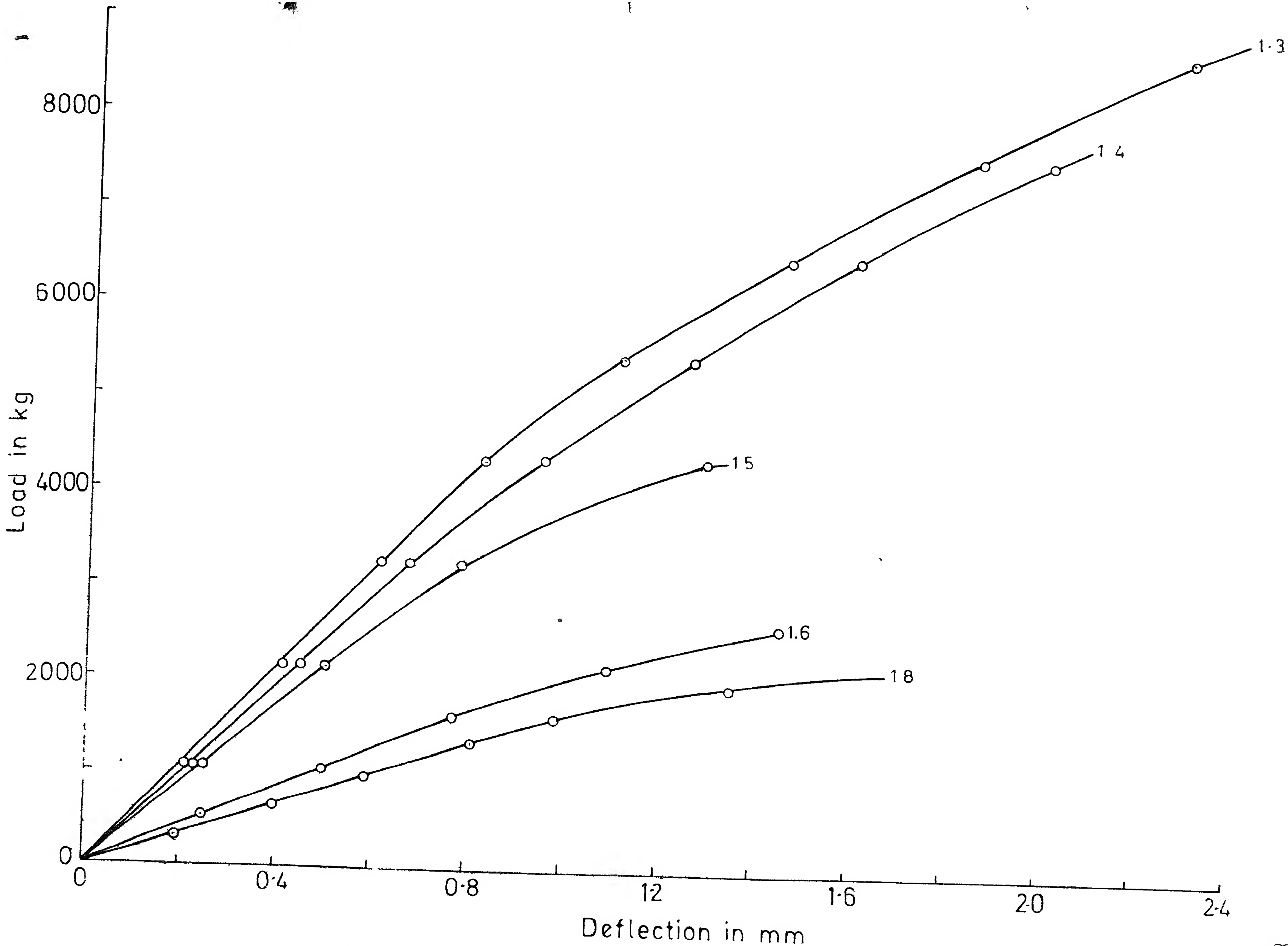

Fig.2·8 Load versus deflection curves for

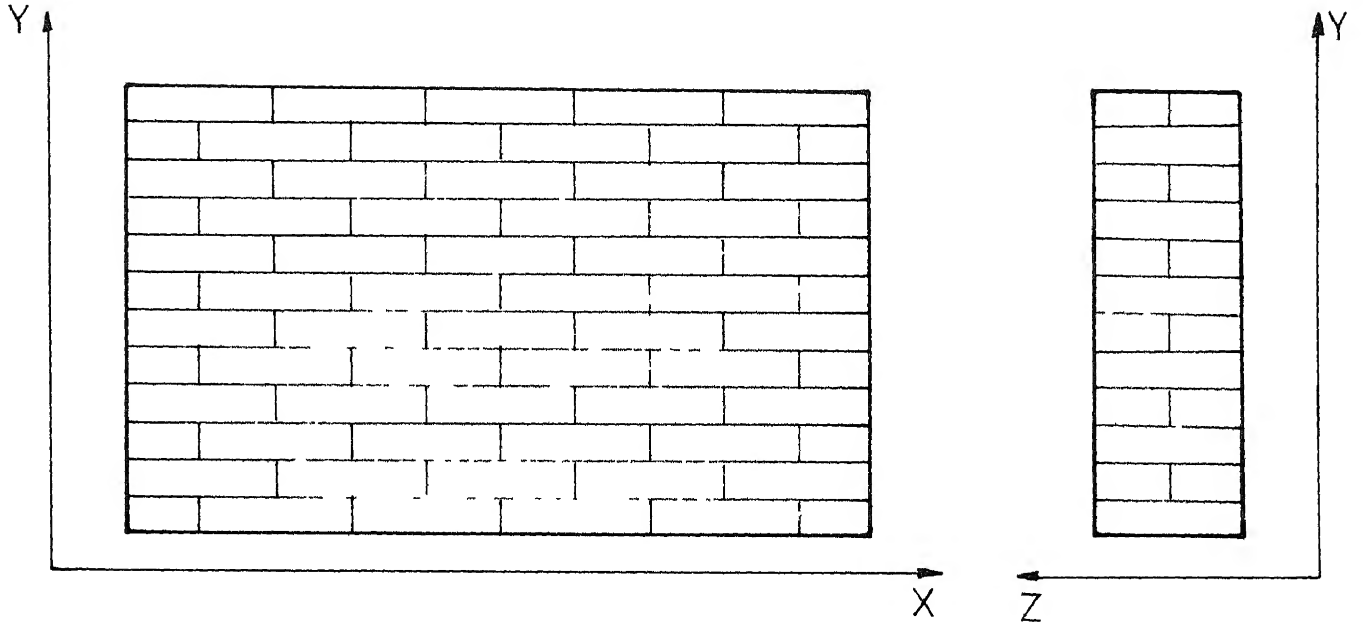

Fig. 2·9 Brickwork element in Global coordinate system

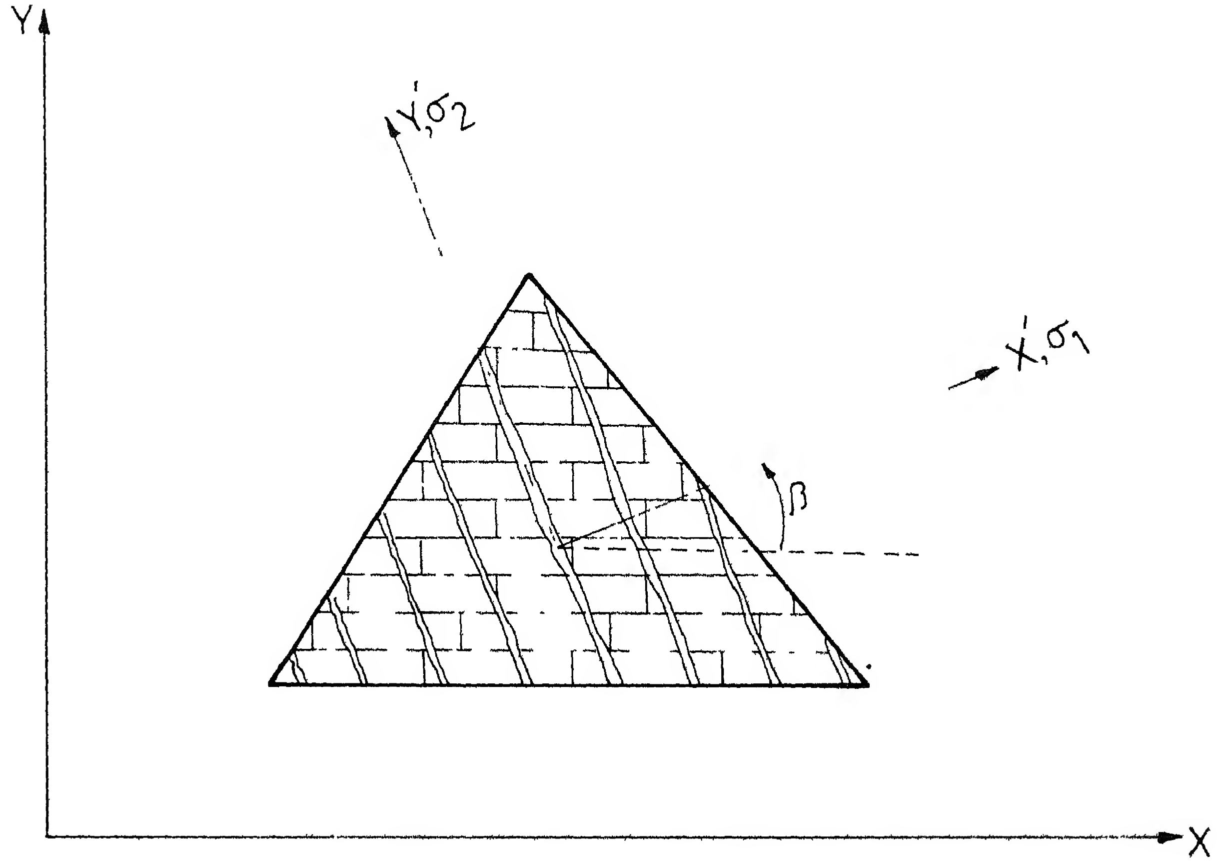

Fig. 2·10 Cracked brickwork element

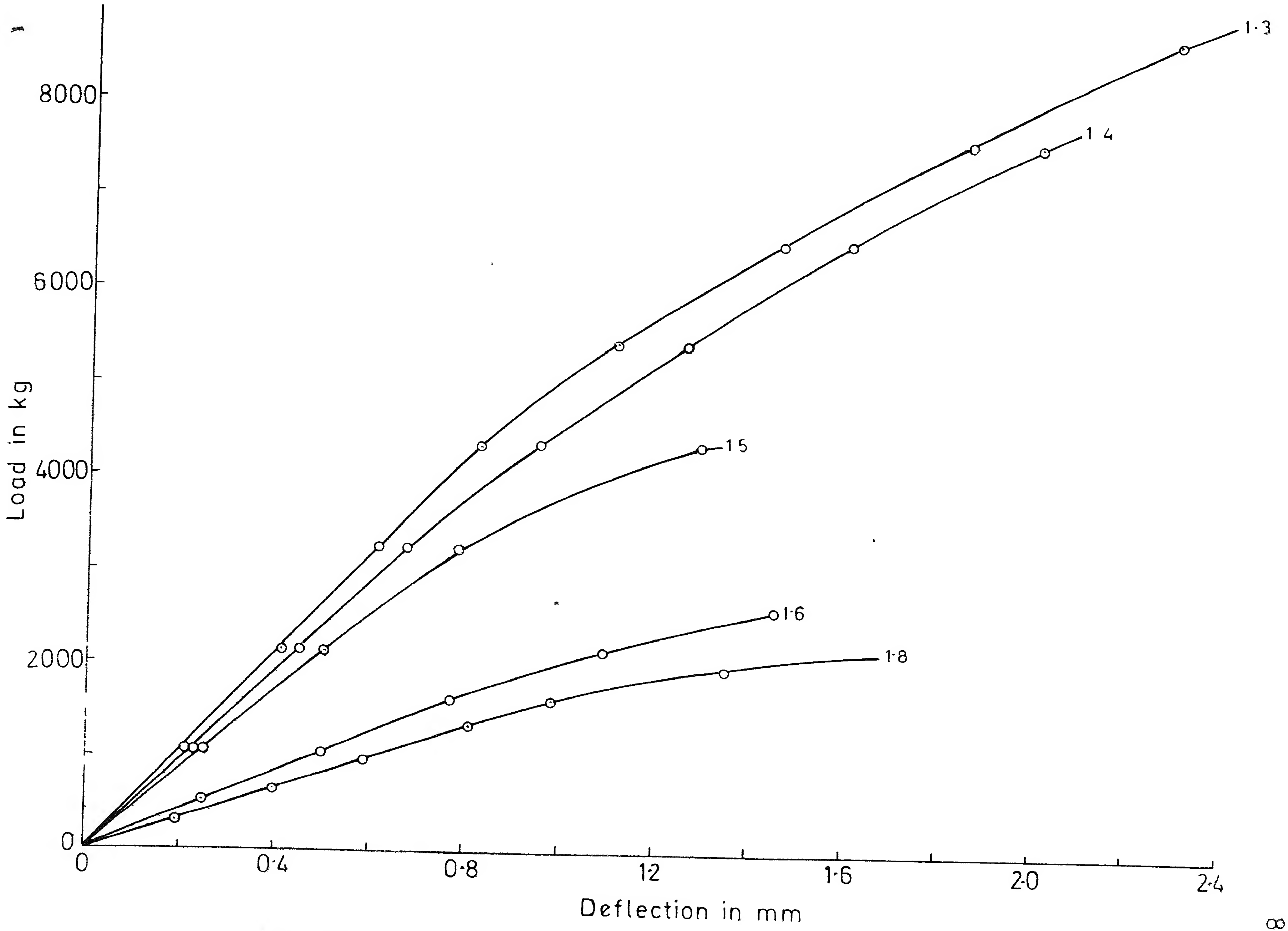

Fig.2·8 Load versus deflection curves for RBM beams

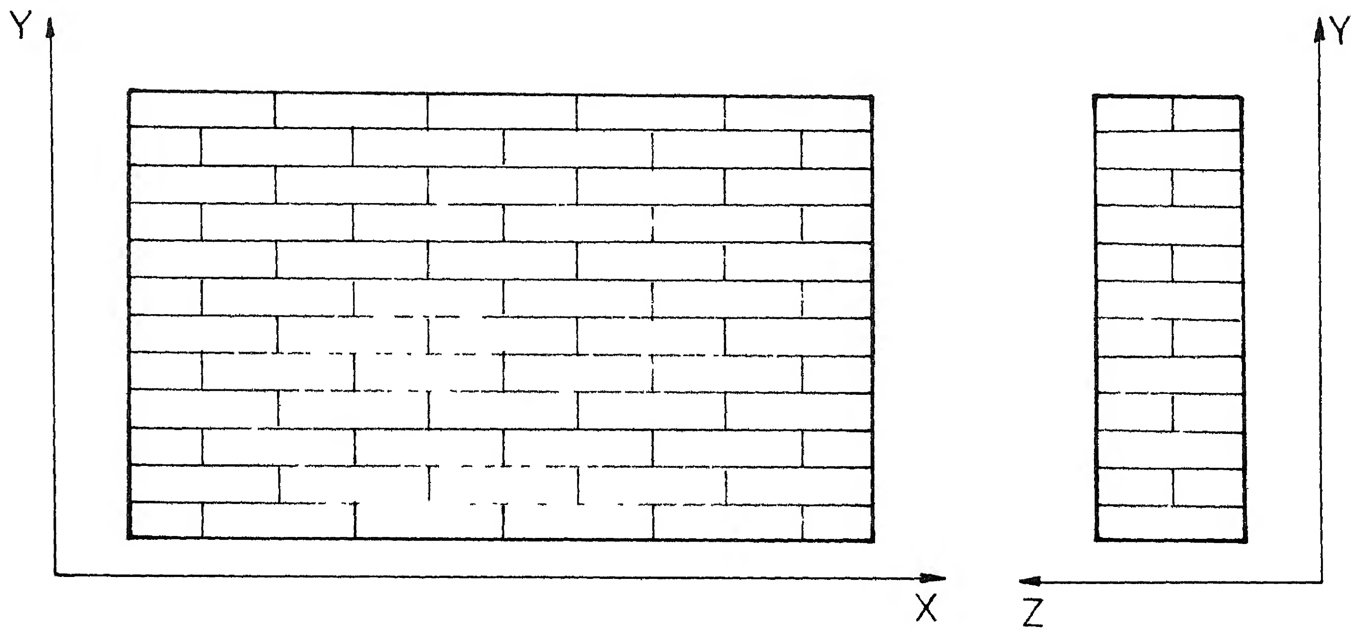

Fig. 2·9 Brickwork element in Global coordinate system

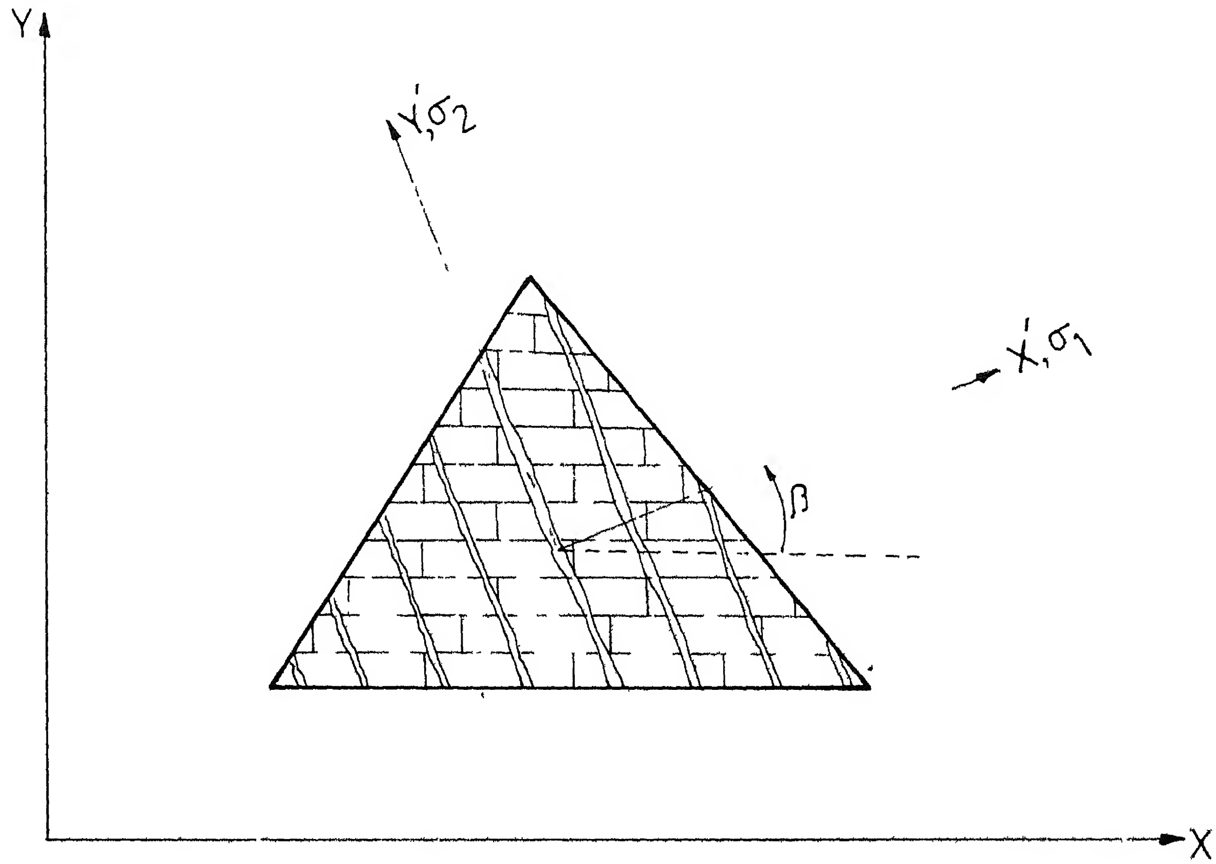

Fig. 2·10 Cracked brickwork element

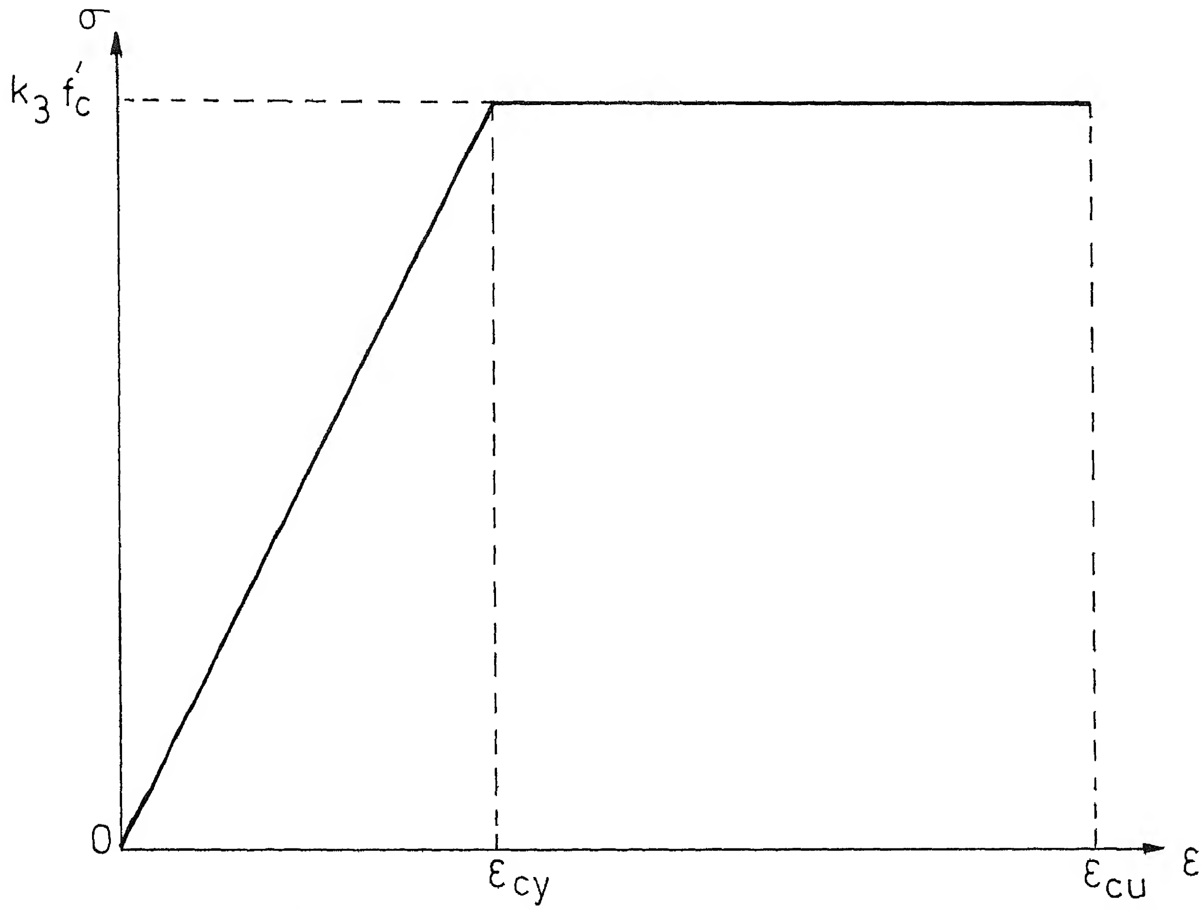

Fig. 2·11 Bilinear stress-strain curve for concrete

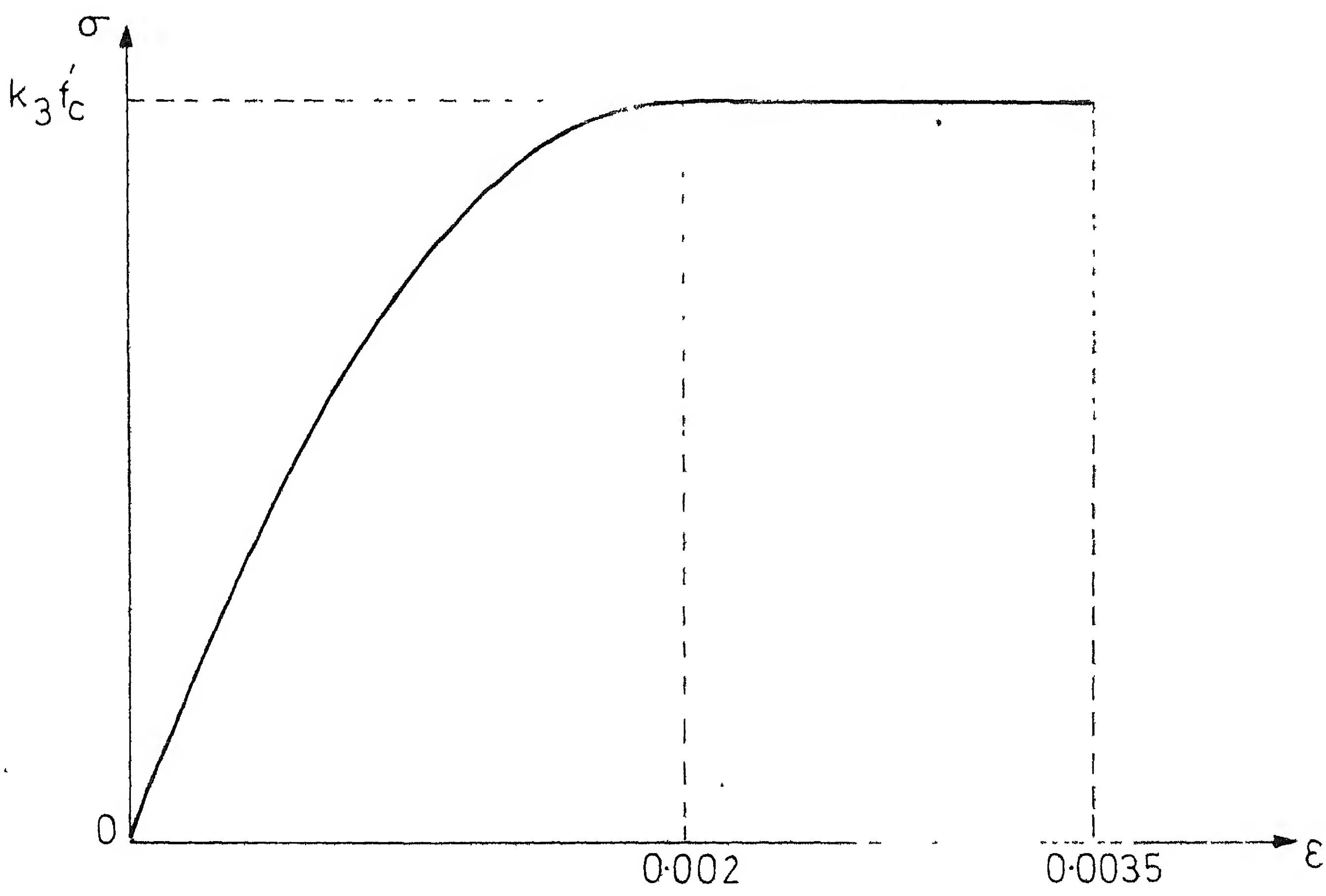

Fig. 2·12 Parabola rectangle stress-strain curve for concrete

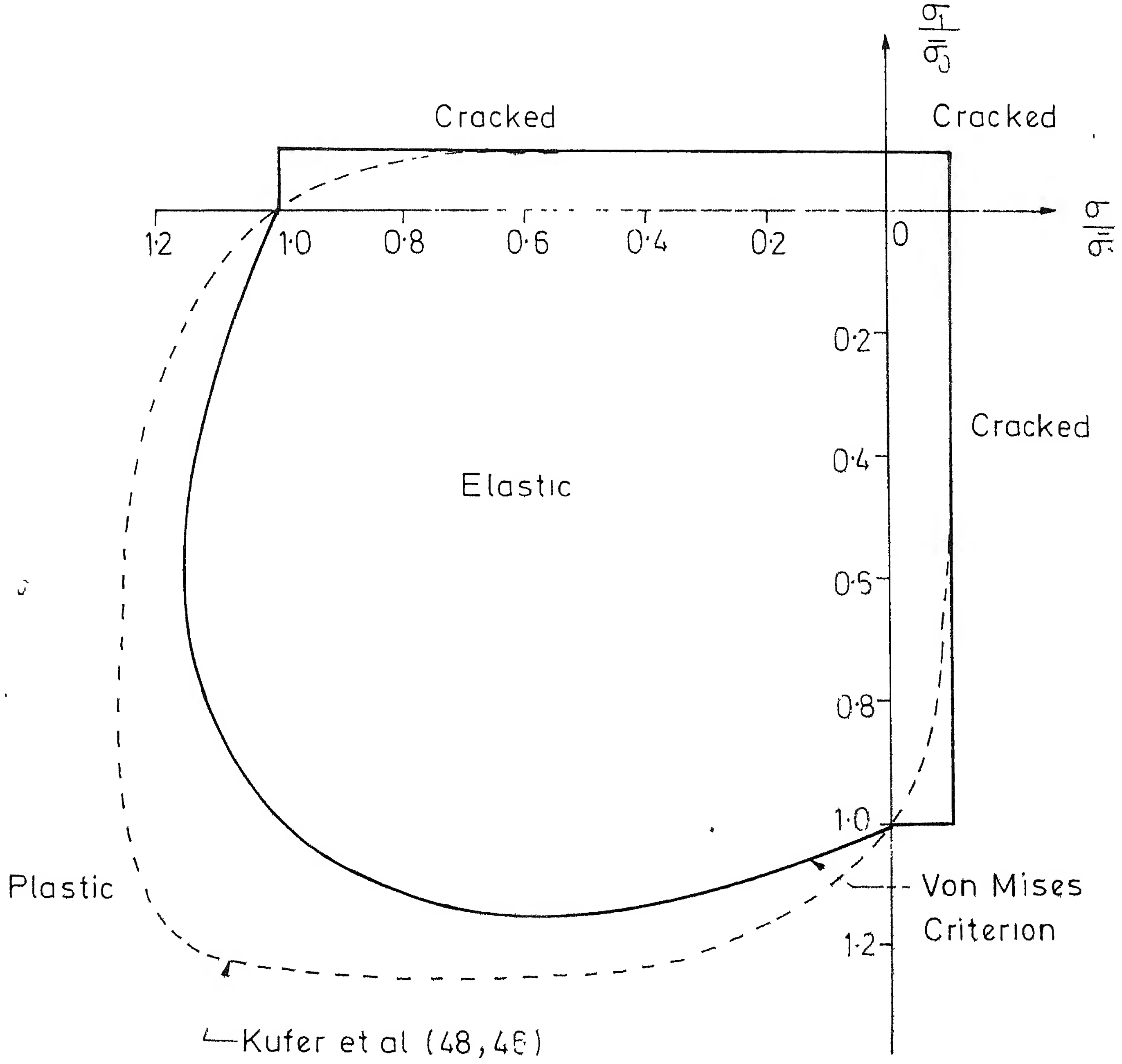

Fig.2·13 Biaxial strength envelope of concrete

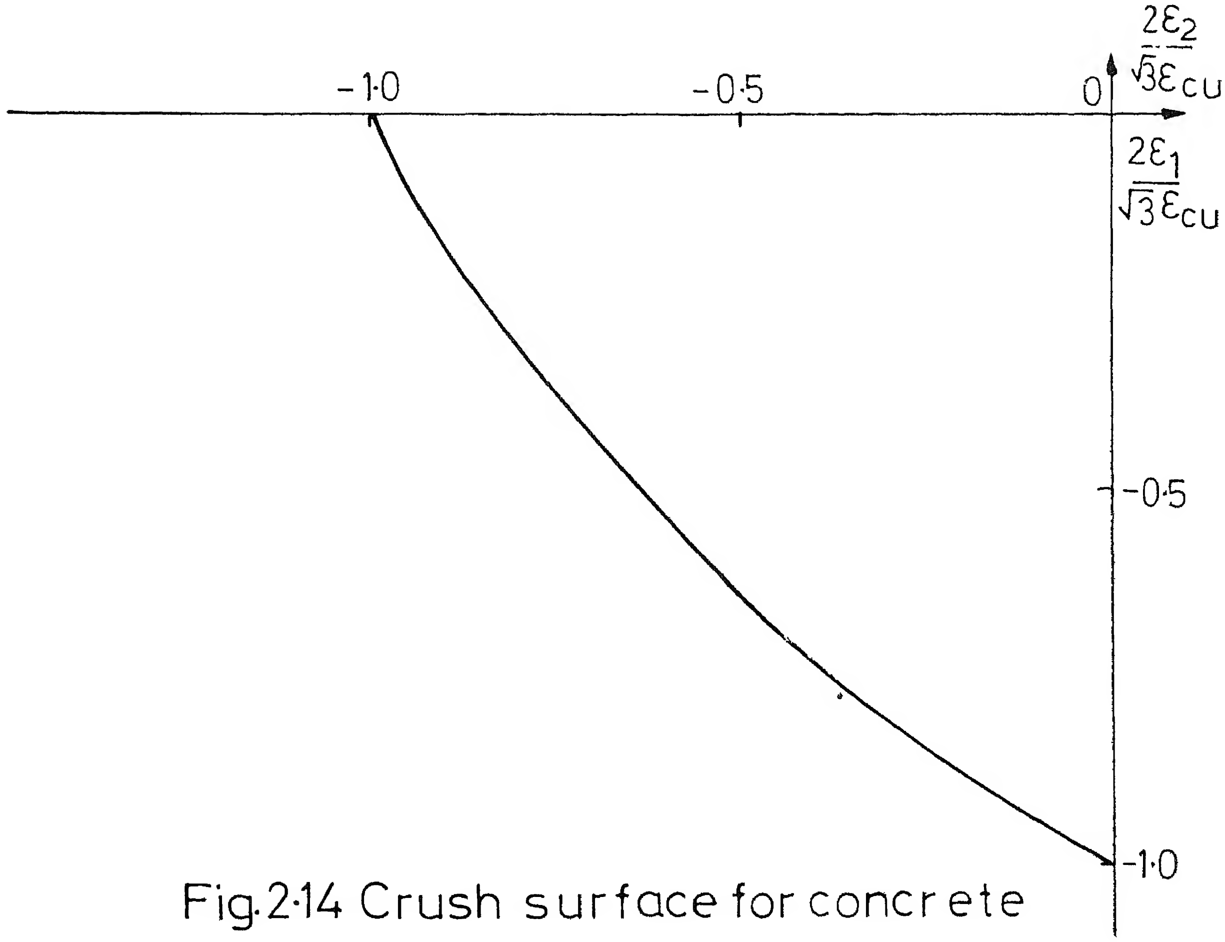

Fig. 2·14 Crush surface for concrete

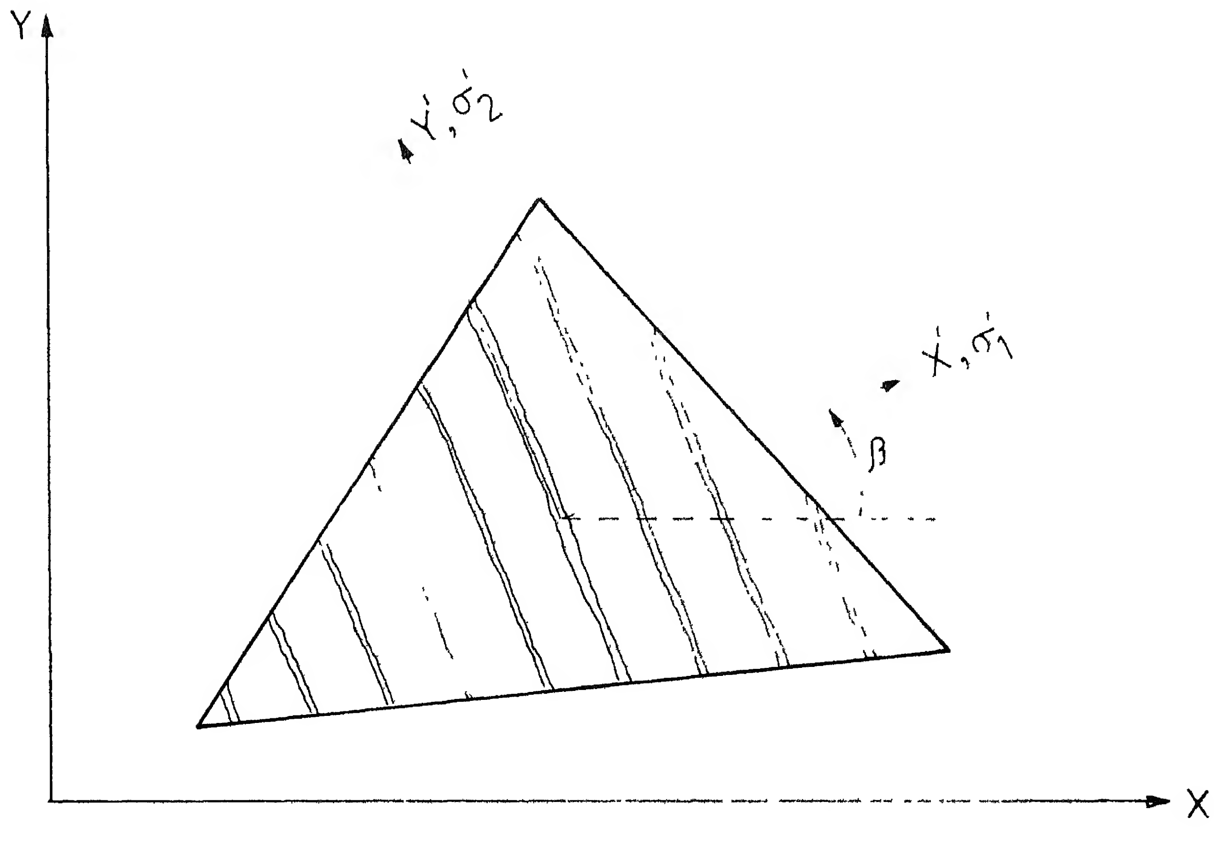

Fig. 2·15 Cracked concrete element

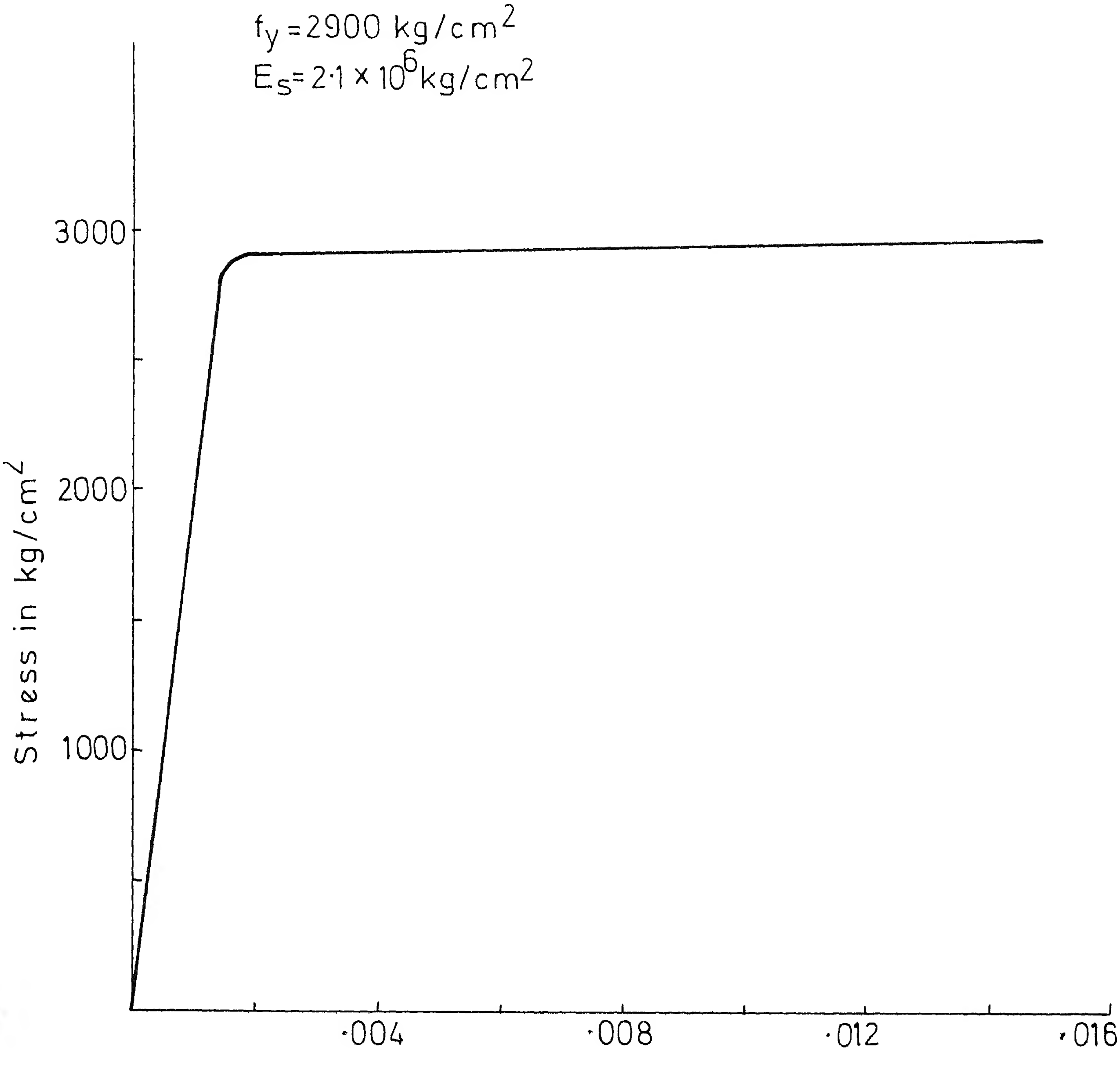

Fig. 2·16 Stress-strain curve for steel

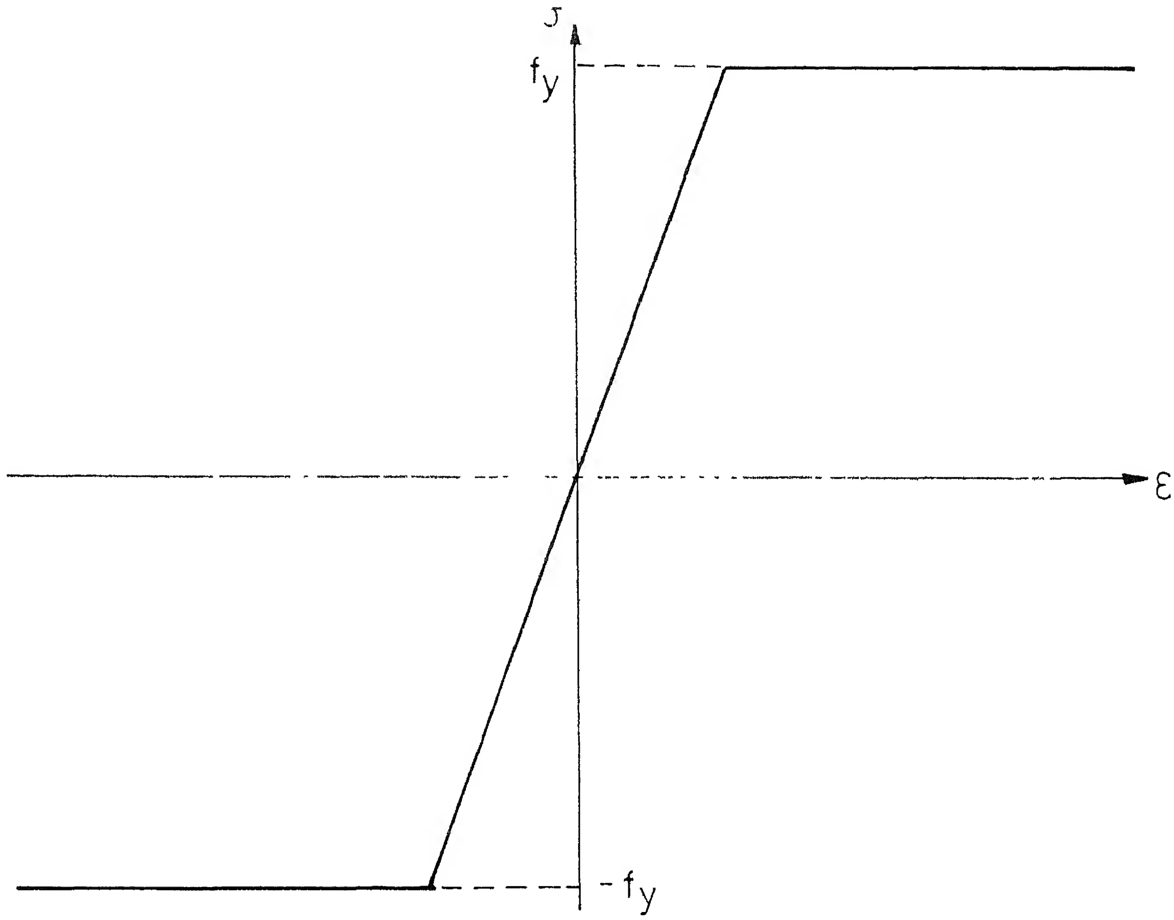

Fig.2.17 Idealised stress-strain curve for steel

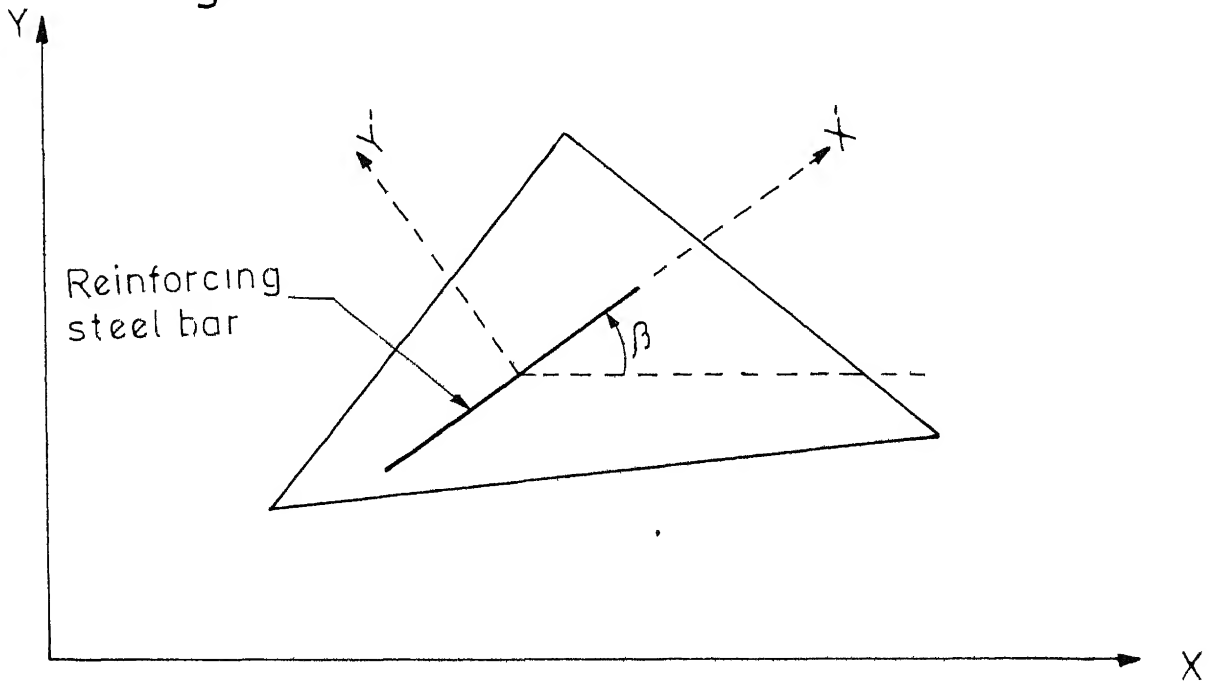

Fig.2.18 Local and Global coordinates for framing constitutive matrix for reinforcing steel

CHAPTER III

EXPERIMENTAL INVESTIGATION

Earlier investigators have reported that no interaction takes place between the brick masonry supported on R.C. beams if the height to span ratio is below 0.5 and the inplane load is applied on the top of brickwork. Furthermore, no interaction is reported for such composite construction, if the inplane load is applied at the junction of brickwork and R.C. beam for any height to span ratio, whatsoever. Wood (7) has suggested for the latter case the use of suitable tensile connectors for the interaction to come into play. Moreover, the general recommendation is that the benefit of such interaction should only be availed, if the brickwork is cast in rich mortars, viz. 1:3. The experimental investigation of interaction between the brick masonry and R.C. beam supporting it, using single legged Z shaped connectors, is the subject matter of study in the present chapter. In other words, composite behaviour of such a construction is experimentally observed for two types of inplane loading on the system mentioned above and for cases (1) of different mortar strength by proportioning its cement sand ratio, (2) of varying height to span ratio of the structure and (3) of different size and location of openings

in the brickwork which is reported herein.

3.1 PREPARATION OF TEST SPECIMEN

3.1.1 Reinforced Concrete Beams

The reinforced concrete beams have been cast in wooden moulds prepared for the purpose. Figs. 3.1(a) and 3.1(b) show respectively the details of wooden moulds used for casting the beams for (i) compressive loading (ii) tensile loading. The size of R.C. beams is kept as 325 cm long, 24 cm wide and 8 cm thick in most cases. Changes in thickness of the beam, if any, are discussed for particular cases. Bending reinforcement in beams consisted of 3 plain round mild steel bars. Diameter of bars varies of course based on height to span ratio. Single legged Z shaped vertical connectors, thirteen in number, were embedded in all concrete beams along their length at a uniform spacing of 25 cm centre to centre according to the modular size of the bricks used in the present work . Limited experimentation has been carried out by varying the size and spacing of the vertical connectors. Beams used for tensile loading had mild steel flats embedded in it all along the length of beam, at a uniform spacing of 25 cm centre to centre, to facilitate the loading arrangement. The mild steel flats were 35 cm long 8 cm wide and 1 cm thick. They were embedded just at the top of concrete. Each mild steel flat

had two 25 mm dia holes at their ends, 30 cm centre to centre. Thus 12 such flats were embedded in each beam. Figures 3.2(a) and 3.2(b) show respectively the beams used for compressive and tensile loading. The beams were cured by putting the moist empty gunny cement bags over it for a period of 4 to 6 days before removing them from moulds. However, the sides of moulds were removed after 24 hours only. After removing the beams from mould, they were kept supported at four points and curing was continued till the construction of brickwork over them.

3.1.2 Brick Masonry Walls

Brick masonry walls, with height to span ratio less than 0.4, were cast is casting yard. Those, with height to span ratio of greater than 0.4, were cast after placing the precast concrete beams over suitable supports (two end supports on rollers and two temporary supports at one third span) right on the test floor. The temporary supports were necessitated due to the fact that the strength of beams after one week of curing was just sufficient to support the self weight. Any appreciable over burden would have caused excessive deflections and consequent failure of beam at the time of specimen preparation. The brickwork was done by two experienced masons. In all cases, brickwork was completed in one day. The bricks were soaked well in

water before using. The ratio of cement and sand in the mortar was taken by weight. The control tests on mortar and bricks were carried out and have already been reported in Chapter II. Care was exercised to maintain the constant mortar thickness. It turned out to be 1 cm for horizontal mortar beds and 1.5 cm for vertical joints. Brick masonry was cured for about 28 days by sprinkling water 2 to 3 times a day over the walls.

3.1.3 Loading

A uniformly distributed load was simulated on the test specimen which was ensured to be horizontal, by applying the load at twelve points. The centre to centre distance between the load points was 25 cm. Twin box type of test floor available in Structural Engineering laboratory at IIT Kanpur was ideally suited for the purpose. Hydraulic jacks were fitted on the channels or box sections which were held down to the test floor with the help of mild steel rods, passing through the fifty cm centre to centre holes of the test floor. These mild steel rods in turn transferred the load to the walls at desired level. In all, nine jacks were used, 3 on each channel or box section. The details of loading arrangement for applying the compressive and tensile type of loads are shown in Figs. 3.3 and 3.4 respectively.

The jacks and the associated hydraulic system were calibrated using a proving ring of 20,000 kg. capacity. The specimens were loaded and unloaded several times to about 25 to 30 percent of first crack load to check the performance of loading system and measuring devices. The loading was incremented at prescribed interval so as to have adequate readings in the elastic and post cracking stage. Electrically operated hydraulic loading was with remote control and therefore loads could be recorded upto failure accurately. However, near the failure load, measuring devices had to be removed in order to protect them from damage due to possible collapse.

3.1.4 Instrumentation

In order to measure strains in brickwork and overall deflection of the composite construction, strain measuring devices were suitably mounted on the test specimen.

3.1.4.1 Dial gauges

The overall deflection of composite construction at various load levels have been recorded with the help of dial gauges of 0.01 mm leastcount mounted at the bottom of R.C. beams. In all, five dial gauges were used for the purpose. The dial gauges were placed at midspan and at 50 and 100 cm from midspan on either side.

3.1.4.2 Strain measuring device

Metalstuds were initially tried to measure the lateral and vertical strains on the surface of composite construction, but had to be abondoned because they gave erratic readings. After this, attempt was made to measure strains in the horizontal direction by 15 cm single wiere 120 ohm electrical resistance strain gauges and 1.5 cm flat grid 120 ohm electrical resistance strain gauge in vertical direction with no success. Finally strains were recorded by fixing the dial gauges between two points 50 cm centre to centre at each horizontal level. For fixing the dial gauges 5.5 mm dia holes were drilled in the masonry with the help of an electric drill using masonry drill bits. One 80 mm long roofing bolt was fixed in each hole with help of a plugging compound. Between these two roofing bolts, the dial gauge was held. The arrangement can be clearly seen in the photographs for cracking pattern. In most of the cases, these gave satisfactory readings.

3.2 PARAMETRIC STUDIES

Experimental study of the interaction between R.C. beam and brick masonry wall has been conducted for both compressive and tensile loading for the different parameters such as (1) ratio of cement and sand used in mortar for brickwork (2) height to span ratio of composite system

(3) symmetric and unsymmetric openings in the masonry wall.

3.2.1 Variation in Cement Sand Ratio in Mortar

In order to study the effect of mortar strength on interaction of composite construction, five cement sand ratios of 1:8 and ranging from 1:6 to 1:3 have been experimented upon, keeping a constant height to span ratio of 0.33. The size of ten specimens numbered 1 to 10, five each tested for compressive and tensile loading is shown in Fig. 3.5. The bending reinforcement is provided for a total working load of 9.0 tonnes and assuming the lever arm to be 0.9 times in depth of composite system, considering it to be an under-reinforced brick beam with zero tensile strength of brick work and concrete.

3.2.2 Variation in Height to Span Ratio

The effect of variation in the height to span ratio on the ultimate load carrying capacity of the composite system has been studied on ten specimens, five each under compressive and tensile loading for height to span ratios of 0.25, 0.33, 0.4, 0.5 and 0.8. The bending reinforcement had to be varied for different height to span ratios as described in preceding subsection. However, the same bending reinforcement was provided for height to span ratio of 0.5 and above as obtained from calculations for H/L of 0.5.

The table on next page gives the details of specimens tested for the purpose.

DETAILS OF SPECIMENS TO STUDY THE EFFECT OF H/L RATIO

H/L	L in cm	H in cm	No. of 6 mm Ø connectors used	Bending reinforcement	Compressive Loading		Tensile Loading	
					Specimen number	Mortar	Specimen number	Mortar
0.25	325	81	13	2 bars 10 mm dia and 1 bar 16 mm dia	11	1:6	15	1:3
0.33	325	108	13	2 bars 10 mm dia and 1 bar 12 mm dia	1	1:6	6	1:3
0.4	325	130	13	3 bars 10 mm dia	12	1:6	16	1:3
0.5	325	162	13	2 bars 8 mm dia and 1 bar 10 mm dia	13	1:6	17	1:3
0.8	325	263	13	2 bars 8 mm dia and 1 bar 10 mm dia	14	1:6	18	1:3

3.2.3 Variation in Size and Location of Openings

The walls of such composite construction shall have door or window openings at suitable locations. How do these openings influence the interaction of composite construction is the subject of experimental study. In the present work, a door opening of 1m x 2m and a window opening 1m x 1m has been considered. While the door opening starts right above the R.C. beam, the sill of window opening has a height of 1m above the R.C. beam. Both of these openings have been placed symmetrically about the vertical centre line and unsymmetrically at a centre of 95 cm from one end of the specimen for purposes of experimentation. A precast concrete member, 8 cm thick and carrying 3 plain mild steel bars of 10 mm dia formed the lintel over the openings. The details of nine specimens numbered 19 to 27 are shown in Fig. 3.6. Specimens number 19 to 23 were cast in mortar 1:6 and have been tested under compressive loading. The rest of the specimens were cast in mortar 1:3 and tested under tensile loading. Specimens number 23 and 27 are similar to specimens number 22 and 25 respectively except for the fact that thickness of R.C. beam in specimens number 23 and 27 is increased to 16 cm. This was necessitated because specimen number 22 failed under its self-weight while making preparations for testing. All specimens had a height to span ratio of 0.8.

3.3 TEST RESULTS

The results of various tests conducted are reported and discussed in this section according to parameters studied.

3.3.1 Effect of Variation in Cement Sand Mortar For Brick Work

The observed test data on deflections at the bottom of R.C. beams at various points along the span, are given in Tables 3.1 to 3.5 for compressive loading and Tables 3.6 to 3.10 for tensile loading respectively. Figs. 3.7 and 3.8 show the plot of load versus deflection for various specimens tested under compressive and tensile loading respectively. Load deflection curves are almost linear in the initial stages and become nonlinear after the appearance of first crack. However, in case of load deflection curves for specimens tested under tensile loading, there is slight deviation from linearity even in the initial stages before separation sets in.

Tables 3.11 and 3.12 reports the observed test data on longitudinal strains for specimens cast in mortars of 1:3 and 1:6 respectively tested under compressive loading. The test data on longitudinal strains for specimens cast in mortars of 1:4, 1:5 and 1:6, and tested under tensile loading is given in Tables 3.13, 3.14 and 3.15 respectively. The strains at a cross section of composite construction, at

mid span, have been plotted in Figs. 3.9(a) and 3.9(b) for specimens tested under compressive and tensile loading respectively. Variation of strains is linear at this cross section. From the linear load deflection curves and the linear variation of longitudinal strains before cracking starts, it can be concluded that composite material behaves linearly in the elastic range. Figs. 3.10(a) and 3.10(b) show the cracking pattern for specimens number 1 to 5 and 6 to 10 and tested under compressive and tensile loading repectively. Specimens number 1 and 2 cast respectively in 1:3 and 1:4 mortar and tested under compressive loading, cracked near the mid span, indicating thereby a bending failure. Specimen number 3 cast in 1:5 mortar and tested under compressive loading has a mixed type of crack pattern i.e. failure is caused jointly by bending and diagonal tension. Specimens number 4 and 5 cast in 1:6 and 1:8 mortar failed due to diagonal tension as the cracks in these specimens developed near the supports only. As is seen from Fig. 3.10(b), all the five specimens numbered 6 to 10 tested under tensile loading failed by horizontal separation at different heights and subsequent development of cracks due to diagonal tension.

Tables 3.16 and 3.17 give the first crack load, failure load, and the load factor for specimens tested under compressive and tensile loading respectively. It is observed from these

tables that the first crack load for specimens tested under compressive loading varies from 12.26 to 22.85 tonnes (including self weight) , while for specimens tested under tensile loading it varies from 5.6 tonnes to 10.7 tonnes (including self weight). The load carrying capacity in elastic range of the thin concrete beam supporting the brick masonry is just its self weight which is around 150 kg. Therefore the composite construction is taking a load in the elastic range which is approximately 37 to 152 times more than the load carrying capacity of the beam it self depending upon the mortar used and the loading condition. In fact, the contention of present work is to demonstrate that for the composite construction under investigation, thinnest possible R.C. beam can be used which is sufficient enough to provide suitable bond and cover to the bending reinforcement and hold the single legged vertical connectors in possition. Not with standing these high ratios, it is clearly observed that the composite construction behaves as a single composite structural element in the elastic range. Furthermore, richer the mortar mix, greater is the interaction in the elastic range between the masonry and R.C. beam connected through single legged Z-shaped stirrups.

The total failure load for specimens tested under compressive and tensile loading varies from 12.26 to 35.24 tonnes and 9.28 to 18.7 tonnes respectively, while the

ultimate load carrying capacity of R.C. beam itself is only 800 kg. Therefore, the interaction observed in the elastic range extends even beyond. In other words, richer the mortar mix greater is the interaction upto failure of the composite structural element.

It is seen from Table 3.17 that the load factor for specimens tested under tensile loading varies from 2.08 to 1.03. All specimens, except the one cast in 1:3 mortar, have a load factor of less than 2.0. I.S. code specifies a load factor of 1.5 for dead load and 2.2 for live load and therefore mortar leaner than 1:3 are not suitable for use when loading is tensile.

For specimens tested under compressive loading the load factor is more than 3 for all specimens cast in mortar 1:6 or richer but it suddenly drops down to 1.36 for specimen cast in 1:8 mortar. It is also observed from Table 3.16 that the first crack load and failure load for specimen in 1.8 mortar are exactly the same meaning thereby a sudden failure of composite system in 1:8 mortar. The reason for this is the bond failure between brickwork and the vertical connectors. Therefore, it can be concluded that the use of 1:8 mortar for brickwork will not provide the desired interaction. Further more, keeping in view that use of 1:6 mortar achieves a load factor of about 3, it can be safely recommended to

cast such composite structural element in 1:6 mortar for cases where loading is compressive.

Based on the above observations, subsequent parametric studies have been conducted on specimens cast in mortars of 1:6 and 1:3 for compressive and tensile loading respectively.

3.3.2 Effect of Variation in Height to Span Ratio

The observed test data on deflections at the bottom of R.C. beam at various points along the span are given in Tables 3.4 and 3.18 to 3.21 for specimens tested under compressive loading while the same for specimens tested under tensile loading are given in Tables 3.6 and 3.22 to 3.25. Figs. 3.11 and 3.12 show the load deflection curves for compressive and tensile loading respectively. For the load deflection curves, it is observed that deflections go on reducing as the height to span ratio increases, meaning thereby that the element is becoming stiffer with the increased height to span ratio.

Tables 3.12 and 3.26 to 3.29 report the observed data on longitudinal strains on the specimens under compressive loading and Tables 3.30 to 3.32 under tensile loading. The strains at a cross section at mid span have been plotted in Figs. 3.13(a) and 3.13(b) for specimens tested under compressive and tensile loading respectively. The variation

of strains is linear upto a height to span ratio of 0.4. It is a bilinear curve for a height to span ratio of 0.5 for specimens under compressive loading and is linear under tensile loading. For a height to span ratio of 0.8 the variation of strains is not clearly obtained. The maximum strains at the top and bottom of specimens under compressive loading in the latter case are of the order of 5×10^{-5} cm/cm. The least count of measuring device leads to a strain of 2×10^{-5} cm/cm. A couple of dial gauges upto quarter height above the R.C. beam recorded constant values leading to zero strains meaning thereby that the strain is less than 2×10^{-5} cm/cm. In the top portion of this specimen the strain variation is clearly nonlinear. For the specimen number 18 of height to span ratio of 0.8 tested under tensile loading meaningful data could not be obtained.

Figures 3.14(a) and 3.14(b) show the cracking pattern of specimens number 11 to 14 and 15 to 18 for compressive and tensile loading respectively. Specimens number 11 and 12 having height to span ratio of 0.25 and 0.4 tested under compressive loading developed cracks near supports meaning thereby a failure in diagonal tension similar to specimen number 4 having height to span ratio of 0.33 cast in 1:6 mortar as discussed before. Specimens numbered 13 and 14 having a height to span ratio of 0.5 and 0.8 failed due to diagonal tension and crushing of concrete and brickwork at the supports.

Photographs showing the failure pattern for these specimens are affixed as Fig. 3.15. All the four specimens numbered 15 to 18, tested under tensile loading, failed by horizontal separation at different heights and subsequent development of cracks due to diagonal tension. Tables 3.33 and 3.34 give the first crack load, failure load and the load factor for specimens tested under compressive and tensile loading respectively. From these tables it is observed that higher is the height to span ratio higher is the load factor. Under compressive loading, the load factor for the specimen of height to span ratio of 0.25 is 1.8 while for others it varies from 3 to 6. The reason for a low value of failure load for specimen of height to span ratio of 0.25 is the possible bond failure between the vertical connectors and the brickwork i.e. a bond length of about 70 cm in 1:6 mortar is sufficient to transfer loads corresponding to the load factor of 1.8 . It is, therefore, concluded that in order to achieve a load factor of 2 or above a rich mortar should be used for height to span ratio of 0.25.

For specimens tested under tensile loading the load factor varies from 1.61 to 2.98. The load factor is below 2.0 for a height to span ratio of 0.25 while, for others, it is more than 2.0. For this height to span ratio, one additional specimen No. 28 was tested. The

specimen was identical to specimen number 15 except that it had 6 mm dia 24 connectors provided at a uniform spacing of 13 cm centre to centre instead of only 13 connectors. The observed data on the deflections for this specimen is given in Table 3.35. The load deflection curve and the cracking pattern is shown in Figs. 3.16 and 3.17. In this case, the deflections are lower as compared to those for specimen No.15 having 13 vertical connectors. For example, the deflection at mid span at a load of 6.77 tonnes is 1.47 mm for specimen number15 while for specimen number 28 it is 0.81 mm for the same load. Furthermore, the horizontal separation starts at a much later stage of loading in specimen number 28 i.e. at a load of 13.5 tonnes instead of 6.77 tonnes in specimen number 15, showing thereby increased resistance to bond slip due to use of more connectors. The load factor for this specimen is 2.08. It is, therefore, concluded that in case of tensile loading and height to span ratio of 0.25, more number of vertical connectors have to be used.

Motivated by the above results, two additional specimens numbered 29 and 30 were cast for a height to span ratio of 0.33 in order to study the effect of the variation of size and number of vertical connectors on the load factor. Specimen number 29 had 13 number 8 mm dia and specimen number 30 had 20 number 6 mm dia plain mild steel

vertical connectors respectively. Thus specimen number 29 had same number of increased diameter connectors while number 30 had increased number of same diameter connectors as specimen number 6. The observed data on deflections for these specimens is given in Tables 3.36 and 3.37 respectively. Load deflection curves for these specimens are shown in Fig. 3.18. Table 3.38 gives the first crack load, failure load and load factor for specimens numbered 6, 29 and 30 for the purposes of comparison. It is observed from Table 3.38 that in specimen number 29 separation started at a load of 6.768 tonnes and it failed at 12.69 tonnes while in case of specimen number 6 separation started at a load of 8.5 tonnes and failure took place at 16.5 tonnes, indicating thereby that increase in the size of connectors has reduced the load carrying capacity. This can only be explained by the fact that 8 mm dia connector has not been able to develop sufficient bond with brickwork through mortar joint about 1.5 cm thick normally used. In specimen number 30, separation started at a load of 13.536 tonnes and it failed at a load of 19.0 tonnes indicating higher load carrying capacity with increased number of connectors. From this limited study, conducted on specimens numbered 28, 29 and 30, it can be concluded that, 6 mm dia connectors provided at spacing closer than 25 cms yields better interaction in

situations where loading is tensile. However, in order to achieve spacing of connectors lower than 25 cms, breaking of the bricks is inevitable.

3.3.3 Effect of Variation in Size and Location of Openings in Brickwork

Tables 3.39 to 3.42 give the observed test data on deflections for specimens number 19, 20, 21 and 23 and tested under compressive loading. Tables 3.43 to 3.46 report the observed data on deflections for specimens number 24 to 27 and tested under tensile loading. Fig. 3.19 and Fig. 3.20 show the plot of load versus deflections for specimens with openings tested under compressive and tensile loading respectively. In addition these figures also show the load deflection curves for solid walls of height to span ratio of 0.8 tested under respective loading for purposes of comparison. Meaningful data on longitudinal strains could not be obtained because of low accuracy of measuring devices. Figs. 3.21 and 3.22 show the cracking pattern of specimens number 19 to 23 and 24 to 27 tested under compressive and tensile loading respectively. In case of compressive loading, specimen No. 19 with a symmetric window opening failed in diagonal tension and crushing of brickwork and concrete at supports. Specimen no. 20 with a symmetric door opening failed in diagonal tension only. Specimen no. 21 having an unsymmetric window opening also failed in

diagonal tension accompanied by shear as is evident from the crack pattern. Specimen no. 22 and 23 failed due to shear only. Photographs affixed as Fig. 3.23 show very clearly the failure patterns discussed.

All specimens tested under tensile loading failed by horizontal separation and subsequent development of cracks due to diagonal tension.

Tables 3.47 and 3.48 give the first crack load, failure load and load factor for specimens tested under compressive and tensile loading respectively. From Table 3.47 and Fig. 3.19, it is observed that symmetric openings do not affect the load carrying capacity of the specimen under compressive loading. However, unsymmetric openings affect the load carrying capacity significantly. The load factor for an unsymmetric window opening is 4.1 against 5.9 for symmetric window opening. The unsymmetric door opening affects the load carrying capacity adversely. Specimen number 22 failed under self-weight while making preparations for the test. The specimen number 23, which had a 16 cm thick R.C. beam failed at a load of 10.04 tonnes thus giving a load factor of only 1.61.

The load carrying capacity of specimens under tensile loading is reduced due to the presence of symmetric or unsymmetric door and window openings. The load factor for

specimen with symmetric and unsymmetric window openings in 2.44 and 2.18 respectively. It may not be out of place to recall that specimen number 6 having height to span ratio of .33 and cast in mortar 1:3 has a load factor of 1.98. The sill of the window openings as described earlier was kept at 1 m height above the R.C. beam meaning thereby that sill height to span ratio is .33. It is, therefore, concluded that specimens with window openings fail at a load only slightly greater than those whose height is equal to the sill height. The load factor for specimen with a symmetric door opening is only 1.57 as against a load factor of 3.0 for corresponding specimen without opening. The load factor for specimen number 27 which has an increased thickness of R.C. beam viz. 16 cm and a symmetric door opening is 2.17. From this it is concluded that inorder to have a load factor of 2.0, such composite construction carrying symmetric door openings be carried out with 16 cm thick R.C. beams.

TABLE 3.1 : DEFLECTIONS

H/L	MORTAR	LOADING
0.33	1:3	COMPRESSIVE

Sl. No.	Pressure on jacks in psi	Load in tonnes	Location of Dial Gauge (Distance from Left End in CM)										Remarks
			62.5		112.5		162.5		212.5		262.5		
			Reading of dial gauge	Deflection in mm	Reading of Dial gauge	Deflection in mm	Reading of Dial Gauge	Deflection in mm	Reading of Dial gauge	Deflection in mm	Reading in Dial Gauge	Deflection in mm	
1.	000	0.00	19.40	0.00	0.11	0.00	12.37	0.00	8.42	0.00	16.94	0.00	
2.	200	4.13	19.53	0.13	0.28	0.17	12.56	0.19	8.58	0.16	17.06	0.12	
3.	400	8.26	19.66	0.26	0.45	0.34	12.76	0.39	8.75	0.33	17.19	0.25	
4.	600	12.39	19.79	0.39	0.61	0.50	12.94	0.57	8.92	0.50	17.32	0.38	
5.	800	16.52	19.92	0.52	0.87	0.76	13.21	0.84	9.17	0.75	17.46	0.52	
6.	1000	20.65	20.11	0.71	1.32	1.21	13.76	1.39	9.61	1.19	17.66	0.72	First crack
7.	1200	24.78	20.38	0.98	1.76	1.65	14.21	1.84	10.02	1.60	17.91	0.97	
8.	1400	28.91	22.05	2.65	6.20	5.09	21.22	8.85	13.42	5.00	20.54	3.60	
9.	1600	33.04	-	-	-	-	-	-	-	-	-	-	Failure

TABLE 3.2 : DEFLECTIONS

H/L	MORTAR	LOADING
0.33	1:4	COMPRESSIVE

Sl. No.	Pressure on jacks in psi	Load in tonnes	Location of Dial Gauge (Distance from Left End in cm)										Remarks
			62.5		112.5		162.5		212.5		262.5		
			Reading of dial gauge	Deflection in mm	Reading of dial gauge	Deflection in mm	Reading of ial gauge	Deflection in mm	Reading of dial gauge	Deflection in mm	Reading in dial gauge	Deflection in mm	
1.	000	0.000	1.86	0.00	0.88	0.00	3.92	0.00	8.90	0.00	13.10	0.00	
2.	100	2.065	1.93	0.07	0.98	0.10	4.03	0.11	8.98	0.08	13.16	0.06	
3.	200	4.130	2.00	0.14	1.09	0.21	4.15	0.23	9.07	0.17	13.22	0.12	
4.	300	6.195	2.07	0.21	1.17	0.29	4.26	0.34	9.16	0.26	13.28	0.18	
5.	400	8.260	2.14	0.28	1.27	0.39	4.37	0.45	9.25	0.35	13.34	0.24	
6.	500	10.325	2.21	0.35	1.36	0.48	4.49	0.57	9.34	0.44	13.40	0.30	
7.	600	12.390	2.28	0.42	1.47	0.59	4.61	0.69	9.43	0.53	13.46	0.36	
8.	700	14.455	2.35	0.49	1.72	0.84	4.95	1.03	9.69	0.79	13.62	0.52	
9.	800	16.520	2.57	0.71	2.06	1.18	5.39	1.47	10.03	1.13	13.84	0.74	First Crack
10.	1000	20.650	3.24	1.38	3.09	2.21	6.52	2.60	11.06	2.16	14.48	1.38	
11.	1200	24.780	4.13	2.27	4.64	3.76	7.98	4.06	12.62	3.72	15.40	2.30	
12.	1400	28.910	-	-	-	-	-	-	-	-	-	-	Failure

TABLE 3.3 : DEFLECTIONS

H/L	MORTAR	LOADING
0.33	1:5	COMPRESSIVE

Sl. No.	Pressure on jack in psi	Load in tonnes	Location of Dial Gauges (Distance from Left End in cm)										Remarks
			62.5		112.5		162.5		212.5		262.5		
			Reading of dial gauge	Deflection in mm	Reading of dail gauge	Deflection in mm	Reading of dial gauge	Deflection in mm	Reading of dial gauge	Deflection in mm	Reading of dial gauge	Deflection in mm	
1.	000	0.00	11.69	0.00	10.46	0.00	13.10	0.00	8.55	0.00	13.63	0.00	
2.	200	1.79	11.77	0.08	10.56	0.10	13.22	0.12	8.66	0.11	13.71	0.08	
3.	400	3.38	11.85	0.16	10.66	0.20	13.34	0.24	8.76	0.21	13.79	0.16	
4.	600	5.08	11.93	0.24	10.77	0.31	13.46	0.36	8.86	0.31	13.87	0.24	
5.	800	6.77	12.01	0.32	10.87	0.41	13.59	0.49	8.97	0.42	13.95	0.32	
6.	1000	8.46	12.09	0.40	10.98	0.52	13.71	0.61	9.09	0.54	14.03	0.40	
7.	1200	10.15	12.18	0.49	11.15	0.69	13.94	0.84	9.25	0.70	14.13	0.50	
8.	1400	11.84	12.28	0.59	11.39	0.93	14.24	1.14	9.49	0.94	14.24	0.61	
9.	1600	13.54	12.50	0.81	11.78	1.32	14.73	1.63	9.90	1.35	14.47	0.84	**First** Crack
10.	1800	15.23	12.76	1.07	12.22	1.76	15.11	2.01	10.29	1.74	14.71	1.08	
11.	2000	16.92	13.00	1.31	12.66	2.20	15.90	2.80	10.87	2.22	14.97	1.34	
12.	2400	20.30	13.64	1.95	13.70	3.24	17.03	3.93	11.72	3.27	15.55	1.92	
13.	2800	23.67	14.86	3.17	15.60	5.14	19.23	6.13	13.75	5.20	16.77	3.14	
14.	3200	-	-	-	-	-	-	-	-	-	-	-	Failure

TABLE 3.4 DEFLECTIONS

H/L	MORTAR	LOADING
0.33	1:6	COMPRESSIVE

Sl. No.	Pressure on jacks in psi	Load in tonnes	Location of Dial Gauges (Distance from Left End in cm)										Remark
			62.5		112.5		162.5		212.5		262.5		
			Reading of dial gauge	Deflection in mm	Reading of dial gauge	Deflection in mm	Reading of dial gauge	Deflection in mm	Reading of dial gauge	Deflection in mm	Reading of dial gauge	Deflection in mm	
1.	000	0.000	7.02	0.00	16.39	0.00	8.94	0.00	11.36	0.00	5.38	0.00	
2.	100	2.065	7.13	0.11	16.53	0.14	9.11	0.17	11.50	0.14	5.50	0.12	
3.	200	4.130	7.24	0.22	16.68	0.29	9.28	0.34	11.63	0.27	5.61	0.23	
4.	300	6.195	7.36	0.34	16.84	0.45	9.45	0.51	11.79	0.43	5.71	0.33	
5.	400	8.260	7.48	0.46	17.00	0.61	9.62	0.68	11.98	0.62	5.84	0.46	
6.	500	10.325	7.62	0.60	17.23	0.84	9.98	1.04	12.20	0.84	6.00	0.62	
7.	600	12.390	7.88	0.86	17.64	1.25	10.64	1.70	12.61	1.25	6.25	0.87	First Crack
8.	700	14.455	8.34	1.32	18.32	1.93	11.28	2.34	13.32	1.96	6.66	1.28	
9.	800	16.520	8.90	1.88	19.12	2.73	12.24	3.30	14.13	2.77	7.30	1.92	
10.	900	18.585	9.20	2.18	19.92	3.43	12.95	4.01	14.80	3.44	7.52	2.14	
11.	1000	20.650	9.70	2.68	21.20	4.81	14.47	5.53	16.26	4.90	8.12	2.74	
12.	1200	-	-	-	-	-	-	-	-	-	-	-	Failure

TABLE 3.5 : DEFLECTIONS

H/L	MORTAR	LOADING
0.33	1:8	COMPRESSIVE

Sl. No.	Pressure on jack in psi	Load in tonnes	Location of Dial Gauges (Distance from Left End in cm)										Remarks
			62.5		112.5		162.5		212.5		262.5		
			Reading of dial gauge	Deflection in mm	Reading of dial gauge	Deflection in mm	Reading of dial gauge	Deflection in mm	Reading of dial gauge	Deflection in mm	Reading of dial gauge	Deflection in mm	
1.	0.0	0.00	0.04	0.00	5.20	0.00	9.78	0.00	8.52	0.00	19.48	0.00	
2.	60	1.24	0.19	0.15	5.45	0.25	10.06	0.28	8.77	0.25	19.63	0.15	
3.	120	2.48	0.34	0.30	5.69	0.49	10.34	0.56	9.02	0.50	19.79	0.31	
4.	180	3.72	0.50	0.46	5.94	0.74	10.62	0.85	9.28	0.76	19.95	0.47	
5.	240	4.96	0.66	0.62	6.19	0.99	10.92	1.14	9.53	1.01	20.12	0.64	
6.	300	6.20	0.82	0.78	6.44	1.24	11.20	1.42	9.78	1.26	20.27	0.79	
7.	400	8.26	1.24	1.20	7.18	1.98	12.01	2.23	10.55	2.03	20.69	1.21	
8.	487	10.06	-	-	-	-	-	-	-	-	-	-	First crack and failure

TABLE 3.6: DEFLECTIONS

H/L	MORTAR	LOADING
0.33	1:3	TENSILE

Sl. No.	Pressure on jacks in psi	Load in tonnes	Location of Dial Gauge (Distance from Left End in cm) 62.5		112.5		162.5		212.5		262.5		Remarks
			Reading of dial gauge	Deflection in mm	Reading of dial gauge	Deflection in mm	Reading of dial gauge	Deflection in mm	Reading of dial gauge	Deflection in mm	Reading of dial gauge	Deflection in mm	
1.	000	0.000	20.84	0.00	16.88	0.00	3.84	0.00	4.53	0.00	2.76	0.00	
2.	200	1.692	20.93	0.09	16.99	0.11	3.96	0.12	4.64	0.11	2.85	0.09	
3.	400	3.384	21.02	0.18	17.11	0.23	4.08	0.24	4.75	0.22	2.94	0.18	
4.	600	5.076	21.12	0.28	17.23	0.35	4.21	0.37	4.87	0.34	3.04	0.28	
5.	800	6.768	21.25	0.41	17.38	0.50	4.37	0.53	5.01	0.48	3.16	0.40	
6.	1000	8.460	21.44	0.60	17.69	0.81	4.79	0.95	5.33	0.80	3.35	0.59	Separation at second layer
7.	1200	10.152	21.90	1.06	18.36	1.48	5.56	1.72	5.99	1.46	3.80	1.04	
8.	1400	11.846	22.64	1.80	19.23	2.35	6.57	2.73	6.83	2.30	4.52	1.76	
9.	1600	13.536	23.73	2.89	20.64	3.76	7.94	4.10	8.24	3.71	5.61	2.85	
0.	1800	15.228	25.16	4.32	22.33	5.45	10.55	6.71	9.92	5.39	7.03	4.27	
1.	1950	16.500	-	-	-	-	-	-	-	-	-	-	Failure

TABLE 3.7 : DEFLECTIONS

H/L	MORTAR	LOADING
0.33	1:4	TENSILE

Sl. No.	Pressure on jacks in psi	Load in tonnes	Location of Dial Gauge (Distance from Left End in cm)										Remarks
			62.5		112.5		162.5		212.5		262.5		
			Reading of dial gauge	Deflection in mm	Reading of dial gauge	Deflection in mm	Reading of dial gauge	Deflection in mm	Reading of dial gauge	Deflection in mm	Reading of dial gauge	Deflection in mm	
1.	000	0.00	23.38	0.00	4.48	0.00	3.07	0.00	4.62	0.00	9.36	0.00	
2.	200	1.69	23.47	0.09	4.63	0.15	3.23	0.16	4.76	0.14	9.47	0.09	
3.	400	3.38	23.58	0.20	4.79	0.31	3.40	0.33	4.92	0.30	9.55	0.19	
4.	600	5.08	23.70	0.32	4.94	0.46	3.56	0.49	5.06	0.44	9.67	0.31	
5.	700	5.92	23.82	0.44	5.09	0.61	3.74	0.67	5.20	0.58	9.78	0.42	
6.	800	6.77	23.97	0.59	5.28	0.80	3.96	0.89	5.40	0.78	9.93	0.57	
7.	900	7.61	24.19	0.81	5.55	1.07	4.25	1.18	5.67	1.05	10.14	0.78	Separation and first crack
8.	1000	8.46	24.59	1.21	6.02	1.54	4.74	1.67	6.12	1.50	10.54	1.18	
9.	1100	9.31	24.93	1.55	6.46	1.98	5.19	2.12	6.59	1.97	10.87	1.51	
10.	1200	10.15	25.95	2.57	7.97	3.48	6.65	3.58	8.04	3.42	11.88	2.52	
11.	1300	11.00	27.72	3.34	10.51	6.03	9.32	6.25	10.52	5.90	12.50	3.14	
12.	1400	11.84	35.40	12.02	19.21	14.73	19.00	15.93	18.59	13.97	20.94	11.58	
13.	1565	13.24	-	-	-	-	-	-	-	-	-	-	Failure

TABLE 3.8 : DEFLECTIONS

H/L	MORTAR	LOADING
0.33	1:5	TENSILE

Sl. No.	Pressure on jacks in psi	Load in tonnes	Location of Dial Gauge (Distance from Left End in cm)										Remarks
			62.5		112.5		162.5		212.5		262.5		
			Reading of dial gauge	Deflection in mm	Reading of dial gauge	Deflection in mm	Reading of dial gauge	Deflection in mm	Reading of dial gauge	Deflection in mm	Reading of dial gauge	Deflection in mm	
1.	000	0.000	20.68	0.00	7.93	0.00	0.09	0.00	8.48	0.00	18.02	0.00	
2.	100	0.846	20.72	0.04	7.99	0.06	0.16	0.07	8.54	0.06	18.06	0.04	
3.	200	1.692	20.77	0.09	8.06	0.13	0.24	0.15	8.60	0.12	18.11	0.09	
4.	300	2.540	20.87	0.19	8.20	0.27	0.40	0.31	8.72	0.24	18.20	0.18	
5.	400	3.400	21.01	0.33	8.40	0.47	0.62	0.53	8.90	0.42	18.32	0.30	
6.	500	4.230	21.15	0.47	8.61	0.68	0.85	0.76	9.15	0.67	18.45	0.43	
7.	600	5.070	21.34	0.66	8.91	0.98	1.18	1.09	9.45	0.97	18.65	0.63	
8.	700	5.920	21.74	1.06	9.50	1.57	1.82	1.73	9.99	1.51	19.06	1.04	
9.	800	6.770	22.38	1.70	10.33	2.40	2.75	2.66	10.88	2.40	19.74	1.72 *	
10.	900	7.614	23.34	2.66	11.86	3.93	4.39	4.30	12.38	3.90	20.62	2.60	
11.	1000	8.460	24.38	3.70	13.87	5.94	6.90	6.81	14.39	5.91	21.69	3.67 **	
12.	1100	9.306	26.15	5.47	16.60	8.67	10.40	10.31	17.54	9.06	23.37	5.35	
13.	1300	11.000	-	-	-	-	-	-	-	-	-	-	Failure

* Separation and first crack ** Separation at top

TABLE 3.9: DEFLECTIONS

H/L	MORTAR	LOADING
0.33	1:6	TENSILE

Sl. No.	Pressure on jacks in psi	Load in tonnes	Location of Dial Gauges (Distance from Left End in cm) 62.5 Reading of dial gauge	62.5 Deflection in mm	112.5 Reading of dial gauge	112.5 Deflection in mm	162.5 Reading of dial gauge	162.5 Deflection in mm	212.5 Reading of dial gauge	212.5 Deflection in mm	262.5 Reading of dial gauge	262.5 Deflection in mm	Remarks
1.	000	0.000	4.59	0.00	3.73	0.00	0.74	0.00	6.38	0.00	1.01	0.00	
2.	100	0.846	4.67	0.08	3.84	0.11	0.89	0.15	6.49	0.11	1.08	0.07	
3.	200	1.692	4.74	0.15	3.97	0.24	1.06	0.32	6.61	0.23	1.15	0.14	
4.	300	2.540	4.84	0.25	4.09	0.36	1.23	0.49	6.73	0.35	1.25	0.24	
5.	400	3.400	4.97	0.38	4.25	0.52	1.47	0.73	6.89	0.51	1.38	0.37	
6.	500	4.230	5.12	0.53	4.49	0.76	1.75	1.01	7.12	0.74	1.52	0.51	
7.	600	5.070	5.33	0.74	4.82	1.09	2.14	1.40	7.45	1.07	1.73	0.72	
8.	700	5.920	5.83	1.24	5.52	1.79	3.13	2.39	8.17	1.79	2.22	1.21 –	First crack and seperation at IInd layer
9.	800	6.770	6.69	2.10	6.93	3.20	4.86	4.12	9.60	3.22	3.05	2.04	
10.	900	7.614	7.59	3.00	8.48	4.75	6.65	5.91	11.14	4.76	3.93	2.92	
11.	1000	8.460	8.84	4.25	10.90	7.17	8.97	8.23	13.45	7.07	5.20	4.19	
12.	1200	10.15	-	-	-	-	-	-	-	-	-	- *	*Failure

TABLE 3.10 : DEFLECTIONS

H/L	MORTAR	LOADING
0.33	1:8	TENSILE

Sl. No.	Pressure on jacks in psi	Load in tonnes	Location of Dial Gauges (Distance from Left End in cm)										Remarks
			62.5		112.5		162.5		212.5		262.5		
			Reading of dial gauge	Deflection in mm	Reading of dial gauge	Deflection in mm	Reading of dial gauge	Deflection in mm	Reading of dial gauge	Deflection in mm	Reading of dial gauge	Deflection in mm	
1.	000	0.000	22.15	0.00	0.63	0.00	24.77	0.00	23.60	0.00	12.54	0.00	
2.	100	0.846	22.15	0.10	0.75	0.12	24.91	0.14	23.72	0.12	12.64	0.10	
3.	200	1.692	22.37	0.22	0.92	0.29	0.12	0.35	23.88	0.28	12.75	0.21	
4.	300	2.540	22.68	0.53	1.33	0.70	0.56	0.79	24.28	0.68	13.06	0.52	
5.	400	3.400	23.22	1.07	2.23	1.60	1.45	1.68	0.19	1.59	13.59	1.05-	Seperation starts
6.	500	4.230	23.99	1.84	3.63	3.00	2.86	3.09	1.56	2.96	14.36	1.82	
7.	600	5.070	0.59	3.44	6.55	5.92	6.04	6.27	4.46	5.86	15.94	3.40	
8.	650	5.500	1.45	4.30	8.30	7.67	8.10	8.33	6.20	7.60	16.76	4.22	
9.	700	5.920	3.32	6.17	11.64	11.01	12.19	12.42	9.52	10.92	18.62	6.08	
10.	750	6.345	4.08	6.93	13.25	12.62	14.11	14.34	11.05	12.45	19.37	6.83	
11.	800	6.770	5.68	8.53	16.20	15.57	18.75	18.98	14.00	15.40	20.94	8.40	
12.	837	7.080	-	-	-	-	-	-	-	-	-	-	Failure

TABLE 3.11: STRAINS

H/L	MORTAR	LOADING
0.33	1:3	COMPRESSIVE

Pressure on jacks in psi			000	200	400	600	800	1000
Total load in tonnes			0.0	4.13	8.26	12.39	16.52	20.65
Location of Dial Gauge (Distance in cm from top of Brickwork)	3.8	Reading of dial guage	11.59	11.61	11.635	11.66	11.685	11.71
		Strain $x10^{-5}$	0.0	-4.0	-9.0	-14.0	-19.0	-24.0
	19.2	Reading of dial gauge	9.34	9.355	9.37	9.39	9.41	9.43
		Strain $x10^{-5}$	0.0	-3.0	-6.0	-10.0	-14.0	-18.0
	34.6	Reading of dial gauge	7.65	7.66	7.67	7.68	7.69	7.705
		Strain $x10^{-5}$	0.0	-2.0	-4.0	-6.0	-8.0	-11.0
	50.0	Reading of dial gauge	2.16	2.165	2.17	2.175	2.18	2.185
		Strain $x10^{-5}$	0.0	-1.0	-2.0	-3.0	-4.0	-5.0

Table contd...on page 122

TABLE 3.11 contd...

<table>
<tr><td colspan="3">Pressure on jacks in psi</td><td>000</td><td>200</td><td>400</td><td>600</td><td>800</td><td>1000</td></tr>
<tr><td colspan="3">Total load in tonnes</td><td>0.0</td><td>4.13</td><td>8.26</td><td>12.39</td><td>16.52</td><td>20.65</td></tr>
<tr><td rowspan="6">Location of Dial Gauge (Distance in cm from top of Brickwork)</td><td rowspan="2">65.4</td><td>Reading of dial gauge</td><td>1.12</td><td>1.12</td><td>1.12</td><td>1.12</td><td>1.12</td><td>1.12</td></tr>
<tr><td>Strain x10^{-5}</td><td>0.0</td><td>0.0</td><td>0.0</td><td>0.0</td><td>0.0</td><td>0.0</td></tr>
<tr><td rowspan="2">80.7</td><td>Reading of dial gauge</td><td>6.035</td><td>6.03</td><td>6.02</td><td>6.015</td><td>6.005</td><td>5.995</td></tr>
<tr><td>Strain x10^{-5}</td><td>0.0</td><td>1.0</td><td>3.0</td><td>4.0</td><td>6.0</td><td>8.0</td></tr>
<tr><td rowspan="2">96.1</td><td>Reading of dial gauge</td><td>0.17</td><td>0.16</td><td>0.145</td><td>0.13</td><td>0.115</td><td>0.10</td></tr>
<tr><td>Strain x10^{-5}</td><td>0.0</td><td>2.0</td><td>5.0</td><td>8.0</td><td>11.0</td><td>14.0</td></tr>
<tr><td colspan="3">Remark</td><td colspan="6">Separation starts</td></tr>
</table>

TABLE 5.12: STRAINS

H/L	MORTAR	LOADING
0.33	1:6	COMPRESSIVE

Location of Dial Gauges (Distance in cm from top of Brickwork)								
Pressure on jacks in psi			000	100	200	300	400	500
Total load in tonnes			0.00	2.065	4.13	6.195	8.26	10.325
	3.8	Reading of dial gauge	7.68	7.71	7.74	7.77	7.80	7.83
	3.8	Strain $x10^{-5}$	0.00	-6.0	-12.0	-18.0	-24.0	-30.0
	19.2	Reading of dial gauge	10.36	10.38	10.405	10.43	10.455	10.48
	19.2	Strain $x10^{-5}$	0.00	-4.0	- 9.0	-14.0	-19.0	-24.0
	34.6	Reading of dial gauge	6.62	6.635	6.65	6.67	6.685	6.705
	34.6	Strain $x10^{-5}$	0.0	-3.0	-6.0	-10.0	-13.0	-17.0
	50.0	Reading of dial gauge	14.62	14.63	14.64	14.65	14.66	14.675
	50.0	Strain $x10^{-5}$	0.0	-2.0	-4.0	-6.0	-8.0	-11.0
	65.4	Reading of dial gauge	16.98	16.985	16.99	16.995	17.00	17.005
	65.4	Strain $x\ 10^{-5}$	0.0	-1.0	-2.0	-3.0	-4.0	-5.0

Table contd..on page 124

Table 3.12 contd..

Pressure on jacks in psi			00	100	200	300	400	500
Total load in tonnes			0.00	2.065	4.13	6.195	8.26	10.325
Location of Dial Gauges (Distance in cm from top of Brickwork.)	80.7	Reading of dial gauge	7.15	7.15	7.15	7.15	7.15	7.15
		Strain $x10^{-5}$	0.00	0.00	0.00	0.00	0.00	0.00
	96.1	Reading of dial gauge	5.97	5.965	5.955	5.95	5.945	5.935
		Strain $x10^{-5}$	0.00	1.0	3.0	4.0	5.0	7.0

TABLE 3.13: STRAINS

H/L	MORTAR	LOADING
0.33	1:4	TENSILE

Location of Dial Gauge (Distance in cm from top of Brickwork)		Pressure on jacks in psi	000	200	400	600	800	900
		Total load in tonnes	0.0	1.69	3.38	5.08	6.77	7.61
	3.8	Reading of dial gauge	10.41	10.44	10.47	10.50	10.53	10.545
		Strain $x10^{-5}$	0.0	-6.0	-12.0	-18.0	-24.0	-27.0
	19.2	Reading of dial gauge	2.34	2.36	2.38	2.405	2.43	2.445
		Strain $x10^{-5}$	0.0	-4.0	-8.0	-13.0	-18.0	-21.0
	34.6	Reading of dial gauge	0.47	0.485	0.50	0.515	0.535	0.545
		Strain $x10^{-5}$	0.0	-3.0	-6.0	-9.0	-13.0	-15.0
	50.0	Reading of dial gauge	1.23	1.24	1.25	1.26	1.27	1.275
		Strain $x10^{-5}$	0.0	-2.0	-4.0	-6.0	-8.0	-9.0

Table contd.. on page 126

Table 3.13 contd....

Pressure on jacks in psi			000	200	400	600	800	900
Total load in tonnes			0.0	1.69	3.38	5.08	6.77	7.61
Location of Dial Gauge (Distance in cm from top of Brickwork)	65.4	Reading of dial gauge	1.47	1.47	1.475	1.48	1.48	1.485
		Strain x10^{-5}	0.0	0.0	-1.0	-2.0	-2.0	-3.0
	80.7	Reading of dial gauge	2.34	2.34	2.335	2.335	2.33	2.325
		Strain x10^{-5}	0.0	0.0	1.0	1.0	2.0	3.0
	96.1	Reading of dial gauge	4.32	4.31	4.30	4.29	4.28	4.275
		Strain x10^{-5}	0.0	2.0	4.0	6.0	8.0	9.0
Remark			Separation starts					

TABLE 3.14 : STRAINS

H/L	MORTAR	LOADING
0.33	1:5	TENSILE

Location of Dial Gauge (Distance in cm from top of Brickwork)		Pressure on jacks in psi	000	200	400	600	700	800
		Total load in tonnes	0.0	1.692	3.4	5.07	5.92	6.77
	3.8	Reading of dial gauge	1.06	1.09	1.13	1.17	1.19	1.21
		Strain $x10^{-5}$	0.0	-6.0	-14.0	-22.0	-26.0	-30.0
	19.2	Reading of dial gauge	7.31	7.34	7.37	7.40	7.415	7.43
		Strain $x10^{-5}$	0.0	-6.0	-12.0	-18.0	-21.0	-24.0
	34.6	Reading of dial gauge	6.38	6.40	6.425	6.445	6.455	6.47
		Strain $x10^{-5}$	0.0	-4.0	-9.0	-13.0	-15.0	-18.0
	50.0	Reading of dial gauge	2.46	2.47	2.485	2.50	2.505	2.515
		Strain $x10^{-5}$	0.0	-2.0	-5.0	-8.0	-9.0	-11.0

Table contd.....on page 128

Table 3.14 contd....

Location of Dial Gauge (Distance in cm from top of Brickwork)		Pressure on jacks in psi	000	200	400	600	700	800
		Total load in tonnes	0.0	1.692	3.4	5.07	5.92	6.77
	65.4	Reading of dial gauge	9.28	9.285	9.29	9.295	9.295	9.30
		Strain $\times 10^{-5}$	0.0	-1.0	-2.0	-3.0	-3.0	-4.0
	80.7	Reading of dial gauge	4.86	4.86	4.855	4.855	4.855	4.85
		Strain $\times 10^{-5}$	0.0	0.0	1.0	1.0	1.0	2.0
	50.1	Reading of dial gauge	1.27	1.26	1.25	1.235	1.23	1.225
		Strain $\times 10^{-5}$	0.0	2.0	4.0	7.0	8.0	9.0
		Remark	Separation starts					

TABLE 3.15: STRAINS

H/L	MORTAR	LOADING
0.33	1:6	TENSILE

Location of Dial Gauge (Distance from top of Brickwork in cm)		Pressure on jacks in psi	000	200	400	500	600	700
		Total load in tonnes	0.0	1.692	3.384	4.23	5.07	5.92
	3.8	Reading of dial gauge	1.36	1.40	1.445	1.47	1.495	1.52
		Strain $x10^{-5}$	0.0	-8.0	-17.0	-22.0	-27.0	-32.0
	19.2	Reading of dial gauge	2.76	2.79	2.83	2.85	2.87	2.89
		Strain $x10^{-5}$	0.0	-6.0	-14.0	-18.0	-22.0	-26.0
	34.6	Reading of dial gauge	7.31	7.335	7.365	7.38	7.395	7.41
		Strain $x10^{-5}$	0.0	-5.0	-11.0	-14.0	-17.0	-20.0
	50.0	Reading of dial gauge	2.005	2.02	2.04	2.05	2.06	2.07
		Strain $x10^{-5}$	0.0	-3.0	-7.0	-9.0	-11.0	-13.0

Table contd... on page 130

Table 3.15 contd....

Pressure on jacks in psi			000	200	400	500	600	700
Total load in tonnes			0.0	1.692	3.384	4.23	5.07	5.92
Location of Dial Gauge (Distance from top of Brickwork in cm)	65.4	Reading of dial gauge	12.54	12.545	12.555	12.56	12.565	12.57
		Strain $\times 10^{-5}$	0.0	-1.0	-3.0	-4.0	-5.0	-6.0
	80.7	Reading of dial gauge	1.76	1.76	1.76	1.76	1.76	1.755
		Strain $\times 10^{-5}$	0.0	0.0	0.0	0.0	0.0	1.0
	96.1	Reading of dial gauge	6.21	6.20	6.19	6.185	6.18	6.17
		Strain $\times 10^{-5}$	0.0	2.0	4.0	5.0	6.0	8.0
		Remark	Separation starts					

TABLE 3.16: FIRST CRACK AND FAILURE LOAD

H/L	LOADING
0.33	COMPRESSIVE

Specimen Number	Mortar	Date of casting	Date of Testing	First crack load in tonnes	Failure load in tonnes	Total failure load including self weight in tonnes =T.F.L.	Load factor = T.F.L. / Working load	Remarks
1	1:3	11.2.78	13.3.78	20.65	33.04	35.24	3.915	Bending failure cracking near mid span
2	1:4	2.6.77	2.7.77	16.52	28.91	31.11	3.45	-do-
3	1:5	18.6.77	20.7.77	13.54	27.07	29.27	3.25	Mixed failure cracking at mid span and supports
4	1:6	14.8.77	13.9.77	12.34	24.78	26.98	3.00	Cracking near supports
5	1:8	18.2.78	18.3.78	10.06	10.06	12.26	1.36	Cracking near supports diagonal tension failure

TABLE 3.17: FIRST CRACK AND FAILURE LOAD

H/L	LOADING
0.33	TENSILE

Specimen Number	Mortar	Date of casting	Date of testing	Ist crack load in tonnes	Failure load	Total failure load including self weight T.F.L.	Load factor= T.F.L. / Working load	Remark
6	1:3	21.2.77	7.4.77	8.46	16.50	18.70	2.08	Horizontal separation and diagonal tension failure
7	1:4	23.1.78	20.2.78	7.61	13.24	15.44	1.71	-do-
8	1:5	24.1.78	23.2.78	6.77	11.00	13.20	1.47	-do-
9	1:6	5.2.78	6.3.78	5.92	10.15	12.35	1.36	-do-
10	1:8	11.3.78	13.4.78	3.40	7.08	9.28	1.03	-do-

TABLE : 3.18 DEFLECTION

H/L	MORTAR	LOAD
0.25	1:6	COMPRESSIVE

Sl. No.	Pressure on jacks in psi	Load in tonnes	Location of Dial Gauge (Distance from Left End in cm)										Remark
			62.5		112.5		162.5		212.5		262.5		
			Reading of dial gauge	Deflection in mm	Reading of dial gauge	Deflection in mm	Reading of dial gauge	Deflection in mm	Reading of dial gauge	Deflection in mm	Reading of dial gauge	Deflection in mm	
1.	000	0.000	12.30	0.00	6.24	0.00	14.08	0.00	11.09	0.00	3.46	0.00	
2.	100	2.065	12.45	0.15	6.49	0.25	14.37	0.29	11.33	0.24	3.61	0.15	
3.	200	4.130	12.60	0.30	6.73	0.49	14.65	0.57	11.58	0.49	3.77	0.31	
4.	300	6.195	12.76	0.46	6.97	0.73	14.93	0.85	11.83	0.74	3.92	0.46	
5.	400	8.260	14.07	1.77	8.52	2.28	16.72	2.64	13.36	2.27	5.12	1.66-	First crack
6.	500	10.325	16.90	4.60	12.33	6.09	20.95	6.87	17.10	6.01	7.98	4.52	
7.	550	11.357	-	-	-	-	-	-	-	-	-	-	
8.	600	12.390	-	-	-	-	-	-	-	-	-	-	
9.	700	14.455	-	-	-	-	-	-	-	-	-	-	Failure

TABLE 3.19: DEFLECTIONS

H/L	MORTAR	LOADING
0.4	1:6	COMPRESSIVE

Sl. No.	Pressure on jacks in psi	Load in tonnes	Location of Dial Gauges (Distance from Left End in cm)										Remarks
			62.5		112.5		162.5		212.5		262.5		
			Reading of dial gauge	Deflection in mm	Reading of dial gauge	Deflection in mm	Reading of dial gauge	Deflection in mm	Reading of dial gauge	Deflection in mm	Reading of dial gauge	Deflection in mm	
1.	000	0.000	21.30	0.00	16.87	0.00	15.53	0.00	0.53	0.00	5.00	0.00	
2.	100	2.065	21.38	0.08	16.97	0.10	15.66	0.13	0.64	0.11	5.08	0.08	
3.	200	4.130	21.47	0.17	17.08	0.21	15.80	0.27	0.74	0.21	5.17	0.17	
4.	300	6.195	21.55	0.25	17.19	0.32	15.93	0.40	0.84	0.31	5.26	0.26	
5.	400	8.260	21.64	0.34	17.30	0.43	16.06	0.53	0.95	0.42	5.34	0.34	
6.	500	10.325	21.72	0.42	17.40	0.53	16.19	0.66	1.06	0.53	5.43	0.43	
7.	600	12.390	21.81	0.51	17.51	0.64	16.31	0.78	1.13	0.65	5.51	0.51	
8.	700	14.455	21.96	0.66	17.69	0.82	16.58	1.05	1.36	0.83	5.65	0.65	
9.	800	16.520	21.29	0.99	18.12	1.25	17.03	1.50	1.79	1.26	5.98	0.98	
10.	900	18.585	22.79	1.49	18.66	1.79	17.58	2.05	2.35	1.83	6.49	1.49-	First crack
11.	1000	20.650	23.64	2.34	19.67	2.80	18.68	3.15	3.39	2.86	7.32	2.32	
12.	1100	22.715	24.67	3.37	20.77	3.90	19.88	4.35	4.43	3.90	8.35	3.35	
13.	1200	24.780	1.30	5.00	22.90	6.03	22.10	6.57	6.53	6.00	9.98	4.98	
14.	1400	28.910	-	-	-	-	-	-	-	-	-	-	Failure

TABLE 3.20: DEFLECTIONS

H/L	MORTAR	LOADING
0.5	1:6	COMPRESSIVE

Sl. No.	Pressure on jacks in psi	Load in tonnes	Location of Dial Gauges (Distance in cm from left end)										Remarks
			62.5		112.5		162.5		212.5		262.5		
			Reading of dial gauge	Delfection in mm	Reading of dial gauge	Deflection in mm	Reading of dial gauge	Deflection in mm	Reading of dial gauge	Deflection in mm	Reading of dial gauge	Deflection in mm	
1.	000	0.000	9.52	0.00	22.16	0.00	14.91	0.00	13.18	0.00	6.86	0.00	
2.	100	2.065	9.57	0.05	22.29	0.08	15.01	0.10	13.26	0.08	6.91	0.05	
3.	200	4.130	9.62	0.10	22.32	0.16	15.11	-.20	13.34	0.16	6.95	0.90	
4.	300	6.195	9.66	0.14	22.40	0.24	15.20	0.29	13.42	0.24	7.00	0.14	
5.	400	8.260	9.71	0.19	22.49	0.33	15.30	0.39	13.52	0.34	7.04	0.18	
6.	500	10.325	9.75	0.23	22.57	0.41	15.40	0.49	13.60	0.42	7.09	0.23	
7.	600	12.390	9.80	0.28	22.65	0.49	15.51	0.60	13.69	0.51	7.15	0.29	
8.	700	14 455	9.85	0.33	22.73	0.57	15.62	0.71	13.78	0.60	7.21	0.35	
9.	800	16 520	9.91	0.39	22.81	0.65	15.73	0.82	13.86	0.68	7.27	0.41	
10.	900	18 585	9.97	0.45	22.89	0.73	15.84	0.93	13.94	0.76	7.33	0.47	
11.	1000	20.650	10.12	0.60	23.09	0.93	16.13	1.22	14.13	0.95	7.48	0.62	
12.	1100	22.715	10.28	0.78	23.31	1.15	16.43	1.52	14.32	1.16	7.65	0.79	- First crack

Contd.....2

Table 3.20 contd...

Sl. No.	Pressure on jacks in psi	Load in tonnes	Location of Dial Gauges (Distance in cm from left end)										Remarks
			62.5		112.5		162.5		212.5		262.5		
			Reading of dial gauge	Deflection in mm	Reading of dial gague	Deflection in mm	Reading of dial gauge	Deflection in mm	Reading of dial gauge	Deflection in mm	Reading of dial gauge	Deflection in mm	
13.	1200	24.780	10.61	1.09	23.82	1.66	17.04	2.13	14.80	1.62	7.96	1.10	
14.	1300	26.845	10.92	1.40	24.41	2.25	17.74	2.83	15.44	2.26	8.28	1.42	
15.	1400	28.910	11.26	1.74	00.01	2.85	18.42	3.51	16.08	2.90	8.62	1.76	
16.	1500	30.975	12.19	2.67	1.75	4.59	21.44	6.53	17.68	4.50	9.56	2.70	
17.	1600	33.040	13.85	4.33	4.15	6.99	24.02	9.11	19.88	6.70	11.26	4.40	Failure

TABLE 3.21: DEFLECTIONS

H/L	MORTAR	LOADING
0.8	1:6	COMPRESSIVE

Sl. No.	Pressure on jacks in psi	Load in tonnes	Location of Dial Gauge (Distance from Left End in cm) 62.5		112.5		162.5		212.5		262.5		Remarks
			Reading of dial gage	Deflection in mm	Reading of dial gauge	Deflection in mm	Reading of dial gauge	Deflection in mm	Reading of dial gauge	Deflection in mm	Reading of dial gauge	Deflection in mm	
1.	000	0.00	23.51	0.00	16.00	0.00	1.39	0.00	19.73	0.00	17.28	0.00	
2.	200	4.13	23.63	0.12	16.14	0.14	1.54	0.15	19.86	0.13	17.41	0.13	
3.	400	8.26	23.75	0.24	16.28	0.28	1.69	0.30	20.00	0.27	17.53	0.25	
4.	600	12.39	23.87	0.36	16.42	0.42	1.84	0.45	20.14	0.41	17.65	0.37	
5.	800	16.52	24.00	0.49	16.57	0.57	2.00	0.61	20.30	0.57	17.78	0.50	
6.	1000	20.65	24.14	0.63	16.74	0.74	2.18	0.79	20.48	0.75	17.91	0.63	
7.	1200	24.78	24.28	0.77	16.92	0.92	2.36	0.97	20.66	0.93	18.06	0.78-	First crack
8.	1400	28.91	24.47	0.96	17.16	1.16	2.62	1.23	20.91	1.18	18.25	0.97	
9.	1600	33.04	24.71	1.20	17.48	1.48	2.98	1.59	21.25	1.52	19.50	1.22	
10.	1800	37.17	0.02	1.51	17.92	1.92	3.51	2.12	21.69	1.96	18.82	1.54	
11.	2000	41.30	0.33	1.82	18.67	2.67	4.21	2.82	22.47	2.74	19.14	1.86	
12.	2200	45.43	0.92	2.41	20.24	4.24	7.51	6.12	24.09	4.36	19.75	2.47	
13.	2400	49.56	-	-	-	-	-	-	-	-	-	-	Failure

TABLE 3.22: DEFLECTIONS

H/L	MORTAR	LOADING
0.25	1:3	TENSILE

Sl. No.	Pressure on jacks in psi	Total loads in tonnes	Location of Dial Gauges (Distance from left end in cm)										Remarks
			62.5		112.5		162.5		212.5		262.5		
			Reading of dial gauge	Deflection in mm	Reading of dial gauge	Deflection in mm	Reading of dial gauge	Deflection in mm	Reading of dial gauge	Deflection in mm	Reading of dial gauge	Deflection in mm	
1.	000	0.000	19.14	0.00	6.24	0.00	3.44	0.00	7.07	0.00	8.12	0.00	
2.	100	0.846	19.20	0.06	6.34	0.10	3.56	.12	7.17	0.10	8.18	0.06	
3.	200	1.692	19.26	0.12	6.44	0.20	3.68	0.24	7.28	0.21	8.24	0.12	
4.	300	2.538	19.32	0.18	6.55	0.31	3.80	0.36	7.38	0.31	8.31	0.19	
5.	400	3.384	19.39	0.25	6.67	0.43	3.94	0.50	7.50	0.43	8.38	0.26	
6.	500	4.230	19.46	0.32	6.79	0.55	4.09	0.65	7.63	0.56	8.45	0.33	
7.	600	5.076	19.54	0.40	6.92	0.68	4.25	0.81	7.76	0.69	8.54	0.42	
8.	700	5.922	19.65	0.51	7.08	0.84	4.45	1.01	7.92	0.85	8.65	0.53	
9.	800	6.768	19.94	0.80	7.48	1.24	4.91	1.47	3.33	1.26	8.97	0.85	- Seperation starts
10.	900	7.614	20.33	1.19	8.31	2.07	5.82	2.38	9.15	2.08	9.35	1.23	
11.	1000	8.460	20.76	1.62	9.08	2.84	6.51	3.07	9.95	2.88	9.77	1.65	
12.	1100	9.306	21.27	2.13	10.15	3.91	7.72	4.28	11.03	3.96	10.31	2.19	
13.	1300	11.000	23.42	4.28	12.45	6.21	12.20	8.76	13.35	6.28	12.48	4.36	
14.	1500	12.690	-	-	-	-	-	-	-	-	-	-	Failure

TABLE 3.23 DEFLECTIONS

H/L	MORTAR	LOADING
0.4	1:3	TENSILE

Sl. No.	Pressure on jacks in psi	Total load in tonnes	Location of Dial Gauges (Distance from left end in cm)								Remarks
			62.5		112.5		162.5		212.5		
			Reading of dial gauge	Deflection in mm	Reading of dial gauge	Deflection in mm	Reading of dial gauge	Deflection in mm	Reading of dial gauge	Deflection in mm	
1.	000	0.000	11.06	0.00	14.70	0.00	1.80	0.00	3.78	0.00	11.90	0.00	
2.	200	1.692	11.10	0.04	14.75	0.05	1.86	0.06	3.83	0.05	11.94	0.04	
3.	400	3.384	11.14	0.08	14.80	0.10	1.92	0.12	3.88	0.10	11.98	0.08	
4.	600	5.076	11.19	0.13	14.85	0.15	1.98	0.18	3.94	0.16	12.02	0.12	
5.	800	6.768	11.25	0.19	14.92	0.22	2.06	0.26	4.01	0.23	12.08	0.18	
6.	1000	8.460	11.33	0.27	15.00	0.30	2.15	0.35	4.09	0.31	12.16	0.26	
7.	1200	10.152	11.41	0.35	15.09	0.39	2.25	0.45	4.17	0.39	12.25	0.35	
8.	1400	11.844	11.50	0.44	15.19	0.49	2.37	0.57	4.28	0.50	12.34	0.44	Seperation starts
9.	1600	13.536	11.84	0.78	15.79	1.09	3.21	1.41	4.89	1.11	12.70	0.80	
10.	1800	15.228	13.16	2.10	17.70	3.00	5.43	3.63	5.80	3.02	14.05	2.15	
11.	2000	16.920	14.20	3.14	19.28	4.58	8.75	6.95	9.65	5.87	15.14	3.24	
12.	2200	18.612	-	-	-	-	-	-	-	-	-	-	Failure

TABLE 3.24: DEFLECTIONS

H/L	MORTAR	LOADING
0.5	1:3	TENSILE

Sl. No.	Pre-ssure on jacks in psi	Total Load in tonnes	Location of Dial Gauges (Distance from left end in cm)										Remarks
			62.5		112.5		162.5		212.5		262.5		
			Reading of dial gauge	Deflection in mm	Reading of dial gauge	Deflection in mm	Reading of dial gauge	Deflection in mm	Reading of dial gauge	Deflection in mm	Reading of dial gauge	Deflection in mm	
1.	000	0.000	9.21	0.00	3.90	0.00	5.83	0.00	0.41	0.00	11.12	0.00	
2.	200	1.692	9.25	0.04	3.95	0.05	5.88	0.05	0.45	0.04	11.16	0.04	
3.	400	3.384	9.29	0.08	4.00	0.10	5.94	0.11	0.50	0.09	11.20	0.08	
4.	600	5.075	9.33	0.12	4.05	0.15	6.00	0.17	0.55	0.14	11.24	0.12	
5.	800	6.768	9.38	0.17	4.11	0.21	6.07	0.24	0.61	0.20	11.28	0.16	
6.	1000	8.460	9.44	0.23	4.17	0.27	6.15	0.32	0.67	0.26	11.34	0.22	
7.	1200	10.152	9.52	0.31	4.25	0.35	6.24	0.41	0.75	0.34	11.41	0.29	
8.	1400	11.844	9.61	0.40	4.34	0.44	6.35	0.52	0.83	0.42	11.50	0.38	
9.	1600	13.535	9.76	0.55	4.55	0.65	6.60	0.77	1.04	0.63	11.65	0.53	*
10.	1800	15.223	10.12	0.91	4.92	1.02	6.96	1.13	1.41	1.00	12.02	0.90	**
11.	2000	16.920	10.92	1.71	5.84	1.94	8.26	2.[illegible]3	2.29	1.88	12.78	1.66	***
12.	2200	18.612	12.47	3.26	7.91	4.01	12.29	6.46	4.27	3.86	14.31	3.19	
13.	2400	20.304	-	-	-	-	-	-	-	-	-	-	Failure

* Separation Ist layer. ** Separation 5th layer. *** Separation at 11th layer

TABLE 3.25: DEFLECTIONS

H/L	MORTAR	LOADING
0.8	1:3	TENSILE

Sl. No.	Pressure on jacks in psi	Total Load in tonnes	Location of Dial Gauge (Distance from left end in cm) 62.5 Reading of dial gauge	62.5 Deflection in mm	112.5 Reading of dial gauge	112.5 Deflection in mm	162.5 Reading of dial gauge	162.5 Deflection in mm	212.5 Reading of dial gauge	212.5 Deflection in mm	262.5 Reading of dial gauge	262.5 Deflection in mm	Remarks
1.	000	0.000	4.90	0.00	2.76	0.00	1.03	0.00	4.98	0.00	0.04	0.00	
2.	200	1.692	4.94	0.04	2.81	0.05	1.08	0.05	5.02	0.04	0.07	0.03	
3.	400	3.384	4.97	0.07	2.85	0.09	1.13	0.10	5.07	0.09	0.11	0.07	
4.	600	5.076	5.01	0.11	2.90	0.14	1.19	0.16	5.12	0.14	0.15	0.11	
5.	800	6.768	5.05	0.15	2.95	0.19	1.25	0.22	5.18	0.20	0.20	0.16	
6.	1000	8.460	5.10	0.20	3.01	0.25	1.32	0.29	5.24	0.26	0.25	0.21	
7.	1200	10.152	5.17	0.27	3.09	0.33	1.41	0.38	5.31	0.33	0.31	0.27	
8.	1400	11.844	5.25	0.35	3.18	0.42	1.51	0.48	5.40	0.42	0.39	0.35	
9.	1600	13.536	5.35	0.45	3.30	0.54	1.66	0.63	5.50	0.52	0.48	0.44–	Separation starts
10.	1800	15.228	5.59	0.69	3.64	0.88	2.08	1.05	5.84	0.86	0.71	0.67	
11.	2000	16.920	5.93	1.03	4.12	1.36	2.76	1.73	6.30	1.32	1.04	1.00	
12.	2200	18.612	6.66	1.76	4.77	2.01	4.17	3.14	6.97	1.99	1.75	1.71	
13.	2400	20.304	8.07	3.17	6.68	3.92	7.31	6.28	8.82	3.84	3.13	3.09	
14.	2650	22.420	-	-	-	-	-	-	-	-	-	-	Failure

TABLE 3 26: STRAINS

H/L	MORTAR	LOADING
0.25	1:6	COMPRESSIVE

Location of Dial Gauge (Distance in cm from top of Brickwork)		Pressure on jacks in psi	000	100	200	300	400
		Total loads in tonnes	0.0	2.065	4.13	6.195	8.26
	3.8	Reading of dial gauge	21.69	21.74	21.79	21.84	-
		Strain $x10^{-5}$	-0.0	-10.0	-20.0	-30.0	-
	11.3	Reading of dial gauge	1.78	1.82	1.865	1.91	-
		Strain $x10^{-5}$	-0.0	-8.0	-17.0	-26.0	-
	26.3	Reading of dial gauge	0.51	0.54	0.57	0.60	-
		Strain $x10^{-5}$	-0.0	-6.0	-12.0	-18.0	-
	41.3	Reading of dial gauge	4.04	4.555	4.07	4.085	-
		Strain $x10^{-5}$	-0.0	-3.0	-6.0	-9.0	

Table contd...on page 143

Table 3.26 contd..

Pressure on jacks in psi			000	100	200	300	400
Total load in tonnes			0.0	2.065	4.13	6.195	8.26
Location of Dial Gauge (Distance in cm from top of Brickwork)	56.3	Reading of dial gauge	11.60	11.60	11.60	11.60	-
		Strain $x10^{-5}$	0.0	0.0	0.0	0.0	
	71.3	Reading of dial gauge	11.80	11.79	11.775	11.76	-
		Strain $x10^{-5}$	0.0	2.0	5.0	8.0	-
Remark							First crack

TABLE 7 27 : STRAINS

H/L	MORTAR	LOADING
0.4	1:6	COMPRESSIVE

Location of Dial Gauge (Distance in cm from top of Brickwork)		Pressure in jacks in psi	000	200	400	600	700	800
		Total load in tonnes	0.0	4.13	8.26	12.39	14.455	16.52
	11.5	Reading of dial gauge	14.82	14.855	14.89	14.93	14.95	14.97
		Strain $x10^{-5}$	-0.0	-7.0	-14.0	-22.0	-26.0	-30.0
	26.7	Reading of dial gauge	1.61	1.64	1.67	1.70	1.715	1.73
		Strain $x10^{-5}$	-0.0	-6.0	-12.0	-18.0	-21.0	-24.0
	42.0	Reading of dial gauge	10.80	10.82	10.84	10.865	10.875	10.89
		Strain $x10^{-5}$	-0.0	-4.0	-8.0	-13.0	-15.0	-18.0
	57.2	Reading of dial gauge	7.40	7.415	7.43	7.445	7.45	7.46
		Strain $x10^{-5}$	-0.0	-3.0	-6.0	-9.0	-10.0	-12.0

Table contd... on page 145

Table 3.27 contd...

Pressure on jacks in psi			000	200	400	600	700	800
Total load in tonnes			0.0	4.13	8.26	12.39	14.455	16.52
Location of Dial Gauge (Distance in cm from top of Brickwork)	72.5	Reading of dial gauge	1.16	1.17	1.18	1.19	1.195	1.20
		Strain $\times 10^{-5}$	-0.0	-2.0	-4.0	-6.0	-7.0	-8.0
	87.8	Reading of dial gauge	0.11	0.11	0.115	0.12	0.12	0.125
		Strain $\times 10^{-5}$	-0.0	-0.0	-1.0	-2.0	-2.0	-3.0
	103.0	Reading of dial gauge	1.79	1.785	1.78	1.775	1.775	1.77
		Strain $\times 10^{-5}$	0.0	1.0	2.0	3.0	3.0	4.0
	118.3	Reading of dial gauge	4.09	4.08	4.065	4.05	4.045	4.035
		Strain $\times 10^{-5}$	0.0	2.0	5.0	8.0	9.0	11.0
		Remark	First crack at 18.585 tonnes					

TABLE 3.28: STRAINS	H/L	MORTAR	LOADING
	0.5	1:6	COMPRESSIVE

Location of Dial Gauge (Distance from top of Brickwork in cm)		Pressure on jacks in psi	000	200	400	600	800	1000
		Total load in tonnes	0.0	4.13	8.26	12.39	16.52	20.65
	6.0	Reading of dial gauge	1.04	1.06	1.085	1.11	1.135	1.16
		Strain $x10^{-5}$	-0.0	-4.0	-9.0	-14.0	-19.0	-24.0
	13.6	Reading of dial gauge	18.84	18.86	18.88	18.905	18.925	18.95
		Strain $x10^{-5}$	-0.0	-4.0	-8.0	-13.0	-17.0	-22.0
	28.8	Reading of dial gauge	5.055	5.07	5.09	5.11	5.13	5.15
		Strain $x10^{-5}$	-0.0	-3.0	-7.0	-11.0	-15.0	-19.0
	44.0	Reading of dial gauge	0.32	0.335	0.35	0.365	0.38	0.40
		Strain $x10^{-5}$	-0.0	-3.0	-6.0	-9.0	-12.0	-16.0
	59.2	Reading of dial gauge	2.24	2.25	2.265	2.275	2.29	2.305
		Strain $x10^{-5}$	-0.0	-2.0	-5.0	-7.0	-10.0	-13.0

Table contd. .. on page

Table 3.28 contd...

Location of Dial Gauge (Distance from top of Brickwork in cm)								
Pressure on jacks in psi			000	200	400	600	800	1000
Total load in tonnes			0.0	4.13	8.26	12.39	16.52	20.65
	74.4	Reading of dial gauge	7.40	7.41	7.42	7.43	7.44	7.45
		Strain $x10^{-5}$	-0.0	-2.0	-4.0	-6.0	-8.0	-10.0
	89.6	Reading of dial gauge	1.0	1.005	1.015	1.02	1.025	1.035
		Strain $x10^{-5}$	-0.0	-1.0	-3.0	-4.0	-5.0	-7.0
	104.8	Reading of dial gauge	5.79	5.79	5.79	5.79	5.79	5.79
		Strain $x10^{-5}$	0.0	0.0	0.0	0.0	0.0	0.0
	120.0	Reading of dial gauge	9.98	9.98	9.98	9.98	9.98	9.98
		Strain $x10^{-5}$	0.0	0.0	0.0	0.0	0.0	0.0
	135.2	Reading of dial gauge	7.26	7.255	7.25	7.24	7.235	7.225
		Strain $x10^{-5}$	0.0	1.0	2.0	4.0	5.0	7.0
	150.4	Reading of dial gauge	6.66	6.65	6.635	6.625	6.61	6.595
		Strain $x10^{-5}$	0.0	2.0	5.0	7.0	10.0	13.0
		Remark	First crack at 22.715 tonnes					

TABLE 3.29: STRAINS

H/L	MORTAR	LOADING
0.8	1:6	COMPRESSIVE

Location of Dial Gauge (Distance from top of Brickwork in cm)		Pressure on jacks in psi	000	200	400	600	800	1000
		Total load in tonnes	0.0	4.13	8.26	12.39	16.52	20.65
3.75		Reading of dial gauge	23.37	23.375	23.385	23.395	23.405	23.415
		Strain $x10^{-5}$	-0.0	-1.0	-3.0	-5.0	-7.0	-9.0
18.75		Reading of dial gauge	21.08	21.085	21.09	21.10	21.105	21.115
		Strain $x10^{-5}$	-0.0	-1.0	-2.0	-4.0	-5.0	-7.0
48.75		Reading of dial gauge	4.31	4.31	4.315	4.315	4.325	4.335
		Strain $x10^{-5}$	-0.0	-0.0	-1.0	-1.0	-3.0	-5.0
78.75		Reading of dial gauge	2.18	2.185	2.19	2.195	2.20	2.205
		Strain $x10^{-5}$	-0.0	-1.0	-2.0	-3.0	-4.0	-5.0

Table contd... on page 149

Table 3.29 contd...

Location of Dial Gauge (Distance from top of Brickwork in mm)		Pressure on jacks in psi	000	200	400	600	800	1000
		Total load in tonnes	0.0	4.13	8.26	12.39	16.52	20.65
	108.75	Reading of dial gauge	9.26	9.26	9.27	9.275	9.28	9.285
		Strain $\times 10^{-5}$	-0.0	-0.0	-2.0	-3.0	-4.0	-5.0
	138.75	Reading of dial gauge	0.36	0.36	0.365	0.37	0.37	0.38
		Strain $\times 10^{-5}$	-0.0	-0.0	-1.0	-2.0	-2.0	-4.0
	168.75	Reading of dial gauge	0.02	0.025	0.025	0.03	0.04	0.045
		Strain $\times 10^{-5}$	-0.0	-1.0	-1.0	-2.0	-4.0	-5.0
	198.75	Reading of dial gauge	1.36	1.36	1.36	1.36	1.36	1.36
		Strain $\times 10^{-5}$	0.0	0.0	0.0	0.0	0.0	0.0
	228.75	Reading of dial gauge	2.73	2.73	2.73	2.73	2.73	2.73
		Strain $\times 10^{-5}$	0.0	0.0	0.0	0.0	0.0	0.0
	251.75	Reading of dial gauge	1.04	1.035	1.03	1.02	1.015	1.005
		Strain $\times 10^{-5}$	0.0	1.0	2.0	4.0	5.0	7.0
		Remark	First crack at 24.78 tonnes					

TABLE 3 30 : STRAINS

H/L	MORTAR	LOADING
0.25	1:3	TENSILE

Location of Dial Gauge (Distance from top of Brickwork in cm)		Pressure on jacks in psi	000	100	200	300	500	700
		Total load in tonnes	0.0	0.846	1.692	2.538	4.23	5.922
3.8	Reading of dial gauge		3.61	3.62	3.635	3.645	3.675	3.705
3.8	Strain $x10^{-5}$		-0.0	-2.0	-5.0	-7.0	-13.0	-19.0
11.3	Reading of dial gauge		0.21	0.22	0.235	0.245	0.27	0.295
11.3	Strain $x10^{-5}$		-0.0	-2.0	-5.0	-7.0	-12.0	-17.0
26.3	Reading of dial gauge		2.13	2.135	2.145	2.15	2.165	2.185
26.3	Strain $x10^{-5}$		-0.0	-1.0	-3.0	-4.0	-7.0	-11.0
41.3	Reading of dial gauge		7.13	7.13	7.135	7.135	7.145	7.155
41.3	Strain $x10^{-5}$		-0.0	-0.0	-1.0	-1.0	-3.0	-5.0

Table contd.... on page 151

Table 3.30 contd....

Pressure on jacks in psi			000	100	200	300	500	700
Total load in tonnes			0.0	0.846	1.692	2.538	4.23	5.922
Location of Dial Gauge (Distance from top of Brickwork in cm)	56.3	Reading of dial gauge	9.86	9.86	9.86	9.86	9.86	9.86
		Strain $x10^{-5}$	0.0	0.0	0.0	0.0	0.0	0.0
	71.3	Reading of dial gauge	2.19	2.19	2.185	2.18	2.17	2.16
		Strain $x10^{-5}$	0.0	0.0	1.0	2.0	4.0	6.0
Remark			Separation starts at 6.768 tonnes					

TABLE 3.31: STRAINS

H/L	MORTAR	LOADING
0.4	1:3	TENSILE

Location of Dial Gauge (Distance from top of Brickwork in cm)		Pressure on jacks in psi	000	200	400	600	800	1000	1200
		Total load in tonnes	0.0	1.692	3.384	5.076	6.768	8.46	10.15
	11.5	Reading of dial gauge	1.76	1.77	1.785	1.795	1.81	1.82	1.835
	11.5	Strain $x10^{-5}$	-0.0	-2.0	-5.0	-7.0	-10.0	-12.0	-15.0
	26.7	Reading of dial gauge	2.01	2.02	2.03	2.04	2.05	2.06	2.07
	26.7	Strain $x10^{-5}$	-0.0	-2.0	-4.0	-6.0	-8.0	-10.0	-12.0
	42.0	Reading of dial gauge	5.71	5.715	5.725	5.73	5.74	5.745	5.755
	42.0	Strain $x10^{-5}$	-0.0	-1.0	-3.0	-4.0	-6.0	-7.0	-9.0
	57.2	Reading of dial gauge	3.18	3.185	3.19	3.195	3.20	3.205	3.21
	57.2	Strain $x10^{-5}$	-0.0	-1.0	-2.0	-3.0	-4.0	-5.0	-6.0

Table contd....on page 153

Table 3.31 contd...

Location of Dial Gauge (Distance from top of Brickwork in cm)									
Pressure on jacks in psi			000	200	400	600	800	1000	1200
Total load in tonnes			0.0	1.692	3.384	5.076	6.768	8.46	10.15
	72.5	Reading of dial gauge	2.14	2.14	2.145	2.145	2.15	2.15	2.155
		Strain $x10^{-5}$	-0.0	-0.0	-1.0	-1.0	-2.0	-2.0	-3.0
	87.8	Reading of dial gauge	7.42	7.42	7.42	7.42	7.42	7.42	7.42
		Strain $x10^{-5}$	0.0	0.0	0.0	0.0	0.0	0.0	0.0
	103.0	Reading of dial gauge	3.76	3.76	3.76	3.755	3.755	3.75	3.745
		Strain $x10^{-5}$	0.0	0.0	0.0	1.0	1.0	2.0	3.0
	118.3	Reading of dial gauge	1.28	1.275	1.27	1.265	1.26	1.255	1.25
		Strain $x10^{-5}$	0.0	1.0	2.0	3.0	4.0	5.0	6.0
Remark			Separation starts at 11.84 tonnes						

TABLE 3.32 : STRAINS

H/L	MORTAR	LOADING
0.5	1:3	TENSILE

Location of Dial Gauge (Distance from top of Brickwork in cm)		Pressure on jacks in psi	000	200	400	600	800	1000	1200	1400
		Total load in tonnes	0.0	1.692	3.384	5.076	6.768	8.46	10.15	11.84
	6.0	Reading of dial gauge	0.41	0.42	0.43	0.44	0.45	0.46	0.475	0.485
	6.0	Strain $x10^{-5}$	-0.0	-2.0	-4.0	-6.0	-8.0	-10.0	-13.0	-15.0
	21.2	Reading of dial gauge	4.99	4.995	5.005	5.015	5.02	5.03	5.04	5.05
	21.2	Strain $x10^{-5}$	-0.0	-1.0	-3.0	-5.0	-6.0	-8.0	-10.0	-12.0
	36.4	Reading of dial gauge	2.12	2.125	2.135	2.14	2.15	2.155	2.165	2.17
	36.4	Strain $x10^{-5}$	-0.0	-1.0	-3.0	-4.0	-6.0	-7.0	-9.0	-10.0
	51.6	Reading of dial gauge	6.28	6.285	6.29	6.295	6.30	6.305	6.31	6.315
	51.6	Strain $x10^{-5}$	-0.0	-1.0	-2.0	-3.0	-4.0	-5.0	-6.0	-7.0
	74.4	Reading of dial gauge	3.51	3.51	3.515	3.515	3.52	3.52	3.525	3.53
	74.4	Strain $x10^{-5}$	-0.0	-0.0	-1.0	-1.0	-2.0	-2.0	-3.0	-4.0

Table contd...on page 155

Table 3.32 contd...

Location of Dial Gauge (Distance from top of Brickwork in cm)		Pressure on jacks in psi	000	200	400	600	800	1000	1200	1400
		Total load in tonnes	0.0	1.692	3.384	5.076	6.768	8.46	10.15	11.84
	89.6	Reading of dial gauge	2.74	2.74	2.74	2.74	2.74	2.74	2.74	2.745
		Strain $x10^{-5}$	-0.0	-0.0	-0.0	-0.0	-0.0	-0.0	-0.0	-1.0
	104.8	Reading of dial gauge	3.41	3.41	3.41	3.41	3.41	3.41	3.41	3.41
		Strain $x10^{-5}$	0.0	0.0	0.0	0.0	0.0	0.0	0.0	0.0
	120.0	Reading of dial gauge	2.16	2.16	2.155	2.155	2.15	2.15	2.145	2.145
		Strain $x10^{-5}$	0.0	0.0	1.0	1.0	2.0	2.0	3.0	3.0
	135.2	Reading of dial gauge	9.24	9.24	9.235	9.23	9.225	9.22	9.215	9.21
		Strain $x10^{-5}$	0.0	0.0	1.0	2.0	3.0	4.0	5.0	6.0
	150.4	Reading of dial gauge	1.79	1.785	1.78	1.775	1.77	1.765	1.755	1.75
		Strain $x10^{-5}$	0.0	1.0	2.0	3.0	4.0	5.0	7.0	8.0
Remark			Separation starts at 13.526 tonnes							

TABLE 3.33 : FIRST CRACK AND FAILURE LOAD

MORTAR	LOADING
1:6	COMPRESSIVE

Speci-men number	H/L	Date of casting	Date of testing	First crack load in tonnes	Failure load in tonnes	Total failure load including self weight etc. =T.F.L. in tonnes	Load factor= T.F.L. / working load	Remarks
11	0.25	7.4.78	7.5.78	8.260	14.455	16.25	1.8	Failed due to diagonal tension
4	0.33	14.8.77	13.9.77	12.390	24.78	26.08	3.0	-do-
12	0.40	19.3.78	23.4.78	18.585	28.91	31.41	3.5	-do-
13	0.50	31.3.78	29.4.78	22.715	33.04	36.04	4.0	Failed due to diagonal tension and cracking of brickwork at supports
14	0.80	2.5.78	30.5.78	24.780	49.56	54.00	6.0	-do-

TABLE 3.34: FIRST CRACK AND FAILURE LOAD

MORTAR	LOADING
1:3	TENSILE

Speci-men number	H/L	Date of casting	Date of testing	First crack load in tonnes	Failure load in tonnes	Total failure load including self weight etc.=T.F.L.	Load factor = $\frac{T.F.L.}{\text{Working load}}$	Remarks
15	0.25	19.7.78	17.8.78	6.768	12.690	14.450	1.610	Failed due to separation and diagonal tension
6	0.33	21.2.77	7.4.77	8.500	16.500	18.700	2.080	-do-
16	0.40	27.7.78	24.8.78	11.844	18.612	21.100	2.340	-do-
17	0.50	7.8.78	7.9.78	13.536	20.304	23.304	2.556	-do-
18	0.80	14.8.78	13.9.78	13.536	22.420	26.920	2.980	-do-

TABLE 3.35: DEFLECTIONS

H/L	MORTAR	LOADING
0.25	1:3	TENSILE

Sl. No.	Pressure on jacks in psi	Total load in tonnes	Location of Dial Gauge (Distance from left end in cm)										Remarks
			62.5		112.5		162.5		212.5		262.5		
			Reading of dial gauge	Deflection in mm	Reading of dial gauge	Deflection in mm	Reading of dial gauge	Deflection in mm	Reading of dial gauge	Deflection in mm	Reading of dial gauge	Deflection in mm	
1.	000	0.000	6.27	0.00	12.98	0.00	7.74	0.00	1.13	0.00	2.88	0.00	
2.	200	1.692	6.39	0.12	13.14	0.16	7.93	0.19	1.19	0.16	2.99	0.11	
3.	400	3.384	6.51	0.24	13.31	0.33	8.12	0.38	1.45	0.32	3.11	0.23	
4.	600	5.076	6.67	0.40	13.47	0.49	8.32	0.58	1.61	0.48	3.27	0.39	
5.	800	6.768	6.87	0.60	13.68	0.70	8.55	0.81	1.81	0.68	3.47	0.59	
6.	1000	8.460	7.09	0.82	13.89	0.91	8.78	1.04	2.03	0.90	3.69	0.81	
7.	1200	10.152	7.33	1.06	14.19	1.21	9.15	1.41	2.31	1.18	3.92	1.04	
8.	1400	11.846	7.64	1.37	14.62	1.64	9.72	1.98	2.73	1.60	4.21	1.33	
9.	1600	13.536	8.09	1.82	15.37	2.39	10.77	3.03	3.46	2.33	4.63	1.75	- Separation starts
10.	1800	15.228	8.73	2.46	17.01	4.03	13.95	6.21	5.11	3.98	5.28	2.40	
11.	2000	16.920	-	-	-	-	-	-	-	-	-	-	Failure

Note: 24 connectors of 6 mm diameter has been used.

TABLE 3.36: DEFLECTIONS

H/L	MORTAR	LOADING
0.33	1:3	TENSILE

Sl. No.	Pre-ssure on jacks in psi	Total load in tonnes	Location of Dial Gauge (Distance from left end in cm)										Remarks
			62.5		112.5		162.5		212.5		262.5		
			Reading of dial gauge	Deflection in mm	Reading of dial gauge	Deflection in mm	Reading of dial gauge	Deflection in mm	Reading of dial gauge	Deflection in mm	Reading of dial gauge	Deflection in mm	
1.	000	0.000	12.76	0.00	3.72	0.00	6.16	0.00	16.30	0.00	13.66	0.00	
2.	200	1.692	12.88	0.12	3.86	0.14	6.30	0.14	16.43	0.13	13.77	0.11	
3.	400	3.384	13.00	0.24	4.00	0.28	6.45	0.29	16.57	0.27	13.89	0.23	
4.	600	5.076	13.13	0.37	4.15	0.43	6.61	0.45	16.72	0.42	14.02	0.36	
5.	800	6.768	13.28	0.52	4.39	0.67	6.91	0.75	16.95	0.65	14.17	0.51-	Separation and first crack starts
6.	1000	8.460	13.76	1.00	5.22	1.50	8.00	1.84	17.78	1.48	14.64	0.98	
7.	1200	10.152	14.90	2.14	7.22	3.50	10.61	4.45	19.76	3.46	15.74	2.08	
8.	1500	12.690	-	-	-	-	-	-	-	-	-	-	Failure

Note: 13 conn·ctors of 8 mm diameter has been used.

TABLE 3.37: DEFLECTIONS

H/L	MORTAR	LOADING
0.33	1:3	TENSILE

Sl. No.	Pressure on jacks in psi	Total load in tonnes	Location of Dial Gauge (Distance from left end in cm)										Remarks
			62.5		112.5		162.5		212.5		262.5		
			Reading of dial gauge	Deflection in mm	Reading of dial gauge	Deflection in mm	Reading of dial gauge	Deflection in mm	Reading of dial gauge	Deflection in mm	Reading of dial gauge	Deflection in mm	
1.	000	0.000	0.10	0.00	0.19	0.00	6.83	0.00	0.00	0.00	0.11	0.00	
2.	200	1.692	0.16	0.06	0.28	0.09	6.93	0.10	0.09	0.09	0.17	0.06	
3.	400	3.384	0.23	0.13	0.38	0.19	7.03	0.20	0.19	0.19	0.24	0.13	
4.	600	5.076	0.30	0.20	0.48	0.29	7.14	0.31	0.29	0.29	0.32	0.21	
5.	800	6.768	0.40	0.30	0.61	0.42	7.33	0.46	0.43	0.43	0.42	0.31	
6.	1000	8.460	0.55	0.45	0.77	0.58	7.46	0.63	0.60	0.60	0.57	0.46	
7.	1200	10 152	0.73	0.63	0.93	0.74	7.63	0.80	0.76	0.76	0.76	0.65	
8.	1400	11.844	0.92	0.82	1.10	0.91	7.81	0.98	0.93	0.93	0.95	0.84	
9.	1600	13.536	2.13	2.03	2.65	2.46	9.61	2.78	2.48	2.48	2.12	2.01	Separation starts
10.	1800	15.228	4.34	4.24	5.36	5.17	12.66	5.83	5.12	5.12	4.39	4.28	
11.	2000	16.920	7.51	7.41	8.88	8.69	16.24	9.41	8.59	8.59	7.46	7.35	
12.	2250	19.035	-	-	-	-	-	-	-	-	-	-	Failure

Note: 20 connectors of 6 mm diameter has been used.

TABLE 3.38: FIRST CRACK AND FAILURE LOAD

H/L	MORTAR	LOADING
0.33	1:3	TENSILE

Speci-men Number	Number and size of Connectors	Date of Casting	Date of Testing	First Crack Load in Tonnes	Failure Load in Tonnes	Total Failure Load including Self Weight etc. in Tonnes =T.F.L.	Load Factor = T.F.L. / Working Load	Remarks
6	13, of 6mm diameter	21.2.77	7.4.77	8.500	16.50	18.7	2.080	Failed due to horizontal seperation and diagonal tension
29	13, of 8 mm diameter	4.3.78	3.4.78	6.768	12.69	14.89	1.654	-do-
30	20, of 6 mm diameter	5.2.78	6.3.78	13.536	19.00	21.20	2.350	-do-

TABLE 3.39:

H/L	MORTAR	LOADING	TYPE OF OPENING
0.8	1:6	COMPRESSIVE	SYMMETRIC OPENING

Sl. No.	Pressure on jacks in psi	Total load in tonnes	Location of Dial Gauge (Distance from left end in cm)										Remarks
			62.5		112.5		162.5		212.5		262.5		
			Reading of dial gauge	Deflection in mm	Reading of dial gauge	Deflection in mm	Reading of dial gauge	Deflection in mm	Reading of dial gauge	Deflection in mm	Reading of dial gauge	Deflection in mm	
1.	000	0.00	7.71	0.00	3.78	0.00	3.35	0.00	2.47	0.00	5.89	0.00	
2.	200	4.13	7.82	0.11	3.92	0.14	3.50	0.15	2.61	0.14	6.01	0.12	
3.	400	8.26	7.94	0.23	4.07	0.29	3.66	0.31	2.76	0.29	6.13	0.24	
4.	600	12.39	8.06	0.35	4.21	0.43	3.81	0.46	2.91	0.44	6.26	0.37	
5.	800	16.52	8.18	0.47	4.36	0.58	3.96	0.61	3.05	0.58	6.38	0.49	
6.	1000	20.65	8.30	0.59	4.51	0.73	4.12	0.77	3.19	0.72	6.49	0.60	
7.	1200	24.78	8.47	0.76	4.70	0.92	4.33	0.98	3.40	0.93	6.66	0.77	First crack
8.	1400	28.91	8.69	0.98	4.92	1.14	4.56	1.21	3.62	1.15	6.88	0.99	
9.	1600	33.09	8.92	1.21	5.17	1.39	4.84	1.49	3.88	1.41	7.12	1.23	
10.	1800	37.17	9.18	1.47	5.45	1.67	5.14	1.79	4.16	1.69	7.38	1.49	
11.	2000	41.30	9.54	1.83	5.84	2.06	5.52	2.17	4.57	2.10	7.75	1.86	
12.	2200	45.43	10.64	2.93	8.42	4.64	9.13	5.78	7.16	4.69	8.87	2.98	
13.	2400	49.56	-	-	-	-	-	-	-	-	-	-	Failure

TABLE 3.40: DEFLECTIONS

H/L	MORTAR	LOADING	TYPE OF OPENING
0.8	1:6	COMPRESSIVE	SYMMETRIC DOOR

Sl. No.	Pressure on jacks in psi	Total load in tonnes	Location of Dial Gauge (Distance from left end in cm)										Remarks
			62.5		112.5		162.5		212.5		262.5		
			Reading of dial gauge	Deflection in mm	Reading of dial gauge	Deflection in mm	Reading of dial gauge	Deflection in mm	Reading of dial gauge	Deflection in mm	Reading of dial gauge	Deflection in mm	
1.	000	0.00	2.08	0.00	2.55	0.00	5.36	0.00	1.72	0.00	3.68	0.00	
2.	200	4.13	2.21	0.13	2.71	0.16	5.54	0.18	1.88	0.16	3.81	0.13	
3.	400	8.26	2.34	0.26	2.87	0.32	5.72	0.36	2.04	0.32	3.94	0.26	
4.	600	12.39	2.47	0.39	3.03	0.48	5.90	0.54	2.21	0.49	4.07	0.39	
5.	800	16.52	2.60	0.52	3.19	0.64	6.08	0.72	2.37	0.65	4.21	0.53	
6.	1000	20.65	2.73	0.65	3.36	0.81	6.27	0.91	2.54	0.82	4.34	0.66	
7.	1200	24.78	2.93	0.85	3.61	1.06	6.55	1.19	2.80	1.08	4.54	0.86	First crack
8.	1400	28.91	3.19	1.11	3.92	1.37	6.90	1.54	3.11	1.39	4.81	1.13	
9.	1600	33.04	3.45	1.37	4.23	1.68	7.30	1.94	3.41	1.69	5.07	1.39	
10.	1800	37.17	3.77	1.69	4.58	2.03	7.73	2.37	3.77	2.05	5.40	1.72	
11.	2000	41.30	4.14	2.06	5.07	2.52	8.29	2.93	4.27	2.55	5.78	2.10	
12.	2200	45.43	5.84	3.76	7.64	5.09	12.74	7.38	6.78	5.06	7.49	3.81	
13.	2400	-	-	-	-	-	-	-	-	-	-	-	

TABLE 3.41: DEFLECTIONS

H/L	MORTAR	LOADING	TYPE OF OPENING
0.8	1:6	COMPRESSIVE	UNSYMMETRIC WINDOW

Sl. No.	Pressure on jacks in psi	Total load in tonnes	Location of Dial Gauge (Distance from left end in cm)										Remark
			62.5		112.5		162.5		212.5		262.5		
			Reading of dial gauge	Deflection in mm	Reading of dial gauge	Deflection in mm	Reading of dial gauge	Deflection in mm	Reading of dial gauge	Deflection in mm	Reading of dial gauge	Deflection in mm	
1.	00C	0.00	0.38	0.00	6.14	0.00	8.65	0.00	2.44	0.00	5.99	0.00	
2.	200	4.13	0.51	0.13	6.31	0.17	8.85	0.20	2.61	0.17	6.10	0.11	
3.	400	8.26	0.64	0.26	6.48	0.34	9.05	0.40	2.78	0.34	6.21	0.22	
4.	600	12.39	0.77	0.39	6.66	0.52	9.25	0.60	2.95	0.51	6.32	0.33	
5.	800	16.52	0.91	0.53	6.85	0.71	9.46	0.81	3.13	0.69	6.44	0.45	First crack
6.	1000	20.65	1.20	0.82	7.25	1.11	9.90	1.25	3.47	1.03	6.66	0.67	
7.	1200	24.78	1.50	1.12	7.65	1.51	10.39	1.74	3.88	1.44	6.93	0.94	
8.	1400	28.91	2.50	2.12	8.95	2.81	11.70	3.05	4.70	2.26	7.63	1.64	
9.	1600	33.04	-	-	-	-	-	-	-	-	-	-	Failure

TABLE 3.42: DEFLECTIONS

H/L	MORTAR	LOADING	TYPE OF OPENING
0.8	1:6	COMPRESSIVE	UNSYMMETRIC DOOR

Sl. No.	Pressure on jacks in psi	Total load in tonnes	Location of Dial Gauge (Distance from left end in cm)										Remarks
			62.5		112.5		162.5		212.5		262.5		
			Reading of dial gauge	Deflection in mm	Reading of dial gauge	Deflection in mm	Reading of dial gauge	Deflection in mm	Reading of dial gauge	Deflection in mm	Reading of dial gauge	Deflection in mm	
1.	000	0.000	15.79	0.00	12.26	0.00	4.77	0.00	12.94	0.00	4.06	0.00	
2.	100	2.065	15.92	0.13	12.45	0.19	5.01	0.24	13.16	0.22	4.19	0.13	
3.	200	4.130	16.05	0.26	12.68	0.42	5.28	0.51	13.39	0.45	4.33	0.27	
4.	300	6.195	16.30	0.51	13.15	0.89	5.54	0.77	13.99	1.05	4.69	0.63	
5.	400	8.26	16.71	0.92	13.76	1.50	6.25	1.48	1[illegible].75	1.81	5.11	1.05	
6.	486	10.04	-	-	-	-	-	-	-	-	-	-	First crack and failure

Note: Supporting R.C. beam thickness 16 cm

TABLE 3.43: DEFLECTIONS

H/L	MORTAR	LOADING	TYPE OF OPENING
0.8	1:3	TENSILE	SYMMETRIC WINDOW

Sl. No.	Pressure on jacks in psi	Total load in tonnes	Location of Dial Gauge (Distance from left end in cm)										Remarks
			62.5		112.5		162.5		212.5		262.5		
			Reading of dial gauge	Deflection in mm	Reading of dial gauge	Deflection in mm	Reading of dial gauge	Deflection in mm	Reading of dial gauge	Deflection in mm	Reading of dial gauge	Deflection in mm	
1.	000	0.000	8.59	0.00	2.36	0.00	5.22	0.00	3.27	0.00	6.60	0.00	
2.	200	1.692	8.63	0.04	2.41	0.05	5.28	0.06	3.31	0.04	6.64	0.04	
3.	400	3.384	8.67	0.08	2.46	0.10	5.34	0.12	3.36	0.09	6.68	0.08	
4.	600	5.076	8.72	0.13	2.51	0.15	5.41	0.19	3.41	0.14	6.73	0.13	
5.	800	6.768	8.78	0.19	2.57	0.21	5.49	0.27	3.47	0.20	6.78	0.18	
6.	1000	8.46	8.84	0.25	2.64	0.28	5.57	0.35	3.54	0.27	6.84	0.24	
7.	1200	10.152	8.91	0.32	2.72	0.36	5.66	0.44	3.62	0.35	6.91	0.31	
8.	1400	11.846	8.99	0.44	2.80	0.49	5.75	0.53	3.70	0.43	6.98	0.38	
9.	1600	13.536	9.07	0.48	2.89	0.53	5.85	0.63	3.78	0.51	7.05	0.45	- Seperation starts
10.	1800	15.228	9.15	0.56	2.98	0.62	5.96	0.74	3.87	0.60	7.13	0.53	
11.	2000	16.920	9.60	1.01	3.68	1.32	6.95	1.73	4.56	1.29	7.59	0.99	
12.	2125	17.98	-	-	-	-	-	-	-	-	-	-	Failure

TABLE 3.44: DEFLECTIONS

H/L	MORTAR	LOADING	TYPE OF OPENING
0.8	1:3	TENSILE	SYMMETRIC DOOR

Sl. No.	Pressure on jacks in psi	Total load in tonnes	Location of Dial Gauge (Distance from left end in cm)										Remarks
			62.5		112.5		162.5		212.5		262.5		
			Reading of dial gauge	Deflection in mm	Reading of dial gauge	Deflection in mm	Reading of dial gauge	Deflection in mm	Reading of dial gauge	Deflection in mm	Reading of dial gauge	Deflection in mm	
1.	000	0.000	6.48	0.00	4.72	0.00	1.90	0.00	3.10	0.00	10.05	0.00	
2.	100	0.846	6.51	0.03	4.77	0.05	2.00	0.10	3.15	0.05	10.08	0.03	
3.	200	1.692	6.55	0.07	4.85	0.13	2.22	0.32	3.23	0.13	10.12	0.07	
4.	300	2.540	6.60	0.12	4.94	0.22	2.46	0.56	3.33	0.23	10.17	0.12	
5.	400	3.384	6.65	0.17	5.05	0.33	2.72	0.82	3.43	0.33	10.22	0.17	
6.	500	4.230	6.71	0.23	5.17	0.45	3.01	1.11	3.55	0.45	10.28	0.23	
7.	600	5.076	6.79	0.31	5.43	0.71	3.63	1.73	3.80	0.70	10.37	0.32	
8.	700	5.920	6.94	0.46	6.01	1.29	5.12	3.22	4.37	1.27	10.51	0.46	
9.	800	8.768	7.24	0.76	6.96	2.24	7.09	5.19	5.30	2.20	10.80	0.75	-Separation starts
10.	900	7.610	7.58	1.10	8.90	4.18	12.02	10.12	7.23	4.13	11.13	1.08	
11.	1000	8.460	7.98	1.50	11.00	6.28	18.13	16.23	9.31	6.21	11.52	1.47	
12.	1100	9.206	8.63	2.15	14.42	9.70	27.35	25.45	12.90	9.60	12.17	2.12	
13.	1200	10.152	-	-	-	-	-	-	-	-	-	-	Failure

TABLE 3.45: DEFLECTIONS

H/L	MORTAR	LOADING	TYPE OF OPENING
0.8	1:3	TENSILE	SYMMETRIC DOOR

Sl. No.	Pressure on jacks in psi	Total load in tonnes	Location of Dial Gauge (Distance from left end in cm)										Remarks
			62.5		112.5		162.5		212.5		262.5		
			Reading of dial gauge	Deflection in mm	Reading of dial gauge	Deflection in mm	Reading of dial gauge	Deflection in mm	Reading of dial gauge	Deflection in mm	Reading of dial gauge	Deflection in mm	
1.	000	0.000	6.50	0.00	3.36	0.00	5.98	0.00	4.35	0.00	9.17	0.00	
2.	100	0.846	6.52	0.02	3.40	0.04	6.03	0.05	4.39	0.04	9.19	0.02	
3.	200	1.692	6.54	0.04	3.44	0.08	6.10	0.12	4.43	0.08	9.21	0.04	
4.	300	2.540	6.56	0.06	3.49	0.13	6.17	0.19	4.47	0.12	9.23	0.06	
5.	400	3.384	6.60	0.10	3.57	0.21	6.29	0.31	4.56	0.21	9.28	0.11	
6.	500	4.23	6.67	0.17	3.71	0.35	6.58	0.60	4.71	0.36	9.36	0.19	
7.	600	5.076	6.76	0.26	3.88	0.52	6.93	0.95	4.88	0.53	9.45	0.28	
8.	700	5.920	6.89	0.39	4.11	0.75	7.29	1.31	5.12	0.77	9.58	0.41	
9.	800	6.768	7.02	0.52	4.37	1.01	7.70	1.72	5.39	1.04	9.72	0.55	- Separation and diagonal tension failure starts
10.	1000	8.460	7.40	0.90	5.11	1.75	8.77	2.79	6.13	1.78	10.10	0.93	
11.	1200	10.152	7.92	1.42	6.09	2.73	10.25	4.27	7.13	2.78	10.63	1.46	
12.	1400	11.846	8.91	2.41	8.12	4.76	13.40	7.42	9.19	4.84	11.64	2.47	
13.	1600	13.536	11.76	5.26	13.37	10.01	20.92	14.94	14.44	10.09	14.50	5.33	
14.	1900	16.074	-	-	-	-	-	-	-	-	-	-	Failure

Note: Supporting beam 16 cm thick

TABLE 3.46: DEFLECTIONS

H/L	MORTAR	LOADING	TYPE OF OPENING
0.8	1:3	TENSILE	UNSYMMETRIC WINDOW

Sl. No.	Pre-ssure on jacks in psi	Total Load in tonnes	Location of Dial Gauge (Distance from Left end in cm)										Remarks
			62.5		112.5		162.5		212.5		262.5		
			Read-ing of dial guage	Defle-ction in mm	Read-ing of dial gauge	Defle-ction in mm	Read-ing of dial gauge	Defle-ction in mm	Read-ing of dial gauge	Defle-ction in mm	Read-ing of dial gauge	Defle-ction in mm	
1.	000	0.000	1.12	0.00	4.46	0.00	8.05	0.00	2.61	0.00	0.00	0.00	
2.	200	1.692	1.17	0.05	4.53	0.07	8.13	0.08	2.68	0.07	0.04	0.04	
3.	400	3.384	1.25	0.13	4.62	0.16	8.22	0.17	2.76	0.15	0.10	0.10	
4.	600	5.076	1.34	0.22	4.71	0.25	8.32	0.27	2.85	0.24	0.19	0.19	
5.	800	6.768	1.50	0.38	4.86	0.40	8.48	0.43	2.98	0.37	0.29	0.29	
6.	1000	8.460	1.66	0.52	5.00	0.54	8.64	0.59	3.1[illegible]	0.51	0.43	0.43	
7.	1200	10.152	1.97	0.85	5.36	0.90	9.03	0.98	3.38	0.77	0.57	0.57	
8.	1400	11.846	2.38	1.26	6.17	1.71	10.13	2.08	3.67	1.06	0.75	0.75	
9.	1600	13.536	5.30	4.18	11.90	7.44	16.34	8.29	7.90	4.39	3.15	3.15	
10.	1850	1[illegible].65	-	-	-	-	-	-	-	-	-	-	Failure

TABLE 3.47 : FIRST CRACK AND FAILURE LOAD

H/L	MORTAR	LOADING
0.8	1:6	COMPRESSIVE

Specimen number	Thickness of R.C. beam in cm	Type of opening	Date of casting	Date of testing	First crack load in tonnes	Failure load in tonnes	Total failure load including self weight T.F.L.etc.	Load factor $=\frac{T.F.L.}{Working\ load}$	Remark
14	8	Nil	2.5.78	30.5.78	24.78	49.56	54.0	6.00	
19	8	Window symmetric	24.8.78	22.9.78	24.78	49.56	53.5	5.94	
20	8	Symmetric door	4.8.78	2.9.78	24.78	49.56	53.0	5.90	
21	8	Unsymmetric window	9.9.78	7.10.78	20.65	33.04	37.04	4.10	
22	8	Unsymmetric door	17.9.78	16.10.78	Nil	Nil	3.50	0.39	
23	16	Unsymmetric door	-	2.6.79	10.04	10.04	14.54	1.61	

TABLE 3.48: FIRST CRACK AND FAILURE LOAD

H/L	MORTAR	LOADING
0.8	1:3	TENSILE

Specimen number	Thickness of R.C. beam in cm	Type of opening	Date of costing	Date of testing	First crack load in tonnes	Failure load in tonnes	Total failure load including self weight etc.	Load factor = T.F.L. / Working load	Remarks
18	8	Nil	14.8.78	13.9.78	13.536	22.42	26.92	2.98	Separation and diagonal tension failure
24	8	Symmetric window	20.9.78	18.10.78	13.536	17.98	22.00	2.44	-do-
25	8	Symmetric door	1.9.78	29.9.78	6.768	10.152	13.65	1.51	R.C.beam failed in compression as well as in tension
26	8	Unsymmetric window	24.9.78	21.10.78	11.844	15.65	19.65	2.18	Separation and diagonal tension failure
27	16	Symmetric door	16.10.78	13.11.78	8.46	16.074	19.57	2.17	-do-

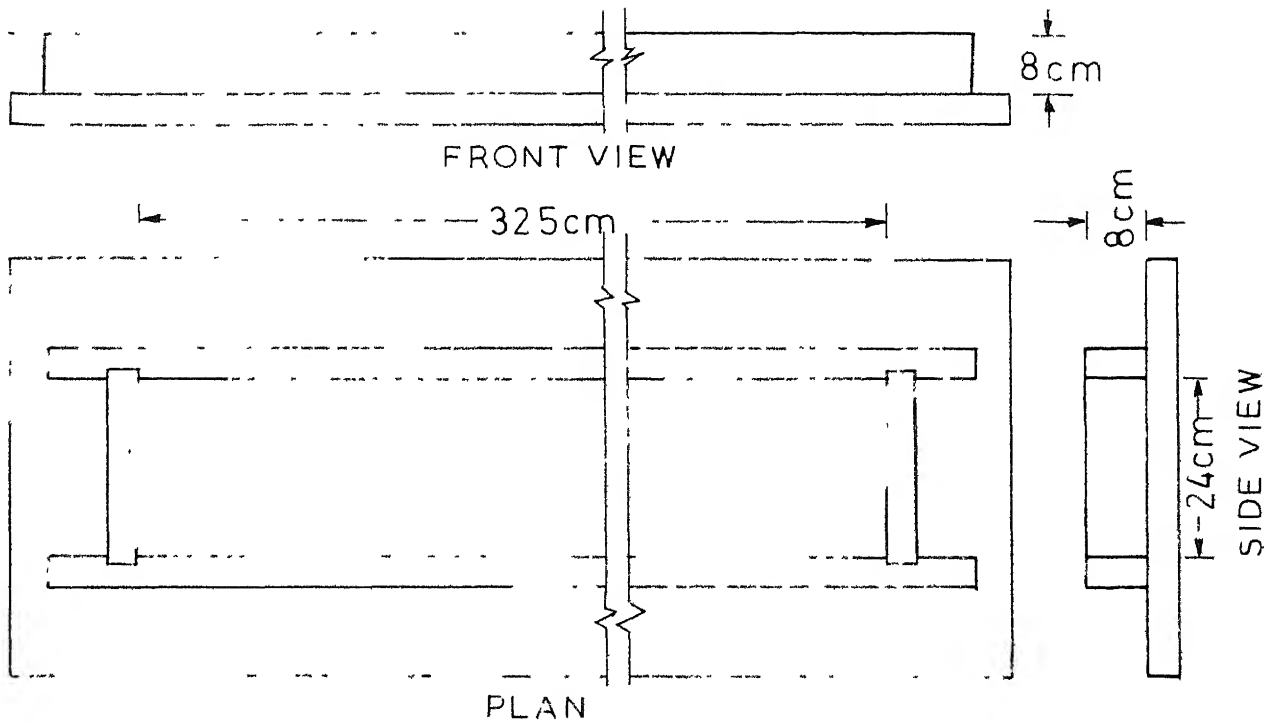

Fig. 3·1 (a) Mould for casting R.C. beams (Compressive loading)

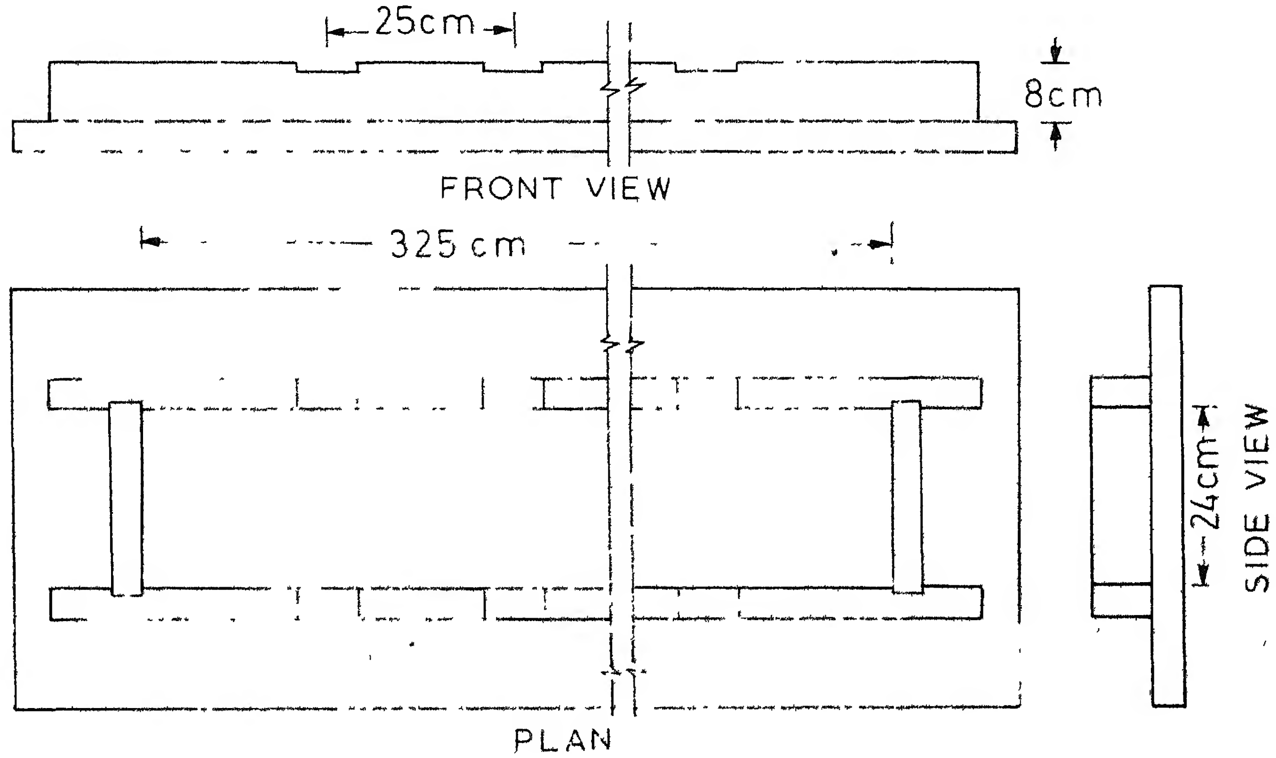

Fig. 3·1 (b) Mould for casting R.C. beams (Tensile loading)

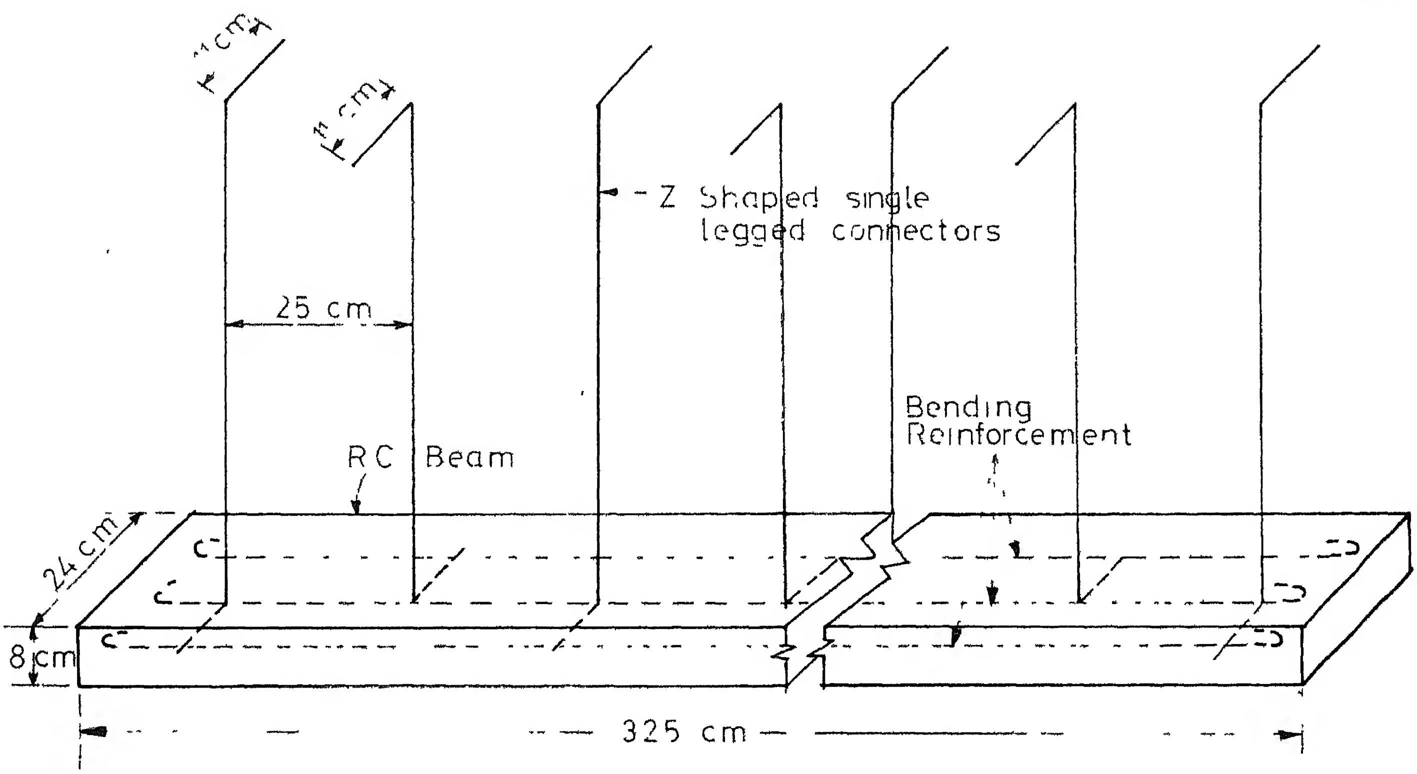

Fig.3·2 a Details of beam (Compressive loading)

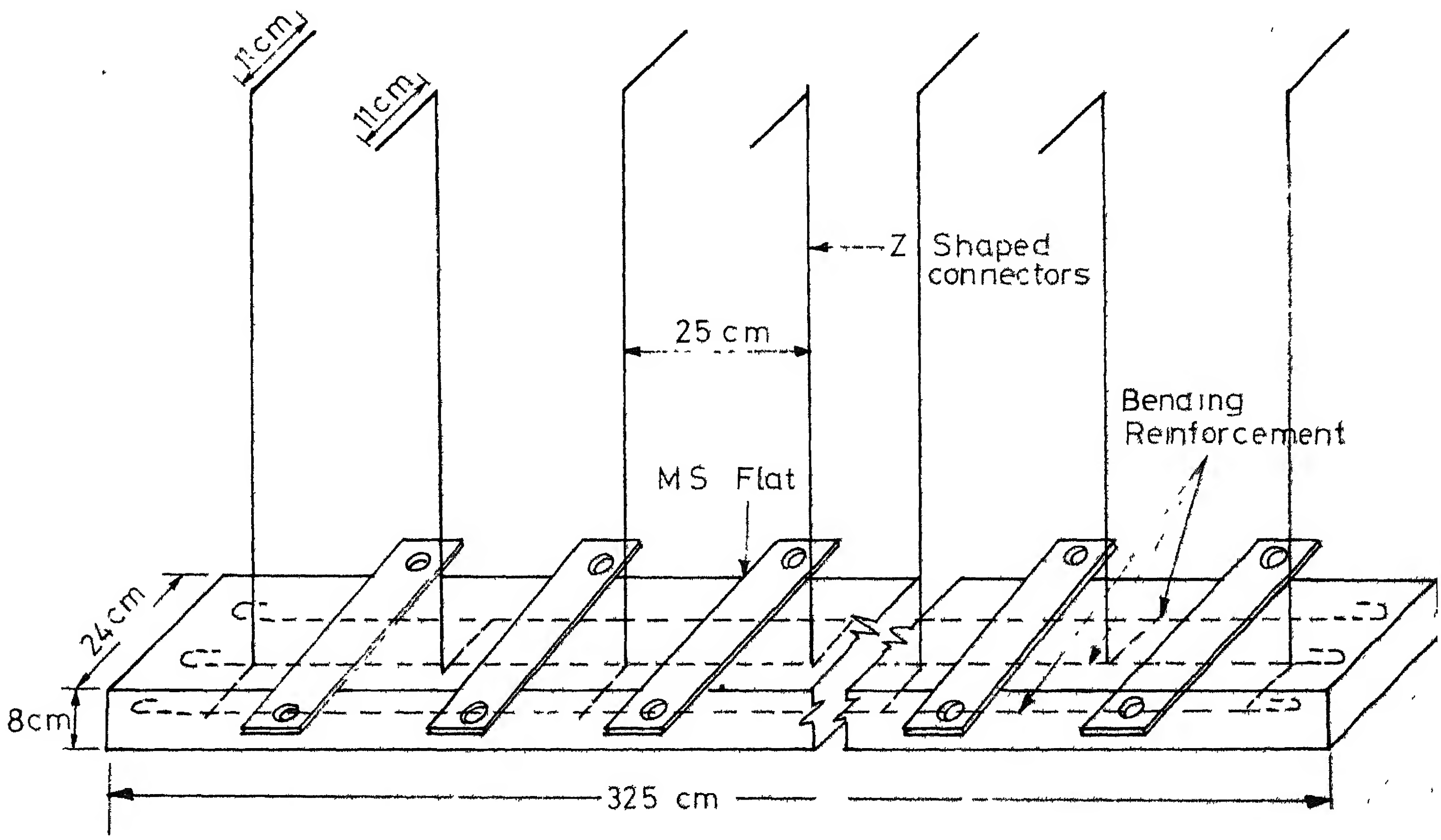

Fig. 3·2 b Details of beam (Tensile loading)

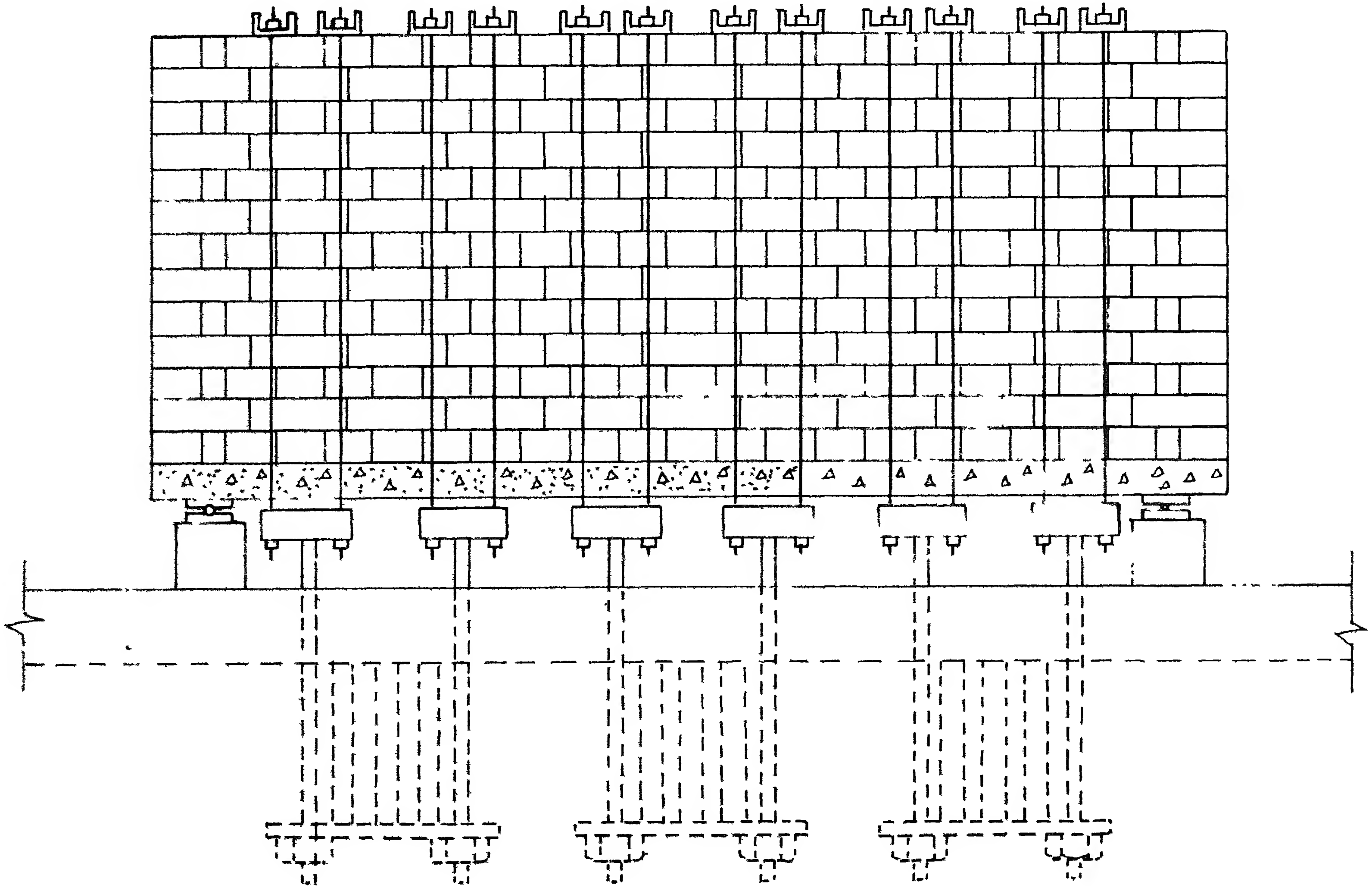

Fig.3·3 Loading arrangement (Compressive loading)

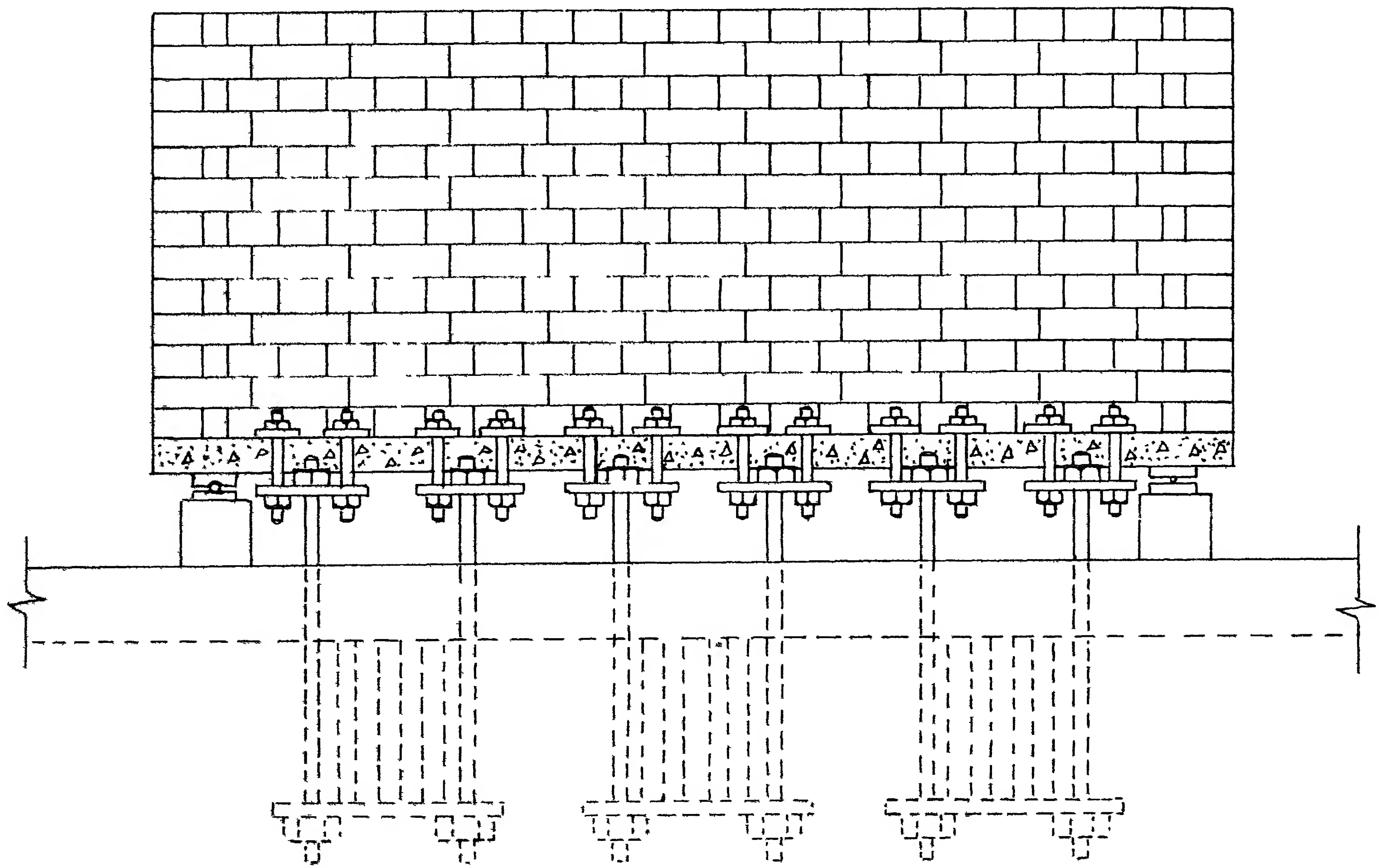

Fig.3·4 Loading arrangement (Tensile loading)

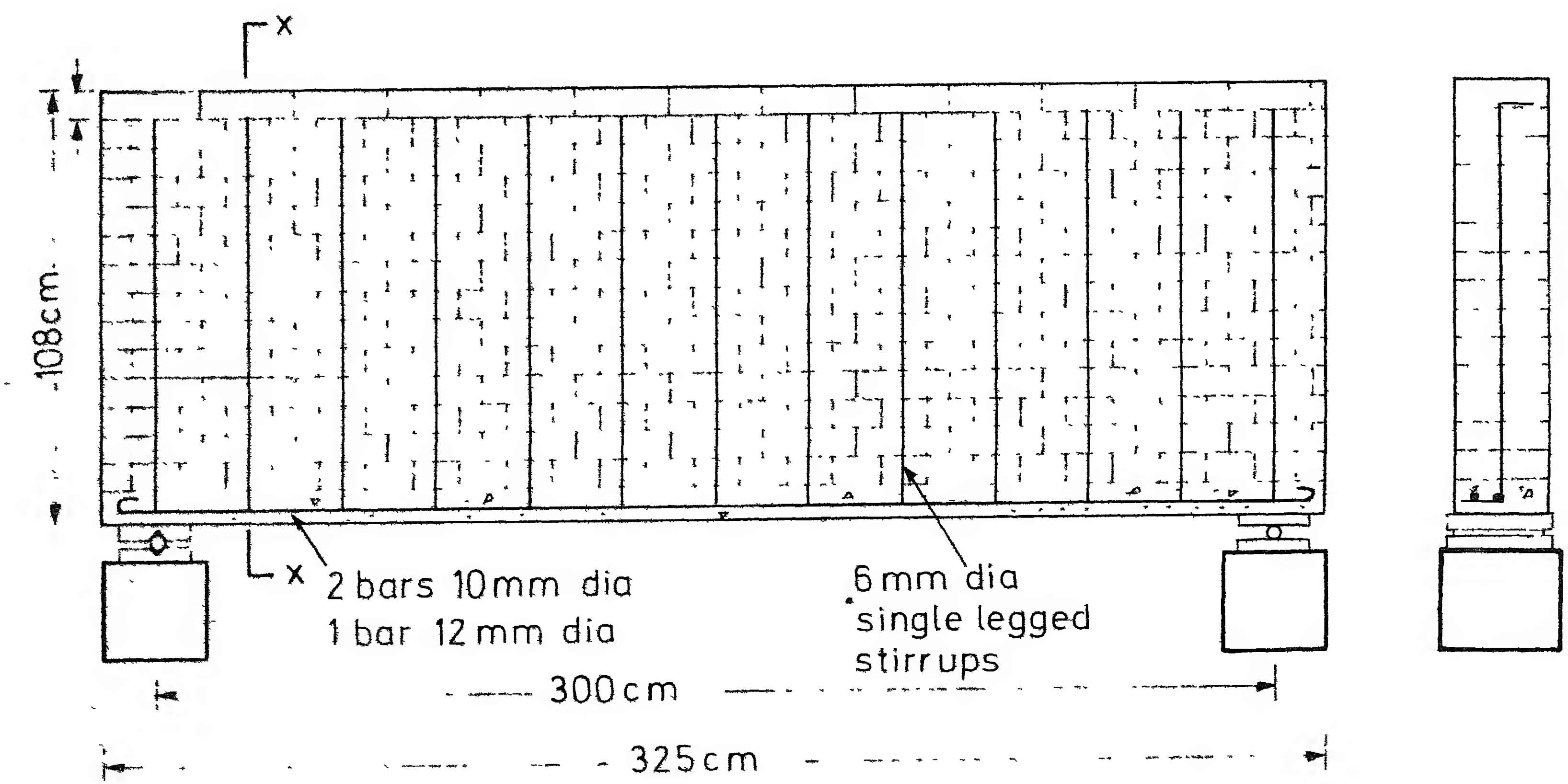

Fig.3·5 A Typical specimen

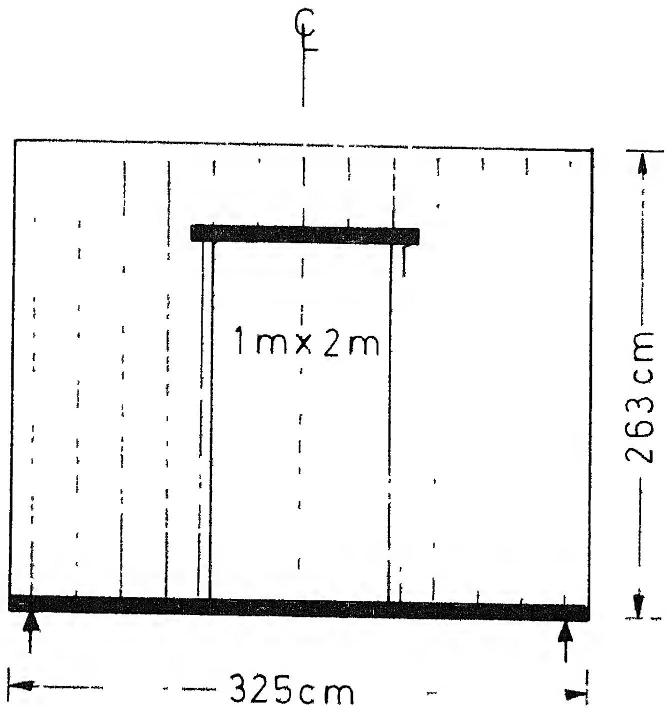

Specimen no. 20 and 25

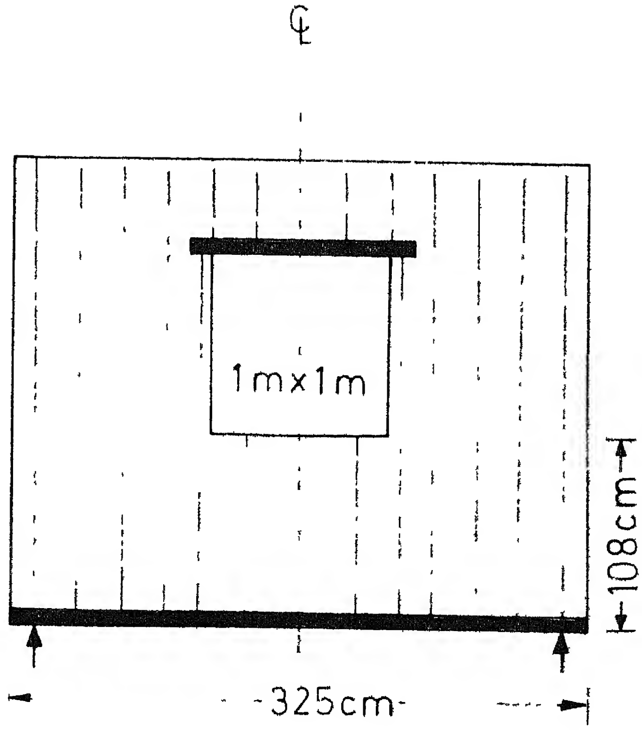

Specimen no. 19 and 24

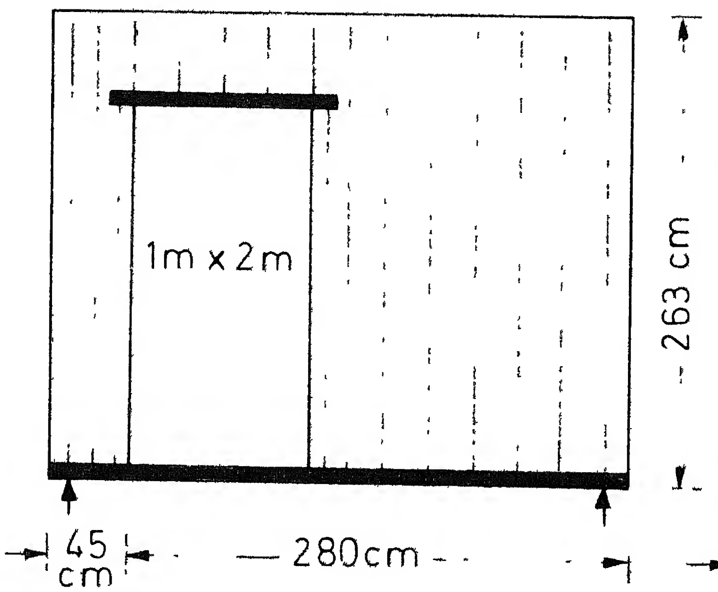

Specimen no. 22

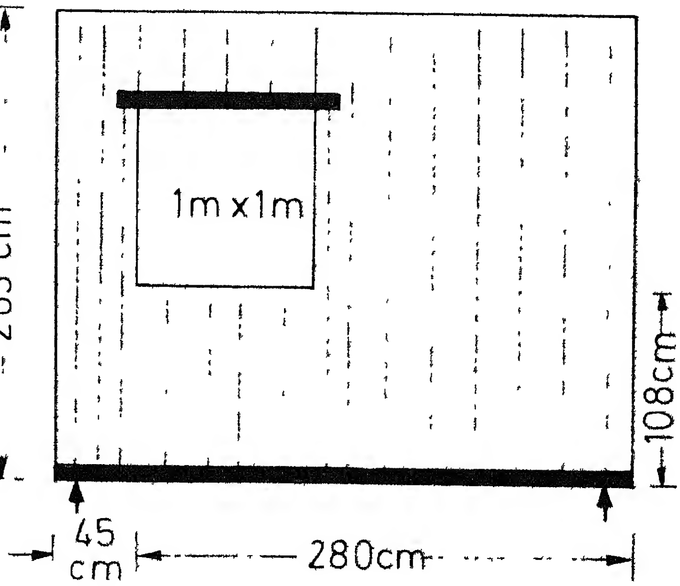

Specimen no. 21 and 26

Fig.3·6 Details of specimen with openings

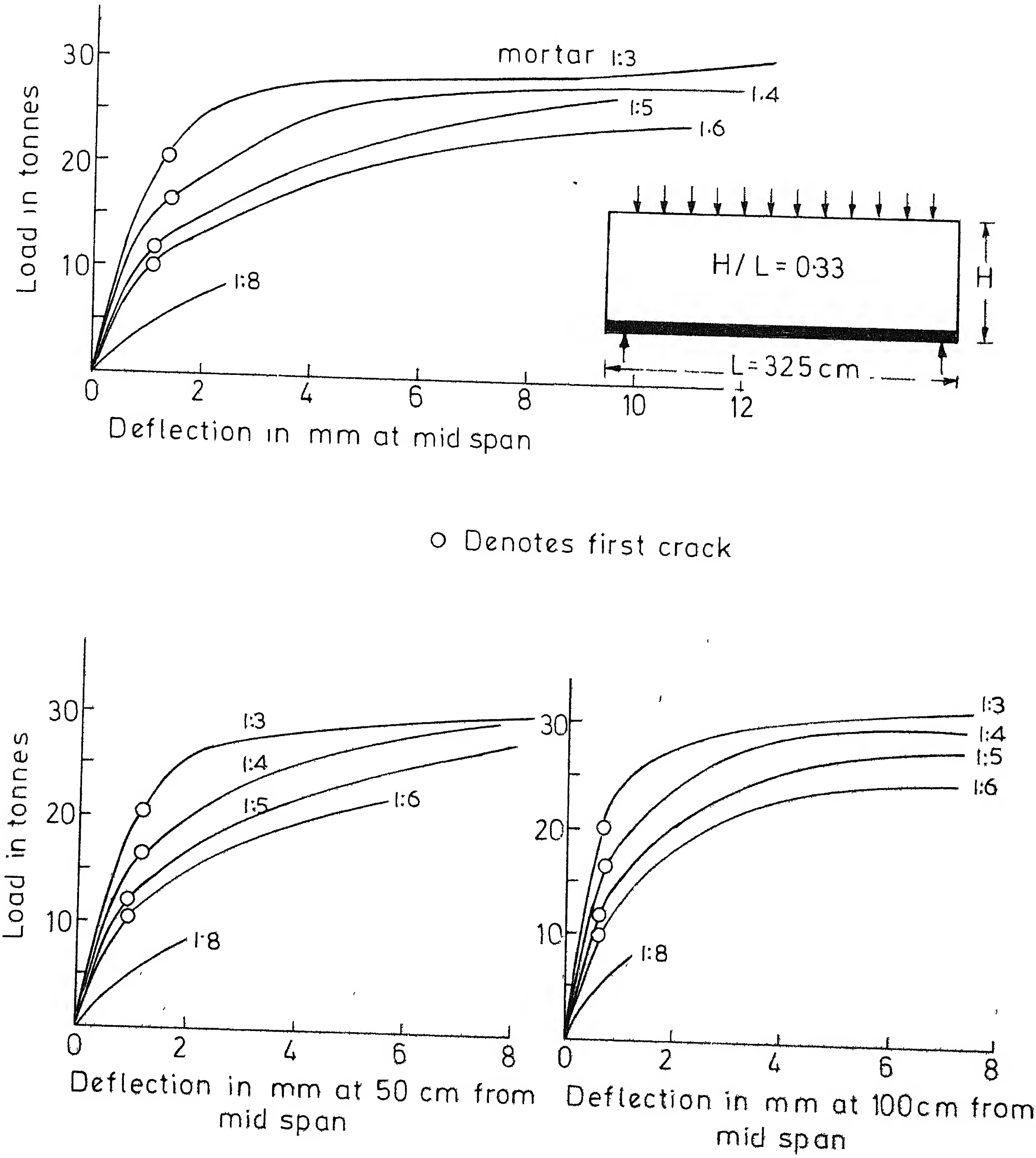

Fig. 3·7 Load versus vertical deflection curves (compressive loading)

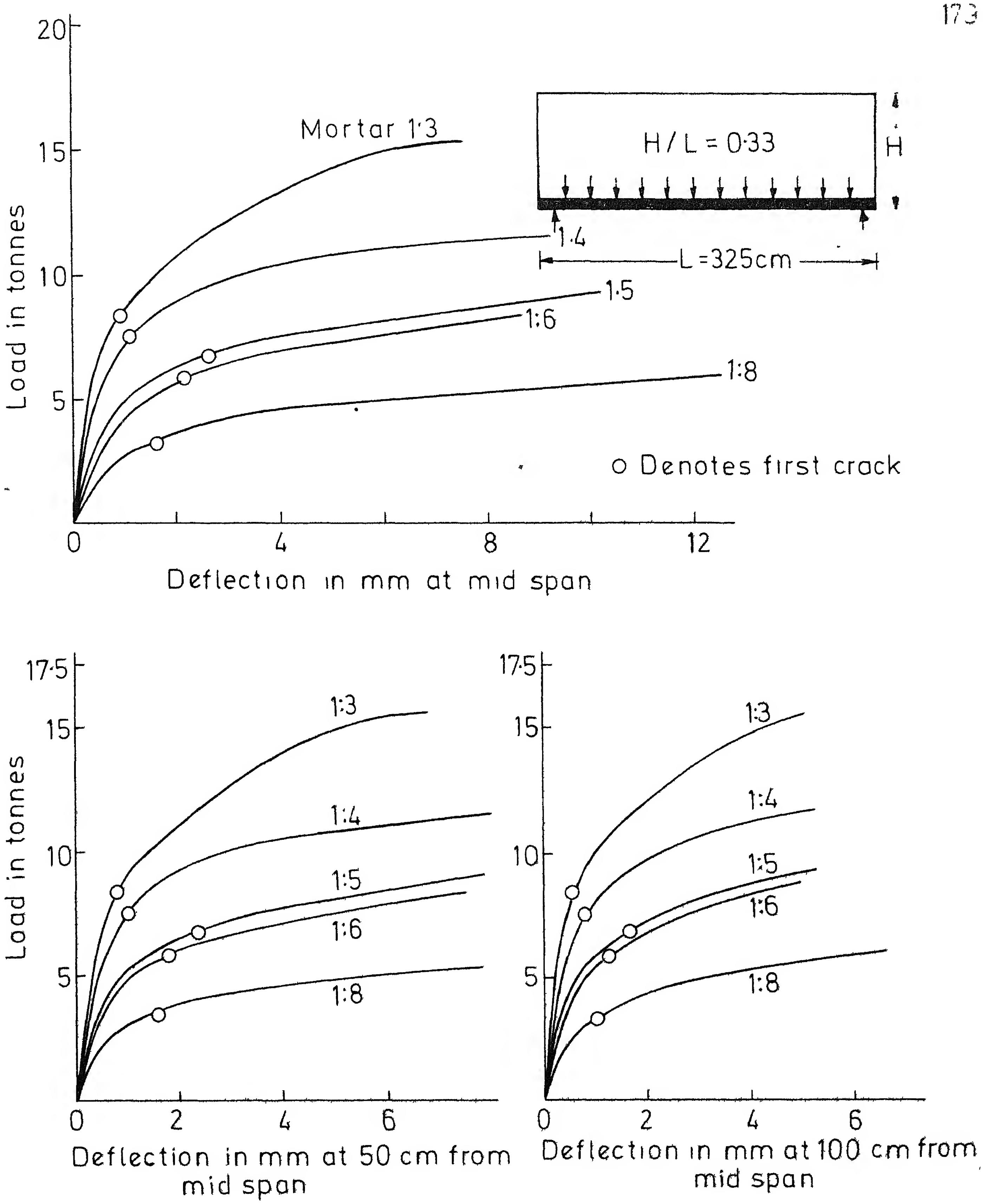

Fig.3·8 Load versus vertical deflection curves (Tensile loading)

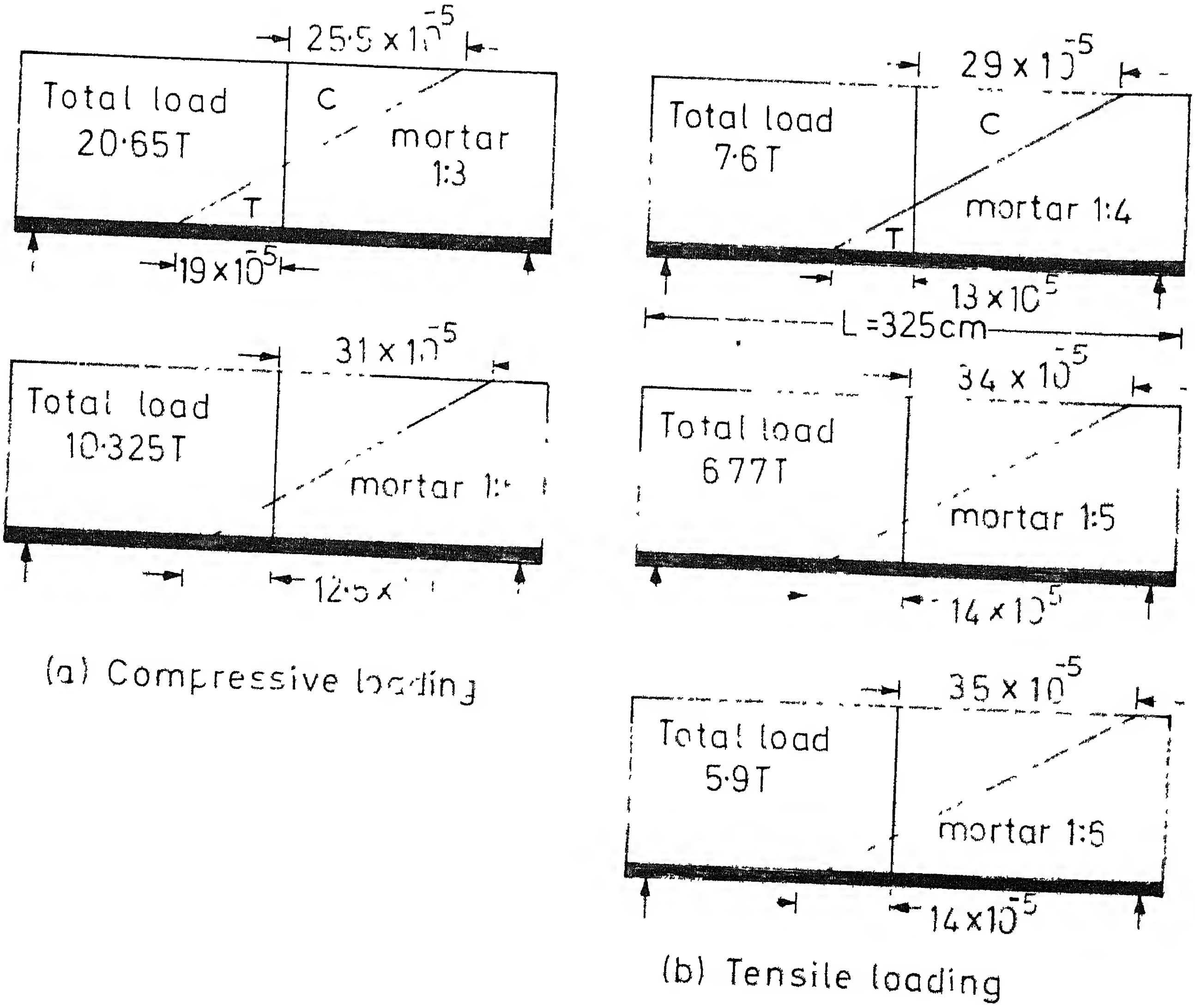

Fig. 3·9 Variation of longitudinal strain at mid span
(H/L = 0·33)

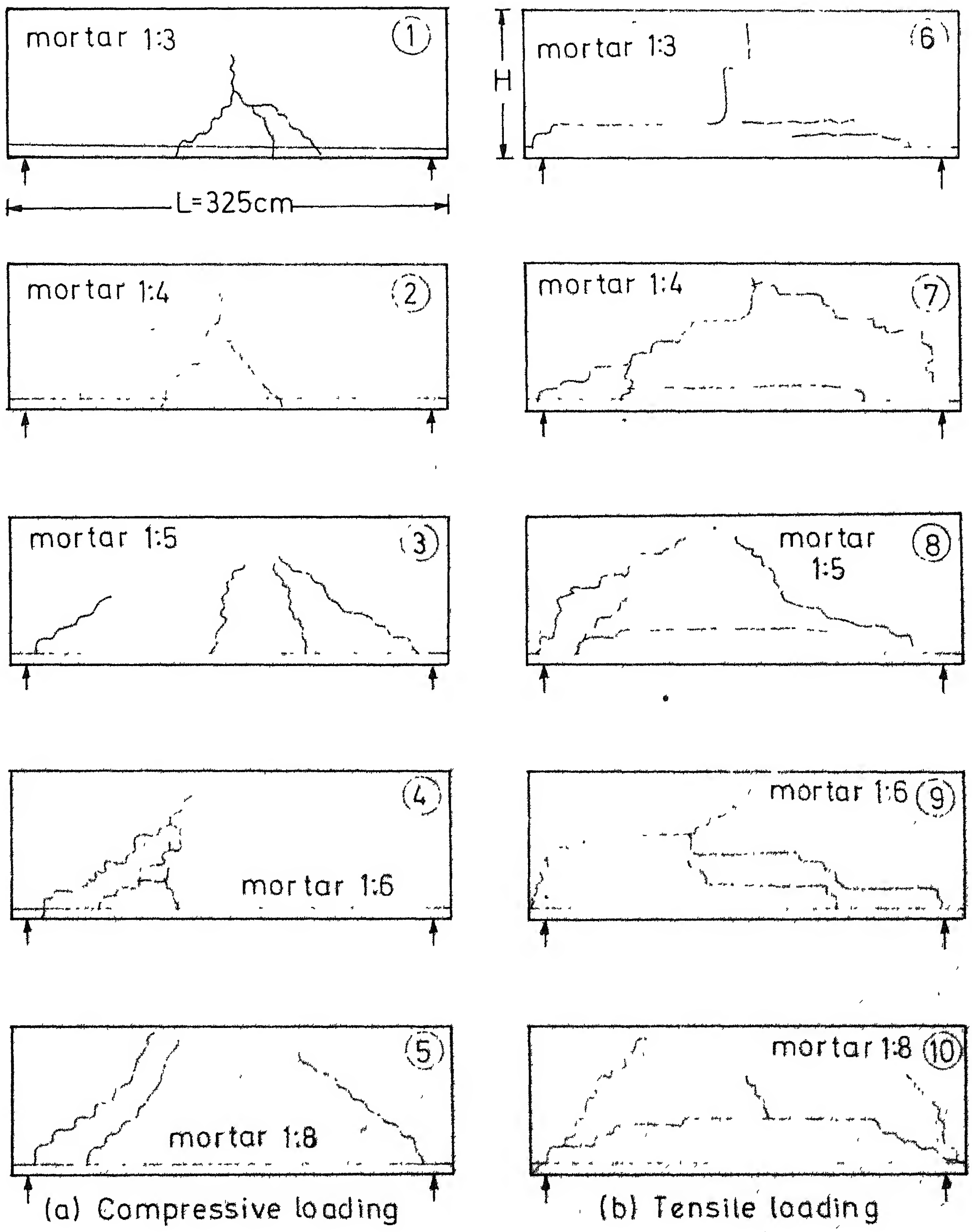

Fig.3·10 Crack pattern at failure (H/L= 0·33)

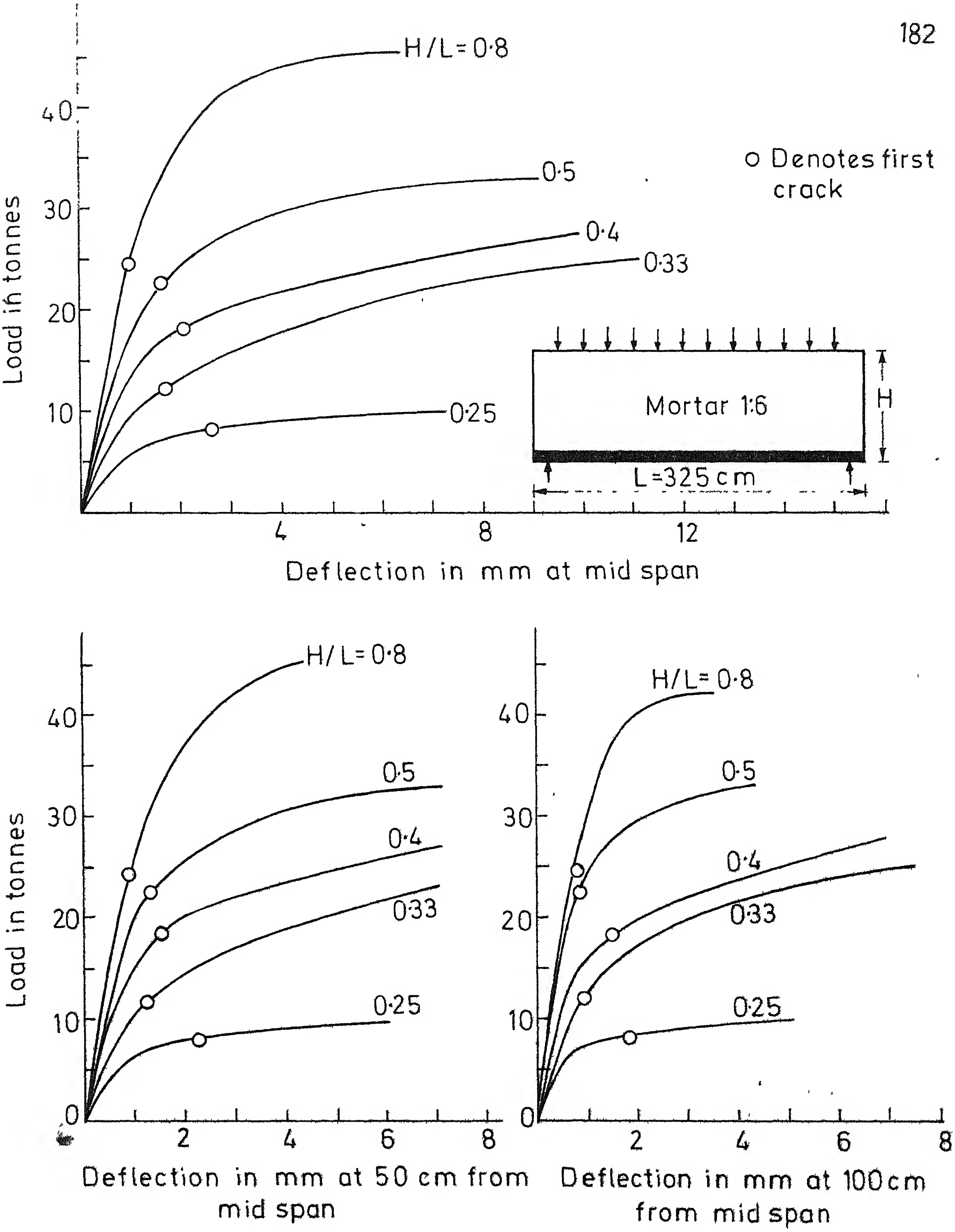

Fig. 3·11 Load versus vertical deflection curves (Compressive loading)

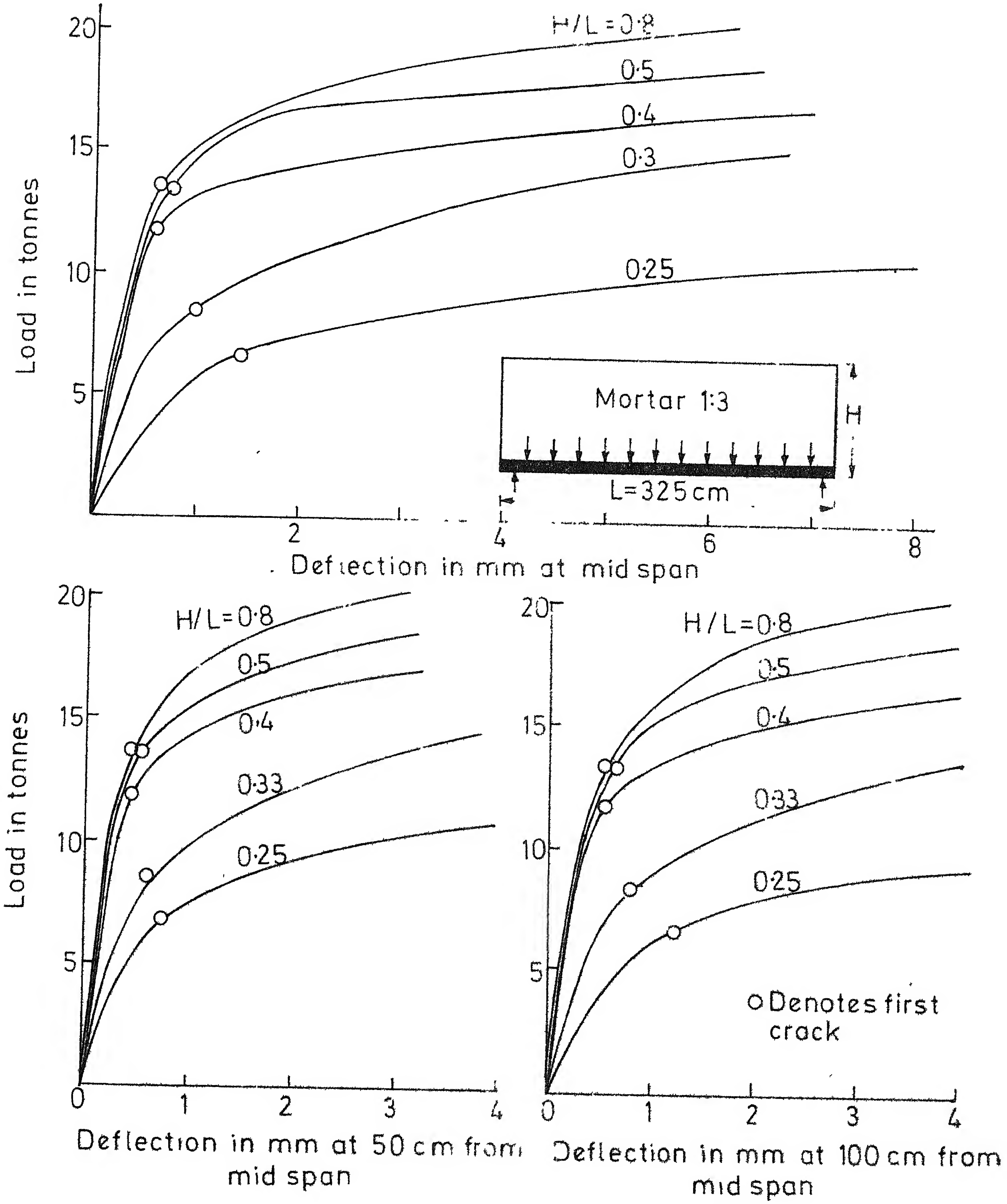

Fig.3·12 Load versus vertical deflection curves (Tensile loading)

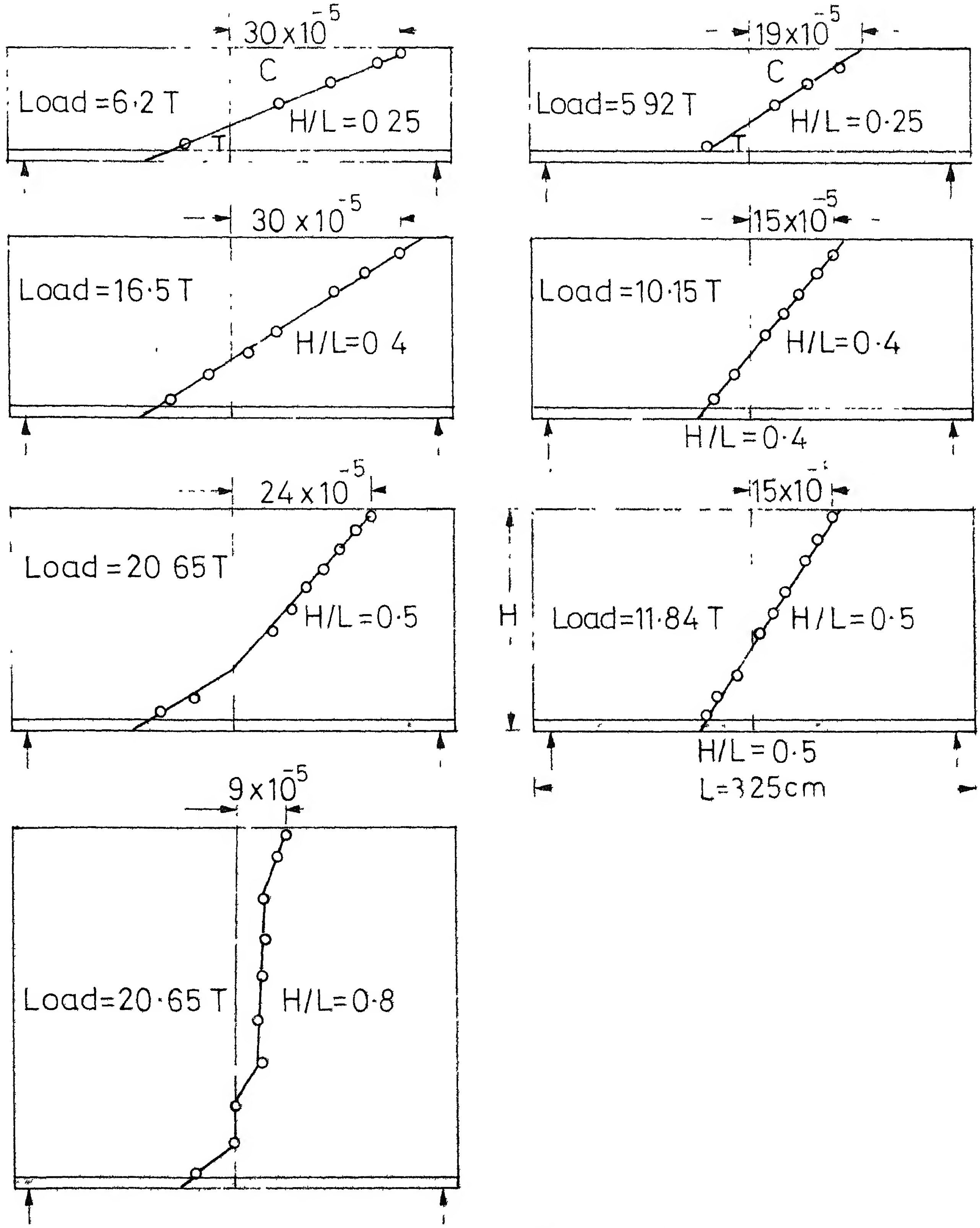

(a) Compressive loading
Mortar 1:6

(b) Tensile loading
Mortar 1:3

Fig.3·13 Variation of longitudinal strains at mid span

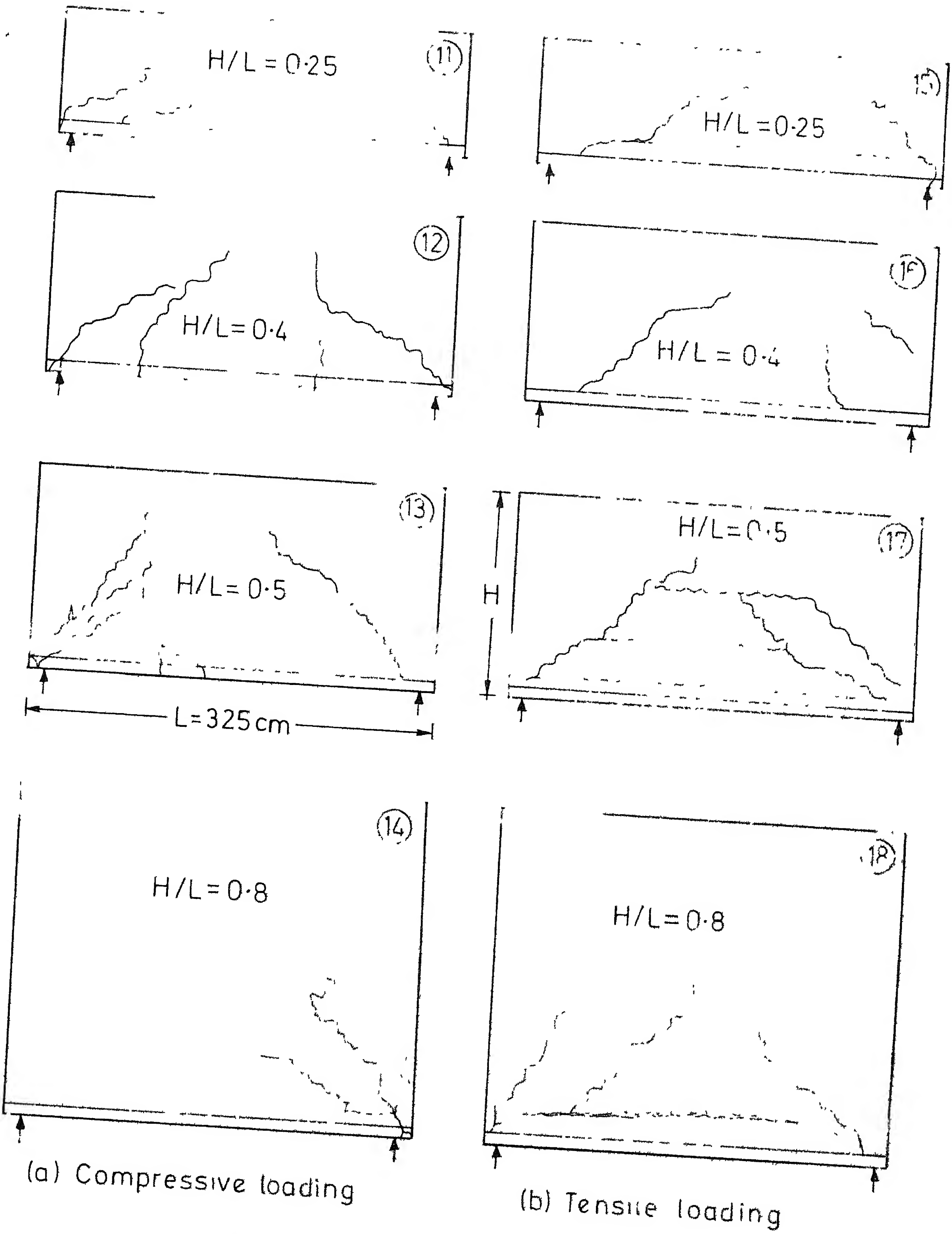

Fig.3·14 Crack pattern at failure

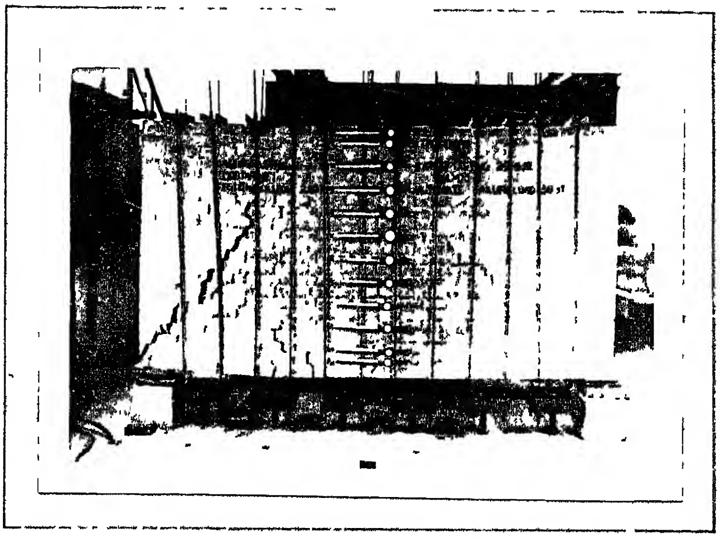

Specimen no. 13 H/L = 0·5, Mortar 1:6
Loading - Compressive

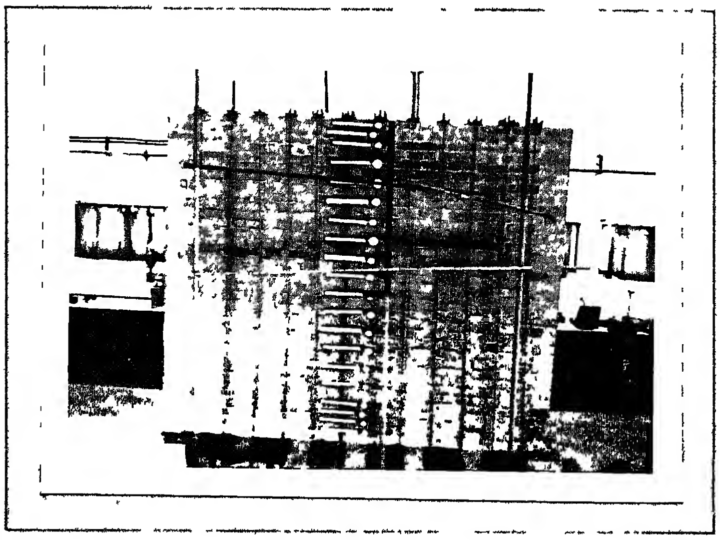

Specimen no. 14 H/L = 0·8, Mortar 1:6
Loading - Compressive

Fig.3·15 Photographs showing failure pattern

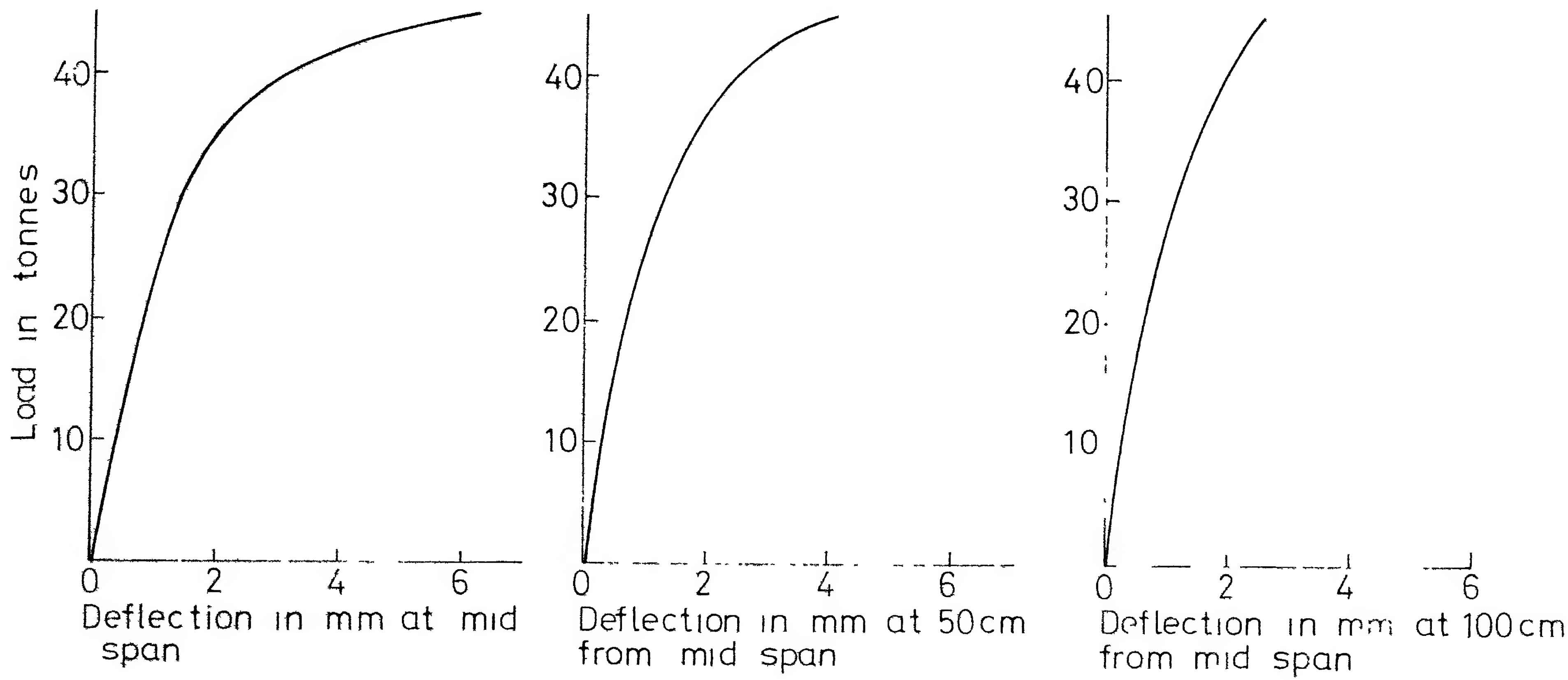

Fig.3·16 Load vs vertical deflection curves

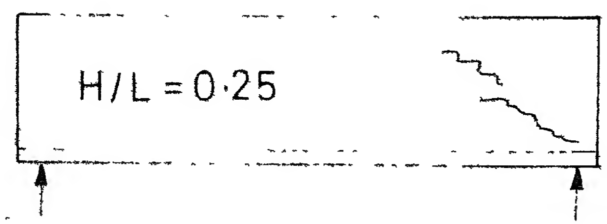

H/L	Mortar	Loading	No. and size of connectors
0·25	1:3	Tensile	24 No 6mm dia

Fig.3·17 Crack pattern at failure

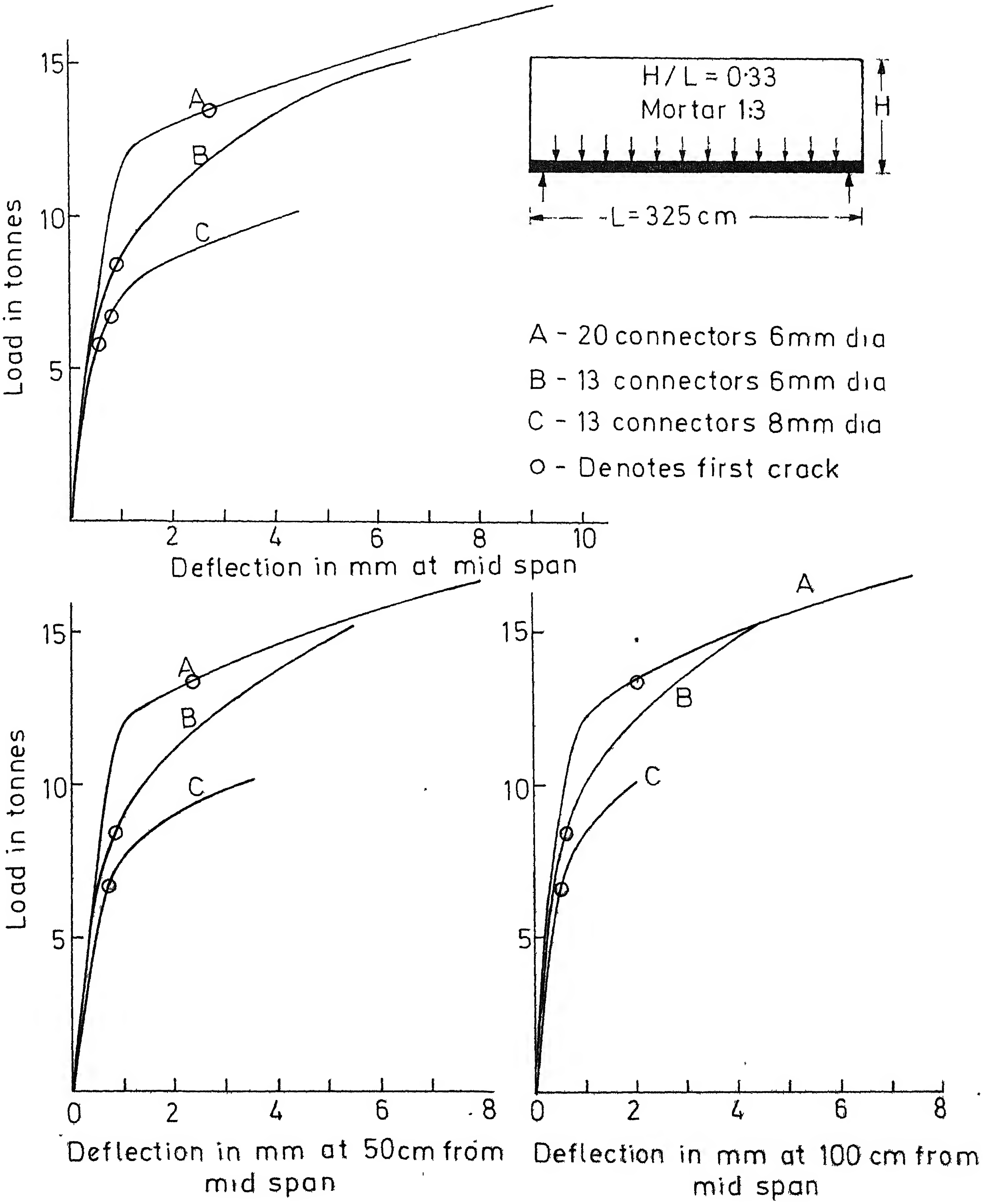

Fig.3·18 Load versus vertical deflection curves (Tensile loading)

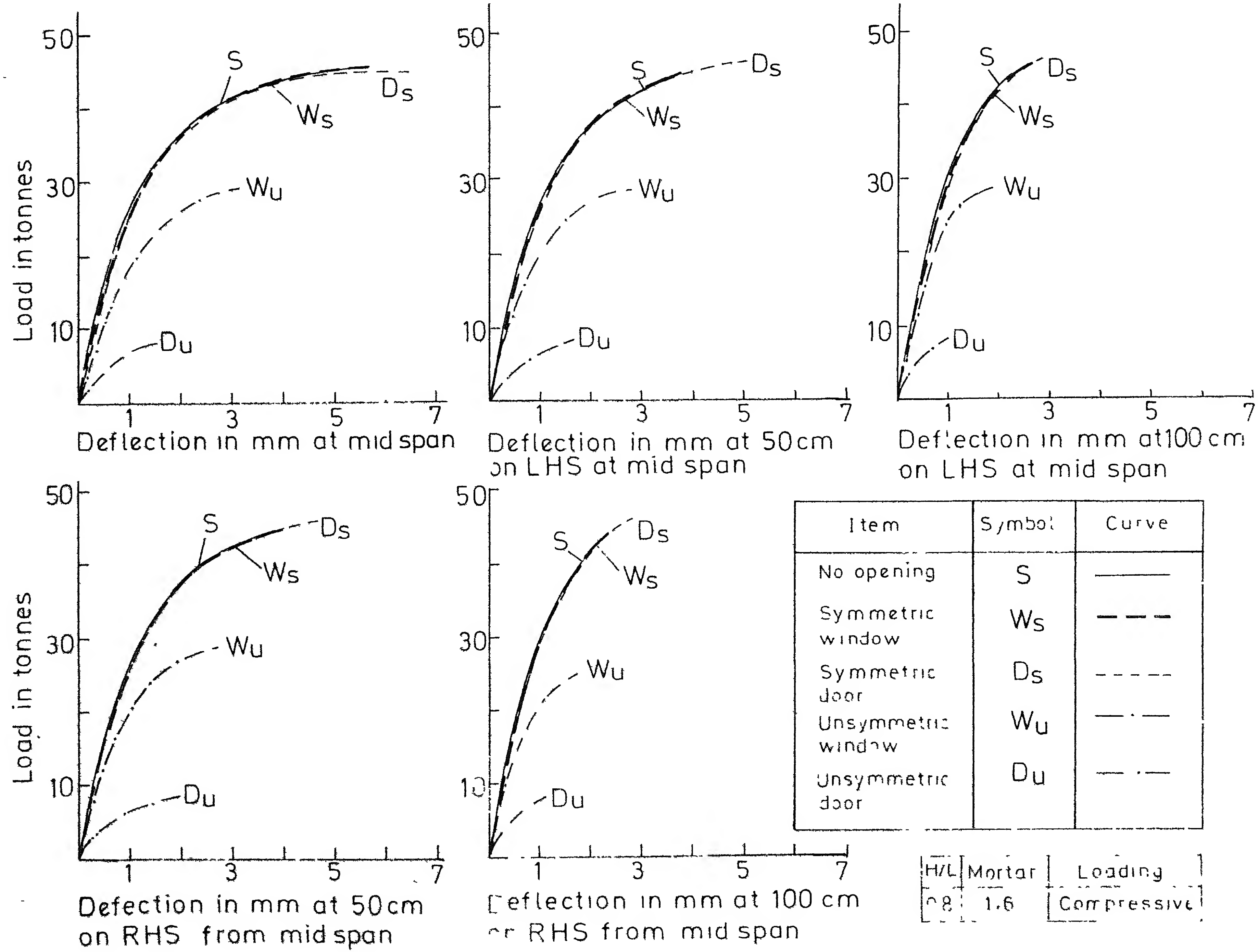

Fig.3·19 Load versus vertical deflection curves

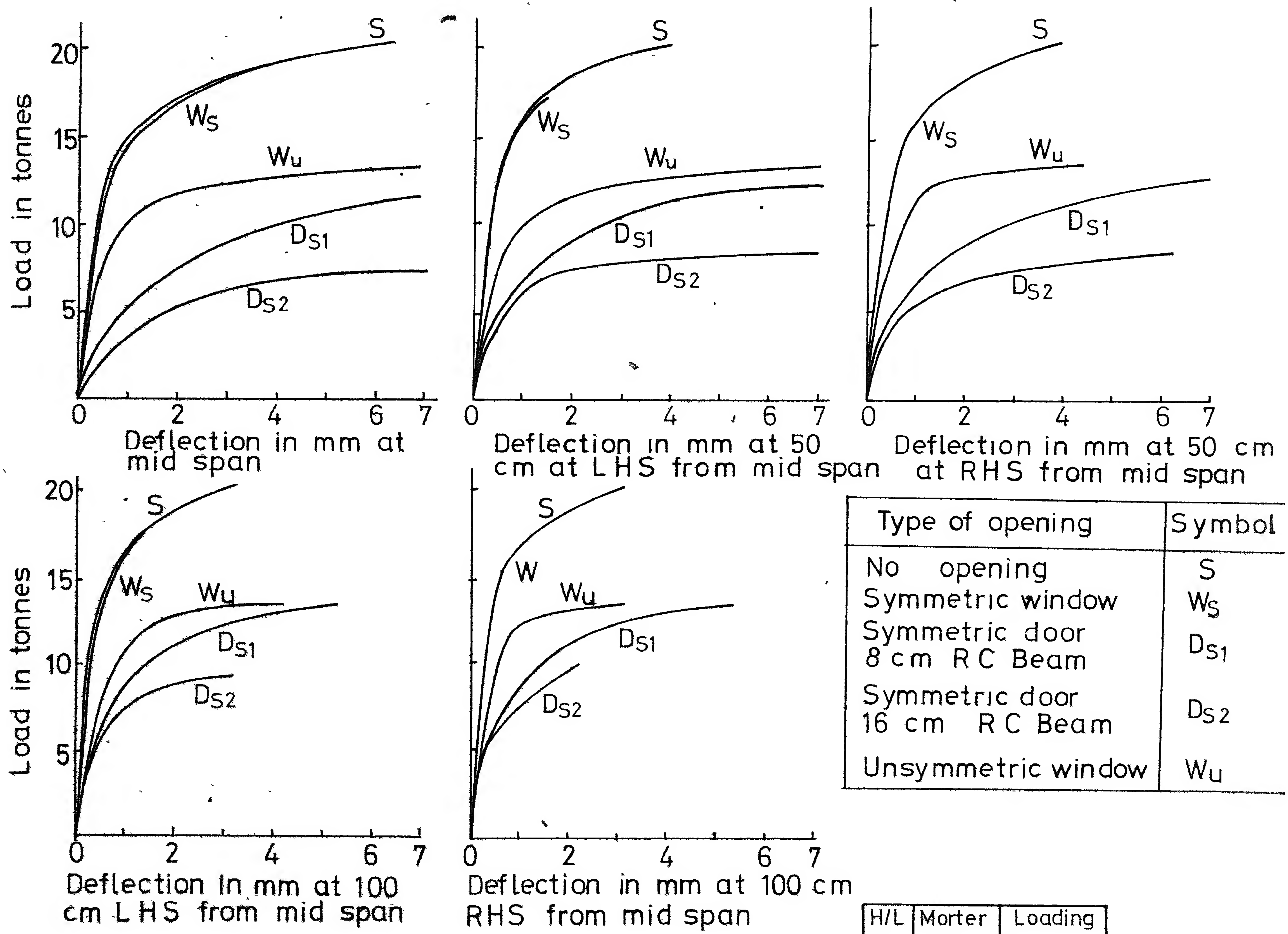

Type of opening	Symbol
No opening	S
Symmetric window	W_S
Symmetric door 8 cm RC Beam	D_{S1}
Symmetric door 16 cm RC Beam	D_{S2}
Unsymmetric window	W_u

H/L	Morter	Loading
0 8	1 3	Tensile

Fig.3·20 Load vs vertical deflection curves

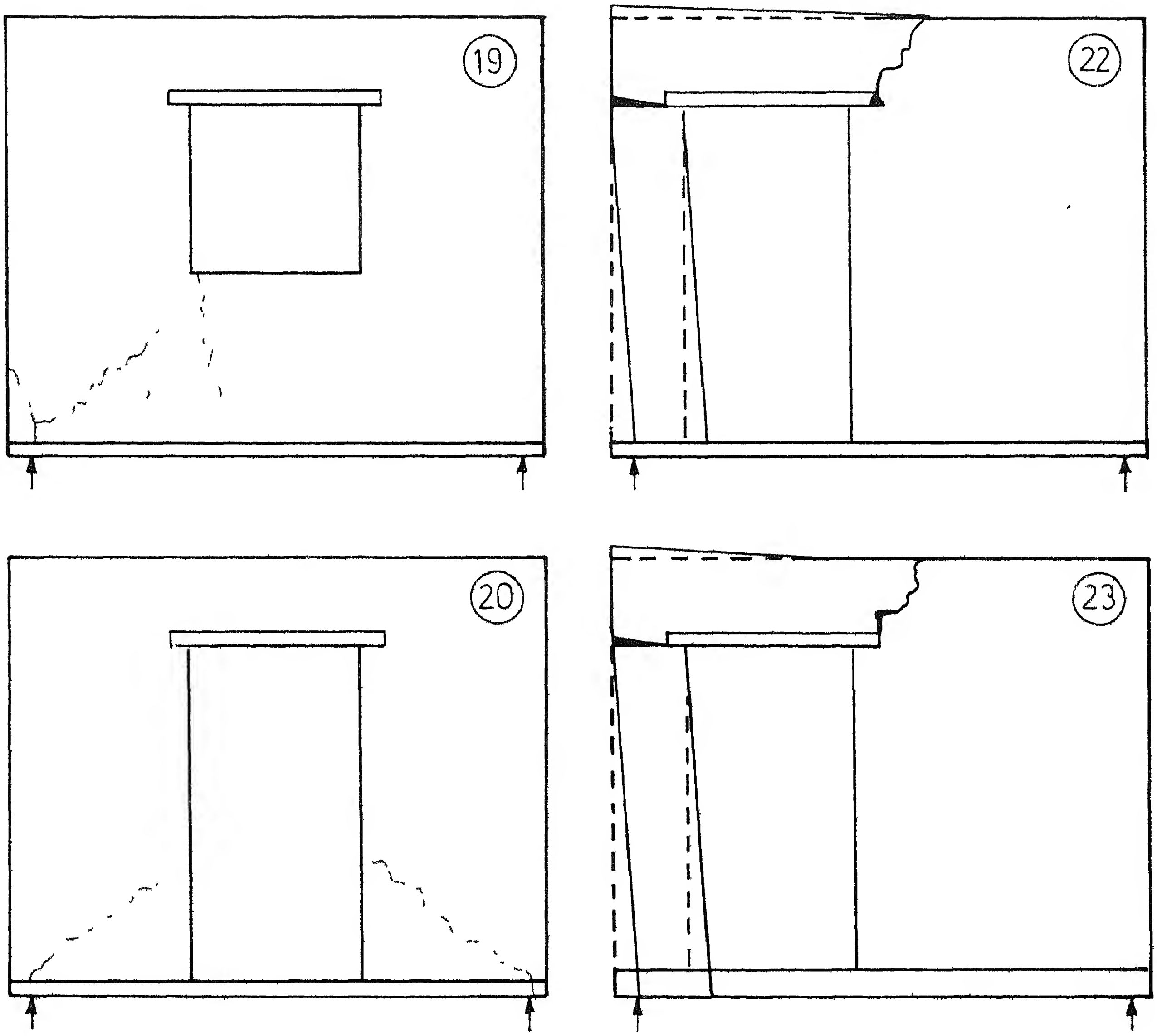

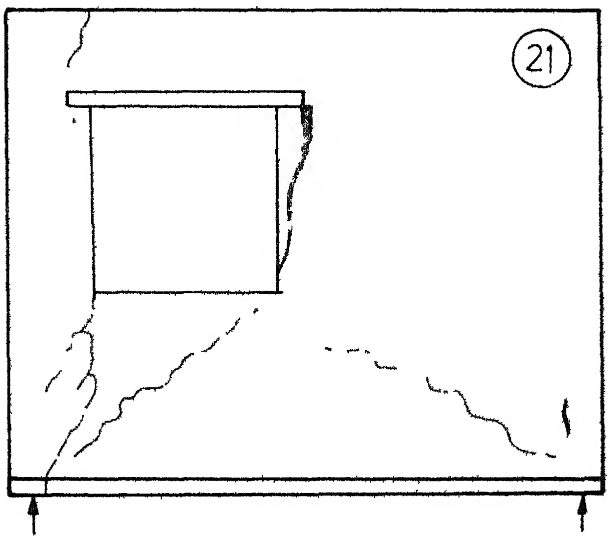

H/L	Mortar	Loading
0·8	1:6	Compressive

Fig. 3·21 Crack pattern at failure

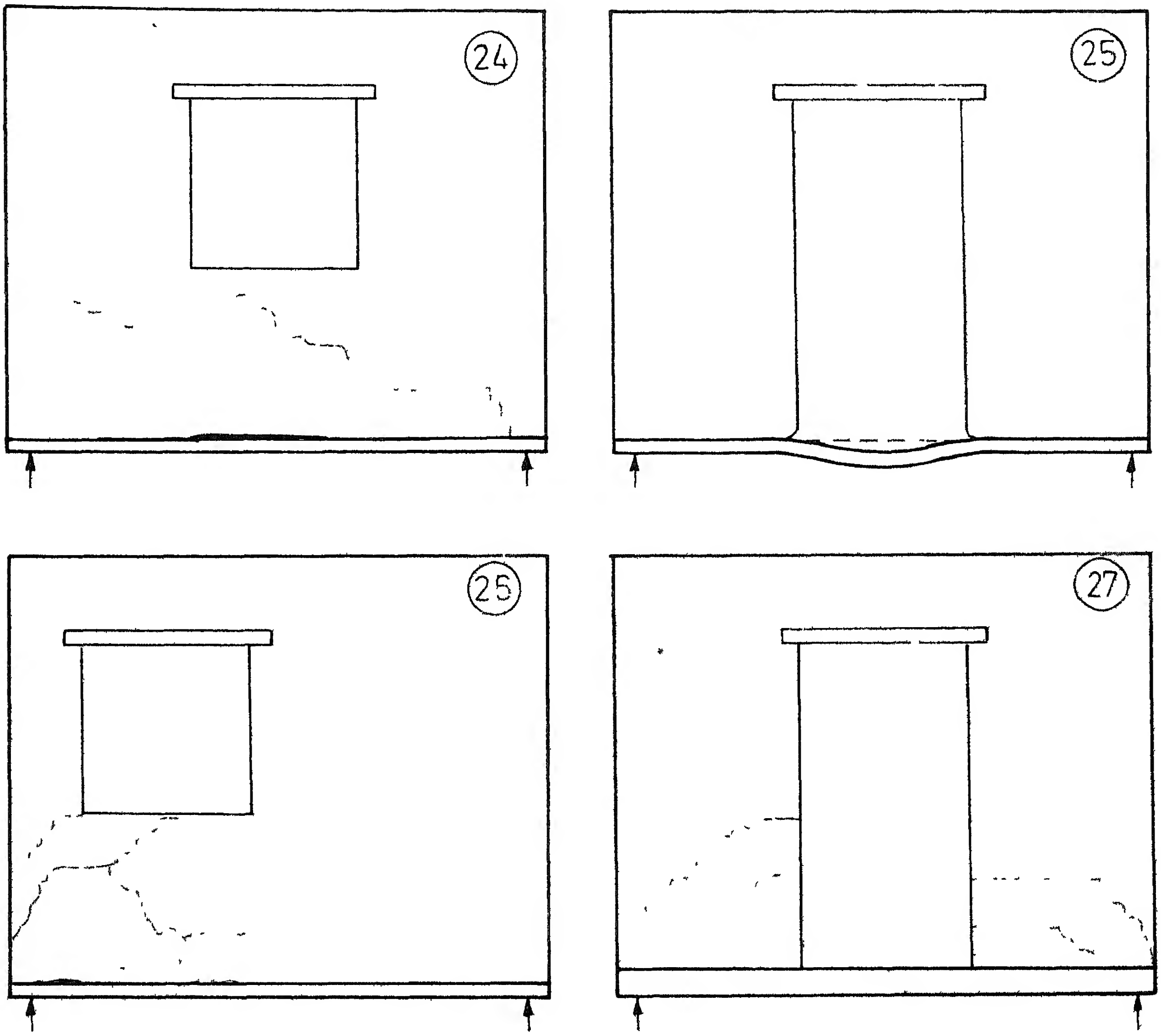

H/L	Mortar	Loading
08	1.3	Tensile

Fig.3·22 Crack pattern at failure

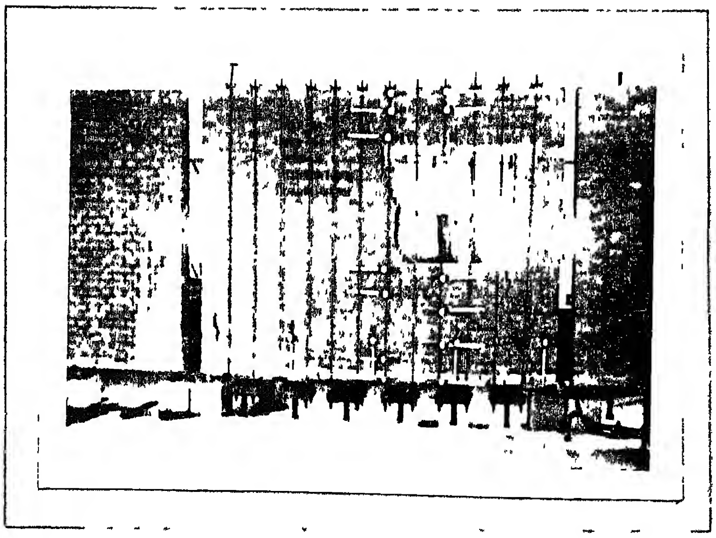

Specimen no.21 Unsymmetric window opening
H/L = 0·8 , Mortar 1:6 , Loading - Compressive

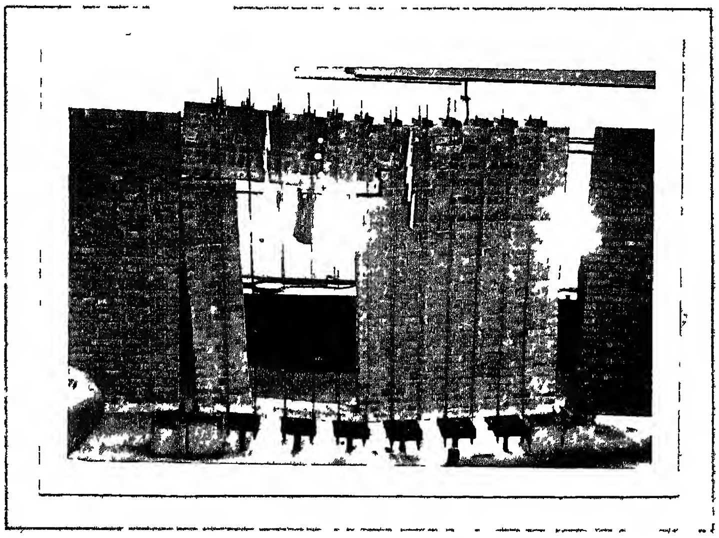

Specimen no.22 Unsymmetric door opening
H/L = 0·8 , Mortar 1 6, Loading - Compressive

Fig.3·23 a Photographs showing failure patterns

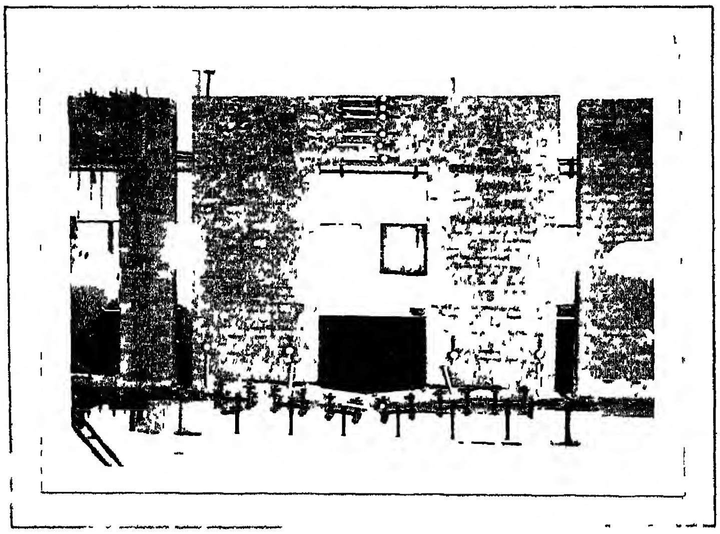

Specimen no 25 symmetric door opening R.C. beam 8 cm thick
H/L = 0·8, Mortar 1:3, Loading -Tensile

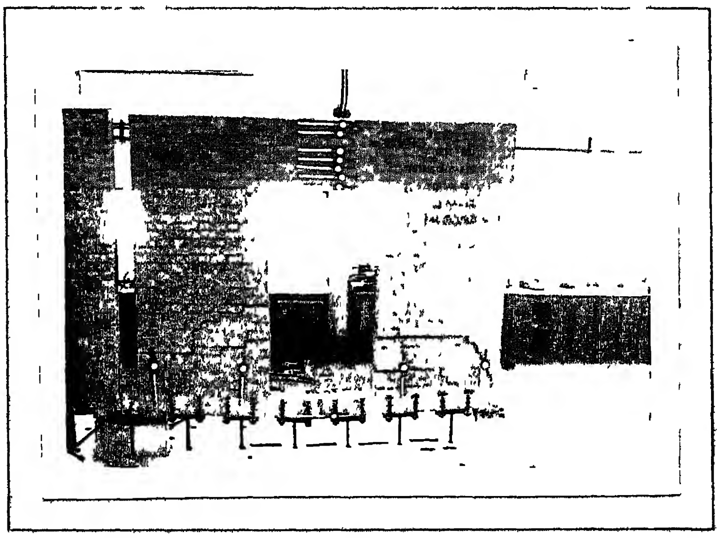

Specimen no 27 symmetric door opening R.C. beam 16 cm thick
H/L= 0·8 , Mortar 1'3 , Loading -Tensile

Fig.3·23 b Photographs showing failure patterns

CHAPTER IV

ANALYTICAL INVESTIGATION

4.1 INTRODUCTION

Brickwork supported on R.C. beams is a composite structure which has been idealized as orthotropic material in Chapter II. In order to carry out a rational analytical study of this class of structure for the purposes of studying crack propagation and obtain load deformation characteristics of the composite system, finite element method seems to be the most useful tool. Hence a computer programme based on finite element method incorporating nonlinearity in the load deformation response arising due to cracking, yielding and crushing of concrete or brickwork and yielding of steel reinforcement has been developed in the present work. The structure has been modelled as a plane stress problem since the composite system considered in the present work is a two dimensional planar structure.

The finite element method is the representation of a continuum by an assemblage of subdivisions called finite elements. The characteristics and properties of all elements are combined to analyse the structure. The simplest element used for two dimensional finite element analysis is a constant

strain triangular element. For two dimensional bending problems, constant strain triangular and quadrilateral elements are not able to represent certain simple stress gradients and that causes inaccuracy in the solution (54). Therefore there is need to use higher order elements. Wilson et al. (54) improved the accuracy of quadrilateral element by adding incompatible displacement modes in the displacement field. These extra displacement modes violate inter element compatability. The other higher order and simple element in use is a linearly varying strain triangular element, which has been used in the present work.

The finite element method employed in this work is based on the stiffness (displacement) approach. Since the method is very well documented in standard text books (55,56, 57) only a brief description of the steps involved in obtaining the 'structure stiffness matrix' is presented in this chapter.

4.2 DISPLACEMENT FORMULATION

In this formulation the displacements u at any point within the element are approximated by a set of functions and can be expressed in terms of nodal displacement δ as

$$\{u\} = [N] \{\delta\} \tag{4.1}$$

where, [N] is called the interpolation or shape function. Having selected the displacement function, the state of strain within the element is given in terms of nodal displacements as

$$\{\epsilon\} = [B] \{\delta\} \tag{4.2}$$

where ϵ is the vector of strain components at any point within the element and [B] is strain-displacement transformation matrix obtained by differentiating [N] .

The stress within the element can now be expressed in terms of strains and material properties as

$$\{\sigma\} = [C] \{\epsilon\} \tag{4.3}$$

where $\{\sigma\}$ is the stress vector at any point within the element, and [C] is the constitutive (stress-strain transformation) matrix.

The potential energy of a deformed solid is given by the sum of the internal strain energy and the potential of the body forces and surface tractions. Thus, for a linearly elastic body,

Potential energy = strain energy-work done by external forces

$$\pi = \frac{1}{2} \int_V \{\epsilon\}^T \{\sigma\} dV - \int_V \{u\}^T \{\bar{X}\} dV - \int_{S_1} \{u\}^T \{p\} dS_1 \tag{4.4}$$

where $\{\bar{X}\}$ is the body force vector;

$\{p\}$ is the surface load vector prescribed over S_1;

and V is the volume of the element.

Substituting the values of σ , $\{\varepsilon\}$ and $\{u\}$ from equations (4.1), (4.2) and (4.3) into equation (4.4), potential energy of the body can be written as

$$\pi = \frac{1}{2} \int_V \{\delta\}^T [B]^T [C][B]\{\delta\} \, dV - \int_V \{\delta\}^T [N]^T \{\bar{X}\} dV$$
$$- \int_{S_1} \{\delta\}^T [N]^T \{p\} \, dS_1 \quad (4.5)$$

Applying the principle of minimum potential energy for the element we obtain

$$\{\delta\}^T \left(\int_V [B]^T [C][B] \int_L \{\delta\} \, dV - \int_V [N]^T \{\bar{X}\} \, dV - \int_{S_1} [N]^T \{p\} \, dS_1\right) = 0 \quad (4.6)$$

Since the variation of nodal displacements $\{\delta \; \delta\}$ are arbitrary, the expression in parenthesis must vanish. This gives the equilibrium equation for the element

$$[K] \{\delta\} = \{P\} \quad (4.7)$$

where $[K]$ is defined as the element stiffness matrix and P is the nodal load vector given by

$$[K] = \int_V [B]^T [C] [B] \, dV \quad (4.8)$$

and $$\{P\} = \int_V [N]^T \{\bar{X}\} dV + \int_{S_1} [N]^T \{p\} \, dS_1 \quad (4.9)$$

Once the element stiffness matrix is found, computing the overall structure stiffness matrix, imposition of boundary conditions and solution of equations follows the standard

direct stiffness method of analysis (55, 57).

4.3 THE LINEARLY VARYING STRAIN TRIANGULAR(L.S.T.) ELEMENT

A linearly varying strain triangular element which has complete quadratic displacement model and satisfies all the convergence requirements has been used in the present work.

4.3.1 Element Stiffness Matrix

A linearly varying strain triangular element (56, 58) ha six nodes out of which 3 are primary nodes at the three corners and 3 secondary nodes at the mid points of three sides. This element has 12 degrees of freedom for plane stress problems as shown in Fig. 4.1. In natural coordinate system, three coordinates L_1, L_2, L_3 are used to define the location of a point but only two of these are independent. Their relation to cartesian coordinates is given by

$$\begin{Bmatrix} X \\ Y \\ 1 \end{Bmatrix} = \begin{bmatrix} X_1 & X_2 & X_3 \\ Y_1 & Y_2 & Y_3 \\ 1 & 1 & 1 \end{bmatrix} \begin{Bmatrix} L_1 \\ L_2 \\ L_3 \end{Bmatrix} \tag{4.10}$$

where (X_1,Y_1), (X_2,Y_2) and (X_3,Y_3) are the cartesian coordinates of primary nodal points and L_1, L_2, L_3 are the natural coordinates of a point inside the element which are defined as

$$L_1 = \frac{A_1}{A}\ , \ L_2 = \frac{A_2}{A}, \ L_3 = \frac{A_3}{A} \tag{4.11}$$

Where A_i is the area of the triangle formed by the vertices j, K and point P and A is the total area of the triangle.

The quadratic displacement field for this element is given by

$$
\begin{aligned}
u &= \alpha_1 + \alpha_2 x + \alpha_3 y + \alpha_4 xy + \alpha_5 x^2 + \alpha_6 y^2 \\
v &= \alpha_7 + \alpha_8 x + \alpha_9 y + \alpha_{10} xy + \alpha_{11} x^2 + \alpha_{12} y^2
\end{aligned}
\qquad (4.12)
$$

where α_i are generalized coordinates.

Using natural coordinates displacement model can be written as

$$
\{U\} = \begin{Bmatrix} u \\ v \end{Bmatrix} = \begin{bmatrix} \{N_1\}^T & \{0\}^T \\ \{0\}^T & \{N_1\}^T \end{bmatrix} \begin{bmatrix} \{\delta u\} \\ \{\delta v\} \end{bmatrix} = [N]\{\delta\} \qquad (4.13)
$$

where

$$\{N_1\}^T = [L_1(2L_1-1),\ L_2(2L_2-1),\ L_3(2L_3-1),\ 4L_1L_2,\ 4L_2L_3,\ 4L_3L_1]$$

$$\{\delta u\}^T = [u_1\ u_2\ u_3\ u_4\ u_5\ u_6]$$

$$\{\delta v\}^T = [v_1\ v_2\ v_3\ v_4\ v_5\ v_6]$$

and u_i's and V_i's are nodal displacements.

Differentiating the expression for u and v we get the strain displacement relation as

$$
\{\epsilon\} = \begin{bmatrix} \{B_1\}^T & \{0\}^T \\ \{0\}^T & \{B_2\}^T \\ \{B_2\}^T & \{B_1\}^T \end{bmatrix} \begin{bmatrix} \{\delta u\} \\ \{\delta v\} \end{bmatrix} = [B]\{\delta\} \qquad (4.14)
$$

where $\{\epsilon\}^T = [\epsilon_x, \ \epsilon_y, \ \gamma_{xy}]$ is the strain vector at any point within the element.

$$\{B_1\} = \frac{1}{2A} \left\{ \begin{array}{c} (4L_1-1)\ b_1 \\ (4L_2-1)\ b_2 \\ (4L_3-1)\ b_3 \\ 4(L_2b_1+L_1b_2) \\ 4(L_3b_2+L_2b_3) \\ 4(L_1b_3+L_3b_1) \end{array} \right\}, \quad \{B_2\} = \frac{1}{2A} \left\{ \begin{array}{c} (4L_1-1)\ a_1 \\ (4L_2-1)\ a_2 \\ (4L_3-1)\ a_3 \\ 4(L_2a_1 + L_1a_2) \\ 4(L_3a_2+L_2a_3) \\ 4(L_1a_3+L_3a_1) \end{array} \right\} \tag{4.15}$$

where

$$\begin{aligned} a_1 &= x_3 - X_2 , \quad & b_1 &= Y_2-Y_3 \\ a_2 &= X_1 - X_3 , \quad & b_2 &= Y_3-Y_1 \\ a_3 &= X_2 - X_1 , \quad & b_3 &= Y_1-Y_2 \end{aligned} \tag{4.16}$$

and (X_1,Y_1), (X_2,Y_2), (X_3,Y_3) are the cartesian coordinates of primary nodal points.

The strain displacement matrix is not constant. Since the strain components are linear function of natural coordinates, they can be written by linear interpolation using strains at three primary nodes. Therefore the nodal strain vector will be

$$\{\epsilon_n\}^T = [\epsilon_{X1} \quad \epsilon_{X2} \quad \epsilon_{X_3} \quad \epsilon_{Y1} \quad \epsilon_{Y2} \quad \epsilon_{Y3} \quad XY1 \quad XY2 \quad XY3] \tag{4.17}$$

where ϵ_{X_i}'s, ϵ_{Y_i}'s and γ_{XY_i}'s are the strains at primary

nodes.

The strains at the primary nodes can be written in terms of nodal displacement by evaluating the matrix [B] of equation (4.14) at primary nodes. This gives

$$\{\varepsilon_n\} = \begin{bmatrix} [B_{n1}]^T & [0]^T \\ [0]^T & [B_{n2}]^T \\ [B_{n2}]^T & [B_{n1}]^T \end{bmatrix} \begin{Bmatrix} \{q_u\} \\ \{q_v\} \end{Bmatrix} = [B_n]\{\delta\} \qquad (4.18)$$

where

$$[B_{n1}]^T = \frac{1}{2A} \begin{bmatrix} 3b_1 & -b_2 & -b_3 & 4b_2 & 0 & 4b_3 \\ -b_1 & 3b_2 & -b_3 & 4b_1 & 4b_3 & 0 \\ -b_1 & -b_2 & 3b_3 & 0 & 4b_2 & 4b_1 \end{bmatrix} \qquad (4.19)$$

$$[B_{n2}]^T = \frac{1}{2A} \begin{bmatrix} 3a_1 & -a_2 & -a_3 & 4a_2 & 0 & 4a_3 \\ -a_1 & 3a_2 & -a_3 & 4a_1 & 4a_3 & 0 \\ -a_1 & -a_2 & 3a_3 & 0 & 4a_2 & 4a_1 \end{bmatrix} \qquad (4.20)$$

and $[B_n]$ is called nodal strain displacement matrix.

Assuming that the material properties are constant with in the element, stresses will also vary linearly within the element. The nodal stress vector is defined as

$$\{\sigma_n\}^T , [\sigma_{X1}\ \sigma_{X2}\ \sigma_{X3}\ \ \sigma_{Y1}\ \sigma_{Y2}\ \sigma_{Y3}\ \tau_{XY1}\ \tau_{XY2}\ \tau_{XY3}] \qquad (4.21)$$

Since both stresses and strains vary linearly within the element, their interpolation models will be identical which are given by

$$\{\sigma\} = [N_\sigma]\{\sigma_n\} \tag{4.22}$$

$$\{\varepsilon\} = [N_\varepsilon]\{\varepsilon_n\} \tag{4.23}$$

where $\{\sigma\}$ and $\{\varepsilon\}$ are stress and strain vector at any point within the element

$$[N_\varepsilon] = [N_\sigma] = \begin{bmatrix} \{N_1\}^T & \{0\}^T & \{0\}^T \\ \{0\}^T & \{N_1\}^T & \{0\}^T \\ \{0\}^T & \{0\}^T & \{N_1\}^T \end{bmatrix} \tag{4.24}$$

and $$\{N_1\}^T = [L_1 \; L_2 \; L_3] \tag{4.25}$$

The stresses and strains are related through material constitutive matrix $[C]$ as

$$\{\sigma\} = [C]\{\varepsilon\} \tag{4.26}$$

The nodal stresses and strains, using equation (4.26) can be written as

$$\{\sigma_n\} = \begin{bmatrix} C_{11}[I] & C_{12}[I] & C_{13}[I] \\ C_{12}[I] & C_{22}[I] & C_{23}[I] \\ C_{13}[I] & C_{23}[I] & C_{33}[I] \end{bmatrix} \{\varepsilon_n\} = [C_n]\{\varepsilon_n\} \tag{4.27}$$,

where C_{ij}'s are element of $[C]$ in equation (4.26)

$[I]$ is a 3x3 identify matrix and

$[C_n]$ is called the nodal stress strain transformation matrix.

The strain energy U of element is given by

$$U = \frac{1}{2} \int_V \{\epsilon\}^T \{\sigma\} \, dV \tag{4.28}$$

Substituting the values of $\{\epsilon\}$ and $\{\sigma\}$ from equation (4.22) and (4.23) in above equation we get

$$U = \frac{1}{2} \{\epsilon_n\}^T \int_V [N_\epsilon]^T [N_\sigma] \, dV \{\sigma_n\} \tag{4.29}$$

Putting the value of $\{\epsilon_n\}$ and $\{\sigma_n\}$ from equations (4.18) and (4.27) in above equation strain energy of element can be written as

$$U = \frac{1}{2} \{\delta\}^T [B_n]^T [\int_V [N_\epsilon]^T [N_\sigma] dV][C_n] [B_n] \{\delta\} \tag{4.30}$$

Therefore stiffness matrix $[K]$ can be defined as

$$[K] = [B_n]^T [D] [C_n] [B_n] \tag{4.31}$$

where

$$[D] = \int_V [N_\epsilon]^T [N_\sigma] \, dV \tag{4.32}$$

For an element of constant thickness, D is given by

$$[D] = t \int_A [N_\epsilon]^T [N_\sigma] \, dA = \begin{bmatrix} [D_1] & [0] & [0] \\ [0] & [D_1] & [0] \\ [0] & [0] & [D_1] \end{bmatrix} \tag{4.33}$$

where $D_1 = t \int_A \{N_1\}\{N_1\}^T \, dA = \frac{Ah}{12} \begin{bmatrix} 2 & 1 & 1 \\ 1 & 2 & 1 \\ 1 & 1 & 2 \end{bmatrix}$ (4.34)

A and t are the area and thickness of the element respectively. Thus element stiffness matrix of linear strain triangular element is given by the expression (4.31) that is by direct multiplication of matrices $[B_n]$, $[D]$ and $[C_n]$.

The matrix $[B_n]$ is based on the displacement vector $\{\delta\}$ in which all degrees of freedom corresponding to x direction are grouped first and then all degrees of freedom corresponding to Y direction. To simplify the assembly of complete stiffness matrix and solution coding, the vector of nodal displacements is rearranged so as to have to components (u,v) at each node together. The modified displacement vector $\{\delta'\}$ is as follows

$$\{\delta'\}^T = \{u_1 \; v_1 \; u_2 \; v_2 \; u_3 \; v_3 \; u_4 \; v_4 \; u_5 \; v_5 \; u_6 \; v_6\} \quad (4.35)$$

The nodal displacement vector $\{\delta\}$ and $\{\delta'\}$ are related through a transformation matrix $[T']$ as

$$\{\delta\} = [T']\{\delta'\} \quad (4.36)$$

where,

$$[T'] = \begin{bmatrix} 1 & 0 & 0 & 0 & 0 & 0 & 0 & 0 & 0 & 0 & 0 & 0 \\ 0 & 0 & 1 & 0 & 0 & 0 & 0 & 0 & 0 & 0 & 0 & 0 \\ 0 & 0 & 0 & 0 & 1 & 0 & 0 & 0 & 0 & 0 & 0 & 0 \\ 0 & 0 & 0 & 0 & 0 & 0 & 1 & 0 & 0 & 0 & 0 & 0 \\ 0 & 0 & 0 & 0 & 0 & 0 & 0 & 0 & 1 & 0 & 0 & 0 \\ 0 & 0 & 0 & 0 & 0 & 0 & 0 & 0 & 0 & 0 & 1 & 0 \\ 0 & 1 & 0 & 0 & 0 & 0 & 0 & 0 & 0 & 0 & 0 & 0 \\ 0 & 0 & 0 & 1 & 0 & 0 & 0 & 0 & 0 & 0 & 0 & 0 \\ 0 & 0 & 0 & 0 & 0 & 1 & 0 & 0 & 0 & 0 & 0 & 0 \\ 0 & 0 & 0 & 0 & 0 & 0 & 0 & 1 & 0 & 0 & 0 & 0 \\ 0 & 0 & 0 & 0 & 0 & 0 & 0 & 0 & 0 & 1 & 0 & 0 \\ 0 & 0 & 0 & 0 & 0 & 0 & 0 & 0 & 0 & 0 & 0 & 1 \end{bmatrix} \qquad (4.37)$$

4.3.2 Consistent Load Vector

Consistent load vector for L.S.T. element (56,58) is calculated from equation (4.9). For uniform body forces, the contribution to load vector is

$$\{P\}^T = \frac{At}{3} \left[0 \; 0 \; 0 \; 0 \; 0 \; 0 \; \bar{x} \; \bar{y} \; \bar{x} \; \bar{y} \; \bar{x} \; \bar{y} \right] \qquad (4.38a)$$

and for a linearly distributed load vector, the contribution to load vector is

$$P = \frac{1}{6} \left\{ \begin{array}{lcl} l_3 p_{x_1}^{(3)} & + & l_2 p_{x_1}^{(2)} \\ l_3 p_{y_1}^{(3)} & + & l_2 p_{y_1}^{(2)} \\ l_3 p_{x_2}^{(3)} & + & l_1 p_{x_2}^{(1)} \\ l_3 p_{y_2}^{(3)} & + & l_1 p_{y_2}^{(1)} \\ l_1 p_{x_3}^{(1)} & + & l_2 p_{x_3}^{(2)} \\ l_1 p_{y_3}^{(1)} & + & l_2 p_{y_3}^{(2)} \\ 2l_3 (p_{x_1}^{(3)} & + & p_{x_2}^{(3)}) \\ 2l_3 (p_{y_1}^{(3)} & + & p_{y_2}^{(3)}) \\ 2l_1 \; (p_{x_2}^{(1)} & + & p_{x_3}^{(1)}) \\ 2l_1 (p_{y_2}^{(1)} & + & p_{y_3}^{(1)}) \\ 2l_2 \; (p_{x_3}^{(2)} & + & p_{x_3}^{(2)}) \\ 2l_2 (p_{y_3}^{(2)} & + & p_{y_1}^{(2)}) \end{array} \right\} \qquad (4.38b)$$

where l is the length of i^{th} side of a triangle, that is the side opposite to node i,

$p_{x_i}^{(j)}$ is the load intensity per unit length at node i in x direction of a linearly varying load that has been applied to side j of the element and

$p_{y_i}^{(j)}$ is the load intensity per unit length at node i in Y direction of a linearly varying load that has been applied to the side j of the element.

4.4 THE LINEARLY VARYING STRAIN BAR ELEMENT(L.S.B.)

The steel reinforcement is idealized as an assembly of one-dimensional bar elements in the present work. Bond between reinforcement and concrete or between reinforcement and brickwork is assumed to be perfect upto failure. Since linear variation of strains have been used for brickwork or concrete elements the bar element should also have linearly varying strains to achieve strain and displacement compatibility.

Fig. 4.2a shows the representation of one dimensional bar element with degrees of freedom in both local and global coordinate systems. The linearly varying strain bar element (56) has three nodes. It has a total of six degrees of freedom in global coordinate system and only three degrees of freedom in local coordinate system as shown in Fig. 4.2b. The axis of element may be at some orientation θ relative to global coordinate system. The local natural coordinate system for bar element is shown in Fig. 4.2c. The relationship between local cartesian coordinate   and natural coordinate L is given by

$$x = \frac{1}{2}(1-L)x_1 + \frac{1}{2}(1+L)\,x_2 \qquad (4.39)$$

which gives

$$L = \frac{x-(x_1+x_2)/2}{(x_2-x_1)/2} = \frac{x - x_3}{l/2}$$

or $$L = \frac{2}{l}\,(x-x_3) \qquad (4.40)$$

where x_1, x_2 and x_3 are the nodal cartesian coordinates in local cartesian coordinate system and l is the length of the bar element. The quadratic displacement function for three noded bar element is given by

$$u = \alpha_1 + \alpha_2 x + \alpha_3 x^2$$

where α_i's are generalized coordinates.

Using natural coordinates, the displacement model interms of interpolation functions can be expressed as

$$u = [N_1 \;\; N_2 \;\; N_3] \begin{Bmatrix} u_1 \\ u_2 \\ u_3 \end{Bmatrix} = [N]^T \; \{\delta\}_l. \qquad (4.41)$$

where

$$\begin{aligned} N_1 &= \frac{1}{2}\, L\,(L-1) \\ N_2 &= \frac{1}{2}\, L\,(L+1) \\ N_3 &= (1-L^2) \end{aligned} \qquad (4.42)$$

and $\{\delta\}_l^T = [u_1 \;\; u_2 \;\; u_3]$ is the nodal displacement vector in local coordinate system.

The strain displacement relation is obtained by differentiating the expression for u and can be written as

$$\epsilon_x = \frac{du}{dx} = \left[\, \frac{1}{l}\,(2L-1),\; \frac{1}{l}\,(2L+1),\; \frac{2}{l}\,(-2L)\, \right] \begin{Bmatrix} u_1 \\ u_2 \\ u_3 \end{Bmatrix} \qquad (4.43)$$

or $\{\varepsilon\} = [B] \{\delta\}_1$ (4.44)

The stress strain relationship is

$$\sigma_x = E_s \, \varepsilon_x \quad (4.45)$$

$$\{\sigma\} = [C]\{\varepsilon\} \quad (4.46)$$

where E_s is the modulus of elasticity of bar material that is reinforcement. Therefore, stiffness matrix of a bar element in local coordinate system can be written as

$$[K]_e = \int_V [B]^T [C] [B] \; dV \quad (4.47)$$

$$= \frac{A_s E_s}{l^2} \int_l \begin{bmatrix} (2L-1)(2L-1) & (2L-1)(2L+1) & -4L(2L-1) \\ (2L-1)(2L+1) & (2L+1)(2L+1) & -4L(2L+1) \\ -4L(2L-1) & -4L(2L+1) & 16L^2 \end{bmatrix} dl$$

(4.48)

where A_s is the cross sectional area of the element. Integration of equation (4.48) gives the stiffness matrix for linear strain bar element as

$$[K]_e = \frac{A_s E_s}{3l} \begin{bmatrix} 7 & 1 & -8 \\ 1 & 7 & -8 \\ -8 & -8 & 16 \end{bmatrix} \quad (4.49)$$

The element stiffness matrix from local coordinate system is to be transferred to global coordinate system. Using the basic displacement transformation $\{\delta\}_1 = [T_1] \{\delta\}$ to relate the displacements in two coordinate system, the desired stiffness matrix transformation is obtained as

$$[K] = [T_1]^T \, [K]_e \, [T_1] \tag{4.50}$$

where $[K]$ is the element stiffness matrix in global coordinate system and

$[T_1]$ is the transformation matrix which transforms the local displacement vector to global displacement vector.

For linear strain bar element, the transformation matrix is given by

$$[T_1] = \begin{bmatrix} \text{Cos}\theta & \text{Sin}\theta & 0 & 0 & 0 & 0 \\ 0 & 0 & \text{Cos}\theta & \text{Sin}\theta & 0 & 0 \\ 0 & 0 & 0 & 0 & \text{Cos}\theta & \text{Sin}\theta \end{bmatrix} \tag{4.51}$$

where θ is the inclination of local coordinate system to global coordinate system.

4.5 PSEUDO LOADS DUE TO CRACKING OR YIELDING

The total potential energy of an elastic uncracked concrete or brick element is given by expression

$$U = U_c + W \tag{4.52}$$

where U_c is the strain energy of concrete or brickwork

W is the potential energy due to external loads.

When this element cracks or yields, material constitutive matrices will change and as a result of this the strain energy will be released. If U_{cc} is the strain energy released

due to cracking and U_{cy} due to yielding of concrete or brickwork, the expression for potential energy can be modified as (30, 33)

$$\pi = U_c - U_{cc} - U_{cy} + W \tag{4.53}$$

For finite element displacement formulation, the potential energy equation (4.53) can be written as follows

$$\pi = \frac{1}{2}\{\delta\}^T[K_c]\{\delta\} - \frac{1}{2}\{\delta\}^T \Big(\int_{V_{cc}} [B]^T[C_{cc}][B]\, dV_{cc} + \int_{V_{cy}} [B]^T[C_{cy}][B]\, dV_{cy}\Big)\{\delta\} - \{\delta\}^T\{P\} \tag{4.54}$$

where $[C_{cc}]$ and $[C_{cy}]$ are the change in material constitutive matrices due to cracking and yielding of concrete or brickwork respectively,

$[K_c]$ is the stiffness matrix of concrete or brickwork element

$[P]$ is the externally applied load vector which includes body force, surface traction and concentrated nodal loads.

Minimizing the potential energy, we obtain,

$$[K_c]\{\delta\} = \{P_{cc}\} + \{P_{cy}\} + \{P\}$$

where $\{P_{cc}\}$ and $\{P_{cy}\}$ are called pseudo loads and are defined as

$\{P_{cc}\} = \Big(\int_{V_{cc}} [B]^T[C_{cc}][B]\, dV_{cc}\Big)\{\delta\}$ = pseudo load vector due to cracking of concrete or brickwork

$\{P_{cy}\} = \Big(\int_{V_{cy}} [B]^T[C_{cy}][B]\, dV_{cy}\Big)\{\delta\}$ = pseudo load vector due to yielding of concrete or brickwork.

Similarly, we can derive the expression for pseudo loads due to yielding of steel reinforcement. The expression will be as follows

$$\{P_{sy}\} = (\int_{V_{sy}} [B]^T [C_{sy}] [B] \, dV_{sy} \{\delta\} \qquad (4.56)$$

where $[C_{sy}]$ is the change in material constitutive matrix due to yielding of steel reinforcement.

The pseudo loads in equation (4.55) are due to the stresses released in the element because of change in material properties. The pseudo loads are computed as follows.

Considering the pseudo load due to cracking

$$\{P_{cc}\} = \int_{V_{cc}} [B]^T [C_{cc}][B] \, dV_{cc} \{\delta\}$$

If $[C]$ is the original constitutive matrix of uncracked and $[C_{cr}]$ is that of cracked element, then $C_{cc} = C - C_{cr}$ and

$$\{P_{cc}\} = \int_{V_{cc}} [B]^T [C] - [C_{cr}] [B]\{\delta\} \, dV_{cc}$$

$$= \int_{V_{cc}} [B]^T [C] - [C_{cr}]\{\varepsilon\} \, dV_{cc}$$

$$= \int_{V_{cc}} [B]^T \{\sigma_0\} \, dV_{cc} \qquad (4.57)$$

where $\{\sigma_0\}$ is the stress released due to cracking.

Similarly pseudo loads due to yielding of concrete or brickwork can be computed in terms of stresses released. This only requires modified material constitutive matrix.

4.5.1 Computation of Pseudo Loads on Concrete/Brickwork Element

In the computational procedure, each element is checked for cracking and yielding at various stages of loading. One of the major advantages of using L.S.T. element is that quite accurate results for linearly elastic analysis of flexural members can be obtained with relatively coarser mesh as shown by Jain, A.K. (41). However the computation of pseudo load vector becomes slightly complicated due to the fact that stresses are not constant over the element and coarser mesh may lead to less accurate results for nonlinear analysis if cracking, yielding etc. are checked at one point (e.g. centroid) only. To overcome this difficulty, the element is further devided into 4 subregions (programme developed accomodates even 16 subregions) as shown in Fig.4.3 for the purpose of pseudo load computations. The strains and stresses are computed at the centroid of each subregion to check for yielding and cracking. The pseudo load vector as given by equation (4.57) for the subregion may be written as

$$\{\Delta P_s\} = \int_{V_r} [B]^T \{\Delta \sigma_o\} \, dV_r$$

where $\{\Delta P_s\}$ is the pseudo load vector for the subregion,

V_r is the volume of subregion that has cracked or yielded and

$\{\Delta \sigma_o\}$ is the vector of stress released in the subregion.

Now for L.S.T. element, it can be written as

$$\{\Delta P_s\} = \int_{V_r} [B_n]^T [N_s]^T \{\Delta\sigma_o\} \, dV_r$$

$$= [B_n]^T \int_{V_r} [N_s]^T \{\Delta\sigma_o\} \, dV_r$$

On integration this gives

$$\{\Delta P_s\} = t \, A_r \, [B_n]^T \begin{Bmatrix} \Delta\sigma_x & L_{1c} \\ \Delta\sigma_x & L_{2c} \\ \Delta\sigma_x & L_{3c} \\ \Delta\sigma_y & L_{1c} \\ \Delta\sigma_y & L_{2c} \\ \Delta\sigma_y & L_{3c} \\ \Delta\tau_{xy} & L_{1c} \\ \Delta\tau_{xy} & L_{2c} \\ \Delta_{xy} & L_{3c} \end{Bmatrix} \qquad (4.58)$$

where A_r is the area of subregion, $\Delta\sigma_x$, $\Delta\sigma_y$ and $\Delta\sigma_{xy}$ are components of stress released vector $\{\Delta\sigma_o\}$, and L_{1c}, L_{2c} and L_{3c} are natural coordinates at the centroid of subregion.

4.5.2 Computation of Pseudo Load Vector on Steel Reinforcement

For the computation of pseudo loads, the steel reinforcement is divided into one or four subregions as shown in Fig. 4.4 and yielding is checked at the centroid of each

subregion. The pseudo load vector on the bar element subregion would be

$$\{\Delta P_s\} = A_s \int_L [B]^T \{\Delta\sigma_o\} \, dL$$

where $[B]$ is the strain-displacement matrix for the bar element, and $\{\Delta\sigma_o\}$ is the stress released in the subregion due to yielding.

If bar is divided in one subregion as shown in Fig. 4.4a the pseudo load vector after integration is

$$\{\Delta P_s\}^T = A_s\Delta\sigma_o \quad \{-1, \quad 1, \quad 0\} \tag{4.59}$$

If bar is divided into four subregions as shown in Fig. 4.4b, the pseudo load vector will be as follows. Pseudo load vector for yielding of subregion 1,2,3 and 4 are

$$\begin{aligned}
\{\Delta P_s\}^T_1 &= \frac{A_s\Delta\sigma_o}{2}\left\{ -\frac{5}{4}, \ -\frac{1}{4}, \ \frac{3}{2} \right\} \\
\{\Delta P_s\}^T_2 &= \frac{A_s\Delta\sigma_o}{2}\left\{ -\frac{3}{4}, \ \frac{1}{4}, \ \frac{1}{2} \right\} \\
\{\Delta P_s\}^T_3 &= \frac{A_s\Delta\sigma_o}{2}\left\{ -\frac{1}{4}, \ \frac{3}{4}, \ -\frac{1}{2} \right\} \\
\{\Delta P_s\}^T_4 &= \frac{A_s\Delta\sigma_o}{2}\left\{ -\frac{1}{4}, \ \frac{5}{4}, \ -\frac{3}{2} \right\}
\end{aligned} \tag{4.60}$$

These pseudo load vectors are in local coordinate system. These are transformed to global coordinate system using the transformation matrix $[T_1]$ of section 4.4. Using transformation

matrix, the pseudo load vector in global coordinate system would be

$$\{\Delta P_s\} = [T_1]^T \{\Delta P_s\} \tag{4.61}$$

4.6 NONLINEAR ANALYSIS

There are two sources of nonlinearity in structural problems. First is the material nonlinearity which results from nonlinear constitutive laws. Second type of nonlinearity arises from the violation of linear strain displacement relationship and is called the geometric nonlinearity. The geometric nonlinearity has been neglected in the present work as the displacements are observed to be small. Besides material nonlinearity, the maximum contribution to the nonlinear behaviour of brick masonry supported on reinforced concrete beams is due to cracking of concrete and brickwork. The way to treat such a situation in the finite element method is to physically define individual cracks as they occur by successively modifying the elements and connectivities of nodal points. But for non-linear analysis the modification of finite element mesh involving renumbering of nodes as the crack propagates has been found to be quite difficult and computationally uneconomical. Therefore, the cracking has been incorporated for the nonlinear analysis, in the present work, by changing the material properties of elements and keeping the topology unaltered.

There are three main approaches to carry out non-linear analysis of structures.

1. Incremental methods
2. Iterative methods
3. Incremental iterative methods.

All the three methods are well documented in standard text books (55, 56) and therefore are not discussed here. Incremental iterative methods are useful and accurate when complete load response of the structure is desired and therefore, this method is used in present work. For completeness of presentation it is briefly described in the subsequent section.

4.6.1 Incremental-Iterative Methods

The incremental-iterative methods uses a combination of incremental and iterative schemes. In this procedure load is applied incrementally, but after each increment successive iterations are performed until the solution converges. The two incremental-iterative methods that are most commonly used in literature are: (i) incremental tangent stiffness method which updates stiffnesses, strains and stresses each time, and (ii) 'initial stress' method which uses the original elastic structure stiffness matrix in all load steps and updates only strains and stresses in each iteration. In both the methods a corrective force is applied at each step to restore the structural equilibrium.

4.6.1.1 Incremental tangent stiffness method

The essence of this method is that at any stage a nodal force system equivalent to the total stress level is evaluated and compared with the prevailing applied loading systems. The difference between the two results is a set of residual forces that can be interpreted as a measure of any lack of equilibrium. To restore equilibrium the residuals are then applied to the structure and problem is resolved after updating the structure stiffness matrix. This process is repeated until residuals are sufficiently small before applying the further load increments. A typical step of the method is described with the aid of Fig. 4.5 which is a single degree of freedom problem. The point B corresponds to the start of the increment i, that is point B is at the end of the increment (i-1). The solution by using the tangent stiffness corresponding to point B leads to the point D, whereas the true solution is at point C. The total deflection corresponding to the point D in multi-degrees of freedom system is given by

$$\{Q_D\} = \{Q_{i-1}\} + \{\Delta Q_i^1\} \tag{4.62}$$

The total load that is equilibrated for $\{Q_D\}$ indicated by point D' is

$$\{P_D'\} = \{P_{i-1}\} + \{\Delta P_i\} - \{\Delta P_{oi}^1\} \tag{4.63}$$

where D D' represents $\{\Delta P^1_{oi}\}$ denoting the unbalanced load for the iteration 1 of load increment i. In general, for j^{th} iteration of i^{th} increment, the total equilibrated load will be

$$\{P^j_i\} = \{P_{i-1}\} + \{\Delta P_i\} - \{\Delta P^j_{oi}\} \tag{4.64}$$

Referring to Fig. 4.5b, the total strains in the element corresponding to structure displacement Q_D' is given by

$$\{\epsilon\}_D = \{\epsilon_{i-1}\} + \{\Delta\epsilon^1_i\} \tag{4.65}$$

Use the tangent stiffness corresponding to the point B gives the stress value at D (Fig. 4.5b) which is higher than the actual stress at D' equilibrated by the strains ϵ_D. Therefore, the total stress that is equilibrated for ϵ_D indicated by point D' is

$$\{\sigma\}_{D'} = \{\sigma_{i-1}\} + \{\Delta\sigma_i\} - \{\Delta\sigma^i_{oi}\} \tag{4.66}$$

where $\{\Delta\sigma^1_{oi}\}$ is the correction stress for iteration 1 of load increment i. In general for the j^{th} increment the total equilibrated stress will be

$$\{\sigma^j_i\} = \{\sigma_{i-1}\} + \{\Delta\sigma_i\} - \{\Delta\sigma^j_{oi}\} \tag{4.67}$$

It can be seen from equations (4.64) and (4.67) (Figs. 4.5a and 4.5b) that the values converge to true solution when correction stress $\{\Delta\sigma_o\}$ and correction load $\{\Delta P_o\}$ tend to zero.

The total stress increment for j^{th} iteration of the i^{th} load increment is expressed as

$$\{\Delta\sigma_i^j\} = [C] \{\Delta e_i^j\} - \{\Delta\sigma_{oi}^j\} \qquad (4.68)$$

where $[C]$ is the constitutive matrix corresponding to the current state of stress. But the determination of current state of stress is not possible without knowing the corresponding constitutive relation. To overcome this difficulty, the solution is found by approximating the material properties corresponding to the stress state of the previous cycle. Now writing the correct stress increment as

$$\{\sigma_{ci}^j\} = [C'] \{\Delta e_i^j\} - \{\Delta\sigma_{oi}^j\} \qquad (4.69)$$

where $[C']$ is the material constitutive matrix corresponding to the previous cycle, the potential energy increment can be written as

$$\Delta\pi = \frac{1}{2} \{\Delta Q\}^T [K_T] \{\Delta Q\} - \{\Delta Q\}^T (\int [B]^T \{\Delta\sigma_o\} \, dV + \{\Delta P\}$$

(4.70)

or the equilibrium equation is given by

$$[K_T] \{\Delta Q\} = \{\Delta P\} + \{\Delta P_o\}$$

or for j^{th} iteration of i^{th} increment, equilibrium equation is as follows

$$[K_T] \{\Delta Q_i^j\} = \{\Delta P_i^j\} + \{\Delta P_{oi}^j\} \qquad (4.71)$$

where $$[K_T] = [K_i^j(\{Q_i^{j-1}\},\{P_i^{j-1}\})] \text{ for } j > 1,$$
$$= [K_i(\{Q_{i-1}\},\{P_{i-1}\})] \text{ for } j = 1, \qquad (4.72)$$

$$\{\Delta P_i^j\} = \{0\} \quad \text{for} \quad j > 1 \qquad (4.73)$$

$$\{\Delta P_{oi}^j\} = \sum_{\text{elements}} [B]^T \{\Delta\sigma_{oi}^{j-1}\} \, dV \text{ for } j > 1$$
$$= \sum_{\text{elements}} [B]^T \{\Delta\sigma_{oi-1}\} \, dV \text{ for } j = 1 \qquad (4.74)$$

The incremental solution of equation (4.18) is obtained by computing the correction load $\{\Delta P_{oi}^j\}$ for each iteration, updating the structure stiffness matrix $[K_T]$ due to change in material property and iterating the process to convergence.

The incremental-iterative method with variable stiffness requires the computation of the structure stiffness matrix at each step of solution procedure. This suffers from an economic disadvantage because a complete reformulation of the stiffness matrix and a new solution of governing equations are required at each iteration. This difficulty can be overcome by adopting a method which uses the same stiffness matrix repeatedly in the solution procedure as described below.

4.6.1.2 Initial Stress Method

As correction loads $\{\Delta P_{oi}^j\}$ in equation (4.71) serve to satisfy the equilibrium, it is not essential that the

tangent stiffness matrix be used. Instead, the tangent stiffness matrix in equation (4.71) can be replaced by the initial stiffness matrix $[K_o]$ corresponding to the original elastic stiffness of the structure. This form of the solution has been called 'initial stress' method (26,27,55). Numerically the 'initial stress' method has a unique advantage of using the same stiffness matrix at every stage of iteration. After the first iteration, each subsequent iteration can be performed in a small fraction of time needed for the first solution since the inverted stiffness matrix is available. The use of the 'initial stress' method where the structure stiffness matrix is computed and inverted only once in the solution procedure has been found computationally advantageous (27). Therefore this method is adopted in the present work.

In each iteration of this method, the difference between the true stress level corresponding to the appropriate strains and that corresponding to an elastic solution is determined. This stress difference is redistributed elastically to restore equilibrium.

Fig. 4.6 shows the essential steps of the 'initial stress' method. The explanation of Fig. 4.6 follows exactly that of Fig. 4.5 except the difference that the line BD remains parallel to the initial tangent. When the original

material properties are used, then potential energy increment of equation (4.70) gets modified to

$$\Delta\pi = \frac{1}{2}\{\Delta Q\}^T K_o\{\Delta Q\} - \{\Delta Q\}^T \left(\int [B]^T\{\Delta\sigma_o\}\, dV + \{\Delta P\}\right) \quad (4.75)$$

or the equilibrium equation is given by

$$[K_o]\{\Delta Q_i^j\} = \{\Delta P_i^j\} + \{\Delta P_{oi}^j\} \quad (4.76)$$

where $[K_o]$ is the initial tangent stiffness matrix which is given by

$$[K_o] = \int_V [B]^T [C_o] [B]\, dV \quad (4.77)$$

where $[C_o]$ being the initial material constitutive matrix. The values of nodal load vectors $\{\Delta P_i^j\}$ and $\{\Delta P_{oi}^j\}$ are given by equations (4.73) and (4.74).

4.7 CONVERGENCE CRITERIA

In the incremental-iterative procedure based on 'initial stress' method used in the present work, the equilibrium equations are solved for nodal displacements. The two most obvious criteria of measuring convergence at the end of an iteration are the magnitude of forces by which equilibrium is violated or the accuracy of the nodal displacements. The violation of equilibrium is measured by the magnitude of the residual unbalanced nodal forces. The accuracy of the nodal displacements can be measured by the magnitude of the additional increments of displacements.

In the present investigation increments of nodal displacements and residual unbalanced nodal forces both are considered to check the convergence. The maximum vector norm is used to measure the error for each component of residual displacement and unbalanced force. The errors are

$$||E_D|| = \max_n ||Q_n|| \text{ for displacement vector; and}$$
$$||E_P|| = \max_n ||P_{on}|| \text{ for unbalanced force vector.}$$

When both the errors become smaller than their convergence criteria, the program will stop the iteration and go on to the next load increment. The residual unbalanced nodal forces will be carried over and added to the next load increment.

The tolerance for convergence could be decided on the basis of the required accuracy of the results which is often dictated by the accuracy of measurement. In the present work the tolerence on unbalanced force has been taken as 1.0 kg. while the same on displacement has been taken as 1×10^{-6} cm.

4.8 RESULTS OF FINITE ELEMENT ANALYSIS

The computer programme developed in Fortran IV in the present work based on foregoing description has been used to analyse the specimens investigated and parametrically studied experimentally. The analytical results are obtained

on DEC system 1090 at IIT Kanpur and these are compared with the experimental results reported in Chapter III. The composite structures and load thereon is simulated to represent identical system as investigated experimentally. Half symmetry of the system has been exploited all through except where unsymmetric openings existed.

Experimental investigation has revealed that the composite system behaves linearly in the initial stages until the load approaches the first crack load. This has been verified analytically as is shown in Fig. 4.13 and Fig. 4.15. Hence, inorder to carry out nonlinear finite element study of the composite system, starting load does not have to be zero load. On the contrary the starting load can be just below the first crack load for each specimen. This ofcourse is not apriori known. Therefore, a numerical experimentation was carried out in each case to decide upon the initial load which was almost 3 tonnes below the first crack load for each specimen. This saved the computational effort as well which would have been otherwise required if the load on the system would have been incremented starting from no load condition. The load was incremented in each case by 3 tonnes in the present analytical study. For each load increment an upper limit of 300 on the number of iterations was imposed to allow the pseudo-loads and deflections to converge. While at

the failure load, pseudo-loads converged in all cases within this limit on the number of iterations the corresponding deflections failed to converge in 300 iterations. Increasing the upper limit on the number of iterations to ensure convergence of deflections at higher loads near the failure would have resulted in prohibitive use of computer time. Therefore, this was not done in the present work. The termination of the programme at 300 iterations or the crushing of concrete whichever occurred earlier was taken to be the on set of failure of the composite system in the present analytical study.

4.8.1 Effect of Variation in Cement Sand Mortar for Brickwork

Specimen number 1 to 10 (described in the previous chapter) are symmetric about a vertical centre line passing through mid span. Therefore, half of the specimen size was modelled by 42 L.S.T. elements for brickwork and concrete and 21 L.S.B. elements for bending reinforcement and vertical connectors as shown in Fig. 4.7.

Figs. 4.8(a) to 4.12(a) respectively show the plot of longitudinal stress, σ_x, at various cross sections for the specimens number 1 to 5 (cast in mortars of 1:3, 1:4, 1:5, 1:6 and 1:8 respectively) at the initial load. From these plots it is seen that the supporting R.C. beam is always

under tension except very near the supports. The compressive stresses are borne by the brickwork. The vertical stresses, σ_y, and the shear stresses, τ_{xy}, have been plotted in Figs. 4.8(b) to 4.12(b) and 4.8(c) to 4.12(c) respectively for the five specimens analysed at the initial load. From these figures it is observed that vertical stress and shear stress concentrate in the R.C. beam and brickwork just above it very near the supports. Figs. 4.8(d) to 4.12(d) show the stress along the bending reinforcement at various loads starting from initial load upto failure. The bending reinforcement in four of the five specimens (i.e. all except one cast in mortar ratio of 1:8) reaches the yield stress at failure. The stress in bending reinforcement increases rapidly as the concrete cracks. Figs. 4.8(e) to 4.12(e) show the vertical deflection at the bottom of specimen along the span at various loads starting from initial load upto failure. From these plots it is seen that the deflection shape has point of inflexion near the supports meaning thereby that the specimens deflect as simply supported beams with small over hang on either side. This is in accordance with the plots shown in Figs. 4.8(a) to 4.12(a) where the nature of longitudinal stresses change from near the supports to the mid span. Fig. 4.13 shows the plot of load versus deflection at mid span obtained analytically. The corresponding experimental deflections obtained are also shown on this

figure for the sake of comparison. From these plots it can be concluded that experimental and analytical results of load versus deflection compare very well all through upto failure load. Fig. 4.14 gives the plot of longitudinal strains for various specimens at the mid span cross section under the initial load. The variation of longitudinal strains is linear as observed experimentally. Table 4.1 gives the first crack load and the failure load for specimen 1 to 5 obtained analytically. The first crack load obtained analytically for specimen number 1 cast in 1:3 mortar is about 25 percent lower than the corresponding experimental value. However, for specimens number 2 to 5 cast in mortar 1:4 to 1:6 and 1:8 respectively these results are approximately 10 percent lower than corresponding values obtained experimentally as given in Table 3.16. The general reason for this discrepancy is probably the fact that specimens investigated experimentally actually cracked earlier than observed. However the large difference in case of specimen number 1 is only attributable to variation in material properties and workmanship of the experimental specimen. The analytical values of failure load is lower by 10 to 20 percent in case of specimens number 1 to 4 cast in mortar 1:3 to 1:6, while for specimen number 5, cast in mortar 1:8 it is higher by 50 percent as compared to corresponding experimental value of failure load.

The failure load analytically obtained corresponds to either crushing of concrete or termination of the programme for each load increment at 300 iterations, whichever is earlier. For the specimens number 1 to 5, the failure load obtained did not result into the crushing of the concrete. In other words, it is corresponding to the premature termination of the programme only due to the limit imposed on the number of iterations without attaining the convergence on deflections. This, however, was unavoidable in the present work because of prohibitively high computational time which would have been otherwise required. It is this premature termination of the programme which has resulted in the lower failure load obtained analytically for specimens number 1 to 4 as compared to the failure load recorded experimentally. However, it would be recalled that during experimental investigation, the dial gauges were removed to ensure safety of the devices and the observers, at a load where the deflections had significantly increased than those in the previous load increment and the failure was expected to be imminent. After the removal of the dial gauges the experimental specimens were further loaded to observe the actual failure load. Significantly, the analytical failure loads obtained are comparing very well with those at which the dial gauges were removed in the experimental

investigation as shown in Table 4.2. From this it can be safely concluded that the analytical method used in the present work is correctly predicting the imminent failure load. Furthermore, the analytical result so obtained is conservative and hence can be safely used for design purposes. Specimen number 5 cast in 1:8 mortar give a higher failure load analytically as compared to the correspon-ding experimental value. The reason for this, as discussed in the previous chapter, is the load failure between the connectors and the brickwork in 1:8 mortar when investigated experimentally while in analytical investigation a perfect bond has been assumed between the connectors and the brick-work. Naturally, therefore, the latter value turns out to be higher.

Figs. 4.8(f) to 4.12(f) show the crack pattern obtained at failure for the five specimens. These crack patterns have been plotted from the computer print out taking into account the information regarding the subregion of the element cracked and the direction of this cracking at the centroid of the subregion. Analytical plot of crack patterns shows more number of cracks in a specimen as compared to those obtained experimentally. The reason for this is that in the analytical work the finite element subregion in which the tensile stress exceeds the allowable

limit is assumed to have cracked and a crack is shown to initiate from that particular element or subregion perpendicular to the direction of the principal tensile stress. Experimentally, however, number of cracks do not develop but the crack already formed initially goes on widening. In any case, the nature of crack obtained both experimentally and analytically is principally the same.

The above analytical study firmly reinforces the conclusions drawn after the experimental investigation in this regard.

Table 4.3 gives the initial load applied, number of load increments and computer time taken for the analytical study of specimens number 1 to 5.

Fig. 4.15 shows the analytical load versus deflection curve under tensile loading for the specimens number 6 to 10 (cast in mortar 1:3, 1:4, 1:5, 1:6 and 1:8 respectively) at the mid span. These results are under the assumption that perfect bond between the connectors and brickwork exists. The corresponding experimental curves are also shown on the same figure for purposes of comparison. From these curves it is observed that deflections obtained experimentally are much higher than those obtained analytically. It is also observed that cracks obtained analytically are linear upto the first crack load while experimental curves show non-

linearity right from zero load. The discrepancy in the analytical and experimental results is due to the fact while experimentally bond slip between the vertical connectors and the brickwork is established, analytically perfect bond between the two has been assumed . Therefore, to obtain a correct analytical load deflection response, introduction of bond link elements is necessary. This however, has not been attempted in the present work and any further analytical study for specimens under tensile loading has been abondoned.

4.8.2 Effect of Variation in Height to Span Ratio

Specimens number 11,4,12,13 and 14 having height to span ratios of 0.25, 0.33, 0.4, 0.5 and 0.8 are analysed under compressive loading by the computer programme developed in the present work and the results so obtained are compared with the corresponding experimental values. All these specimens being symmetrical about the vertical line passing through the mid span, half symmetry has been exploited in the analytical study. Specimens number 11, 12 and 13 were modelled by 42 L.S.T. elements for brickwork and concrete and 21 L.S.B. elements for bending reinforcement and connectors. Specimen number 14 having a height to span ratio of 0.8 was, however, modelled by 56 L.S.T. elements for brickwork and concrete and 28 L.S.B. elements for bending reinforcement and vertical connectors.

Figs. 4.16(a) to 4.19(a) respectively show the plot of longitudinal stress, σ_x, at the initial load at various cross sections for the specimen number 11 to 14. From these plots and from Fig. 4.8(a) which is for the longitudinal stress , σ_x, for a height to span ratio of 0.33 it is seen that the supporting thin R.C. beam is always in tension except very near the supports as was the case for specimens number 1 to 5. It is further observed that the variation of longitudinal stress, σ_x, in brickwork is almost linear upto a height to span ratio of 0.5. For specimen number 14, having a height to span ratio of 0.8 the longitudinal stress at various cross sections are very small and these do not vary linearly. Infact the brickwork is relatively free from the longitudinal stress in all specimens investigated. It is further observed from these plots that the neutral axis at initial load (i.e. for uncracked section) is at a depth almost equal to 2/3rd the height of composite system. Vertical stresses, σ_y, and the shear stresses, τ_{xy}, have been plotted in Figs. 4.16(b) to 4.19(b) and 4.16(c) to 4.19(c) respectively for the four specimens number 11 to 14. It is observed from these plots that concentration of vertical stress and shear stress takes place near the supports in the R.C. beam and the brickwork just above it. Figs. 4.16(d) to 4.19(d) gives the stress in steel along the bending reinforcement at various loads starting

from initial load upto failure. At failure, the stress in bending reinforcement in all specimens reaches the yield stress. Figs. 4.16(e) to 4.19(e) show the vertical deflection at the bottom of composite system along the span at various loads starting from initial load upto failure. From these curves it is seen that higher is the height to span ratio lower are the deflections for the same load. Fig. 4.20 shows the plot of load versus deflection at mid span obtained analytically. The corresponding deflections obtained experimentally at various loads are also shown on this figure for purposes of comparison. From these curves it can be concluded that the experimental and analytical results of load versus deflection compare very well upto the failure load except for specimen number 11, which has a height to span ratio 0.25. In case of specimen number 11, the experimental and analytical load deflection curves upto first crack load overlap each other but beyond first crack load experimental deflections are much higher than obtained analytically. The reason for this difference is that, the length of connectors is not sufficient to transfer the load and therefore bond slip starts after the first crack load and this bond slip causes higher deflections and subsequent early failure of the specimen. However, since perfect bond has been assumed in the analytical work,

analytical results show lower deflections and higher failure loads. Table 4.4 gives the first crack load and the failure load for specimens number 4 and 11 to 14 having various height to span ratios. The first crack load for all specimens are slightly lower than observed experimentally for the corresponding specimens as given in Table 3.33 except in the case of specimen number 12 having a height to span ratio of 0.4 where the analytical value is around 20 percent lower than the experimental value. This difference in two values for specimen number 12 is only attributable to variation in material properties and workmanship of the experimental specimen. The failure load obtained analytically is about 10 percent lower than the corresponding failure load obtained experimentally except in case of specimen number 11 where experimental failure load is lower than the analytical value for reasons explained earlier. The reason for the lower analytical failure load is again the premature termination of computer programme because of the limit imposed on the number of iterations for a load increment as discussed in the preceeding section. Figs. 4.16(f) to 4.19(f) show the crack patterns obtained for the four specimens. The nature of cracks is basically the same as obtained experimentally. However, analytical plot of crack pattern show more number of cracks in a specimen as compared to those obtained

experimentally for reasons explained in preceeding section.

This study reinforces the conclusions drawn from the experimental work that higher is the height to span ratio, higher is its load carrying capacity. Furthermore, the analytical results for the first crack load as well as the failure load are slightly conservative from designers point of view.

Table 4.5 gives the initial load applied, number of load increments and computer time taken for the analytical study of specimen number 11 to 14.

4.8.3 Effect of Variation in Size and Location of Openings

Specimens number 19 to 23 having openings as detailed in the table on next page, have been analytically analysed by the computer programme developed in the present work. Half symmetry has been exploited wherever possible. The table also gives the details of finite element model for each specimen.

Figs. 4.21(a) to 4.24(a) gives respectively the plot of longitudinal stress, σ_x, at the initial load at various cross sections for specimen number 19 to 22. From these plots it is seen that behaviour of the composite system with symmetric door and window opening as well the unsymmetric window opening is more or less same as that of composite wall

DETAILS OF FINITE ELEMENT MODEL OF SPECIMENS WITH OPENINGS

Specimen number	Type of opening	Location	No. of nodes	Number of L.S.T. elements		Number of L.S.B elements	
				In concrete	In brickwork	In bending reinforcement	In connectors
19	Window	Symmetric	161	20	46	10	23
20	Door	Symmetric	157	20	42	10	21
21	Window	Unsymmetric	312	40	92	20	47
22	Door	Unsymmetric 8 cm thick R.C. beam	298	40	84	20	43
23	Door	Unsymmetric 16 cm thick R.C. beam	356	68	84	20	43

without opening except at the lintel level. Refering to Figs. 4.21(a) and 4.22(a) we observe that the lintel is under longitudinal compression and the brickwork above it is almost free of longitudinal stress. On the contrary we see in Fig. 4.23(a) that the lintel is under longitudinal tension and the brickwork over it is in longitudinal compression. The reason for this is the fact that the load through the brickwork above the unsymmetric window opening is directly transferred on to the lintel while for symmetric openings the load gets transferred through arching action. Comming to Fig. 4.24(a) we observe that the supporting R.C. beam experiences longitudinal tension at the centre of the opening. This is easily explained from Fig. 4.24(e) where the corresponding deflected shape shows hogging moment at this cross section. The behaviour at the lintel level and above in this case is identical to the one discussed for the case of unsymmetric window opening. Vertical stress, σ_y, is plotted along the span at various heights of the wall for specimens number 19 to 22 and is shown in Figs. 4.21(b) to 4.24(b) respectively. Concentration of vertical stress takes place near the supports and brickwork above it as observed in corresponding solid composite system and also at the ends of the R.C. lintel provided at the top of the openings. In case of symmetric door and window openings, the magnitude

of vertical stress at the supports and brickwork above it is same at various heights under identical load. Moreover, the values also compare well at the corresponding heights of the composite system without openings under identical load. This is as anticipated since load transference in either case is through arching action meaning thereby that symmetric openings about the vertical centre line of the composite system do not affect the over all behaviour of the composite structure. Figs. 4.29(c) to 4.24(c) show respectively the plot of shear stress, τ_{xy}, at various cross sections for specimens number 19 to 22. The concentration of shear stress in all cases is incidentally at locations where the concentration of vertical stress occurs viz. at the supports in R.C. beam and at the two ends of R.C. lintel above the openings. Figs. 4.21(d) to 4.24(d) show the plot of stress in steel along bending reinforcement at various loads starting from intial load to failure load. In specimens number 19 and 20 having symmetric window and door openings bending reinforcement reaches the yield stress at the failure load but for the remaining two specimens number 21 and 22 having unsymmetric openings, the stress in bending reinforcement is below yield value even at the failure load. Figs. 4.21(e) to 4.24(e) show the vertical deflection at the bottom of specimens all along the span at various loads starting from initial to

failure load. Plots of Figs. 4.21(e) and 4.22(e) are almost identical to the corresponding plot of composite system without opening. The slight difference in the values of deflections at various points under the identical load is qualitatively accounted for from the fact that the stiffness of composite system due to openings reduces. From Fig. 4.24(e) it is observed that there is a marked increace in the deflections at various points along the span from the initial to the failure load.

Fig. 4.25 shows the plot of load versus deflection at mid span of all the specimens obtained analytically. The corresponding deflections obtained experimentally are also shown on this figure for purposes of comparison. From these curves it is concluded that the analytical and experimental results of load versus deflections compare well upto failure for all specimens except number 22 for which experimental load deflection curve is not available. Since it failed under its self weight. Table 4.6 gives the first crack load and the failure load for specimens number 19 to 23. Analytical value of first crack load are slightly lower than those obtained experimentally (given in Table 3.47) in case of specimens number 19, 20, 21 and 23. Analytical value of failure loads is lower by about 10 percent to 15 percent for all specimens except number 22 for which no experimental data

is at hand. The reason for the conservative analytical failure load has already been discussed. Fig. 4.21(f) to 4.24(f) show~~s~~ the crack pattern obtained from analytical results. The crack pattern is basically the same as obtainted experimentally.

From this study it is concluded that symmetric openings do not appreciably affect the load carrying capacity of the composite system. However the unsymmetric window opening affects the load carrying capacity significantly while unsymmetric door opening affects the load carrying capacity adversly. It would be recalled that same conclusions were drawn from experimental investigations.

TABLE 4.1 : FIRST CRACK AND FAILURE LOAD $\frac{\text{H/L LOADING}}{\text{0.33 COMPRESSIVE}}$

Specimen Number	Mortar	Ist crack load in tonnes	Failure load in tonnes	Remarks
1	1:3	15.0	27.0	Bending reinforcement at mid span has yielded. The first crack was at mid span
2	1:4	15.0	24.0	-do-
4	1:5	12.0	24.0	Bending reinforcement at mid span and brickwork at top has yielded. The first crack was at mid span.
5	1:6	12.0	21.0	-do-
6	1:8	9.0	15.0	The first crack in concrete was in the mid span region while that in brickwork was near the support. The ultima failure took place because of yielding of brickwork

TABLE 4.2 : IMMINENT FAILURE LOADS $\frac{\text{H/L LOADING}}{\text{0.33 COMPRESSIVE}}$

Specimen number	Mortar	Analytical failure load in tonnes	Experimental imminent failure load in tonnes
1	1:3	27.0	28.91
2	1:4	24.0	24.78
3	1:5	24.0	23.67
4	1:6	21.0	22.71
5	1:8	15.0	8.26

TABLE 4.3 : COMPUTER TIME

H/L	LOADING
0.33	COMPRESSIVE

Specimen number	Mortar	Initial load in tonnes	Number of subsequent load increment	Computer time
1	1:3	3.0	8	58 min 30 secs
2	1:4	3.0	7	52 min 24 secs.
3	1:5	9.0	5	50 min 27 secs
4	1:6	9.0	4	41 min 23 secs
5	1:8	6.0	3	34 min 53 secs

TABLE 4.4: FIRST CRACK AND FAILURE LOAD

MORTAR	LOADING
1:6	COMPRESSIVE

Specimen number	H/L	First crack load in concrete in tonnes	First crack load in brick-work in tonnes	Failure load in tonnes	Remarks
11	0.25	9.0	9.0	18.0	Brickwork at top and bending reinforcement reaches the yield stress
4	0.33	12.0	12.0	21.0	Bending reinforcement at mid span has yielded
12	0.40	15.0	15.0	24.0	Brickwork at top and bending reinforcement midspan has yielded
13	0.50	21.0	21.0	30.0	-do-
14	0.80	24.0	24.0	45.0	Concrete at the supports has crushed and bending reinforcement has yielded

TABLE 4.5: COMPUTER TIME

MORTAR	LOADING
1:6	COMPRESSIVE

Specimen number	H/L	Initial load in tonnes	Number of subsequent load increments	Computer Time
11	0.25	6.0	4	35 min 40 secs
12	0.40	12.0	4	56 min 57 secs
13	0.50	18.0	4	58 min 54 secs
14	0.80	21.0	8	96 min 41 secs

TABLE 4.6: FIRST CRACK AND FAILURE LOAD

H/L	MORTAR	LOADING
0.8	1:6	COMPRESSIVE

Specimen number	Type of opening	First crack load in tonnes	Failure load in tonnes	Remarks
19	Symmetric window	24.0	45.0	Concrete at supports has crus and bending rein- forcement has yielded
20	Symmetric door	24.0	45.0	-do-
21	Unsymmetric window	18.0	24.0	Shear failure
22	Unsymmetric door	3.0	9.0	-do-
23	Unsymmetric door 16 cm R.C. beam	3.0	9.0	-do-

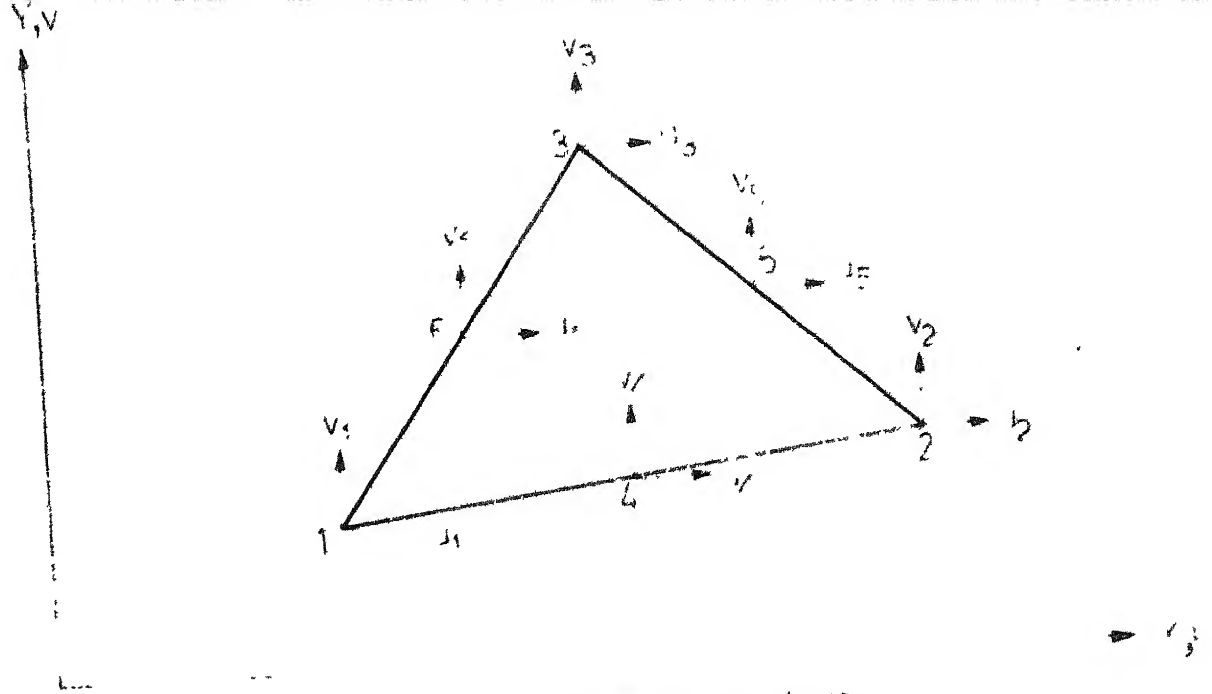

(a) Global coordinate system

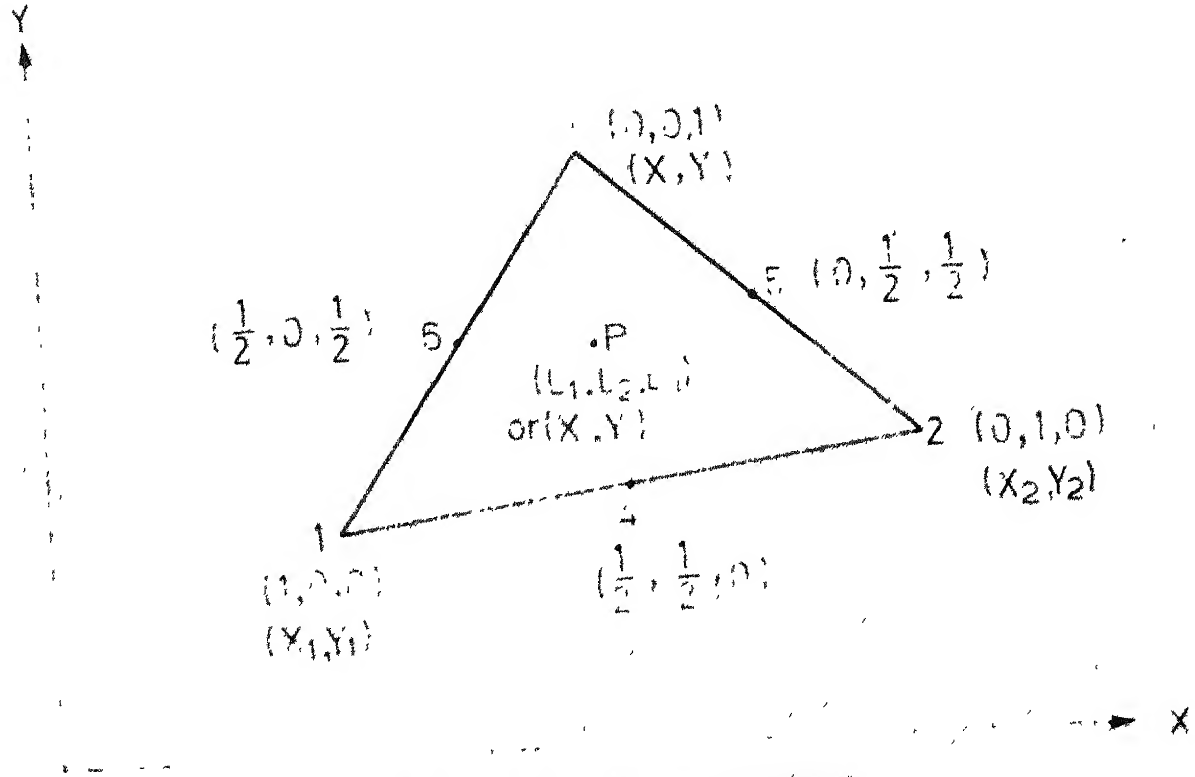

(b) Natural coordinate system

Fig. Linear strain triangular element (LST)

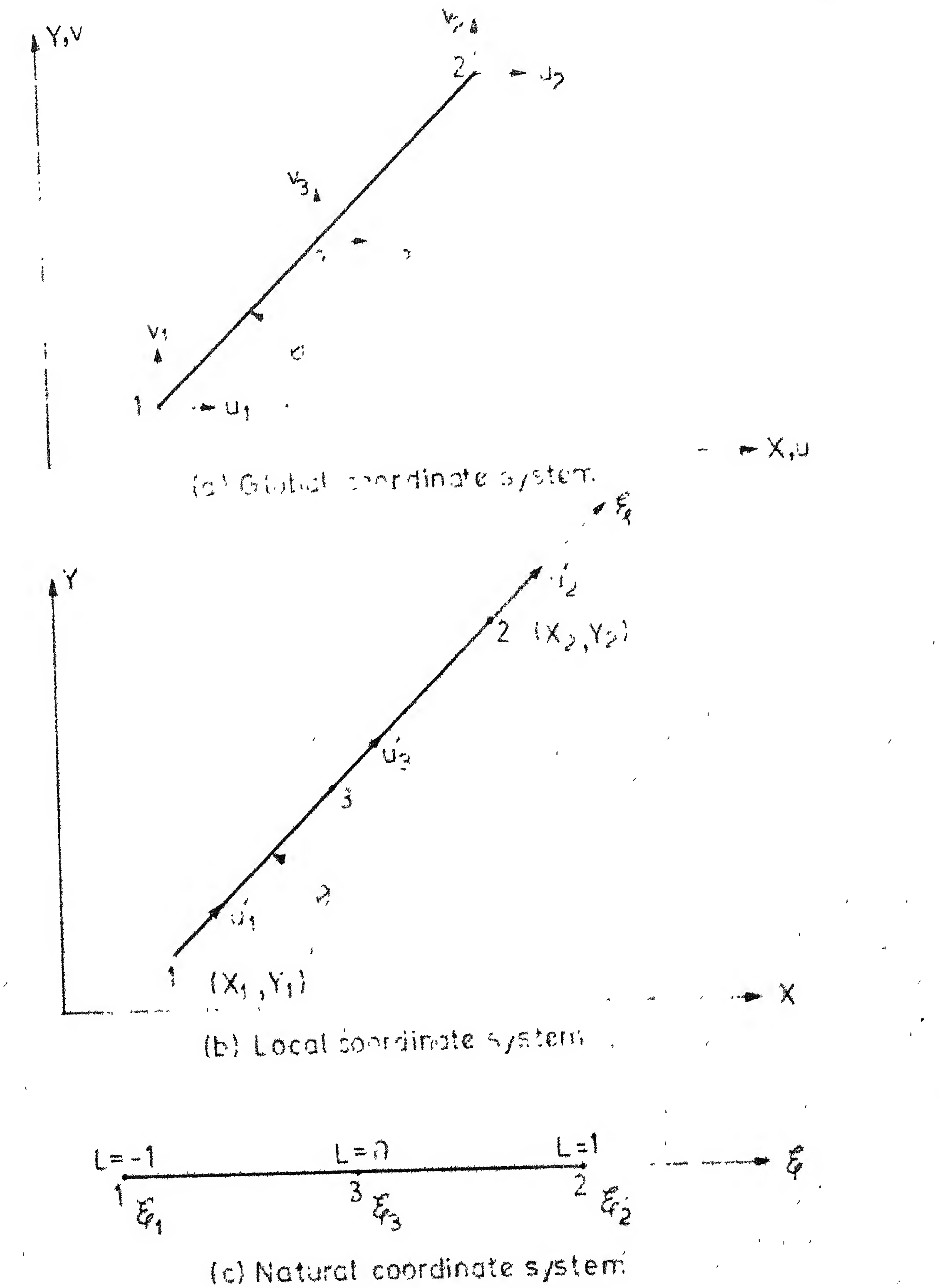

Fig.4.2 Linearly varying strain bar element (LSB)

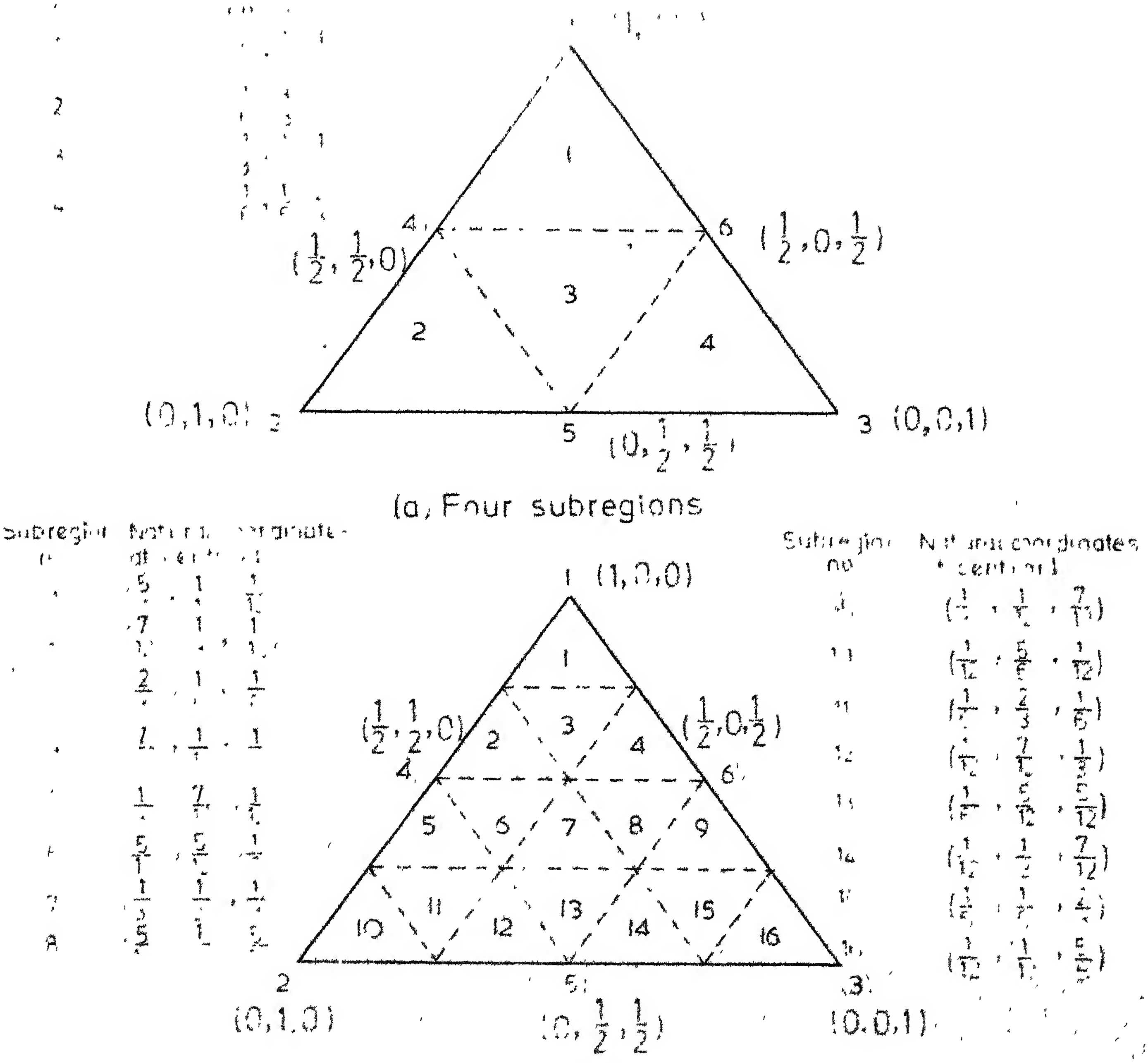

(a) Four subregions

(b) Sixteen subregions

Fig 4.3 Subregioning of triangular element

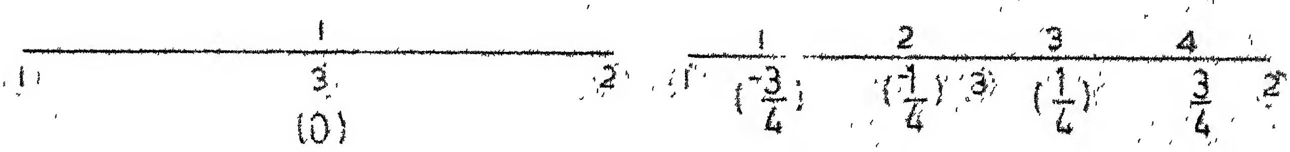

(a) One subregion

(b) Four subregions

Fig.4.4 Subregioning of bar element

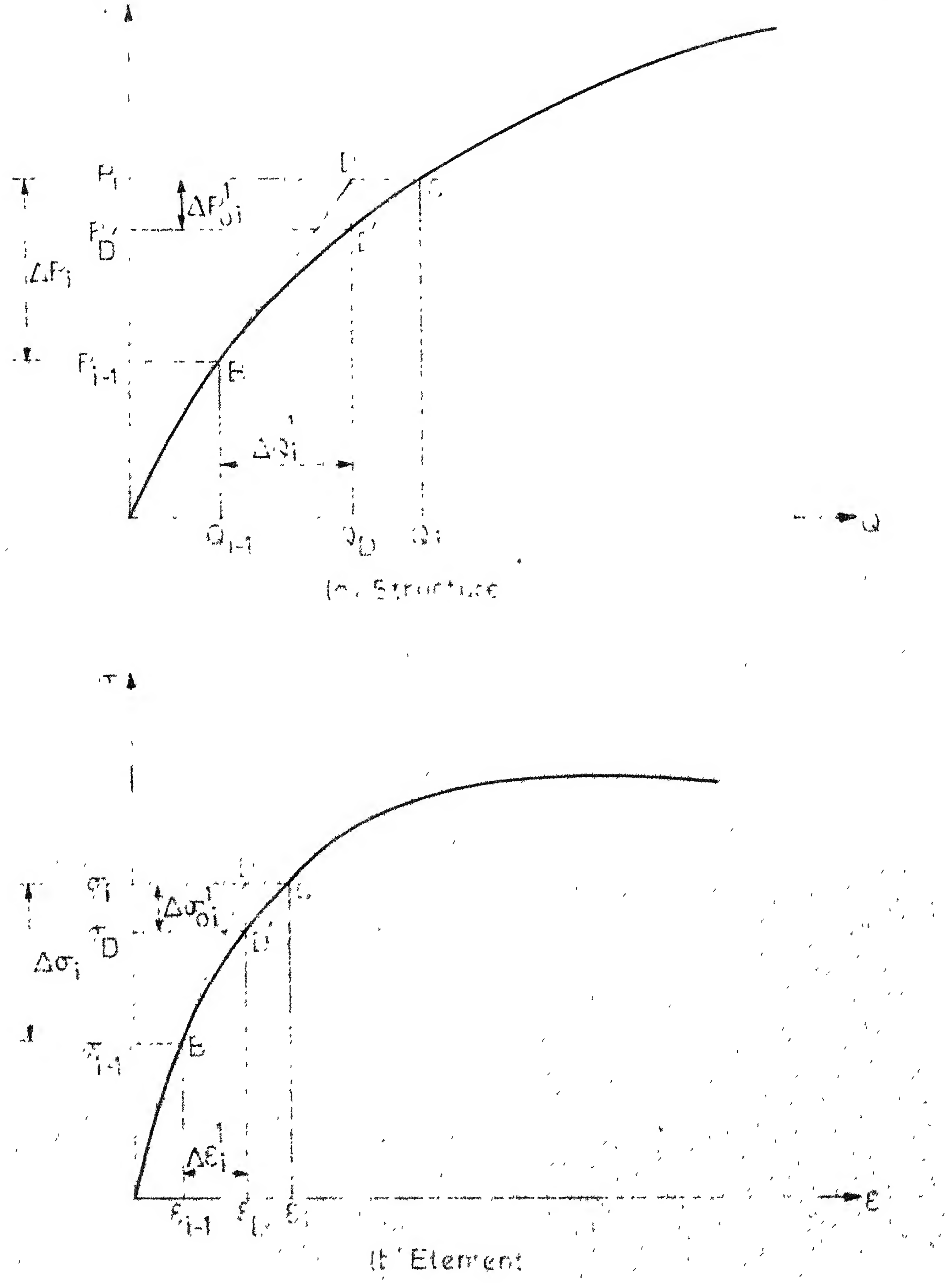

Fig.45 Incremental iterative tangent stiffness metho

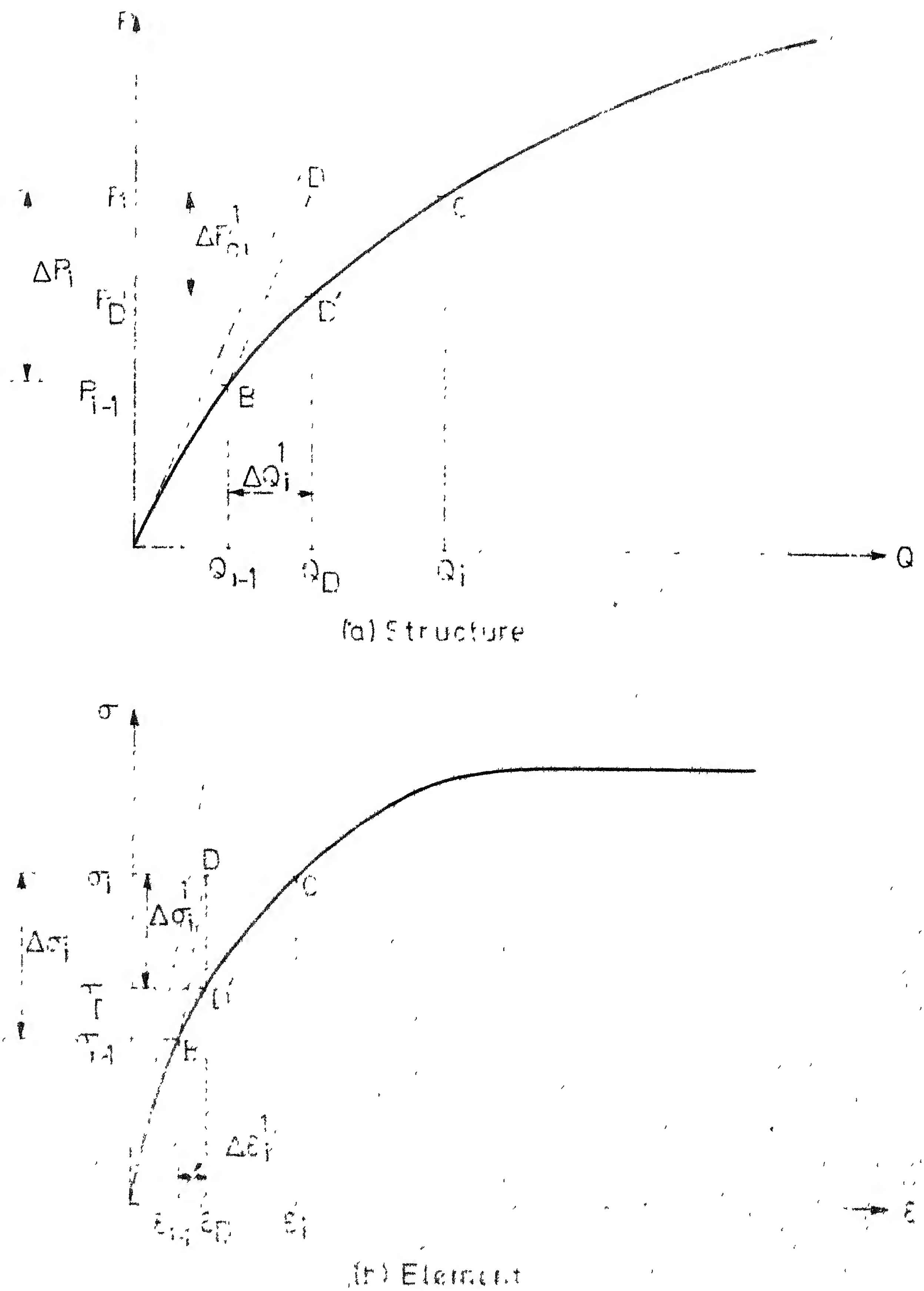

Fig. 4·6 Incremental iterative initial stress method

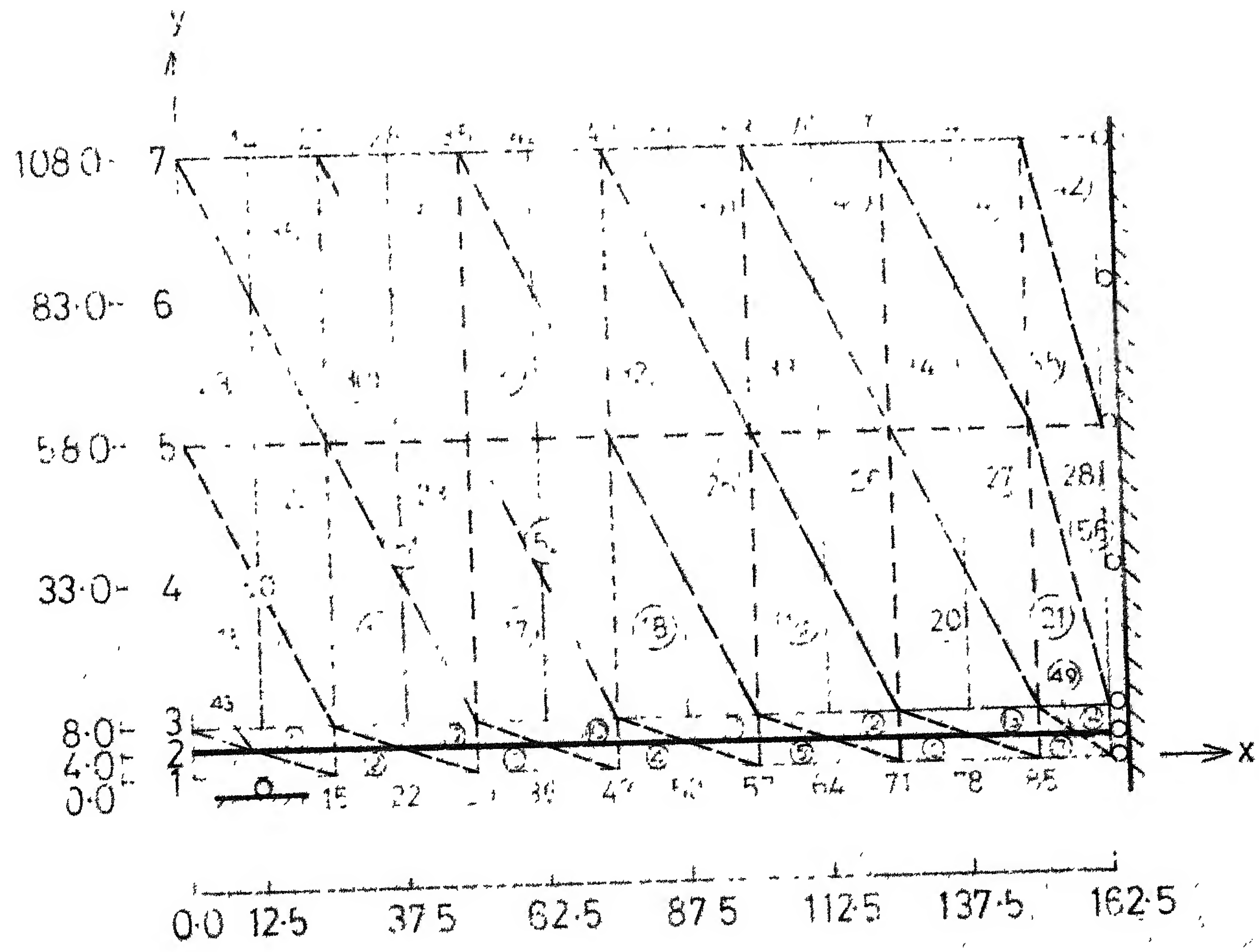

Fig. 4.7 Finite element idealization of a typical specimen

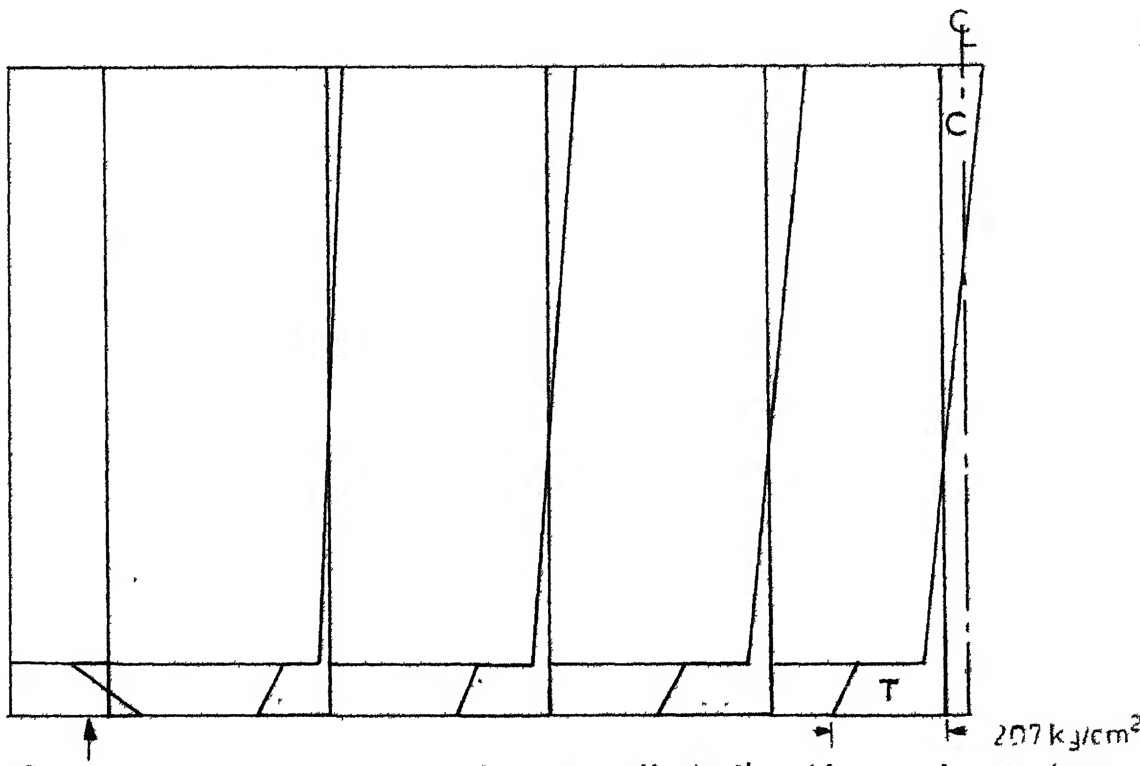

Fig. 4·8 a Longitudenal stress distribution at various cross sections

H/L	Mortar	Loading	Initial load
0·55	1:3	Compressive	12 T

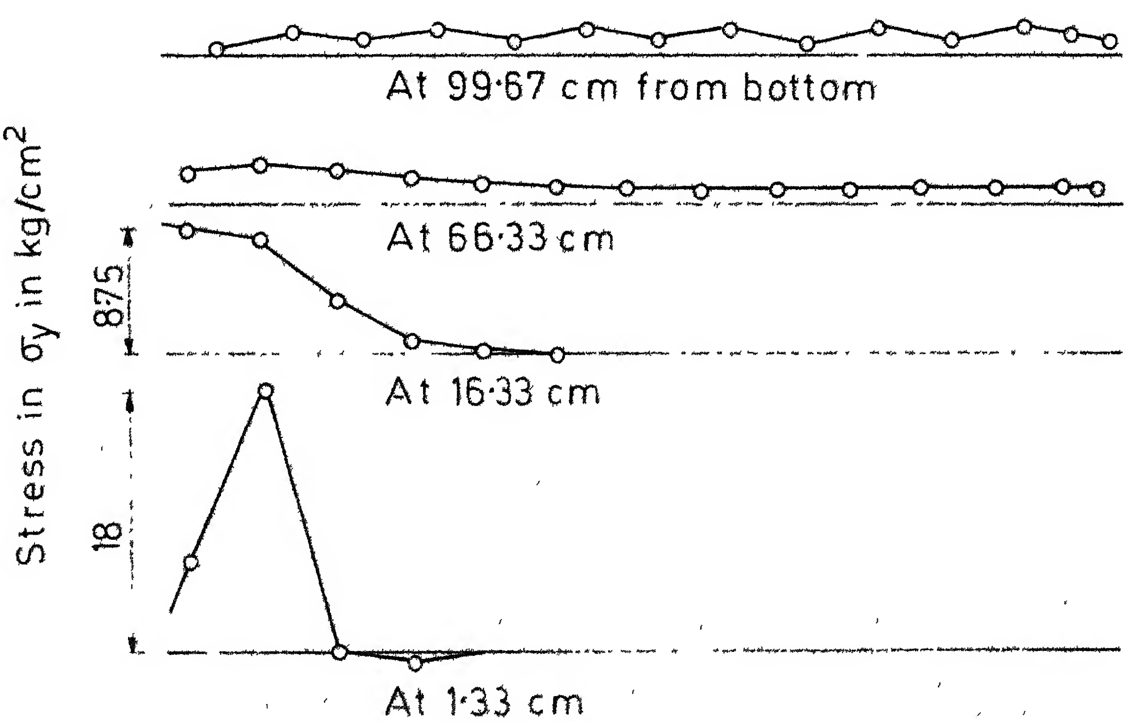

Fig. 4·8 b Vertical stress distribution along span at various heights

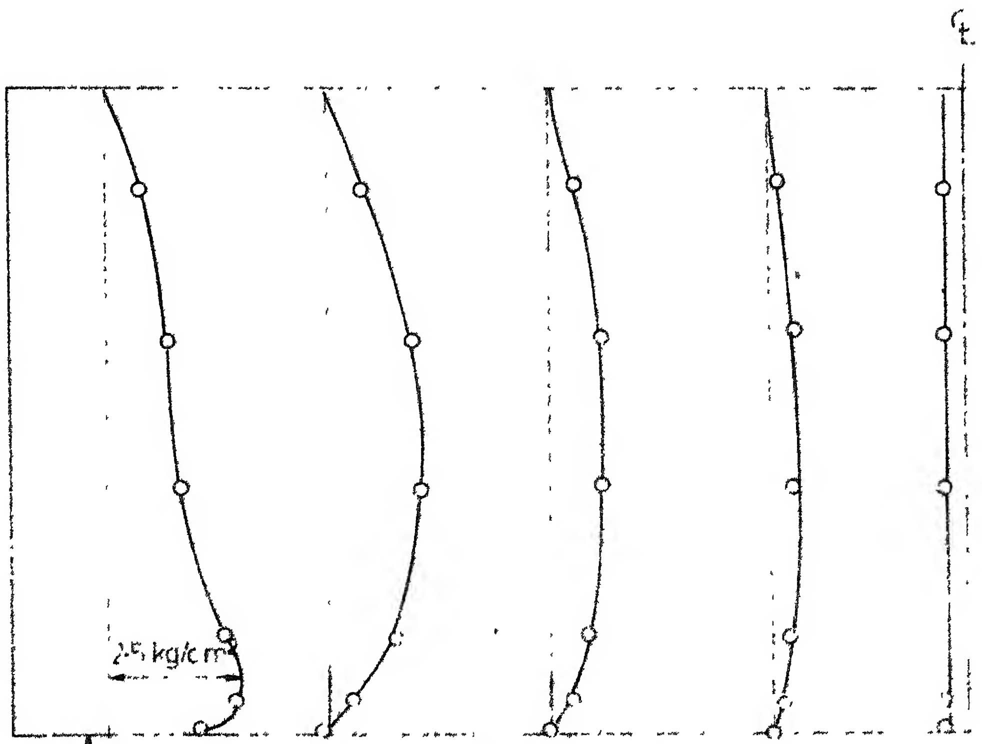

Fig.4·8 c Shear stress distribution at various cross sections

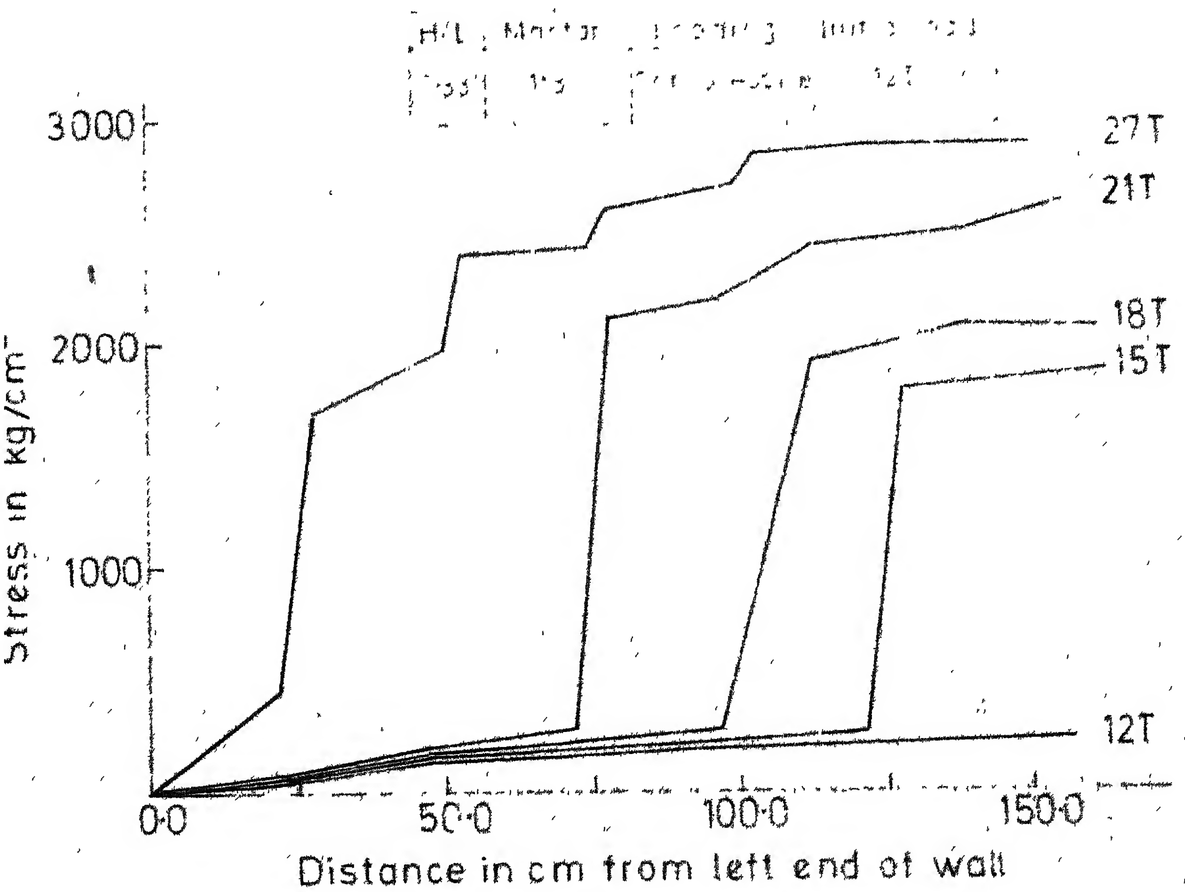

Fig.4·8d Variation of stress in bending reinforcement along span at various loads

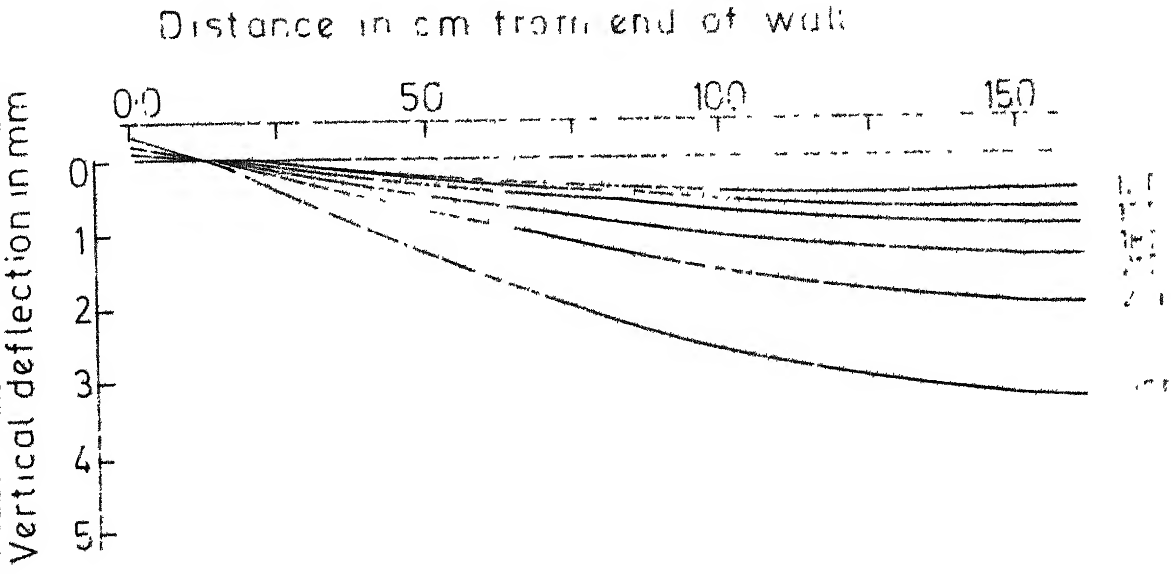

Fig. 4·8 e Vertical deflection of wall along span at various loads

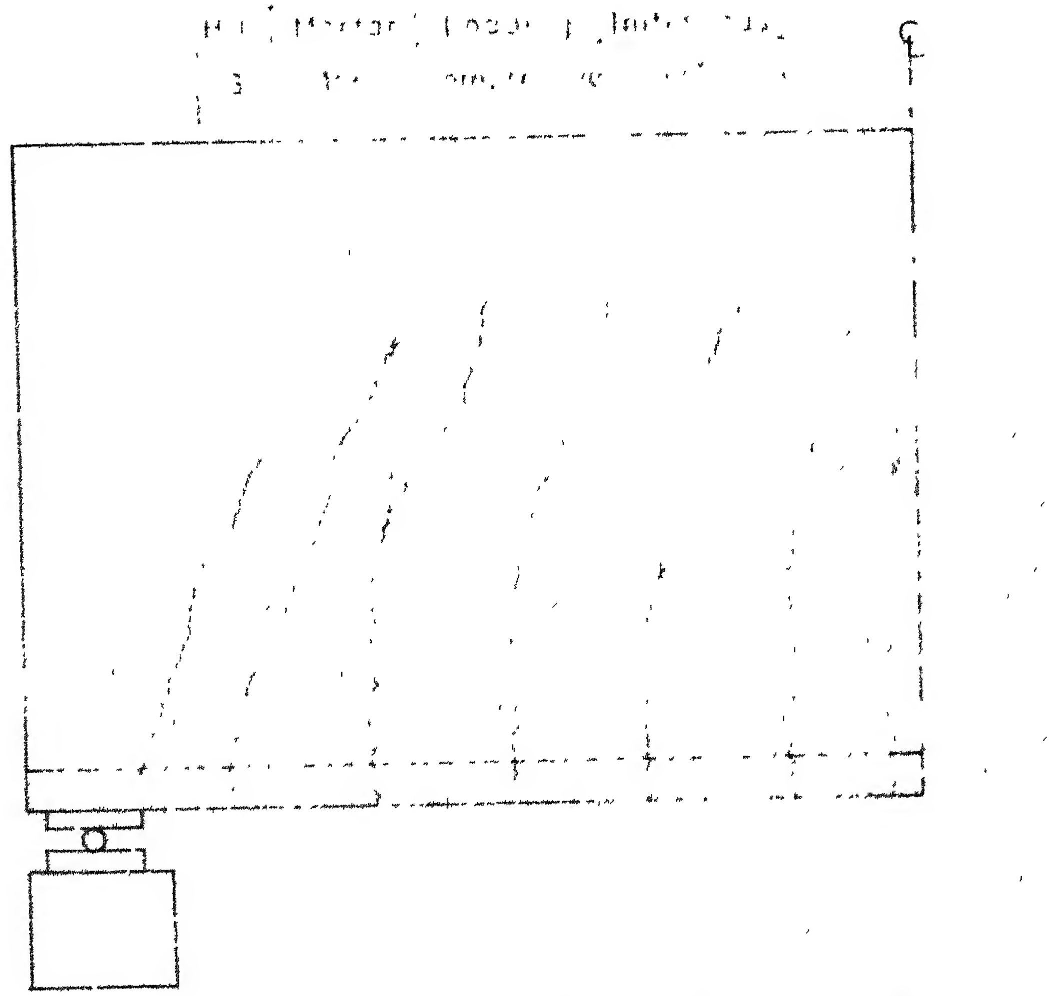

Fig 4·8 f Crack pattern at failure

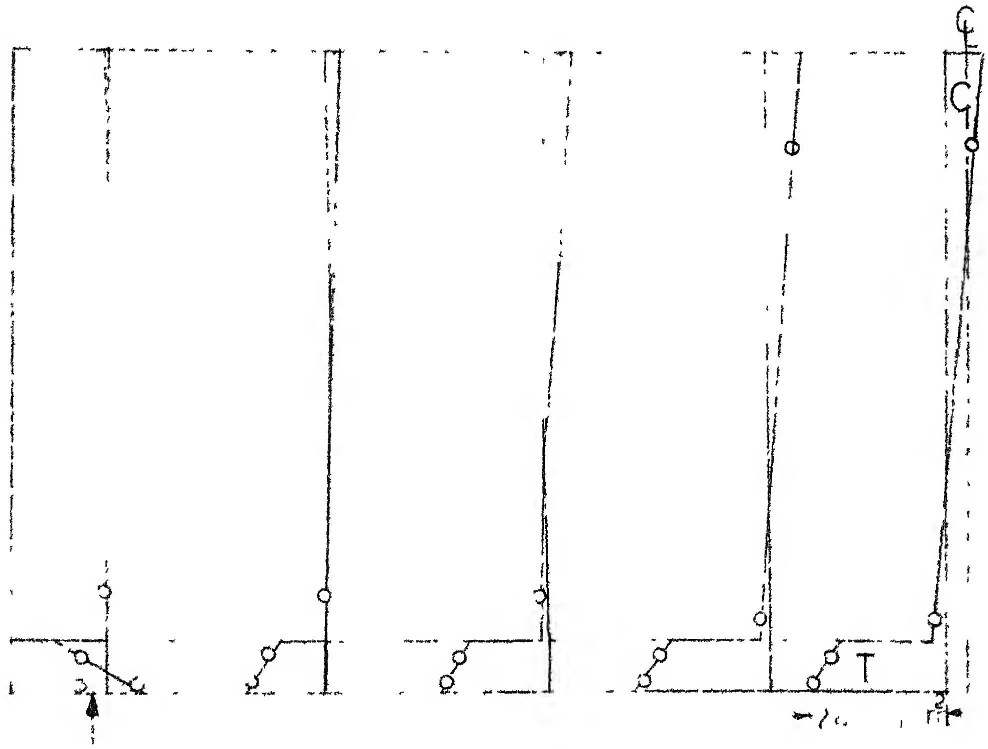

Fig 4·9 a Longitudinal stress distribution at various cross sections

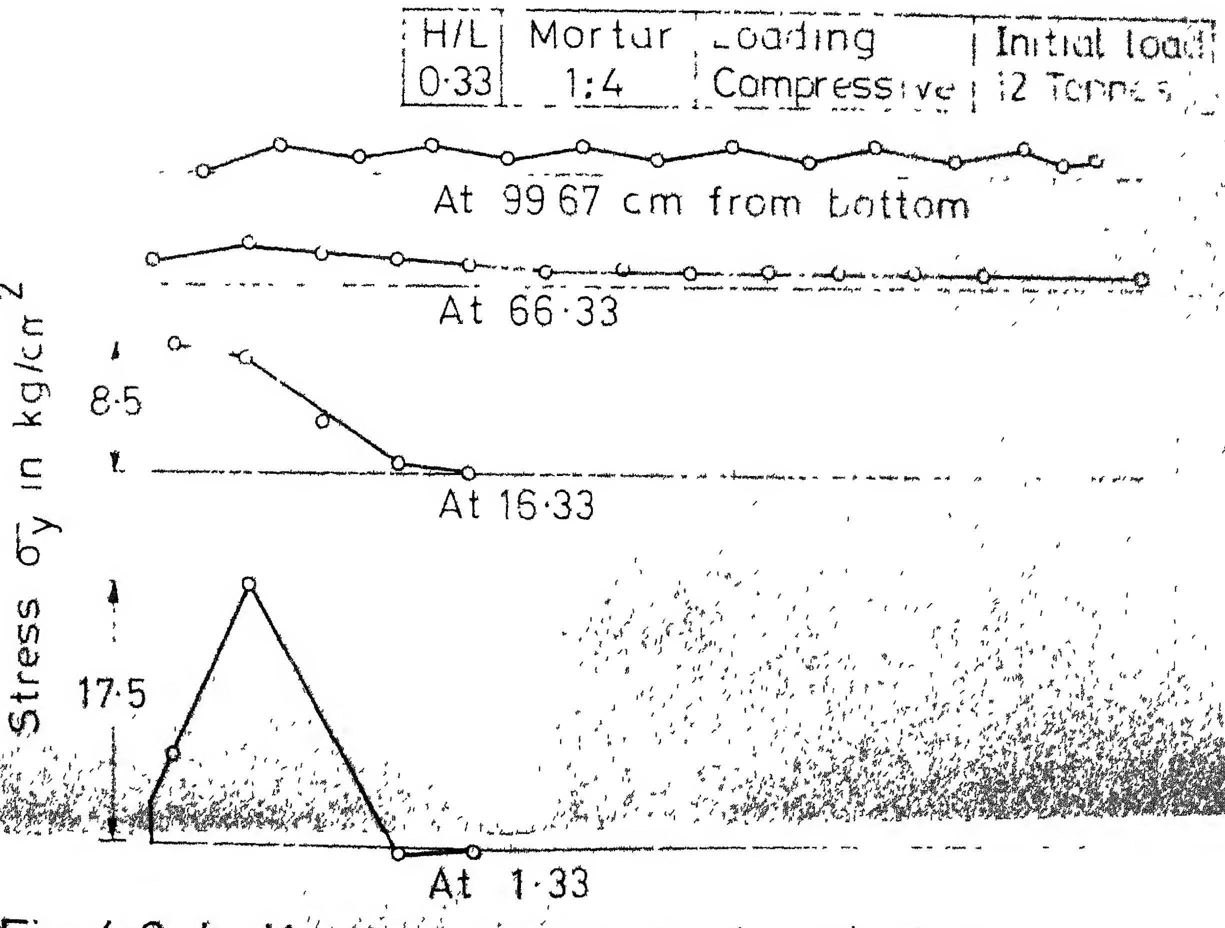

Fig. 4·9 b Vertical stress σ_y distribution along span at various heights.

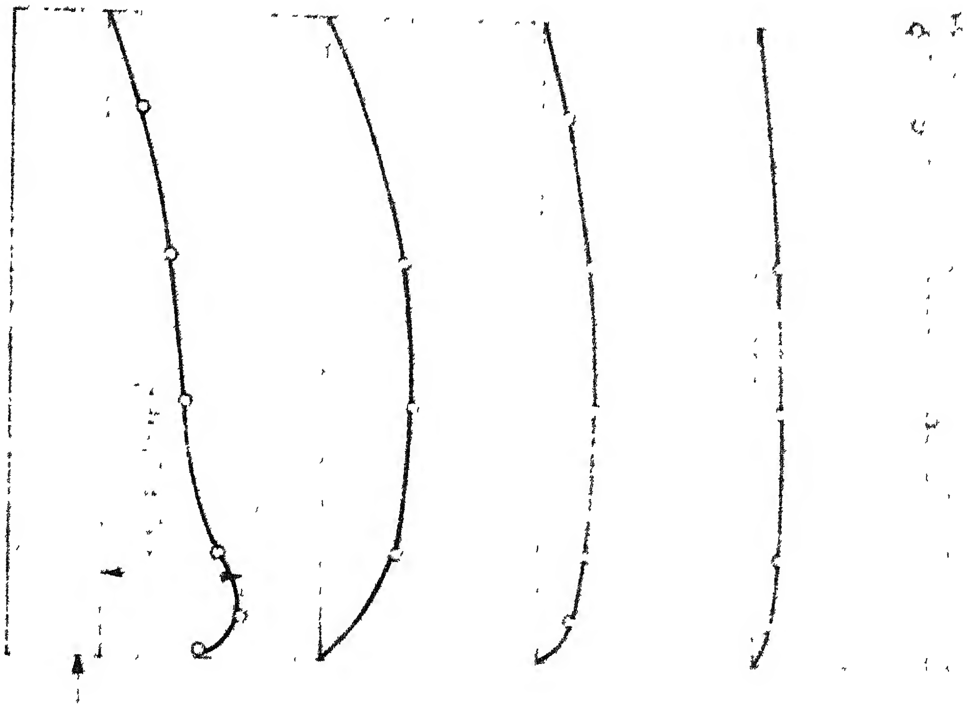

Fig.4·9 c Shear stress distribution at various cross sections

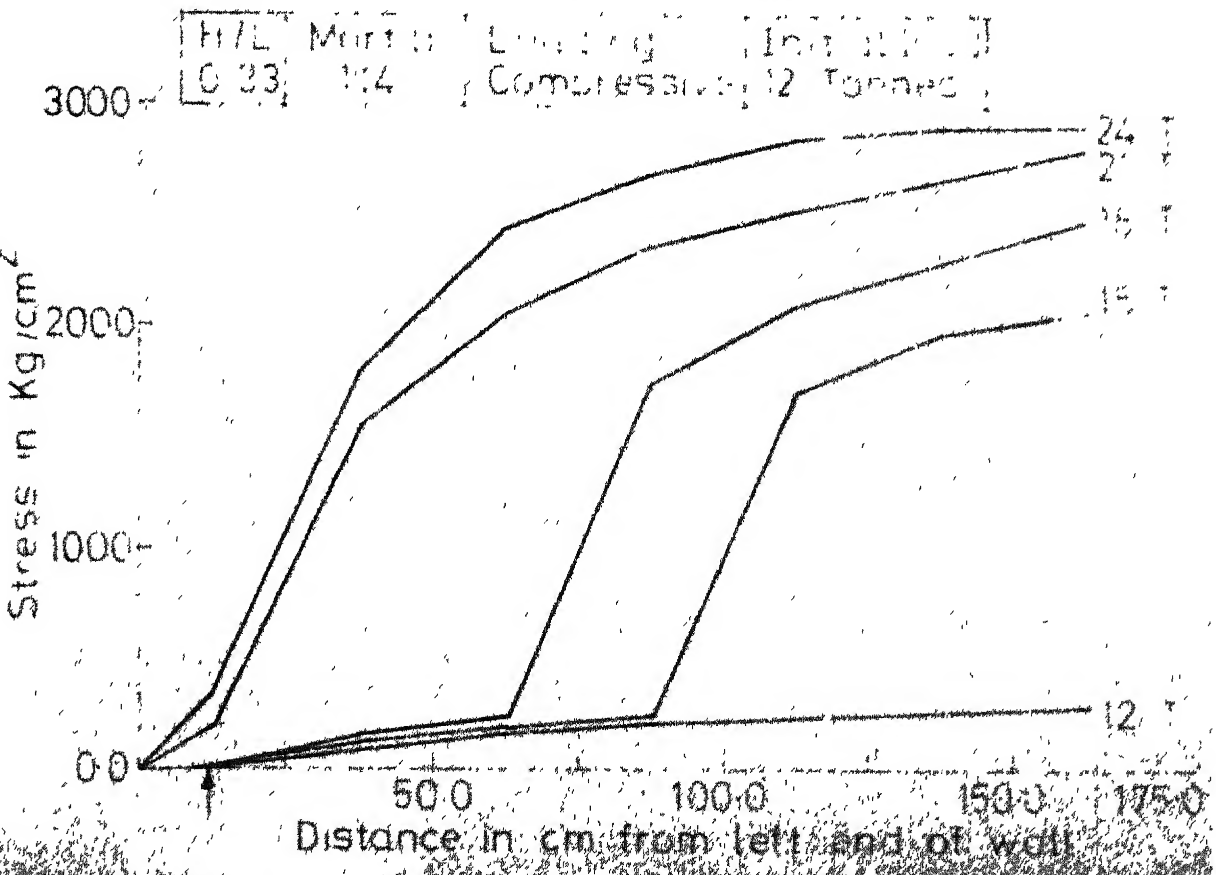

Fig.4·9 d Variation of stress in bending reinforcement along span at various loads

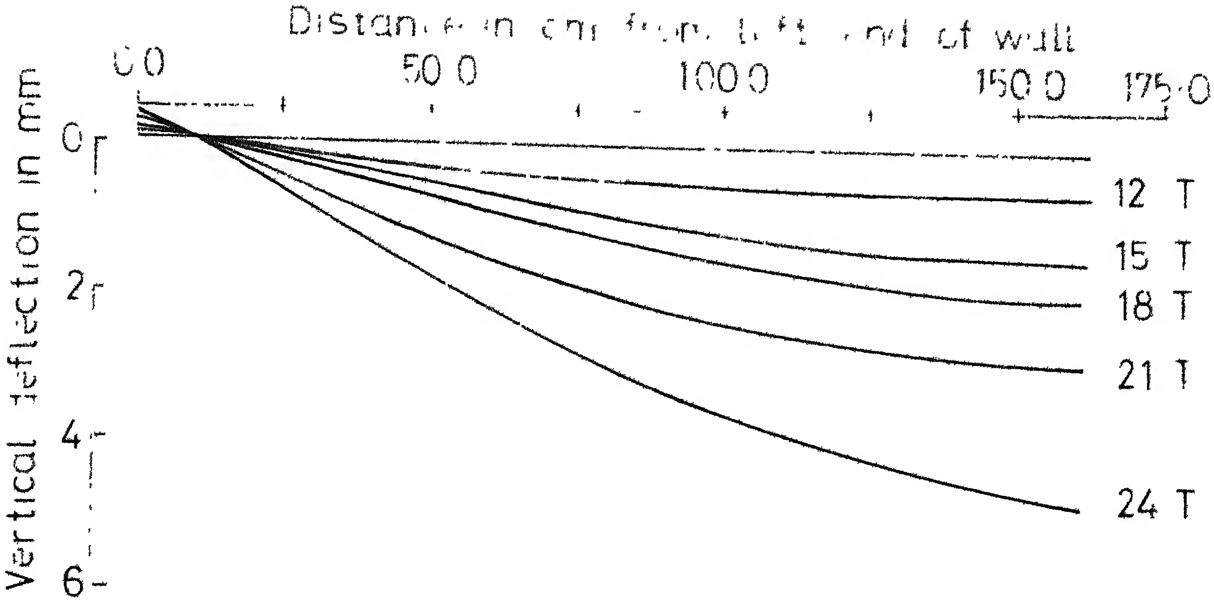

Fig. 4·9 e Vertical deflection of wall along span at various loads

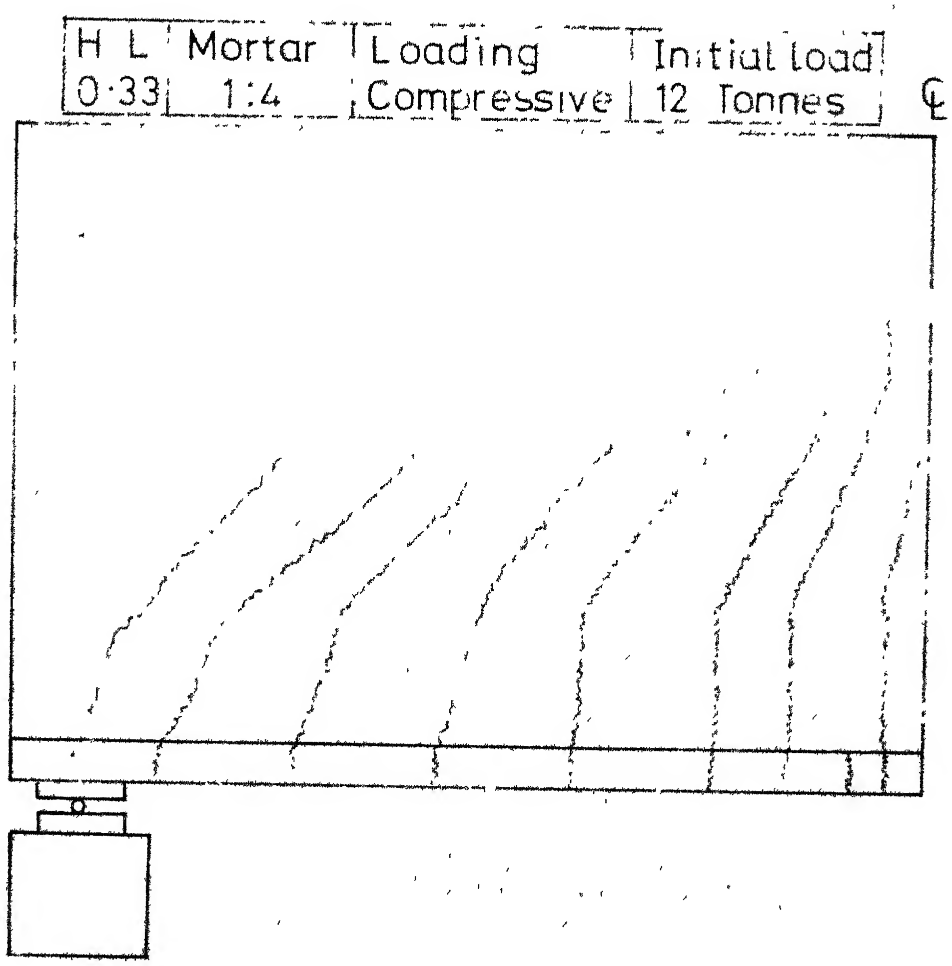

Fig. 4·9 f. Crack pattern at failure

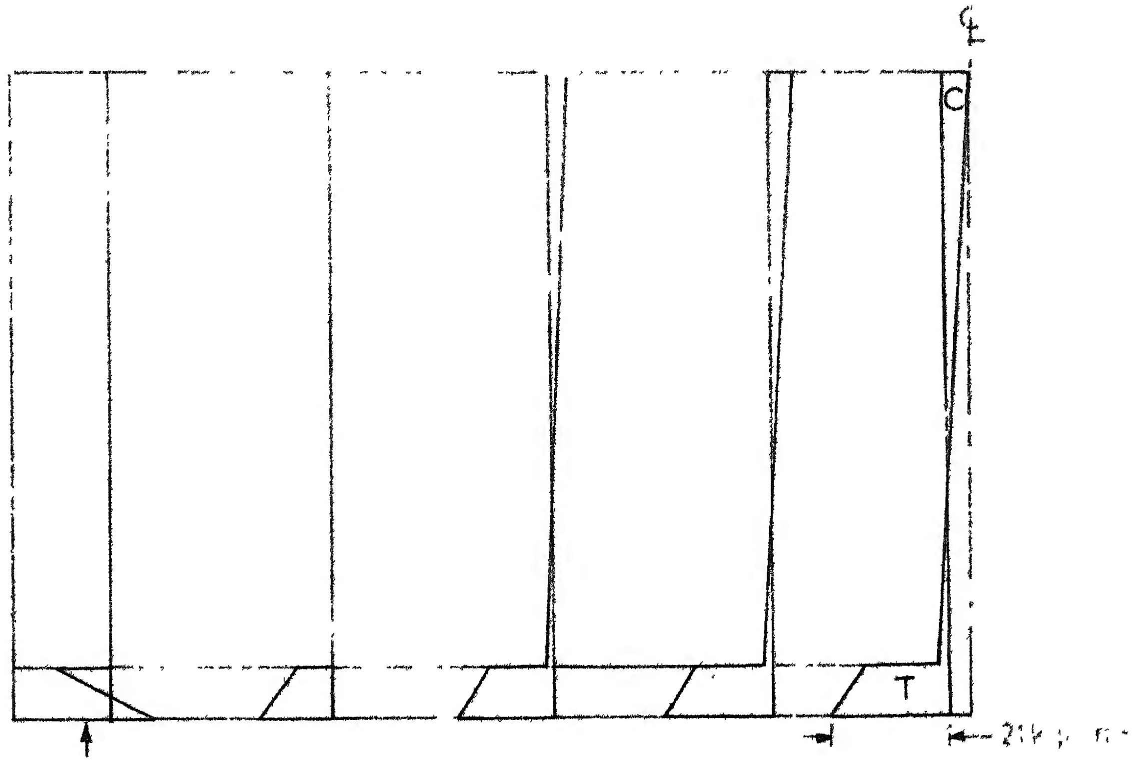

Fig. 4·10a Longitudinal stress distribution at various cross sections

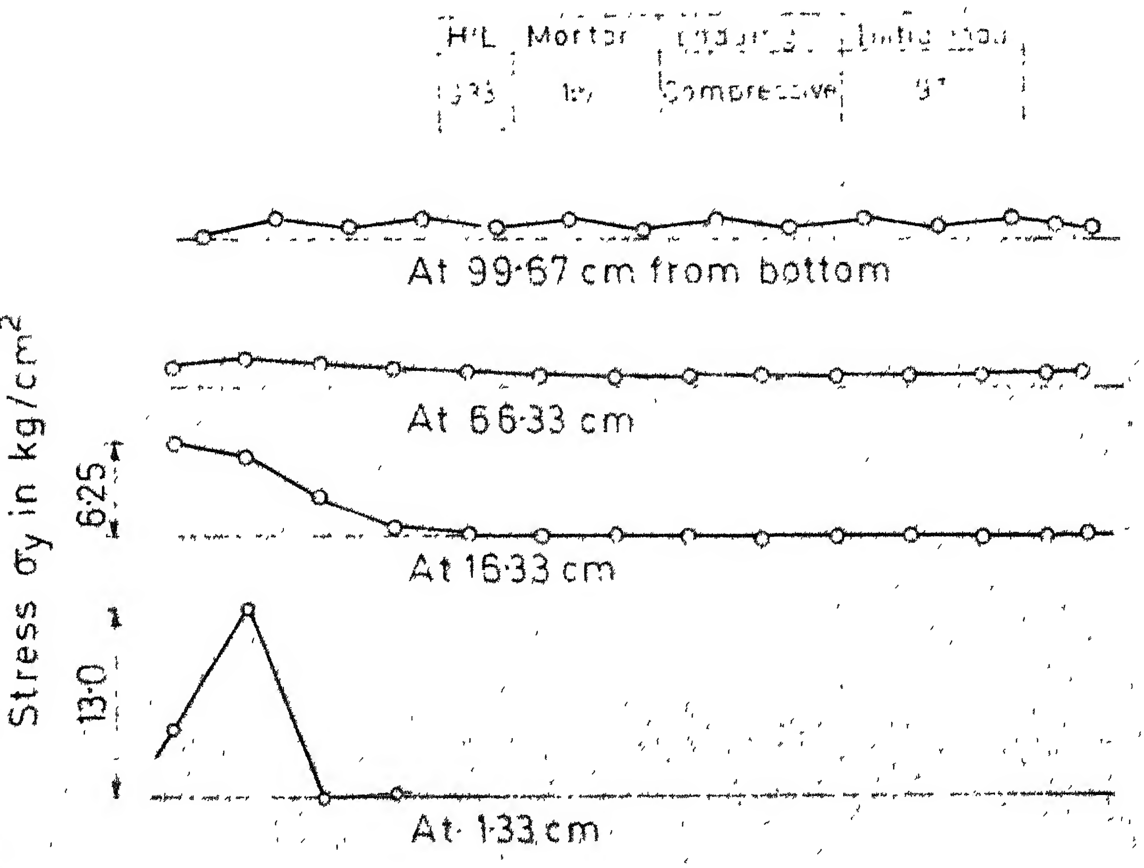

Fig. 4·10 b Vertical stress distribution along span at various heights

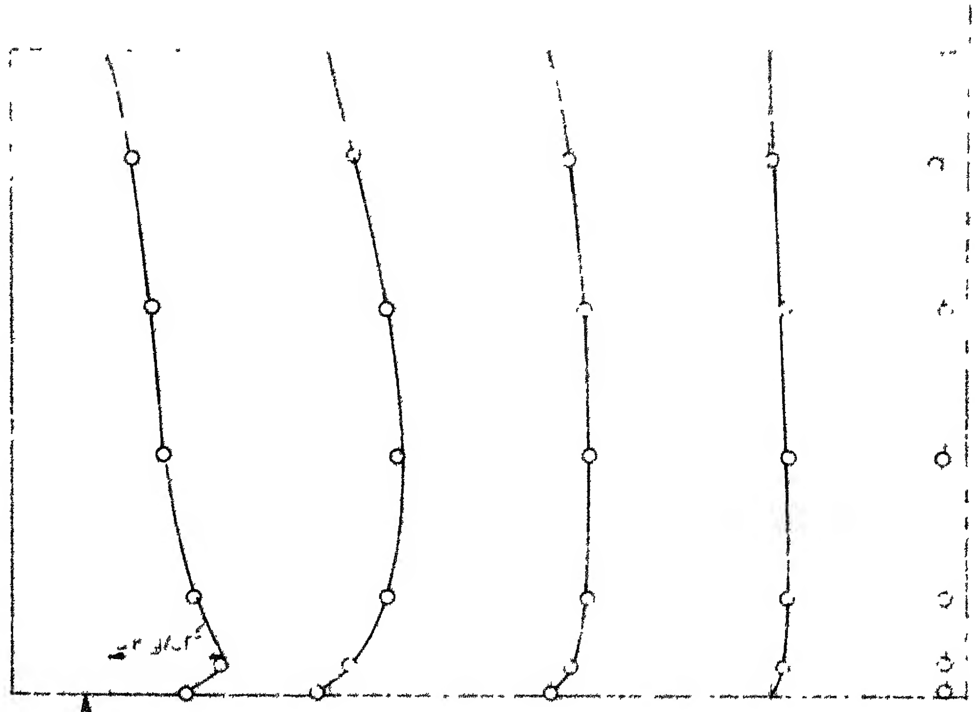

Fig.4·10 c Shear stress distribution at various cross sections

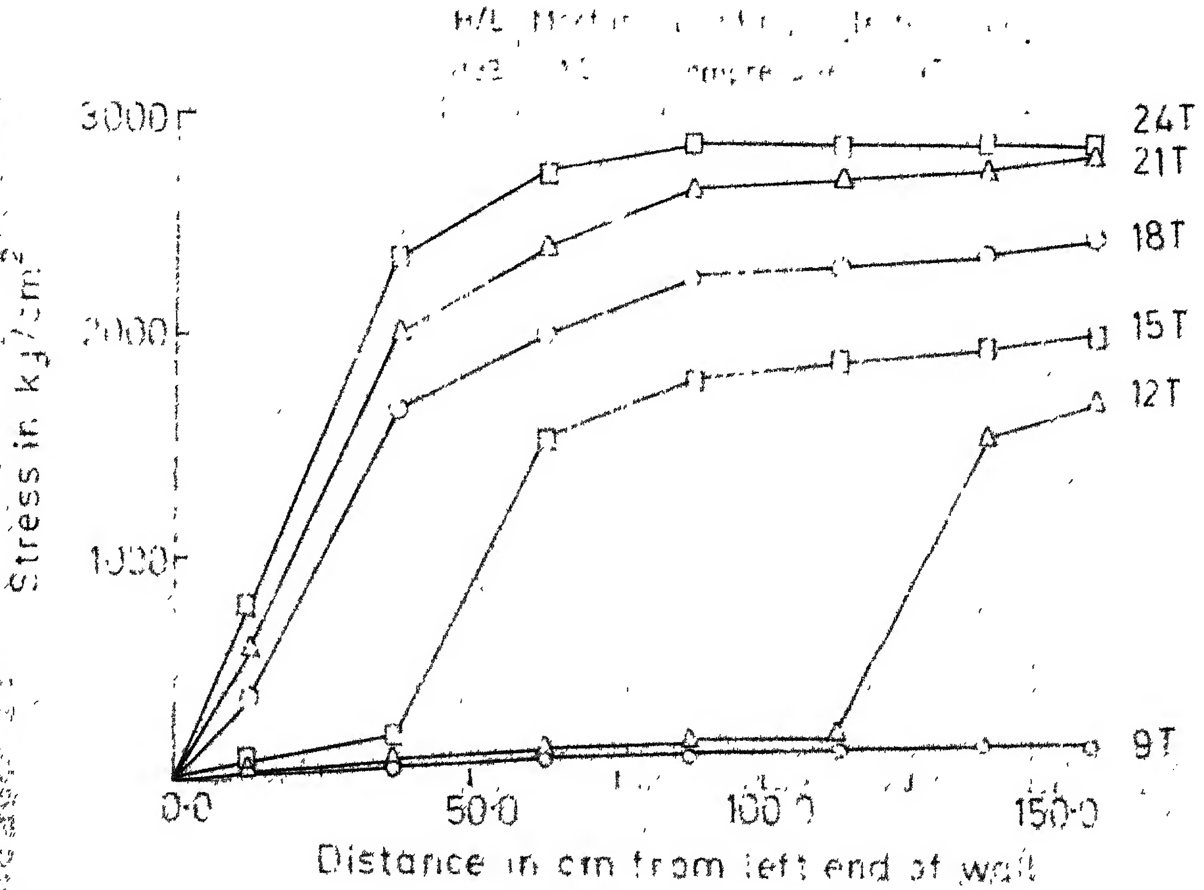

Fig.4·10 d Variation of stress in bending reinforcement along span at various loads

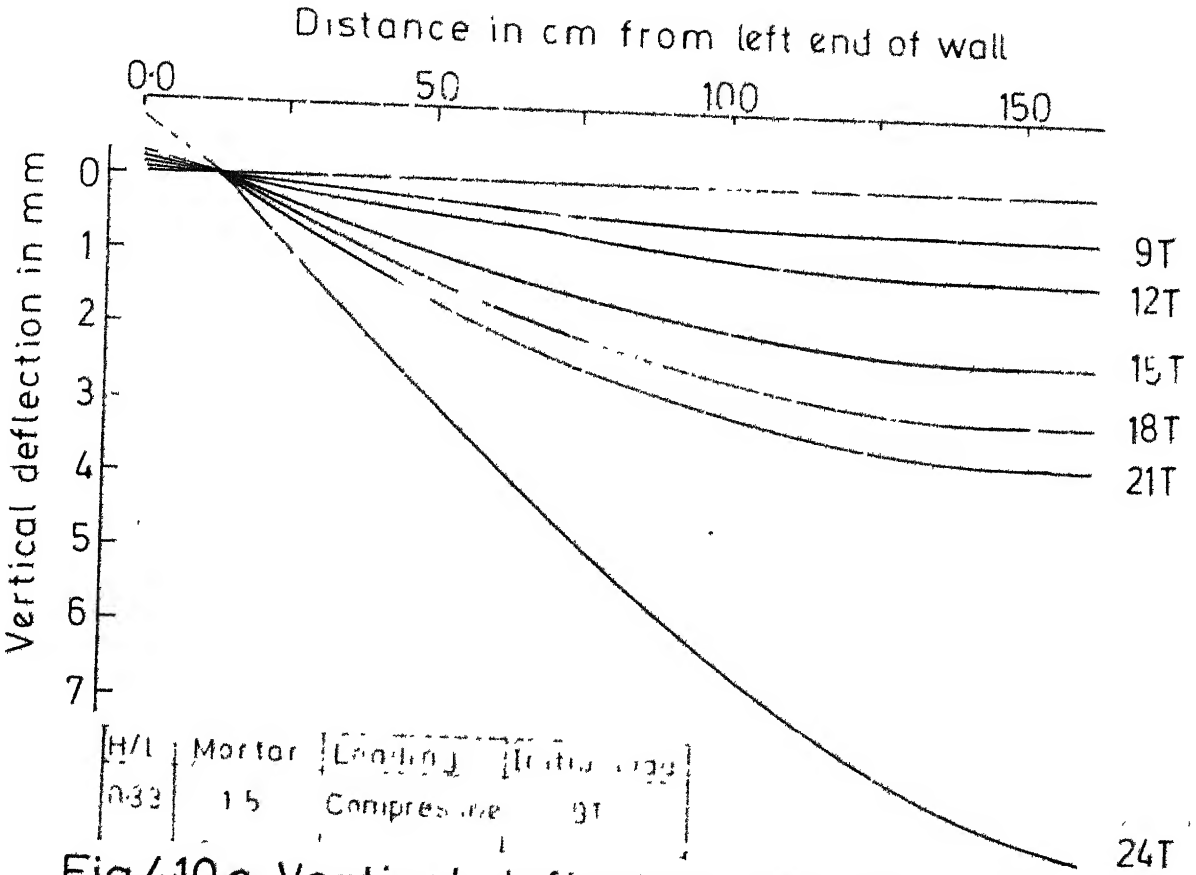

Fig.4·10e Vertical deflection of wall along span at various loads

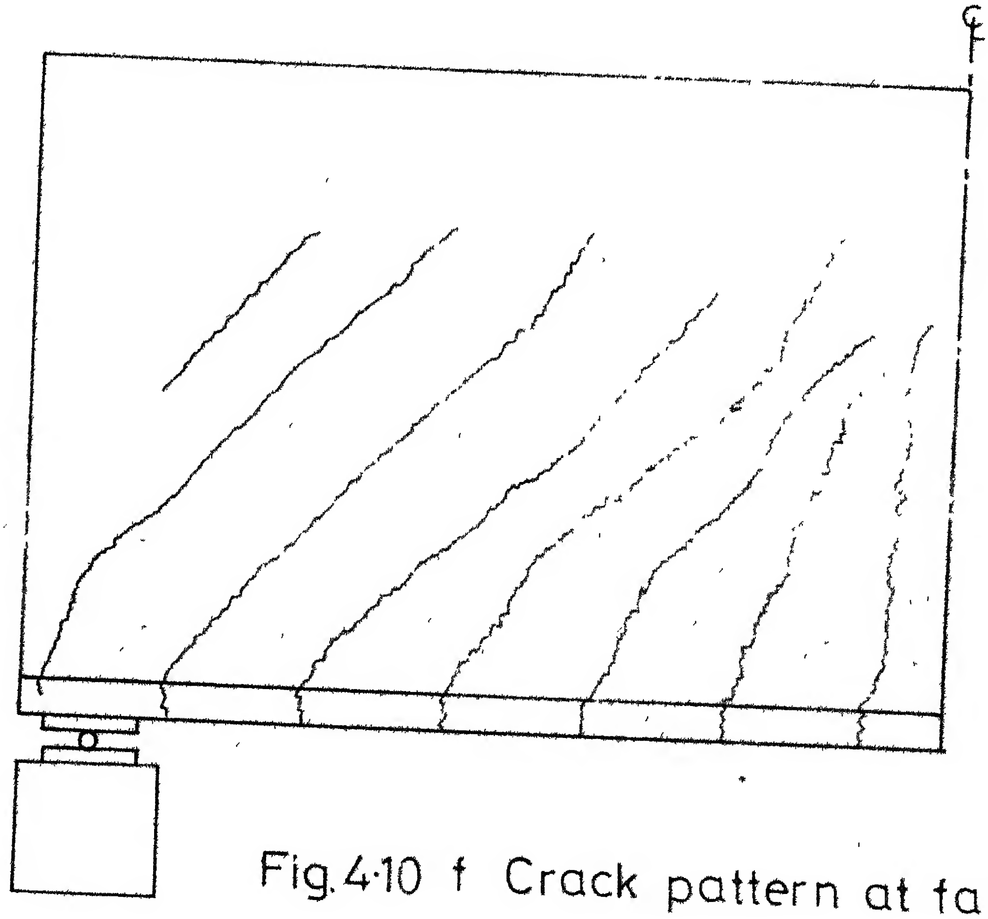

Fig.4·10 f Crack pattern at failure

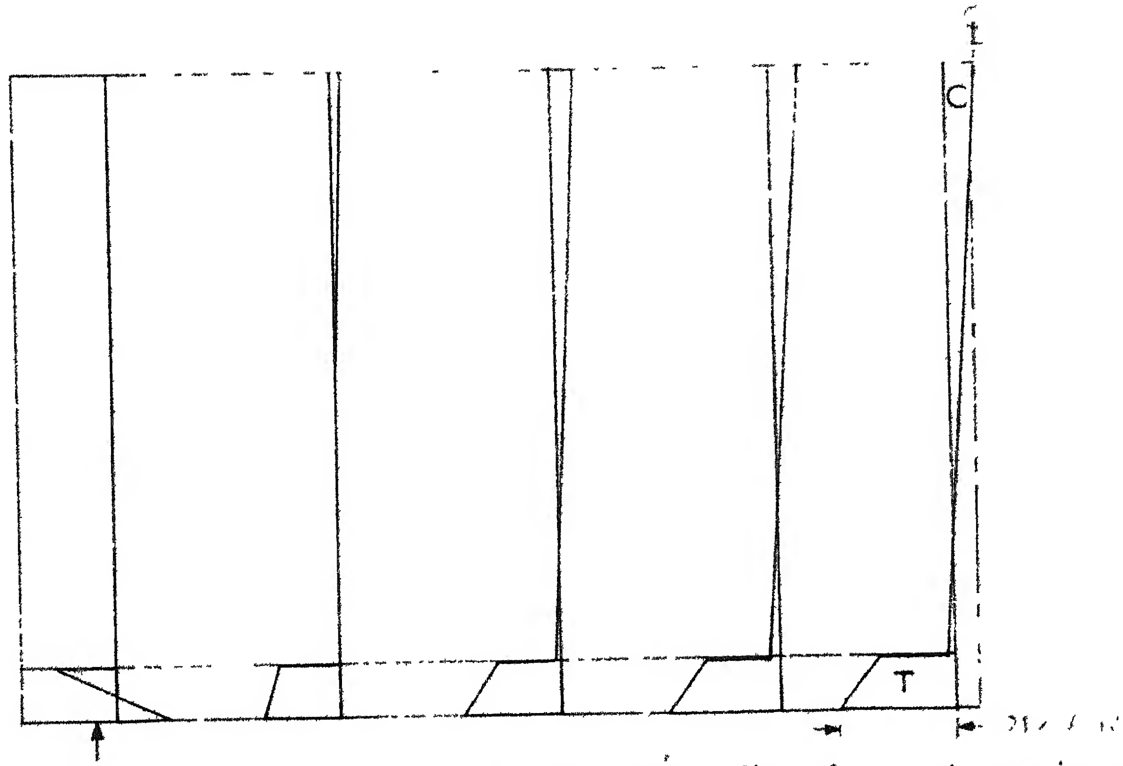

Fig.4.11a Longitudinal stress distribution at various cross sections

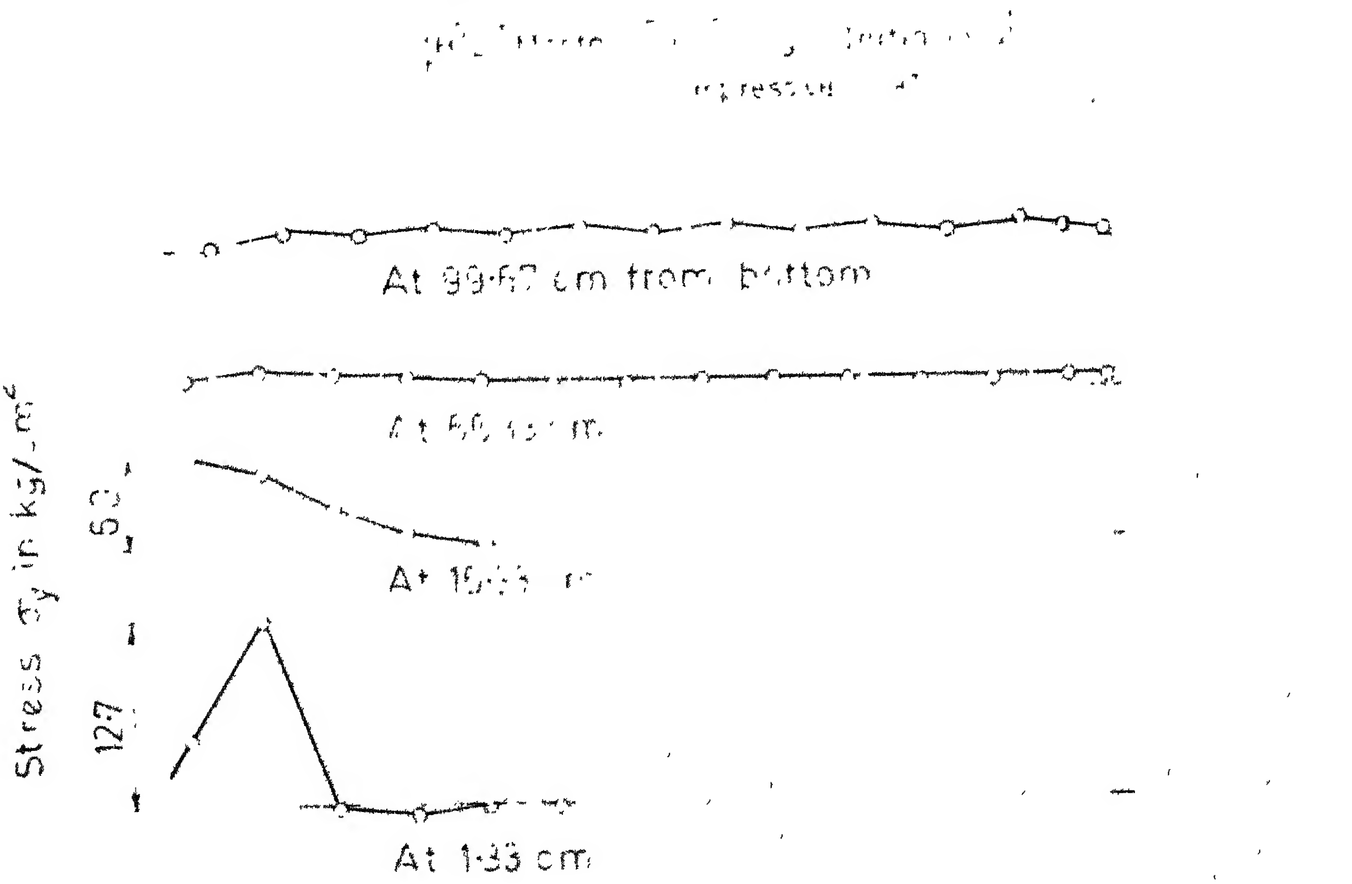

Fig.4.11b Vertical stress distribution along span at various heights

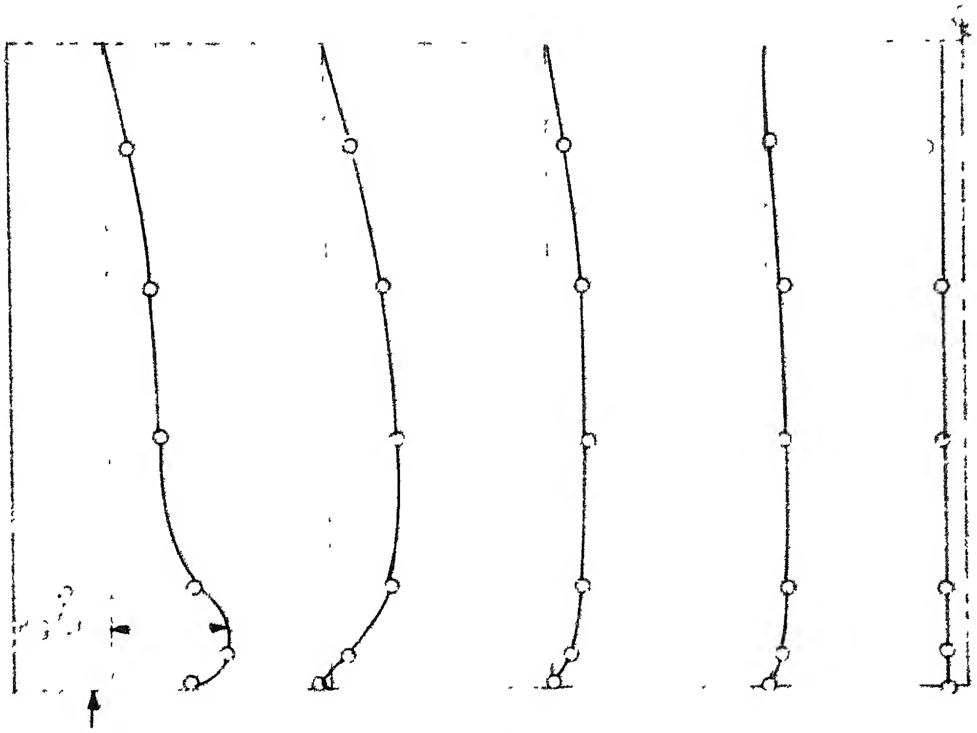

Fig.4·11 c Shear stress distribution at various cross sections

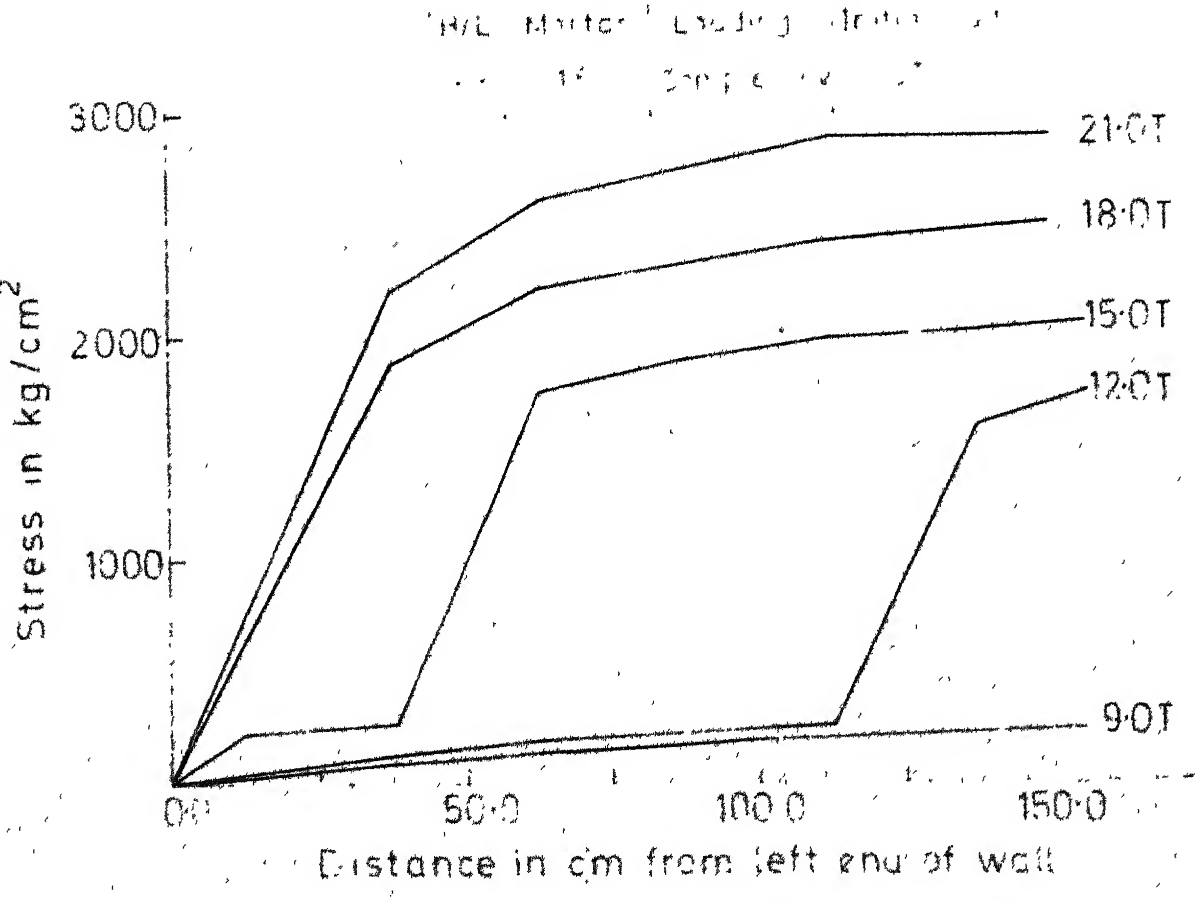

Fig.4·11d Variation of stress in bending reinforcement along span at various loads

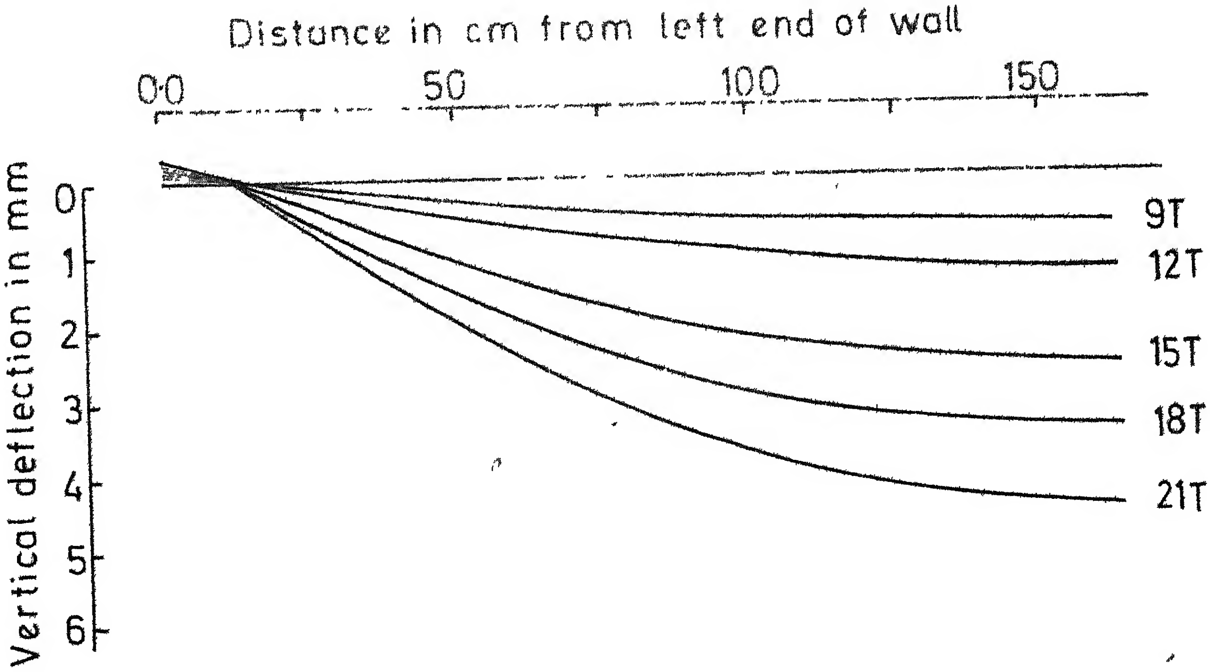

Fig.4·11e Vertical deflection of wall along span at various loads

H/L	Mortar	Loading	Initial load
0·33	1:6	Compressive	9T

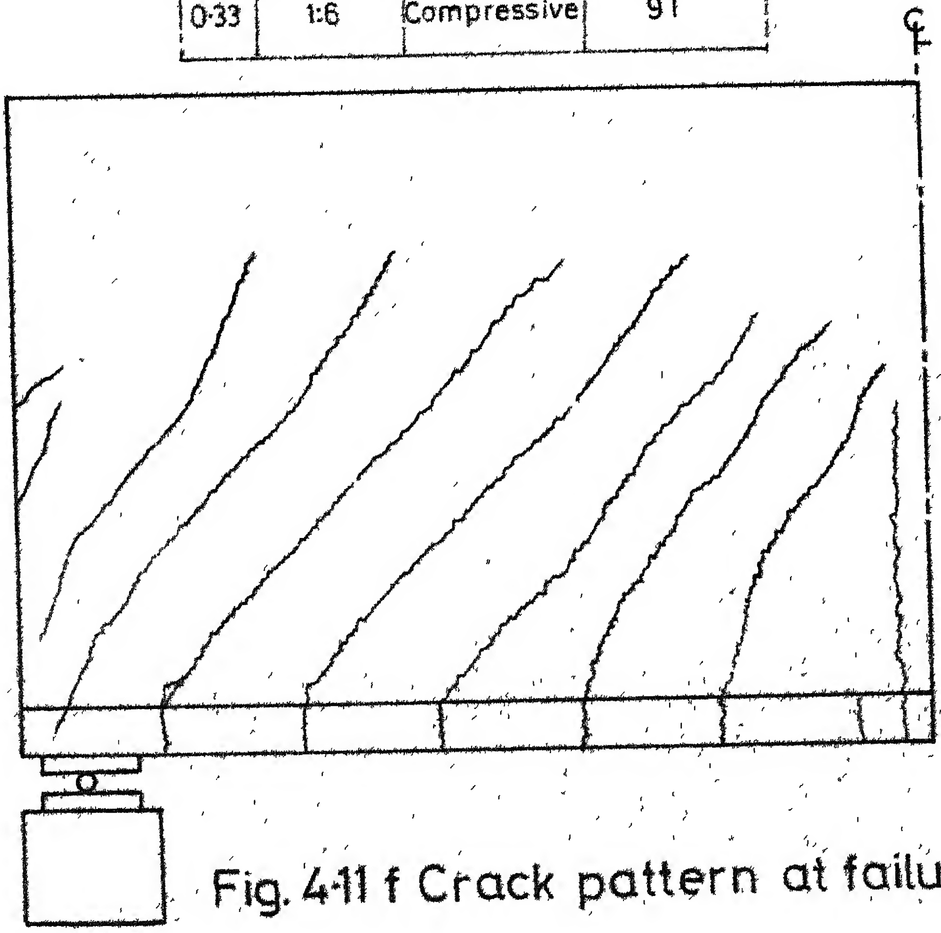

Fig. 4·11 f Crack pattern at failure

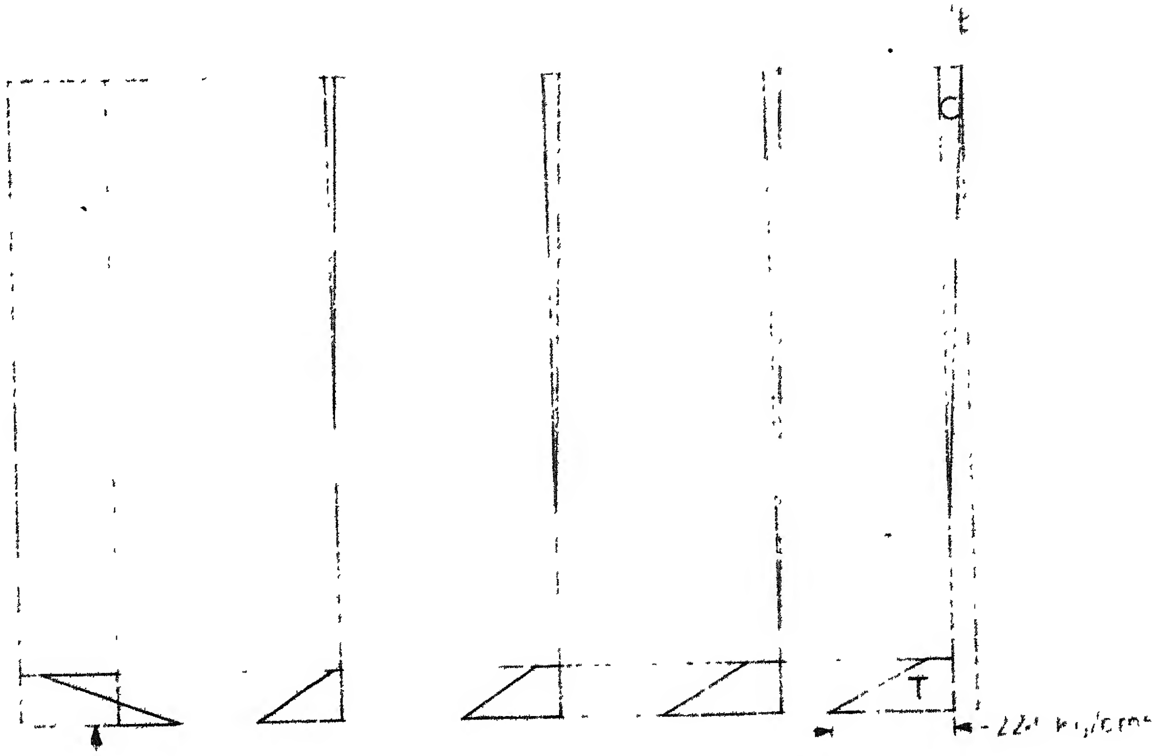

Fig. 4·12a Longitudinal stress distribution at various cross sections

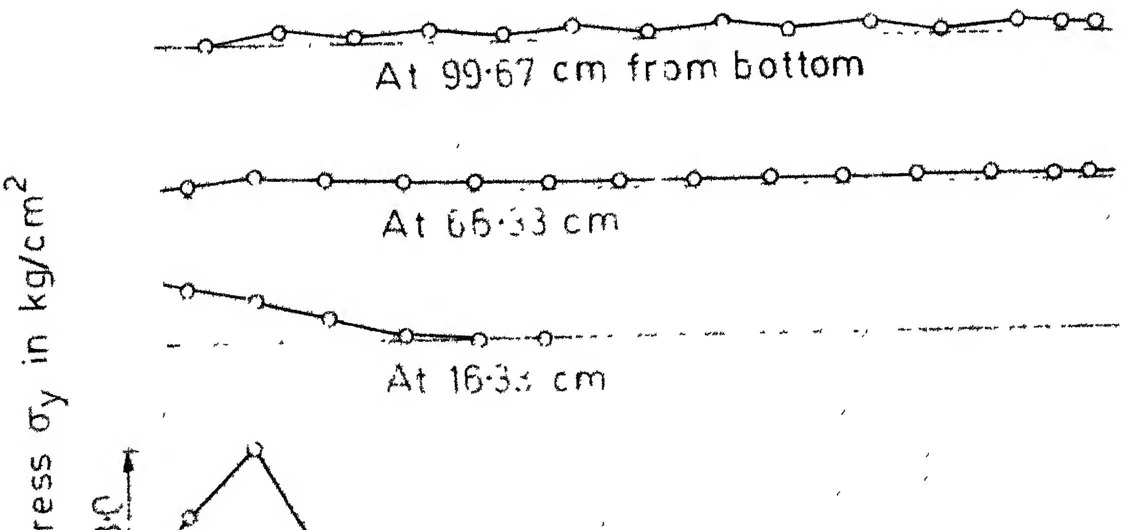

Fig. 4·12 b Vertical stress σ_y distribution along span at various heights

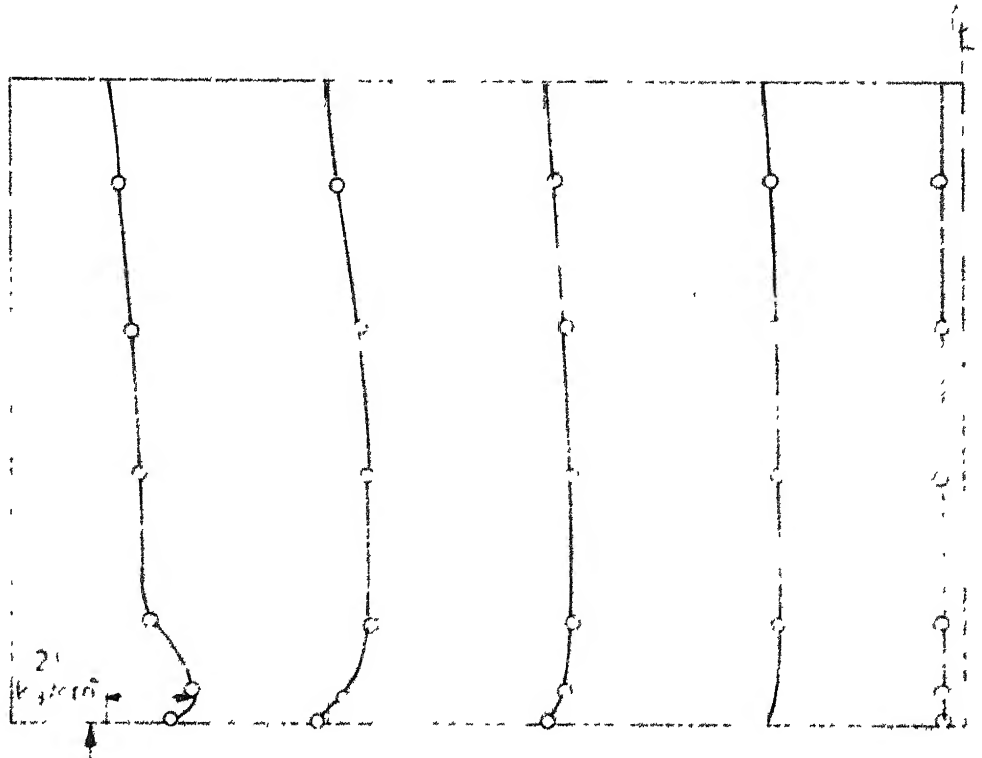

Fig.4·12 c Shear stress distribution at various cross sections

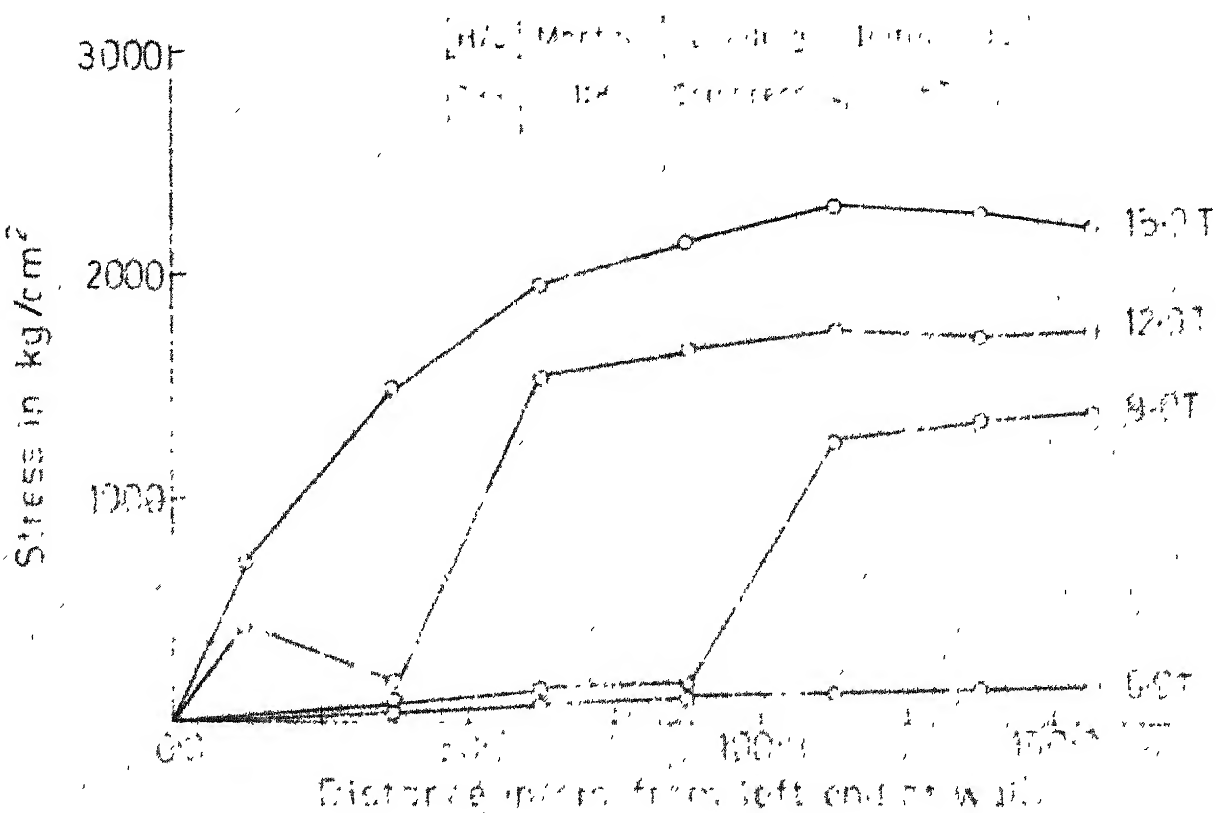

Fig.4·12 d Variation of stress in bending reinforcement along span at various loads

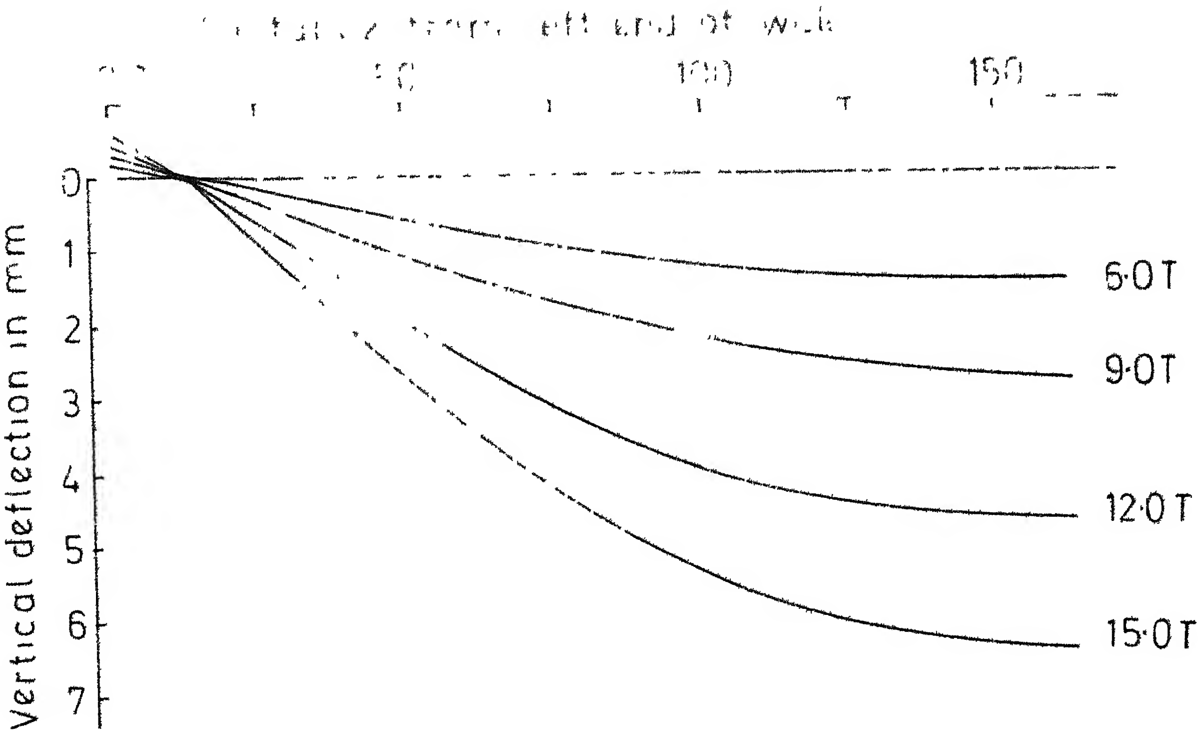

Fig.4·12e Vertical deflection of wall along span at various loads

H/L	Mortar	Loading	Initial load
0·33	1:8	Compressive	6T

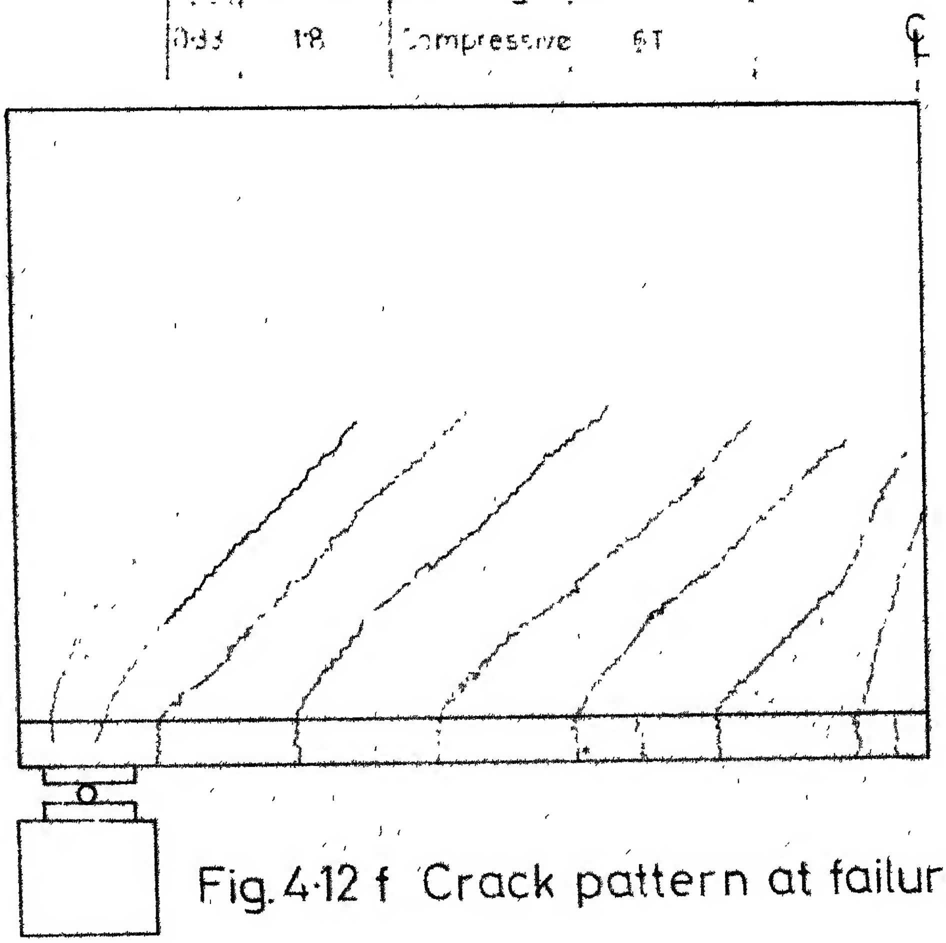

Fig. 4·12 f Crack pattern at failure

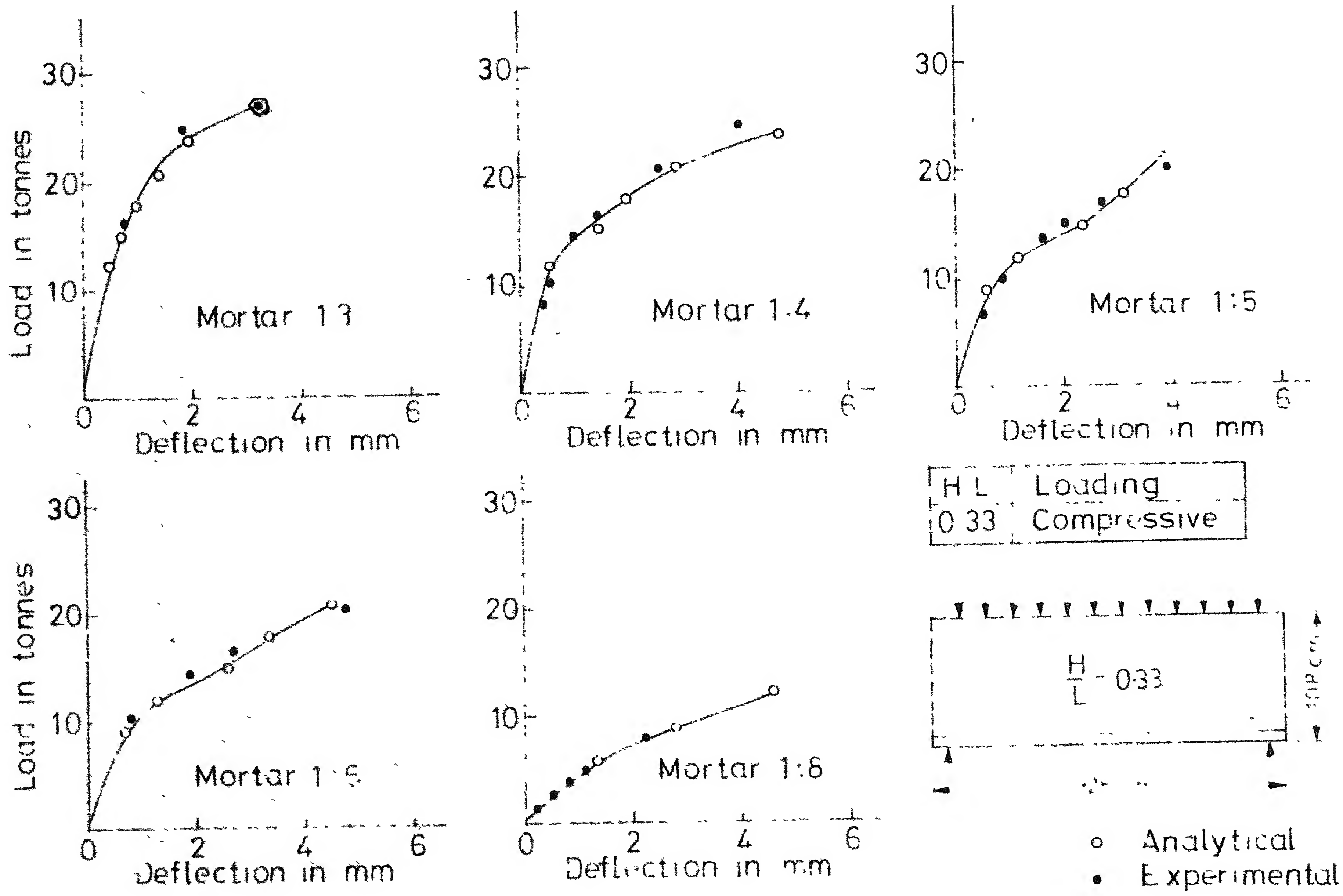

Fig. 4·13 Load vs deflection curves

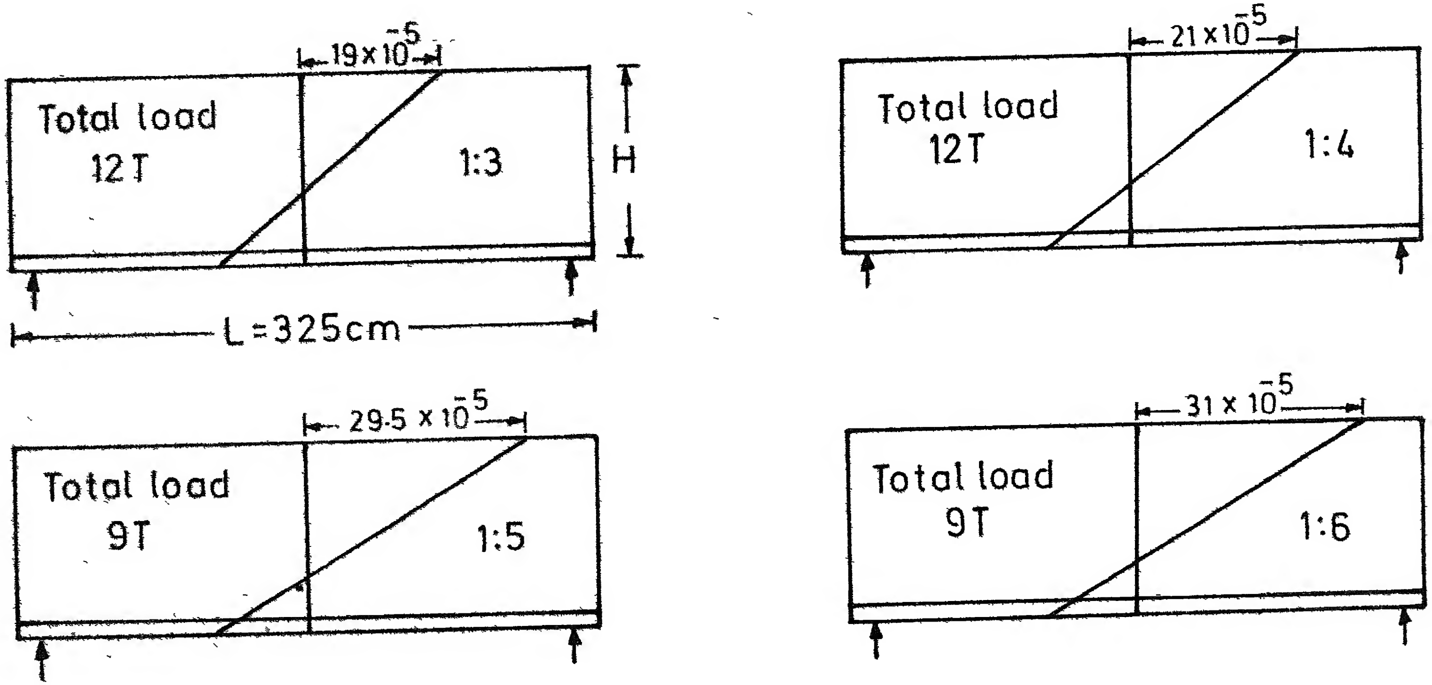

Fig. 4.14 Variation of longitudinal strains at mid span (H/L = 033) Loading (Compressive)

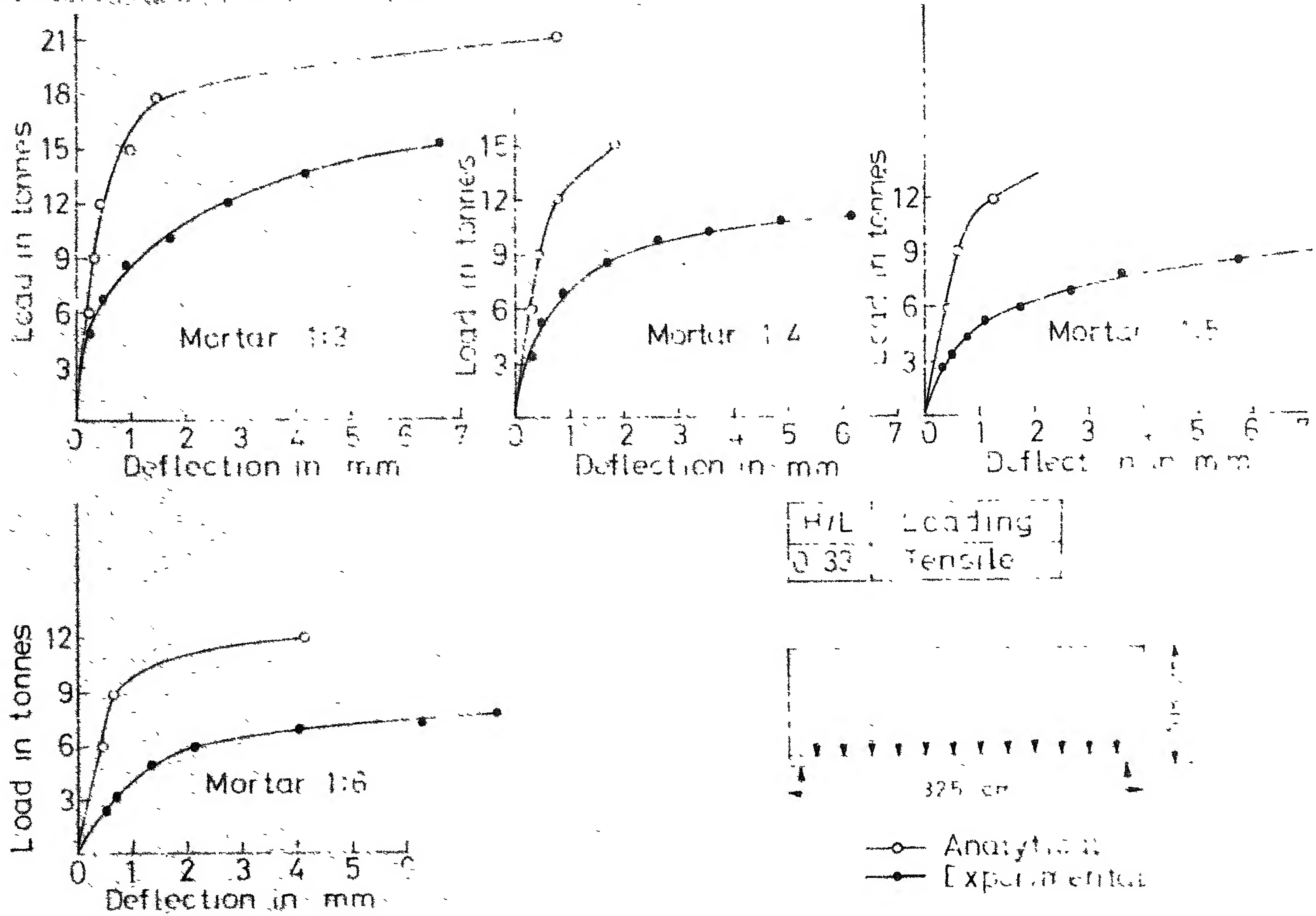

Fig. 4·15 Load vs deflection curves

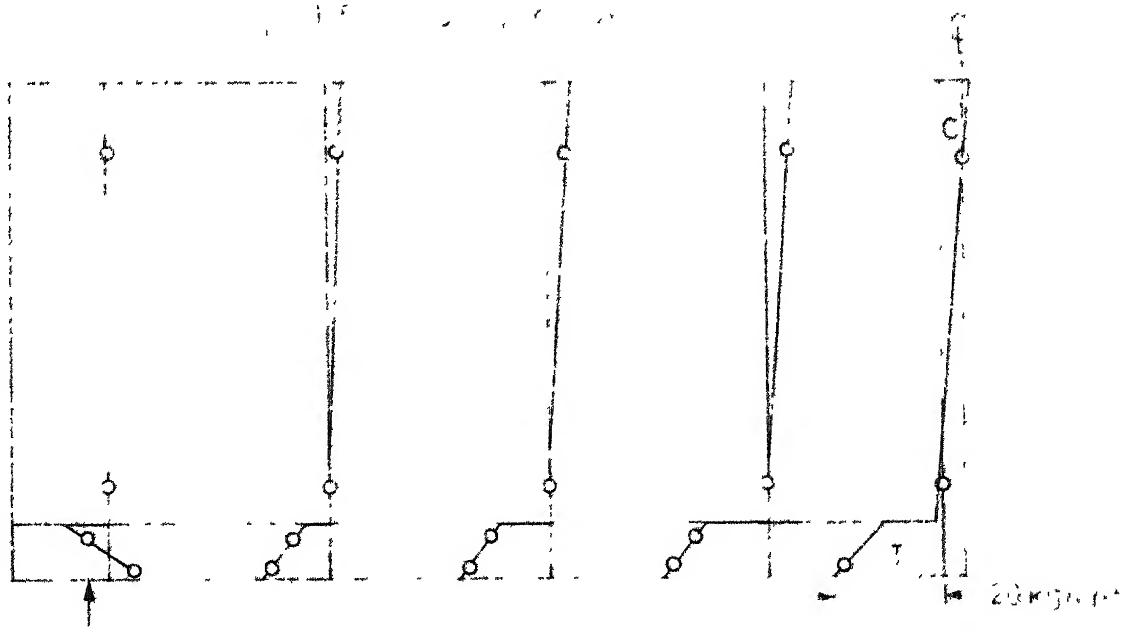

Fig. 4·16 a Longitudinal stress distribution at various cross sections

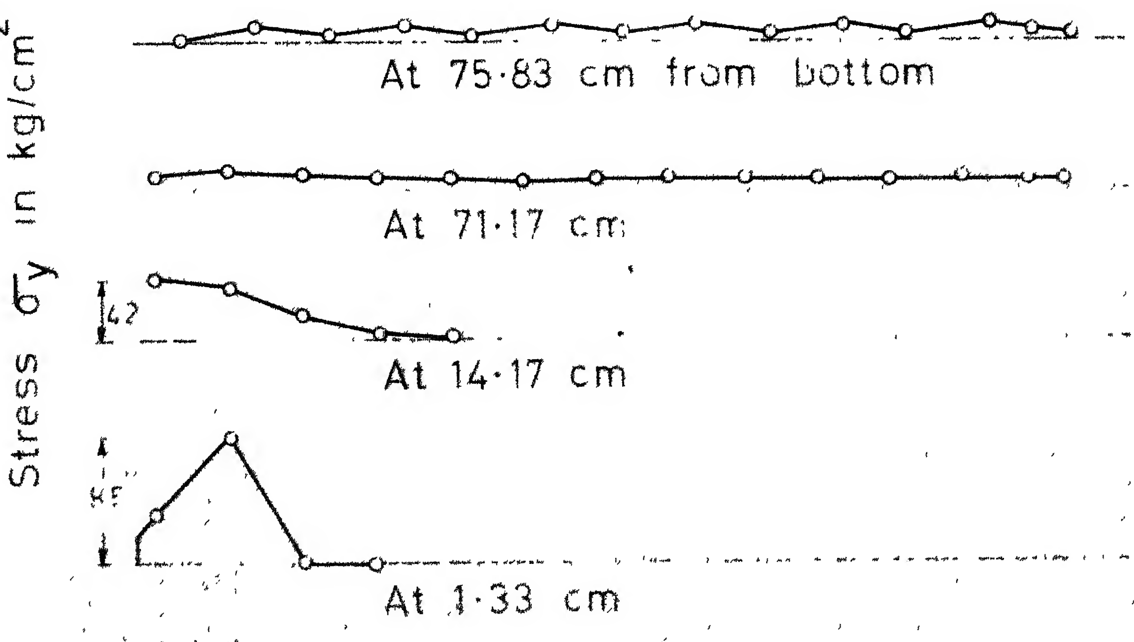

Fig. 4·16 b Vertical stress σ_y distribution along span at various heights

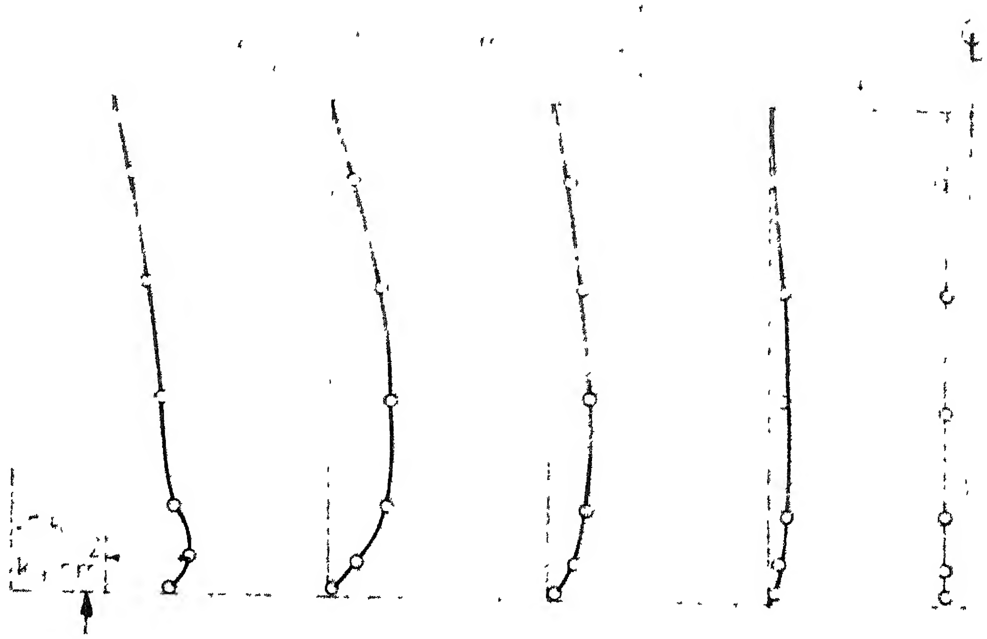

Fig. 4·16 c   Shear stress distribution at various cross sections

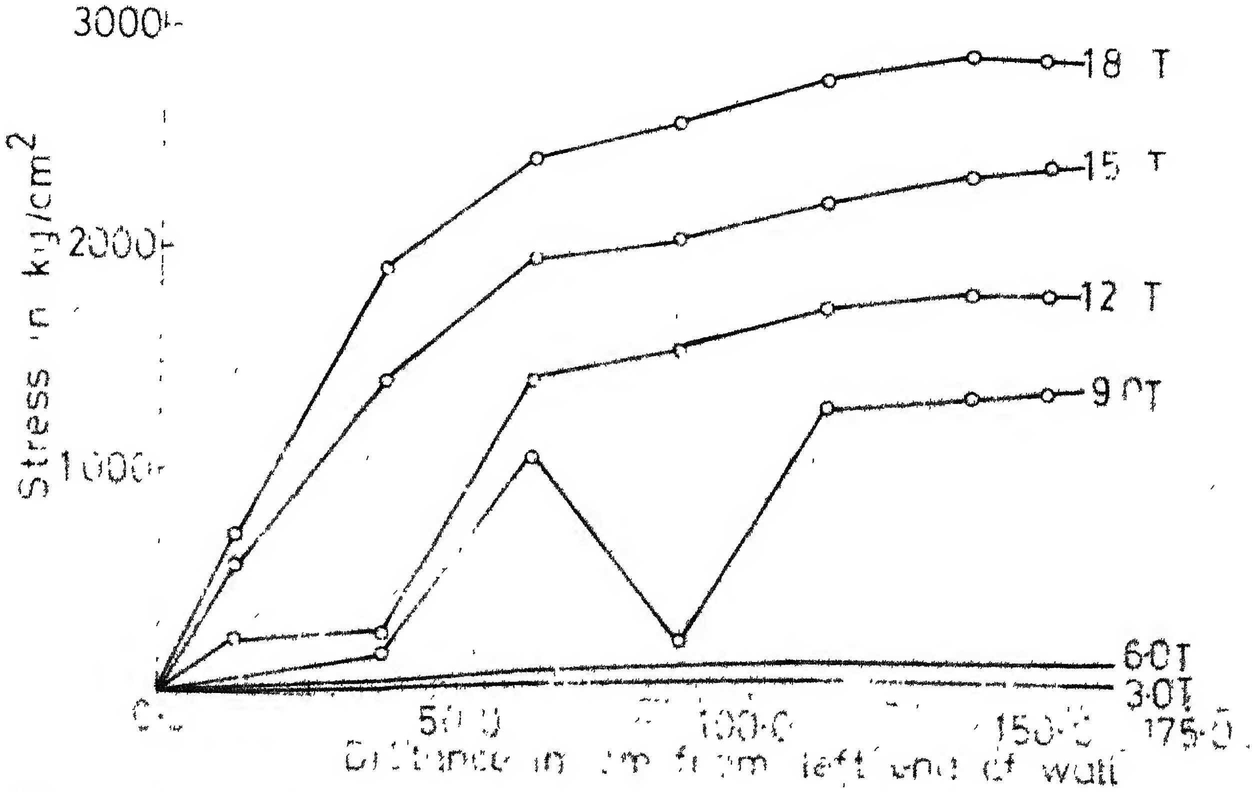

Fig. 4·16 d Variation of stress in reinforcement along span at various loads

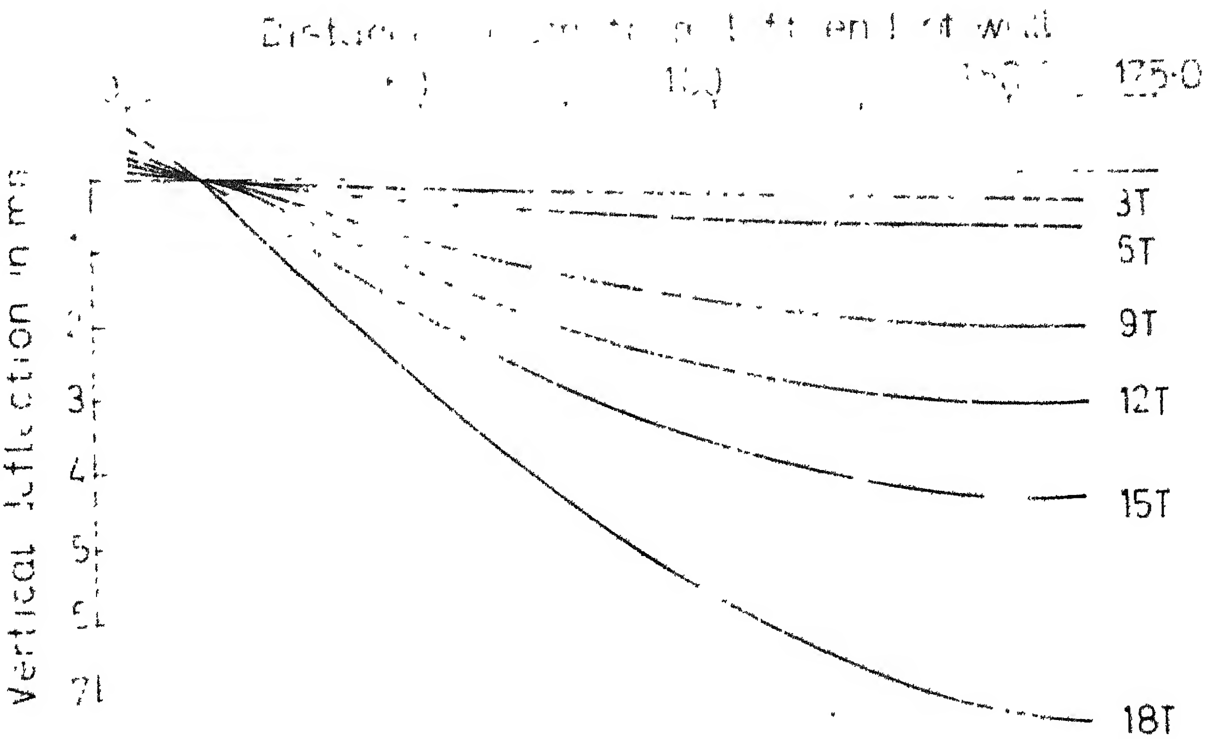

Fig 4·16 e Vertical deflection of wall along span at various loads

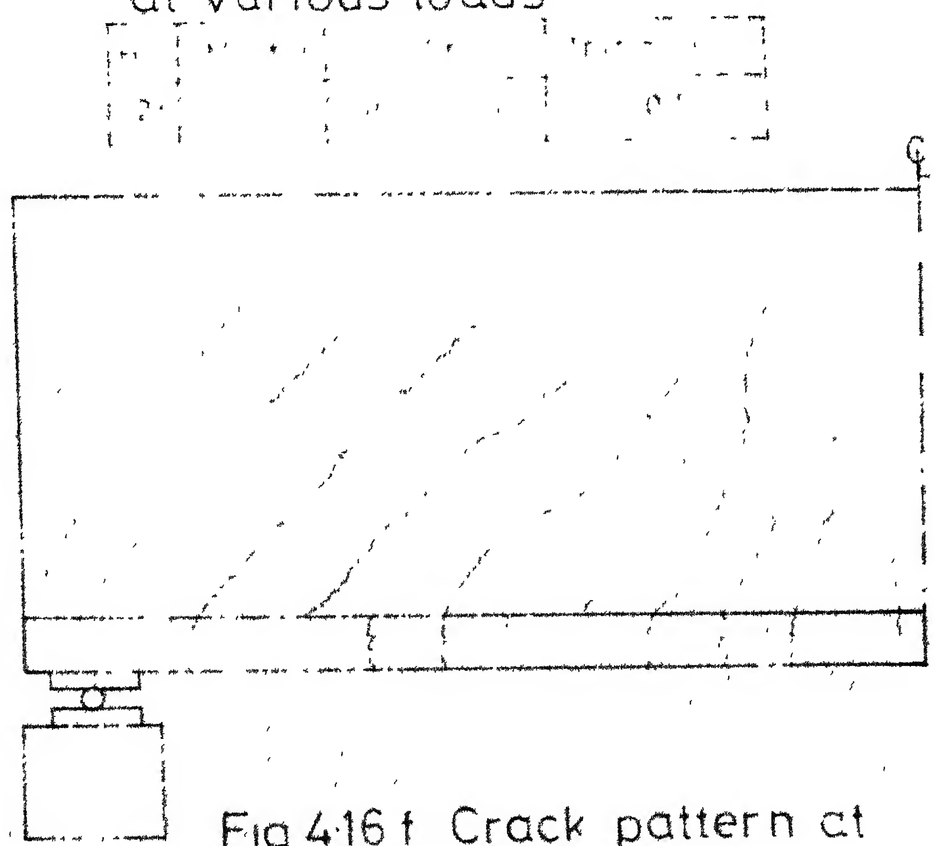

Fig 4·16 f Crack pattern at failure

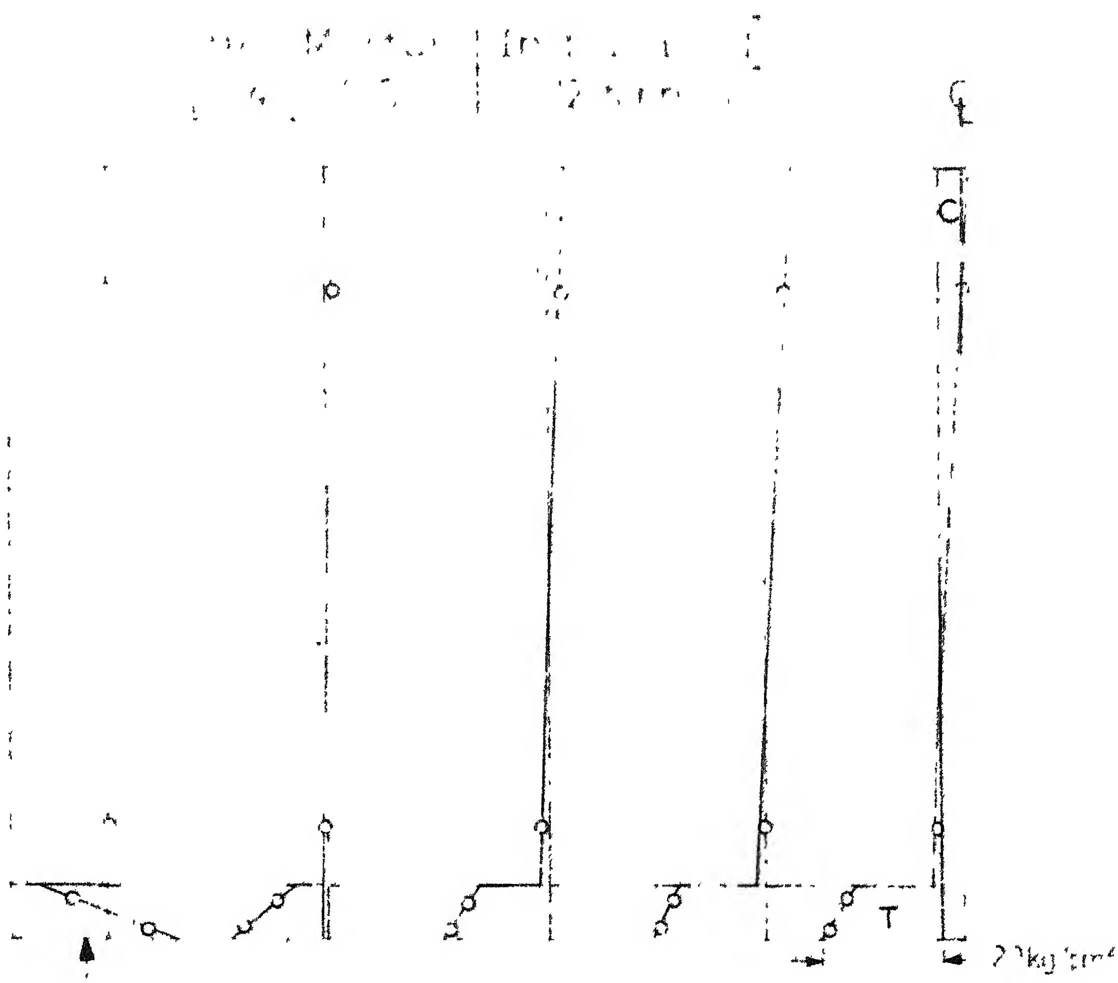

Fig.4·17a Longitudinal stress distribution at various cross sections

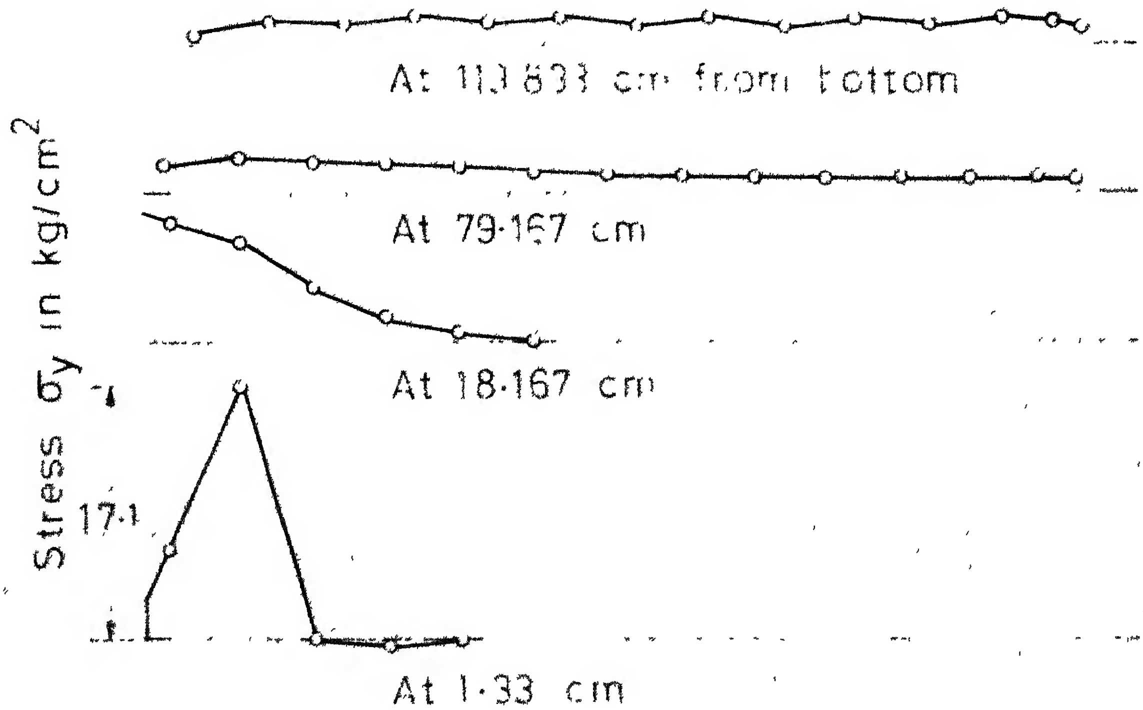

Fig. 4·17 b Vertical stress σ_y distribution at various heights

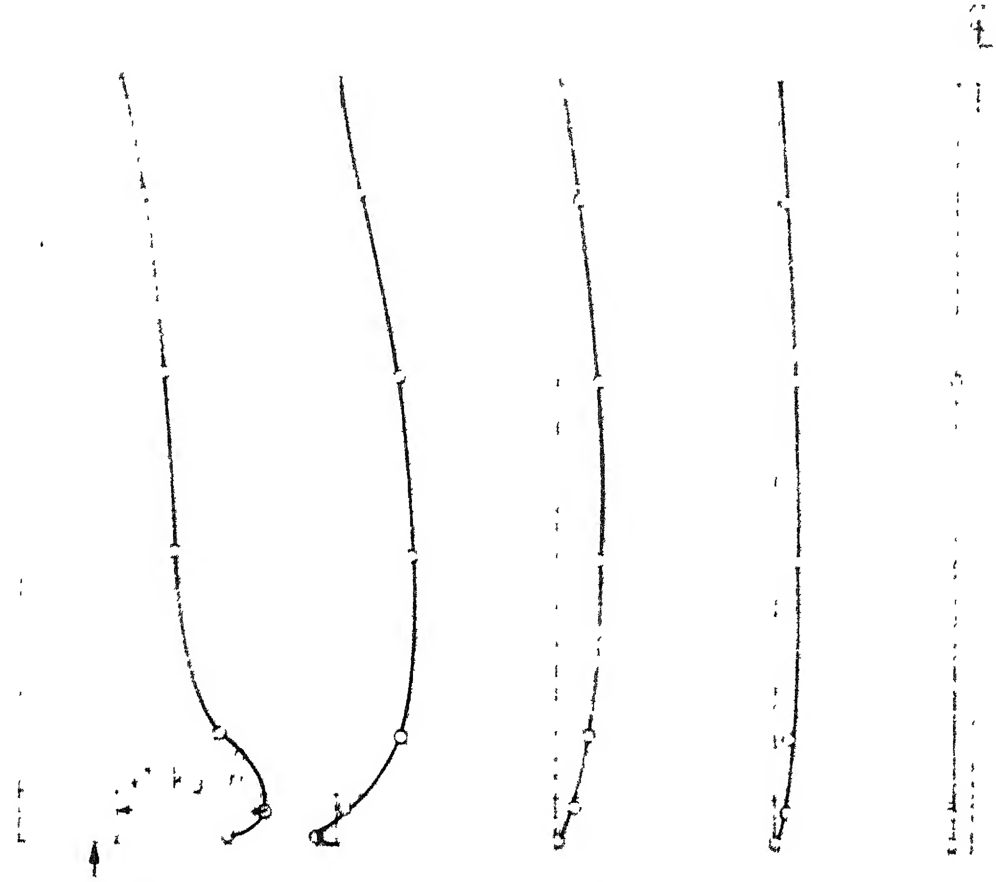

Fig.4.17 c Shear stress distribution at various cross sections

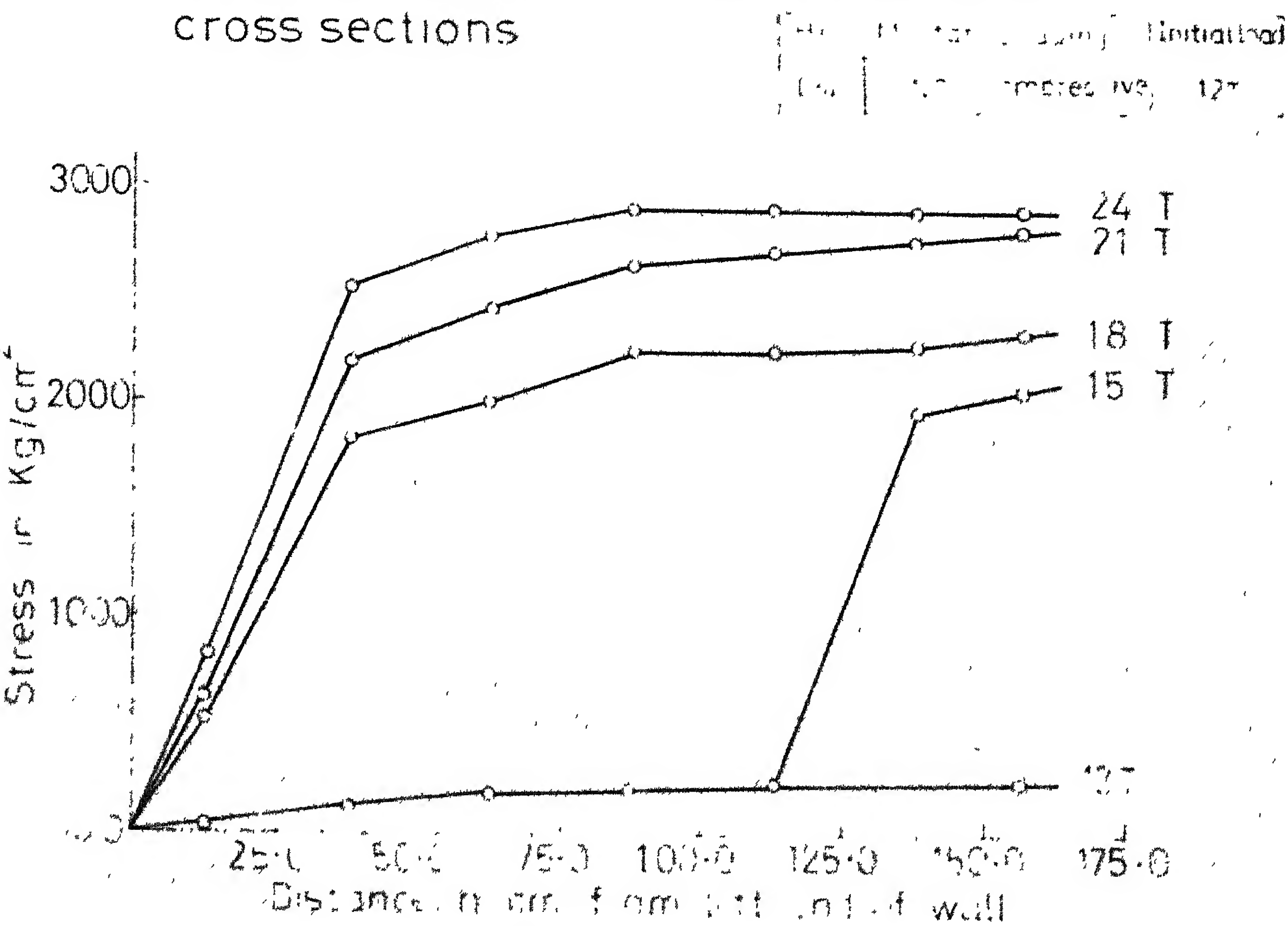

Fig 4.17 d Variation of stress in bottom reinforcement along span at various loads

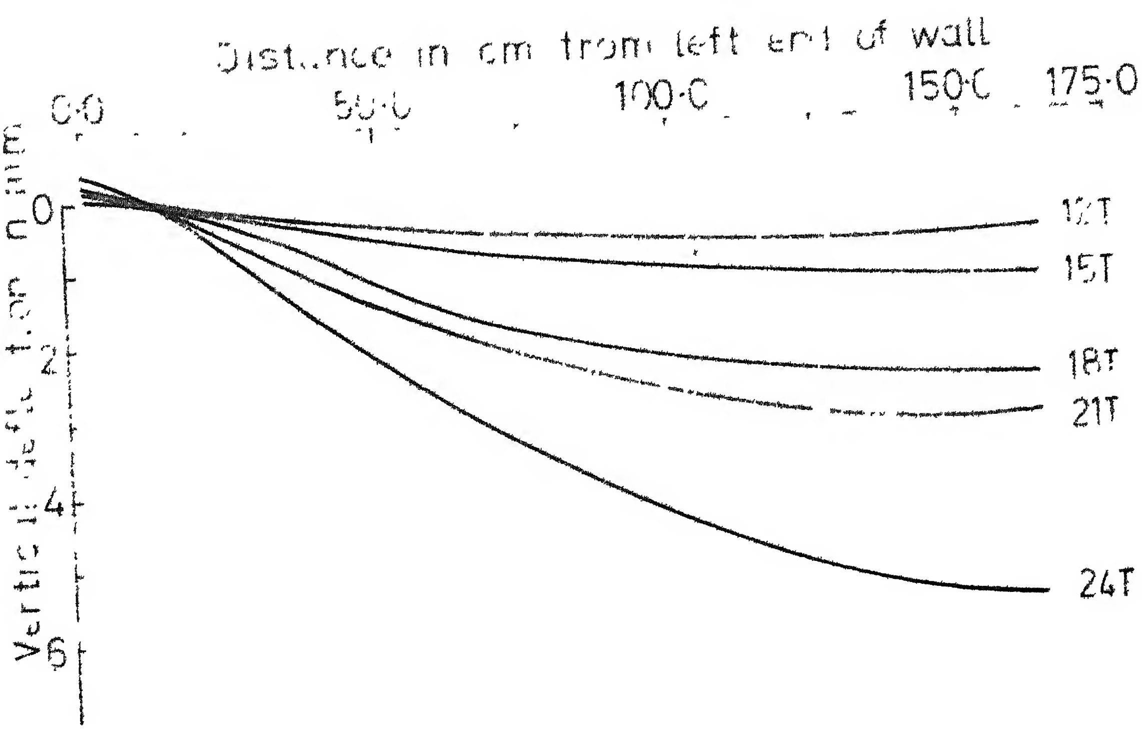

Fig.4.17 e Vertical deflection of wall along span at various loads

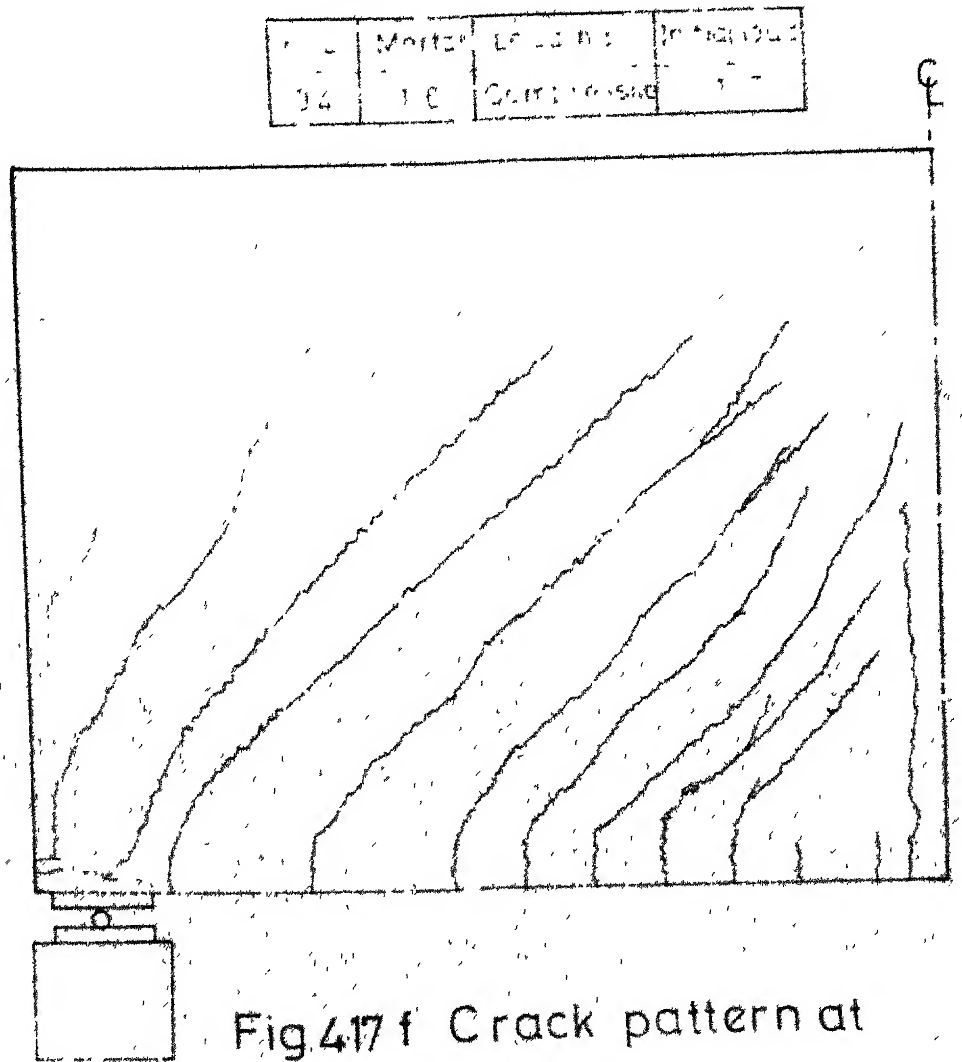

Fig.4.17 f Crack pattern at failure

H/L	Mortar	Loading	Initial load
0·5	1:6	Compressive	18 T

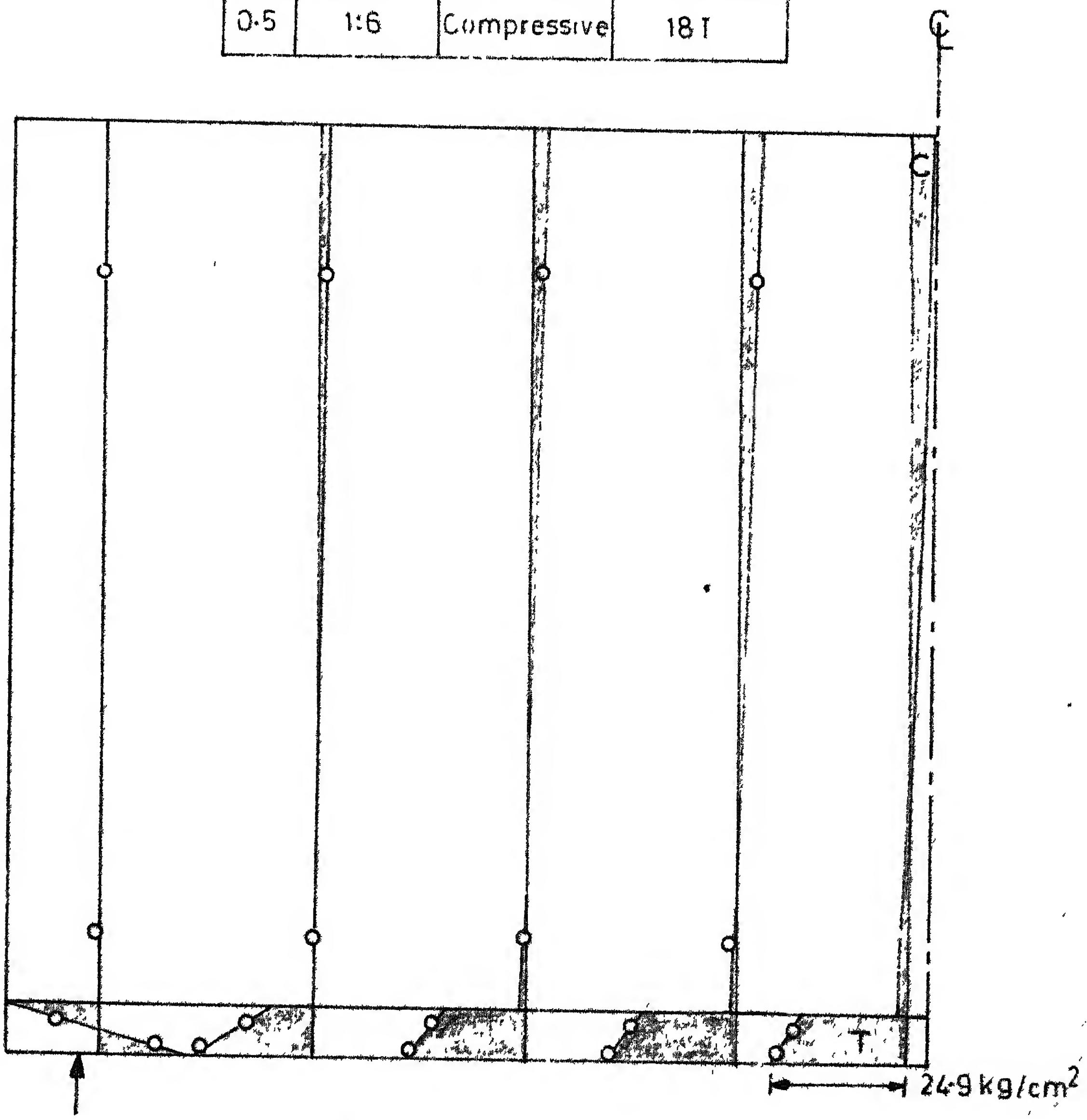

Fig. 4·18 a Longitudinal stress distribution at various cross sections

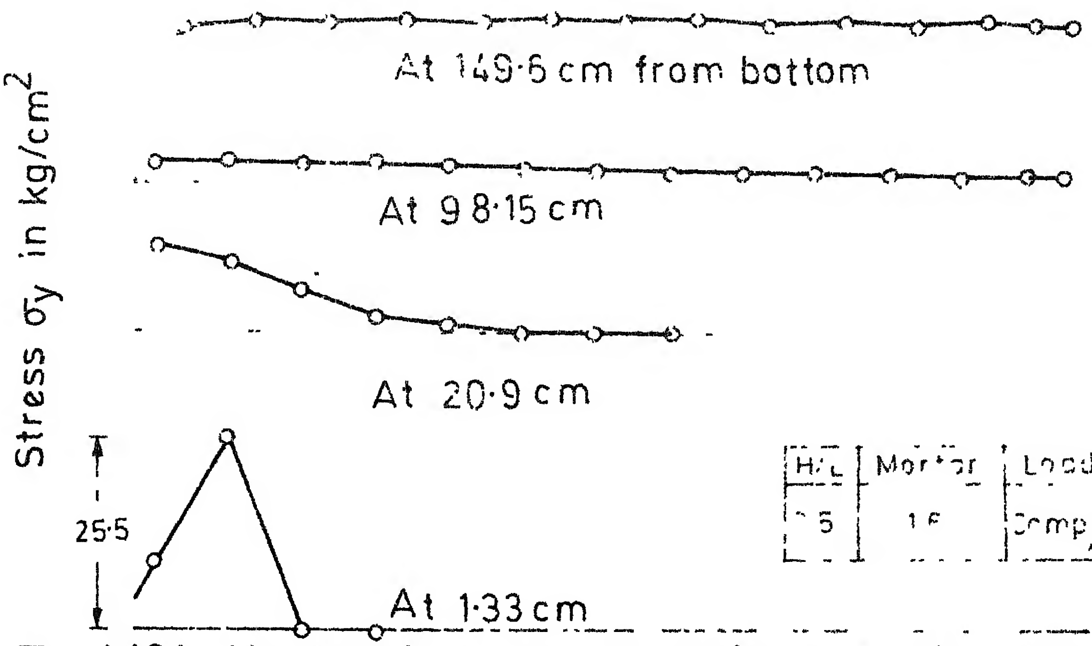

H/L	Mortar	Loading	Initial load
·5	1:6	Compressive	18 T

Fig.4·18 b Vertical stress distribution along span at various heights

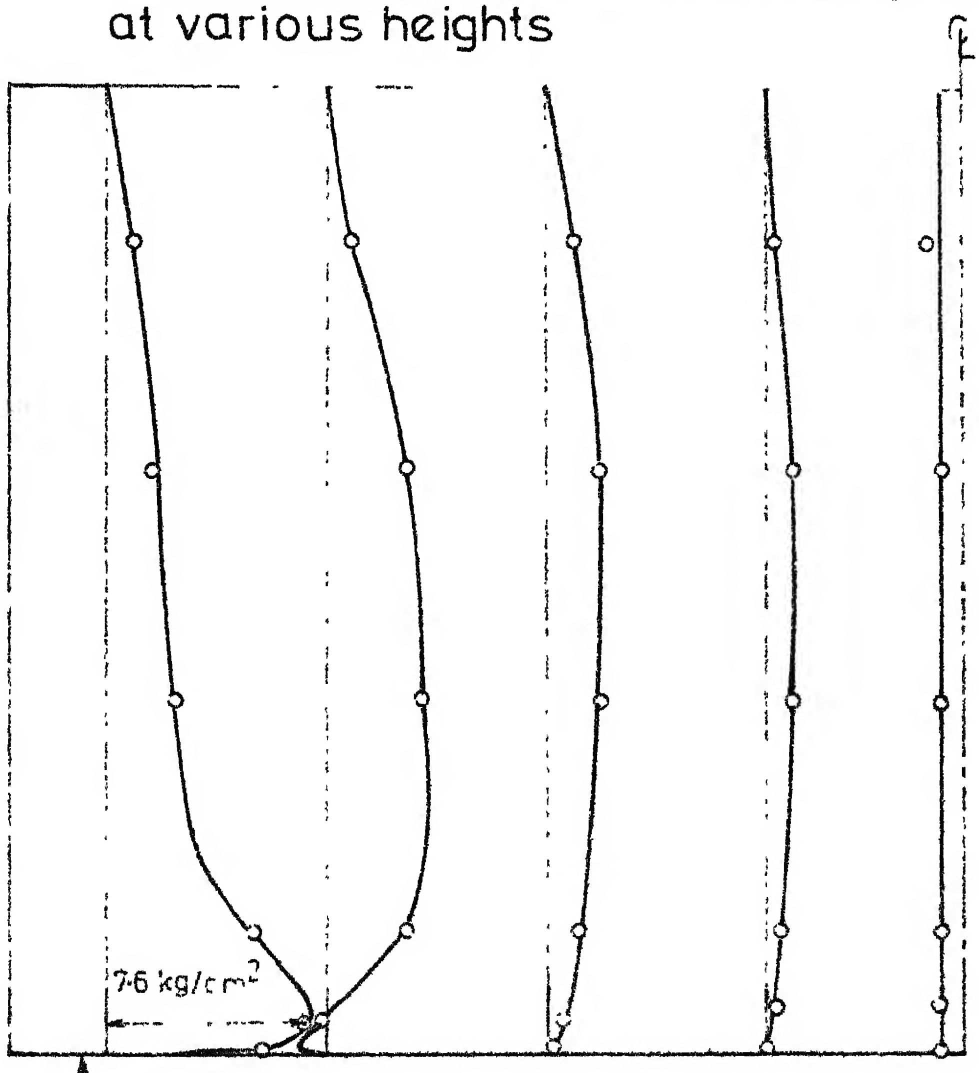

Fig.4·18 c Shear stress distribution at various cross sections

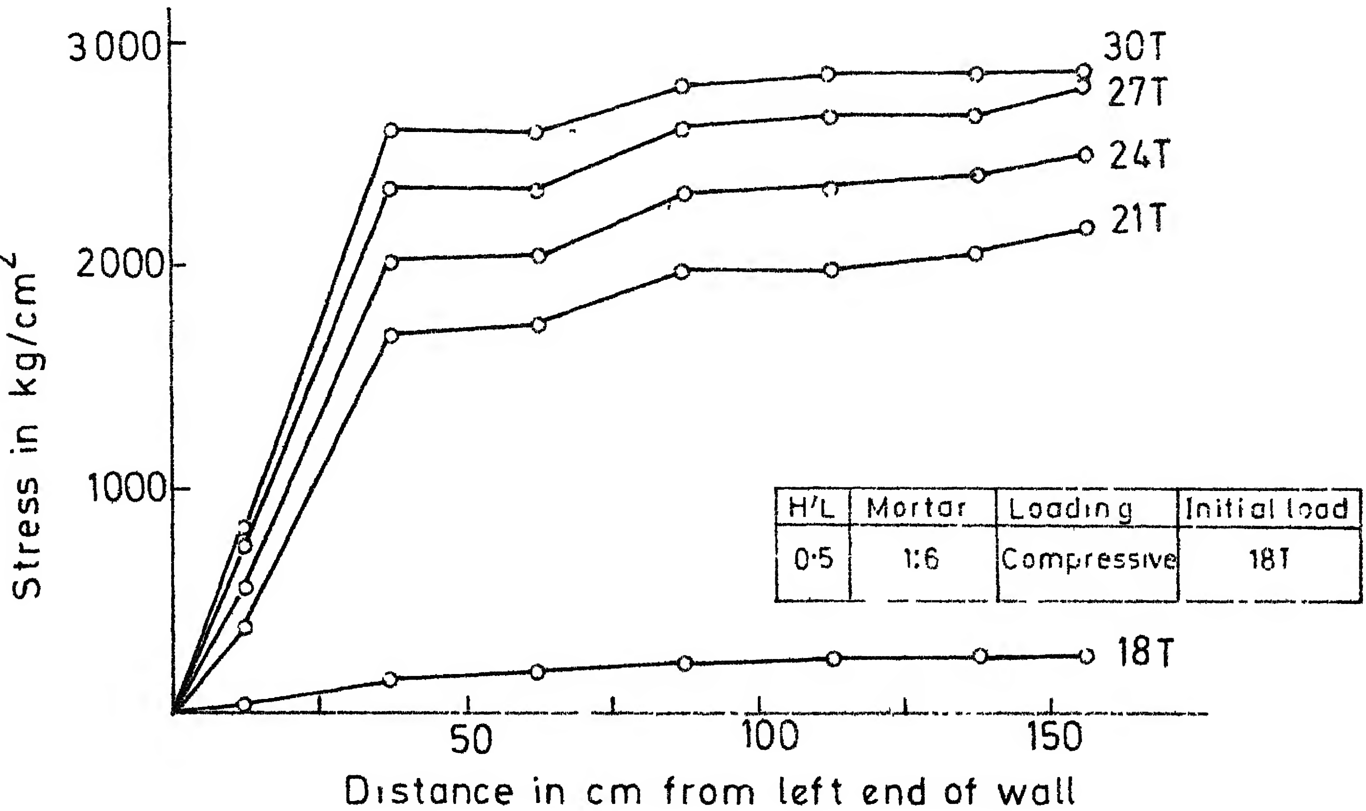

Fig. 4·18 d Variation of stress in bottom reinforcement along span at various loads

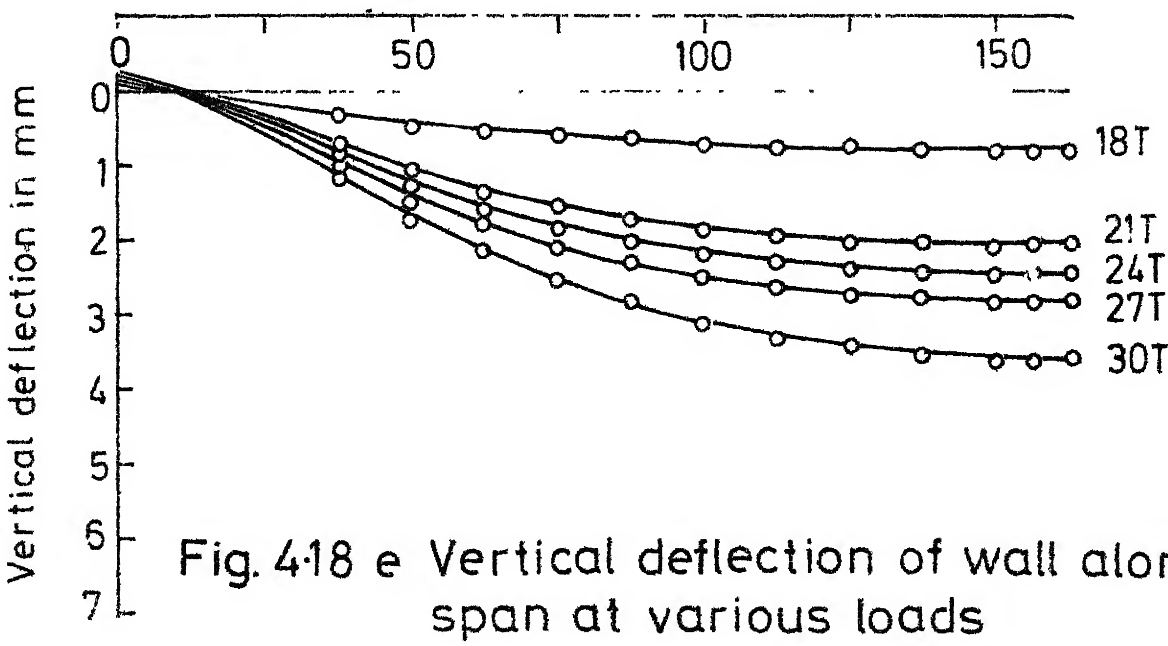

Fig. 4·18 e Vertical deflection of wall along span at various loads

H/L	Mortar	Loading	Initial load
05	1:6	Compressive	18T

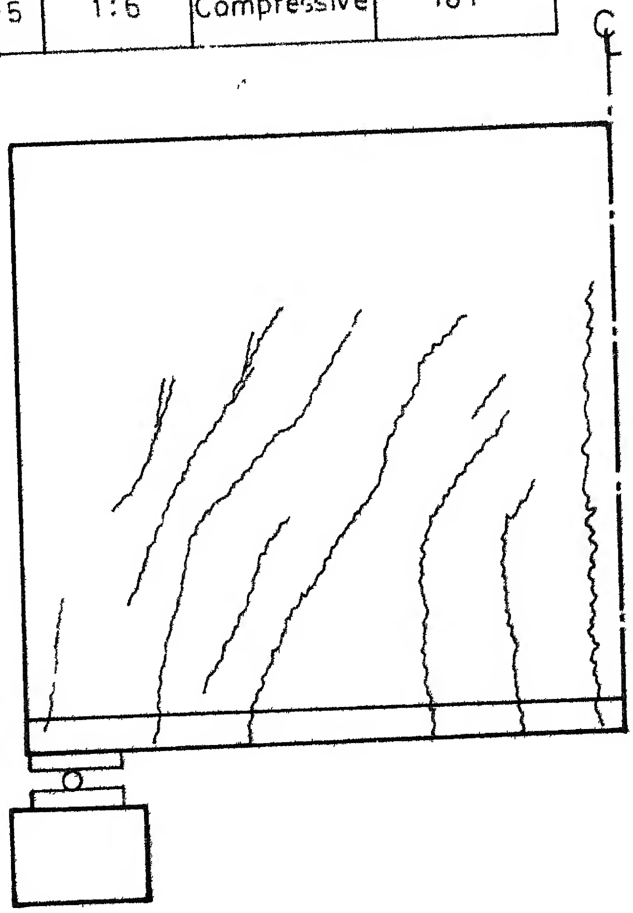

Fig. 4·18 f Crack pattern at failure

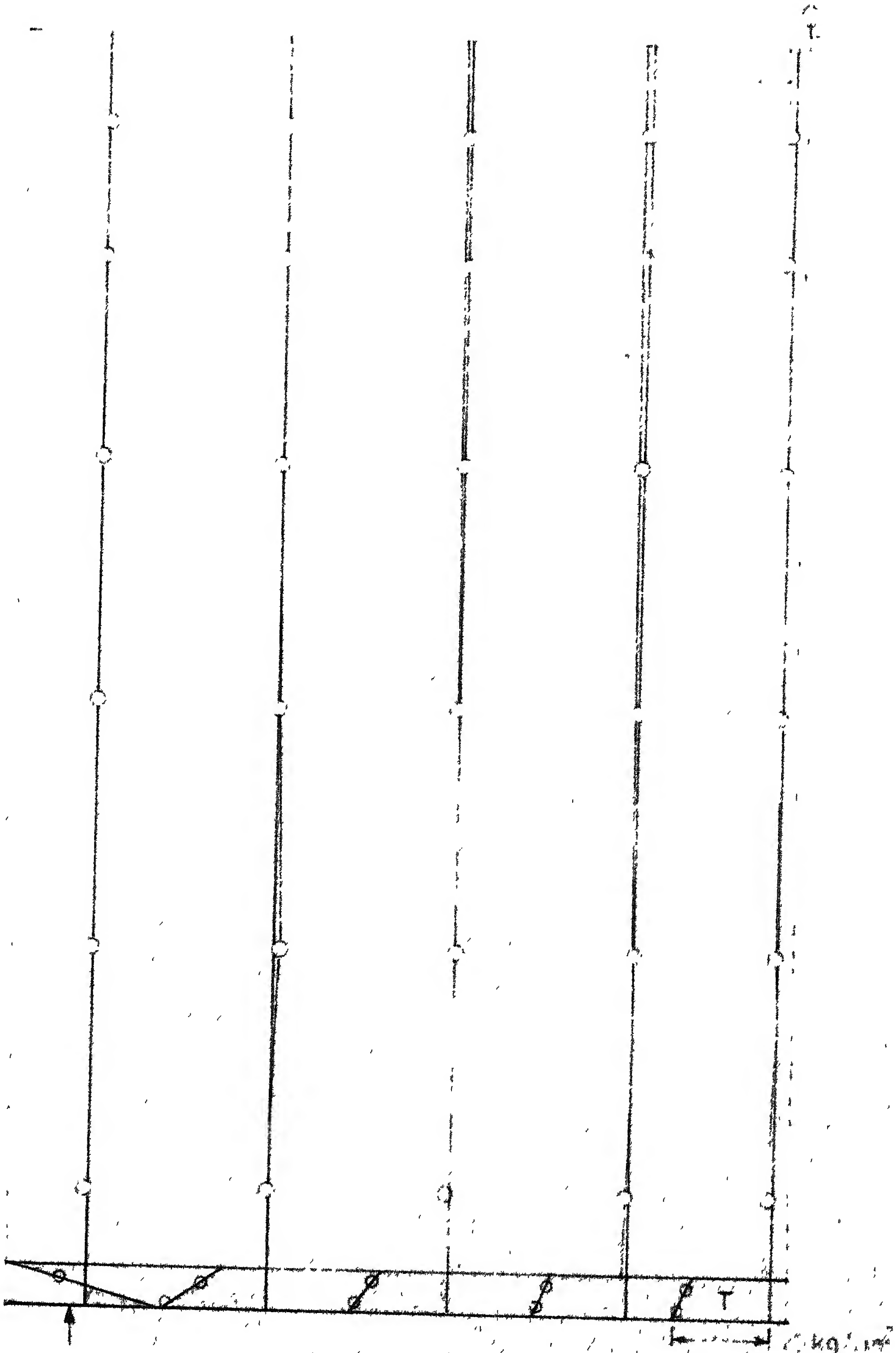

Fig.4·19 a Longitudinal stress distribution at various cross section

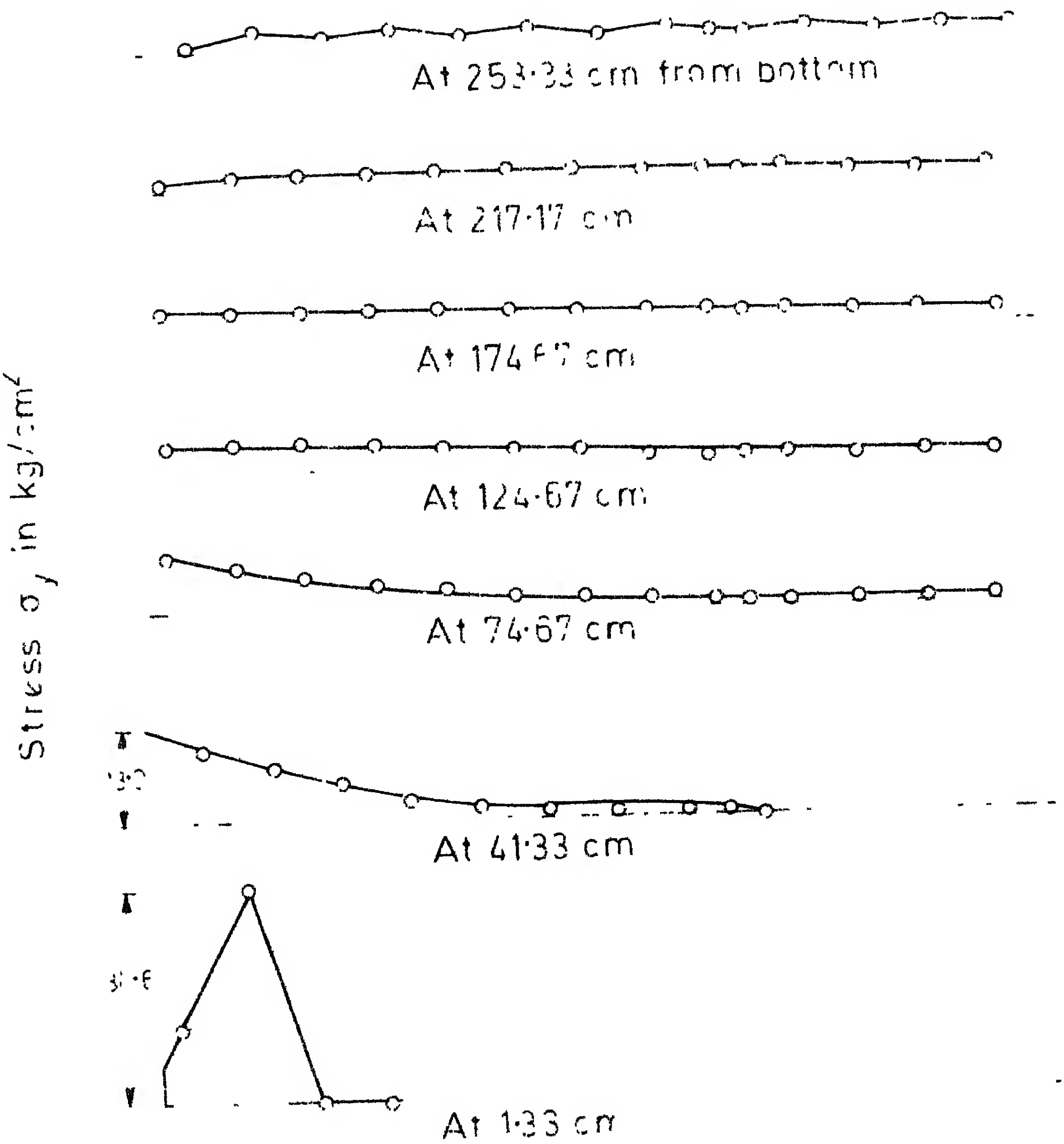

Fig.4·19b Vertical stress σ_y distribution along span at various heights

Fig. 4·19 c Shear stress distribution at various cross sections

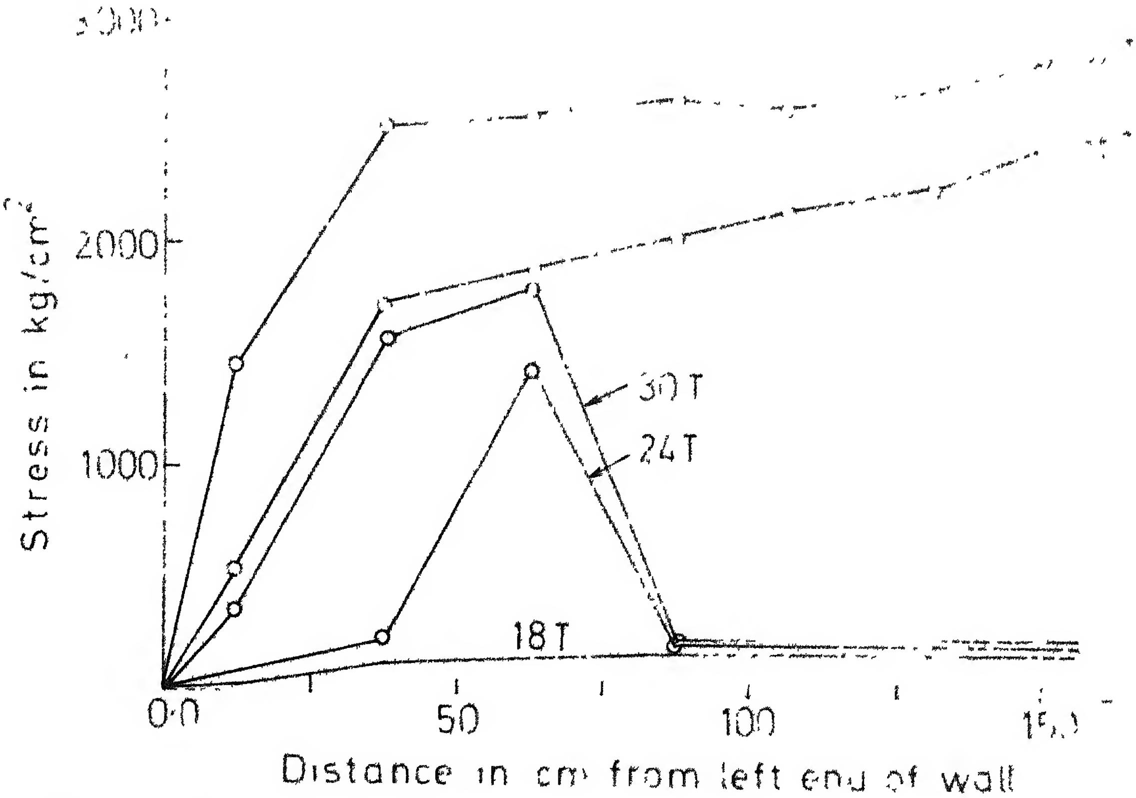

Fig.4·19 d Variation of stress in bottom reinforcement along span at various loads

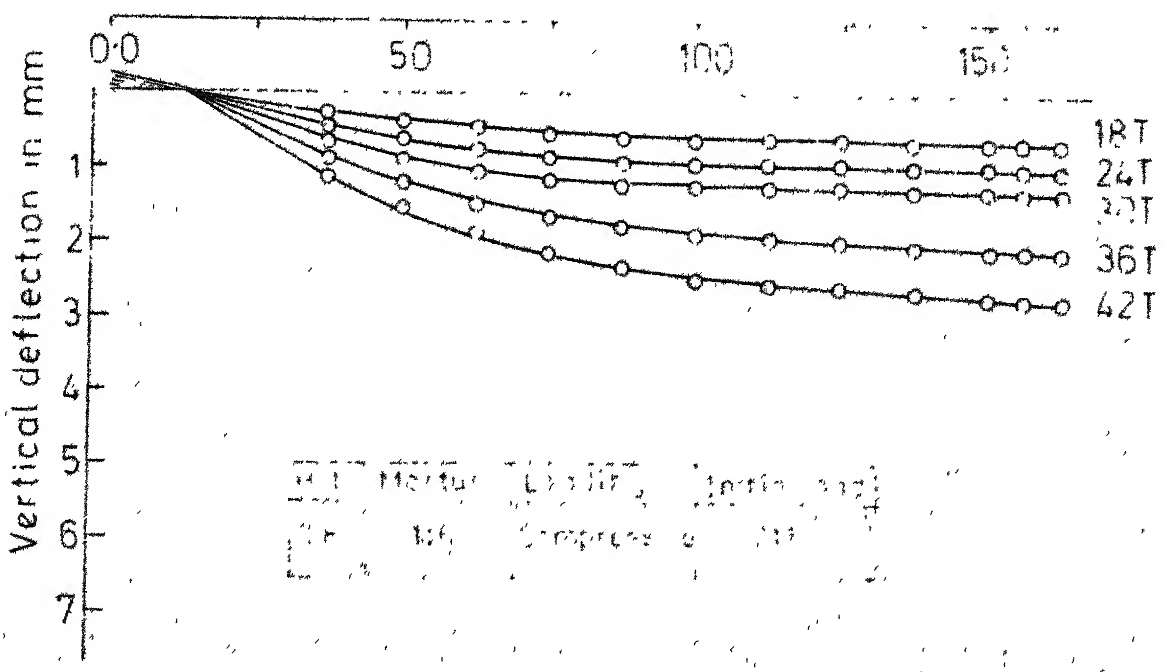

Fig.4·19 e Vertical deflections of wall along span at various loads

H/L	Mortar	Loading	Initial load
0·8	1:6	Compressive	21 T

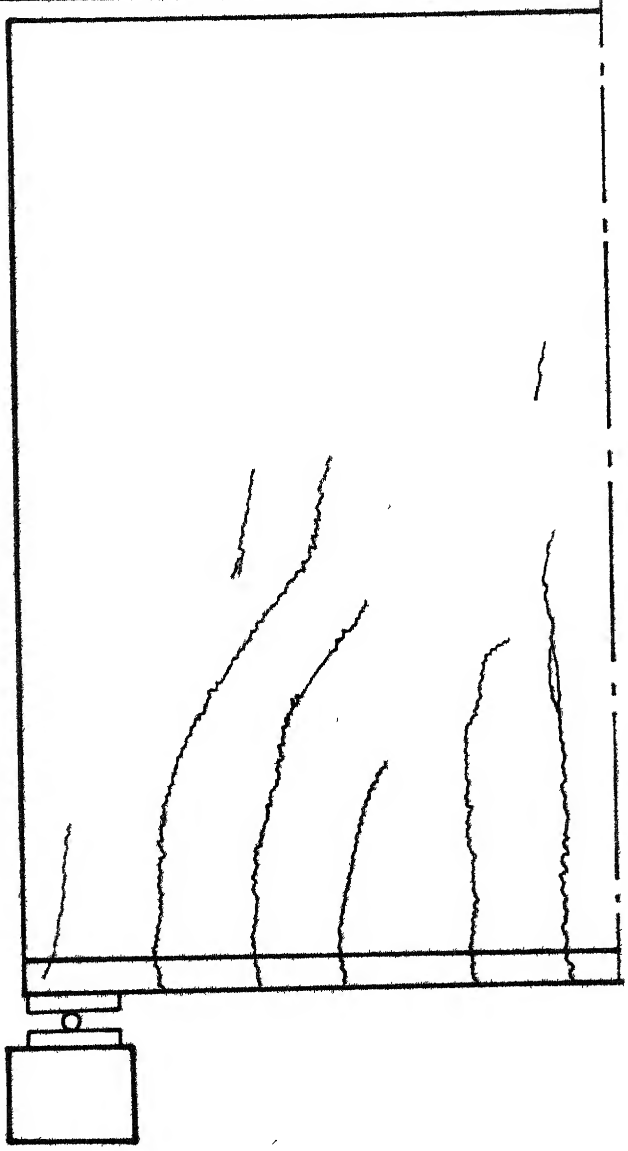

Fig. 4·19 f Crack pattern at failure

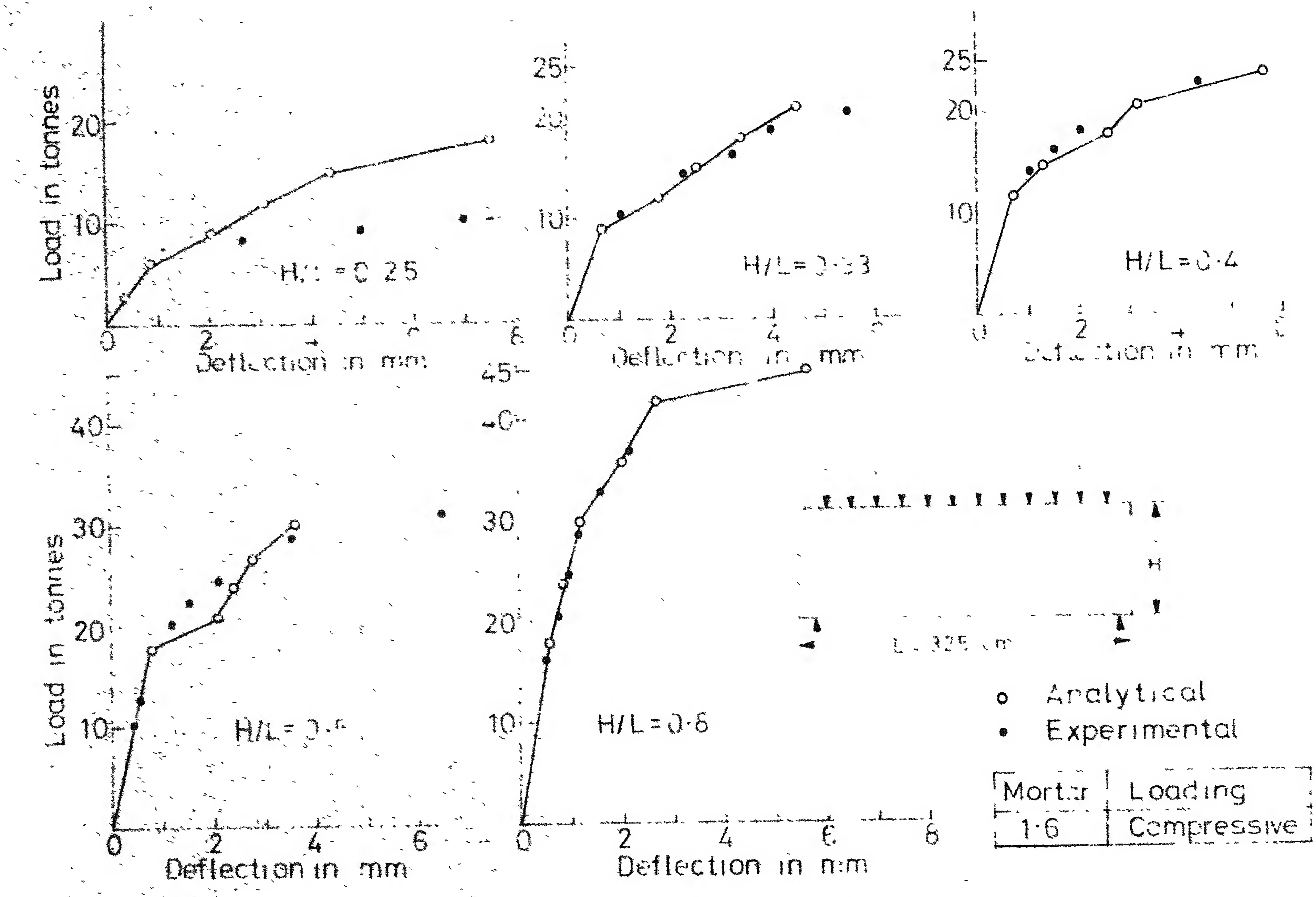

Fig. 4·20 Load vs deflection curves at mid span

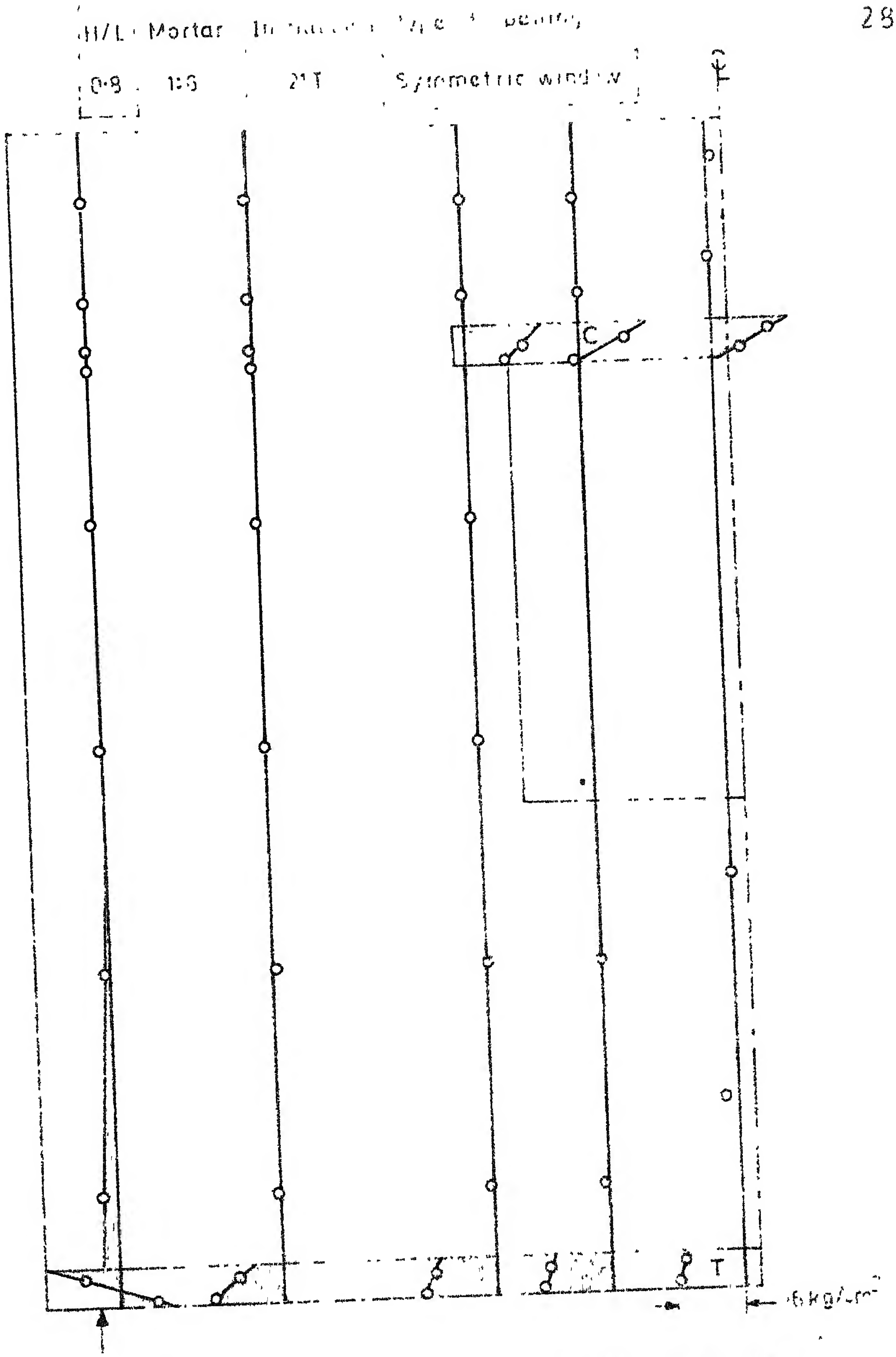

Fig.4.21a Longitudinal stress distribution at various cross section

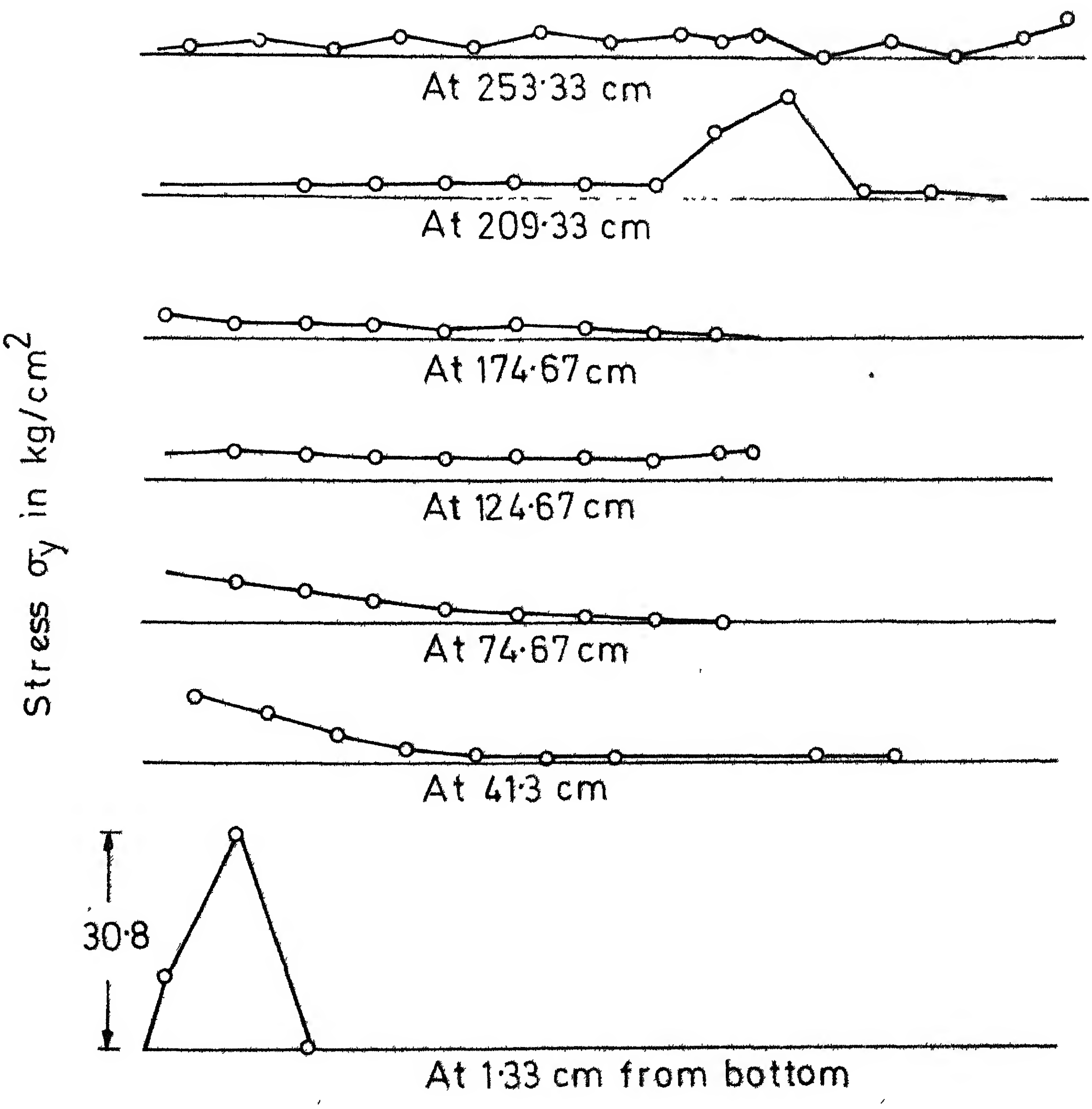

Fig.4·21 b Vertical stress distribution along span at various heights

H/L	Mortar	Initial load	Type of opening
0·8	1:6	21T	Symmetric window

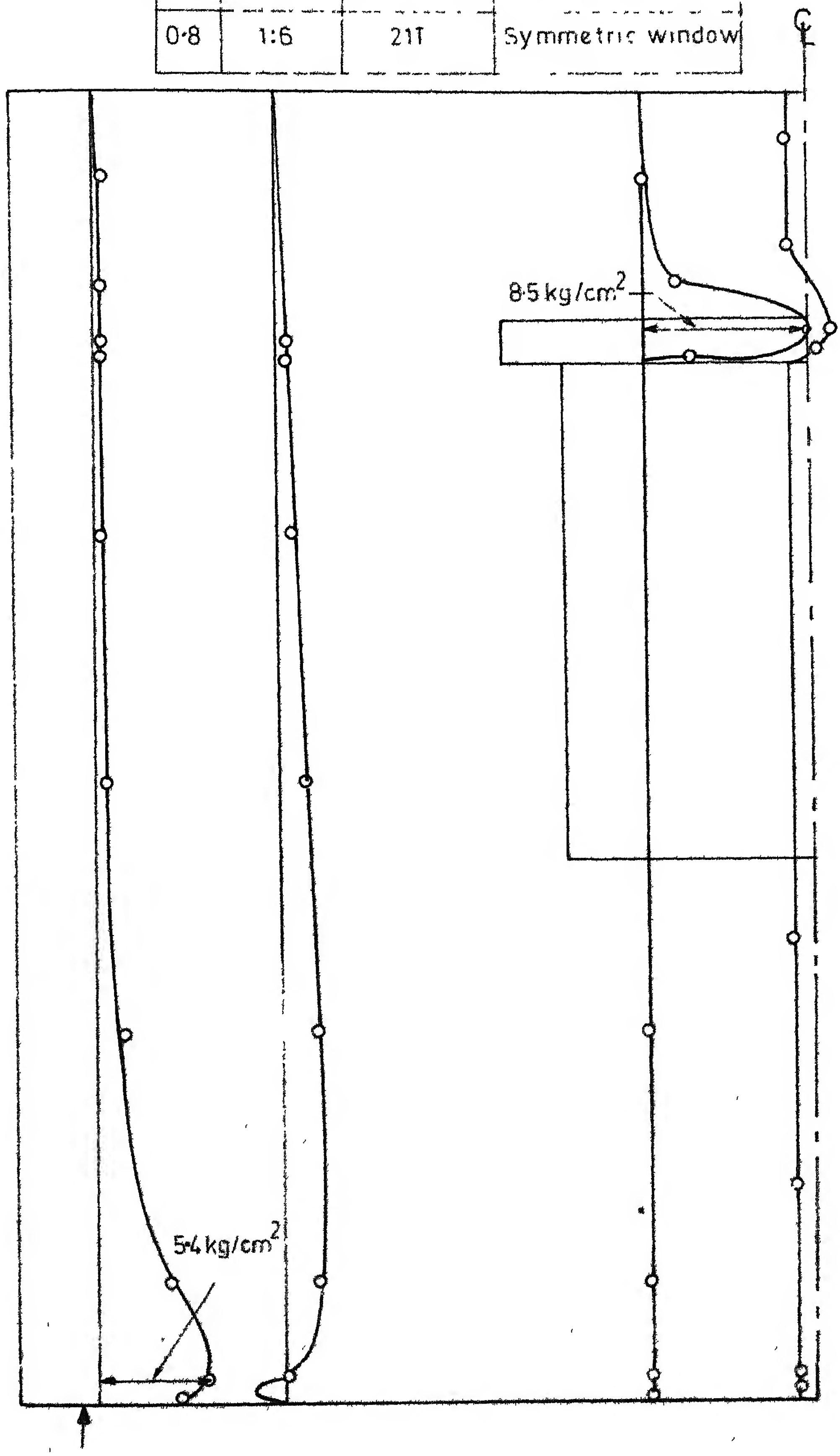

Fig 4·21 c Shear stress distribution at various cross sections

H/L	Mortar	Initial load	Type of opening
0·8	1:6	21T	Symmetric window

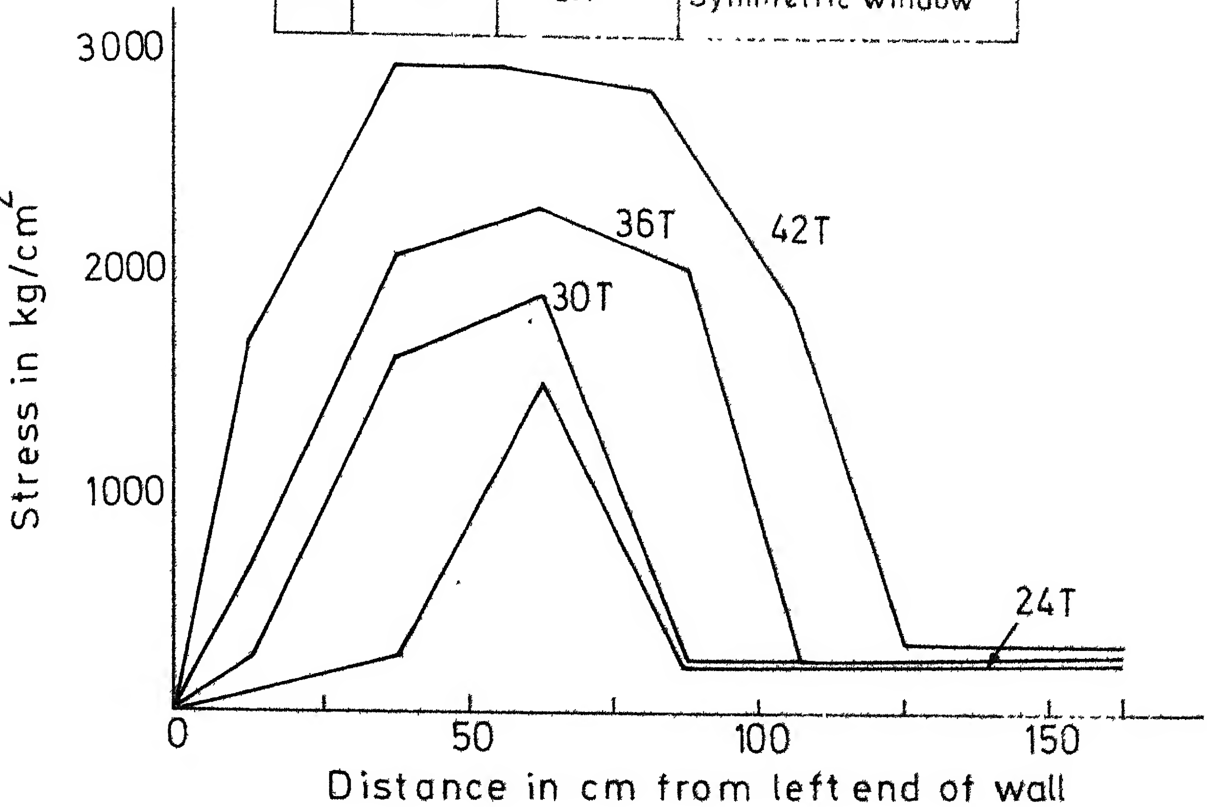

Fig.4·21 d Variation of stress in bottom reinforcement along span at various loads

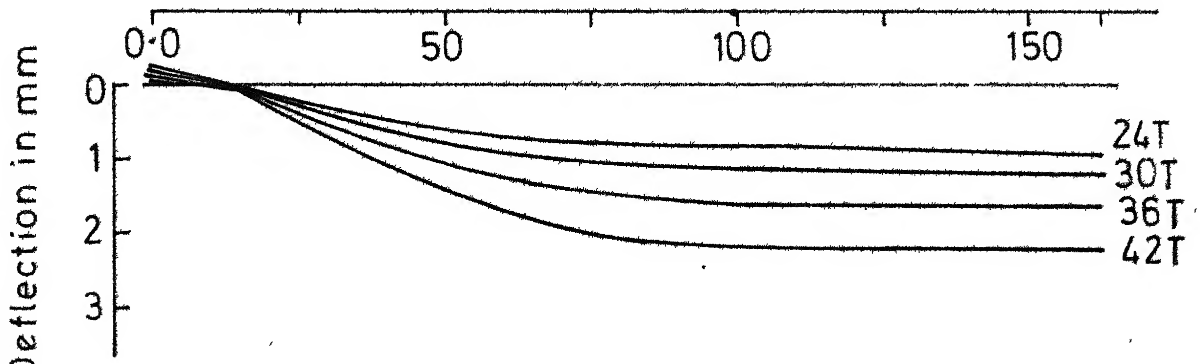

Fig.4·21 e Vertical deflection of wall along span at various loads

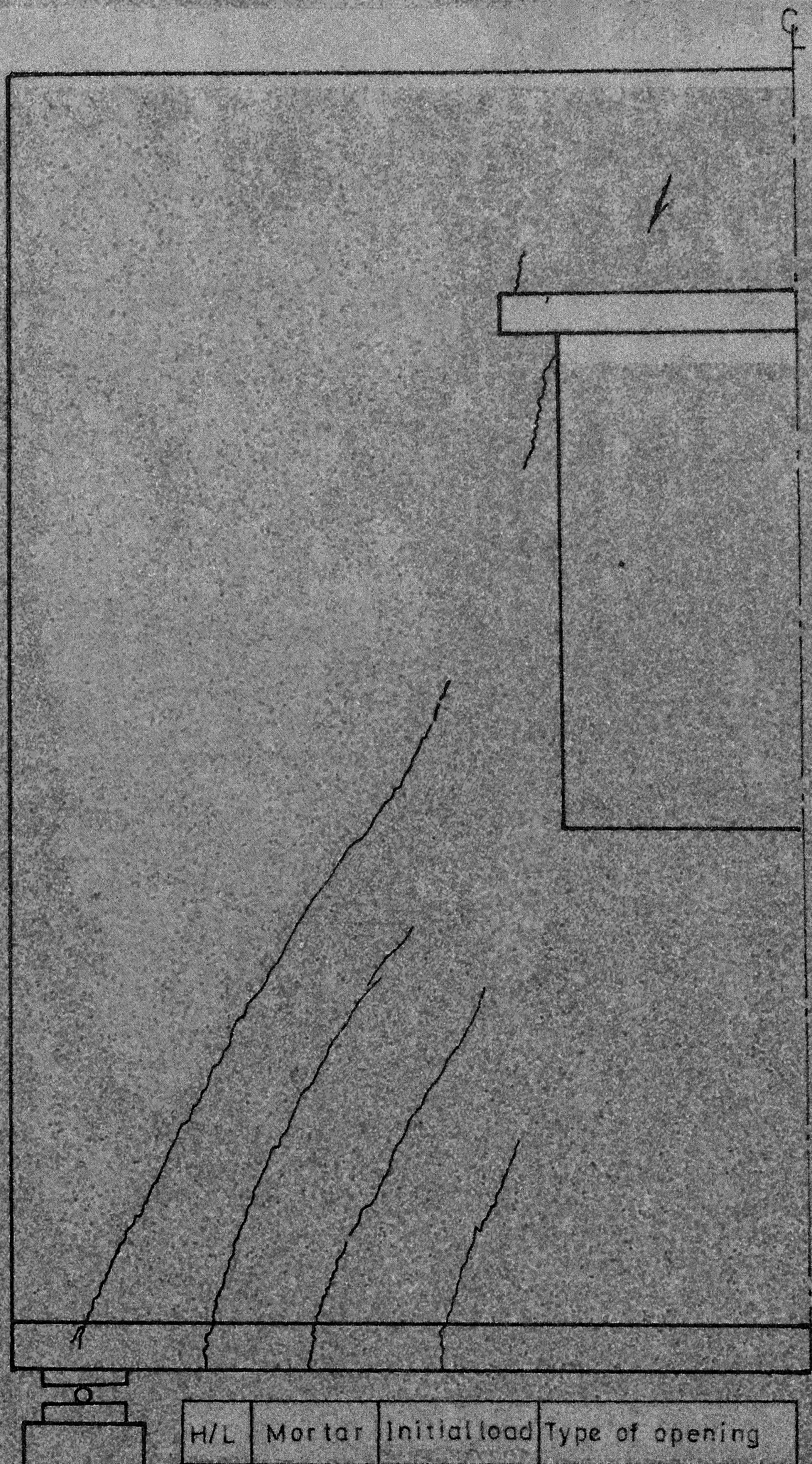

H/L	Mortar	Initial load	Type of opening
0·8	1:6	21T	Symmetric window

Fig.421f Crack pattern at failure

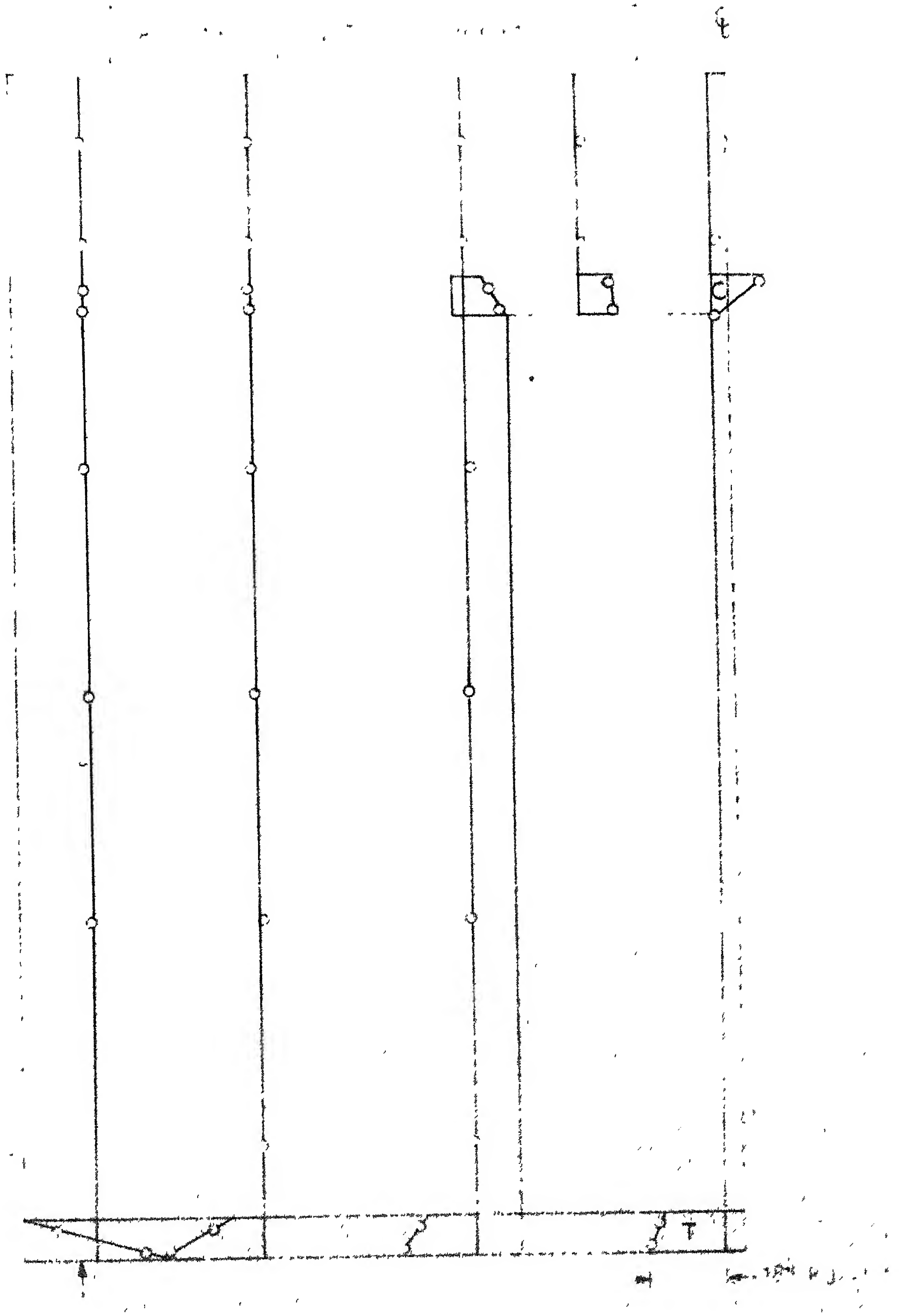

Fig. 4.22 a Longitudinal stress distribution at various cross section

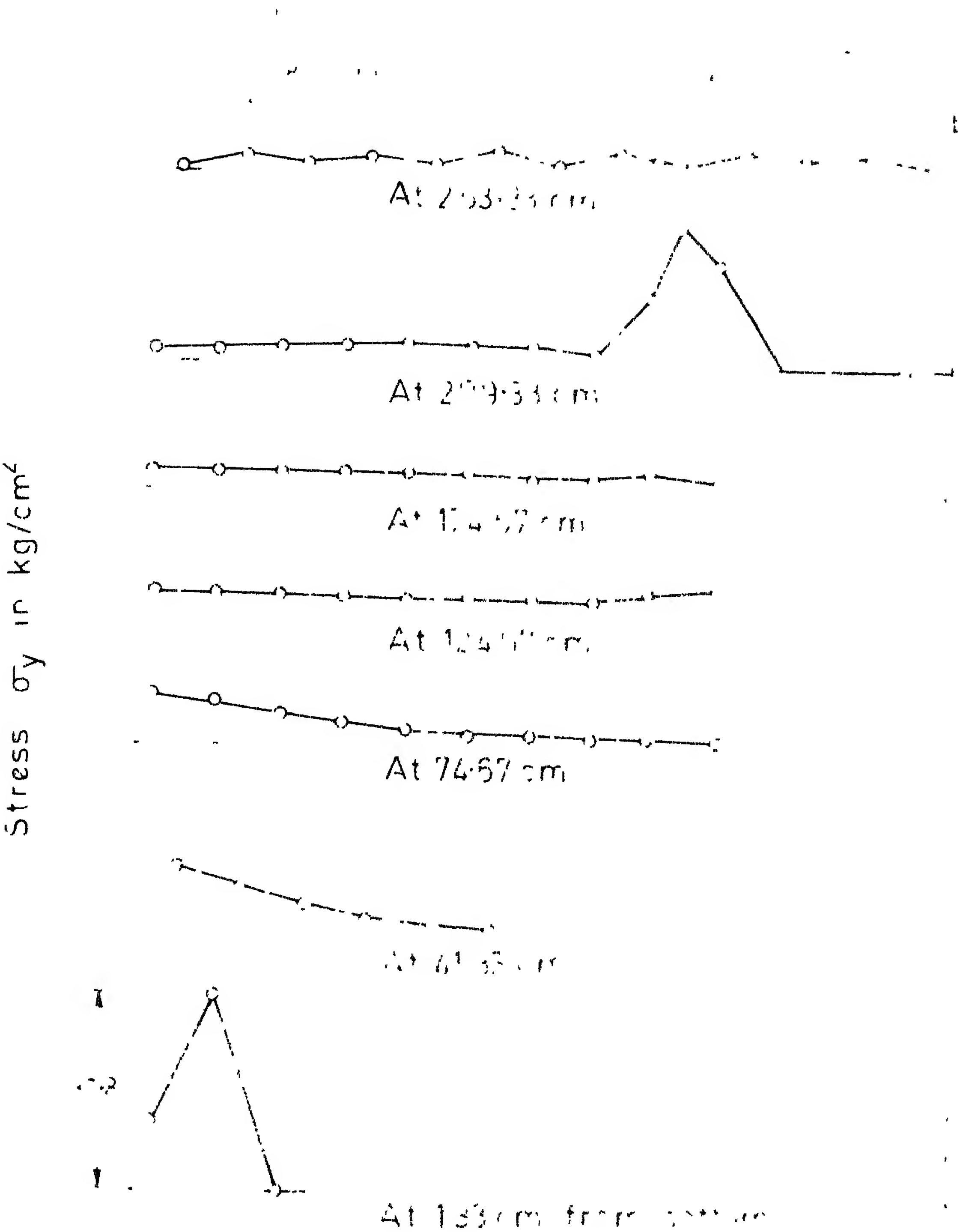

Fig.4.22 b Vertical stress σ_y distribution along span at various heights

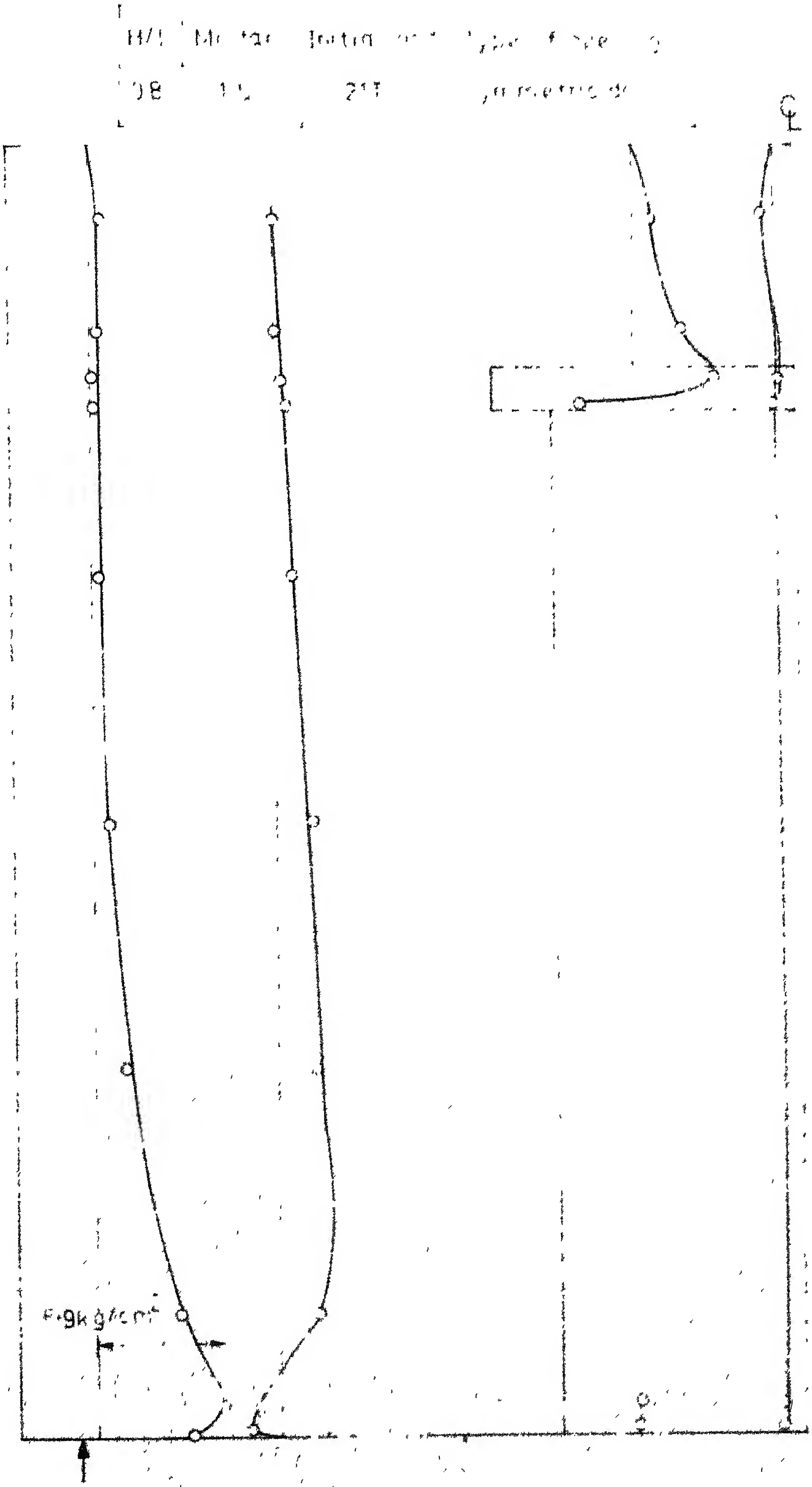

Fig. 4.22 c Shear stress distribution at various cross-section

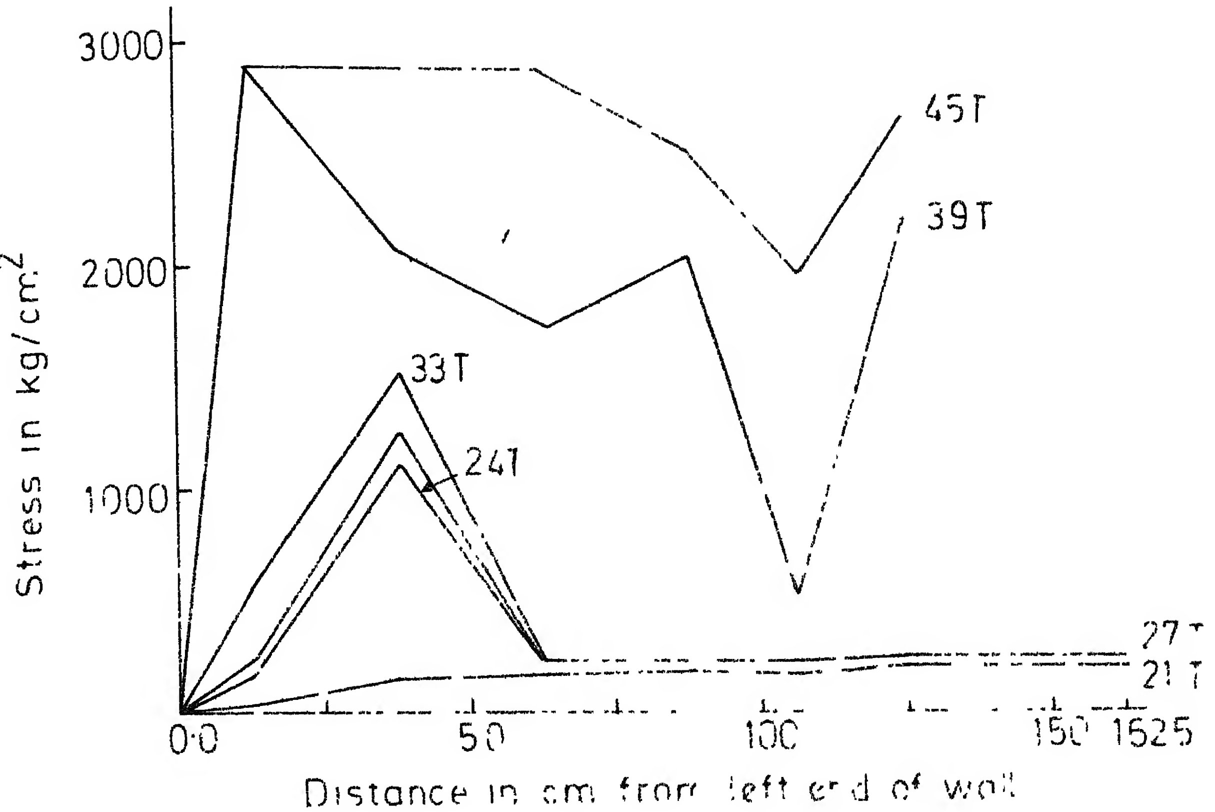

Fig. 4·22 d Variation of stress in bending reinforcement along span at various loads

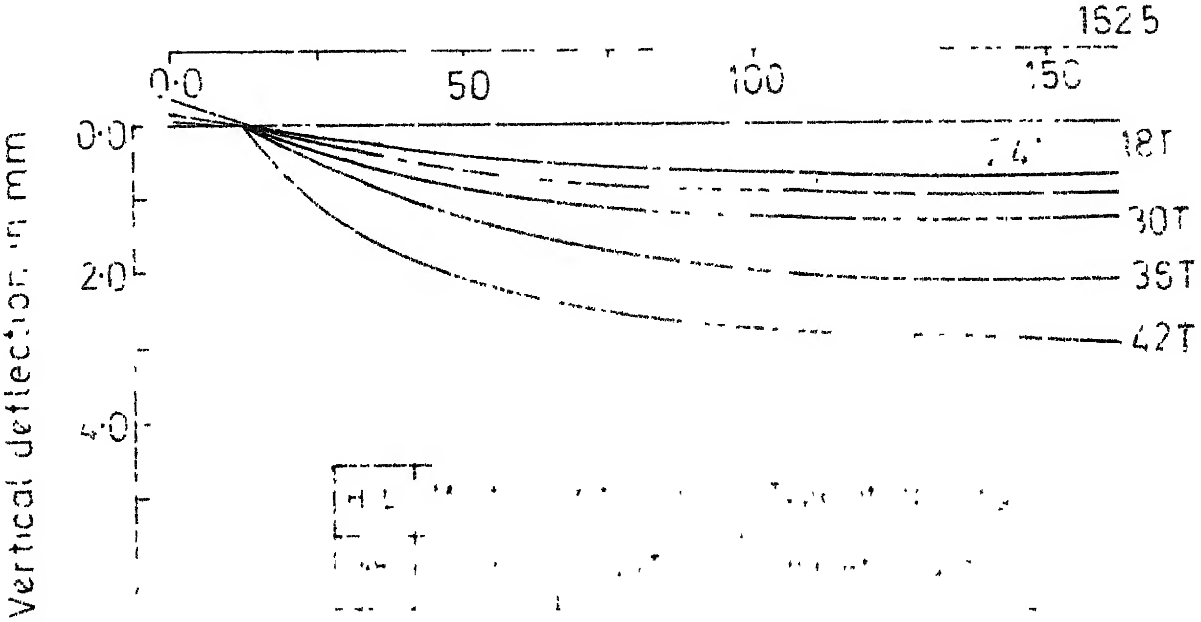

Fig. 4·22 e Vertical deflection of wall along span at various loads

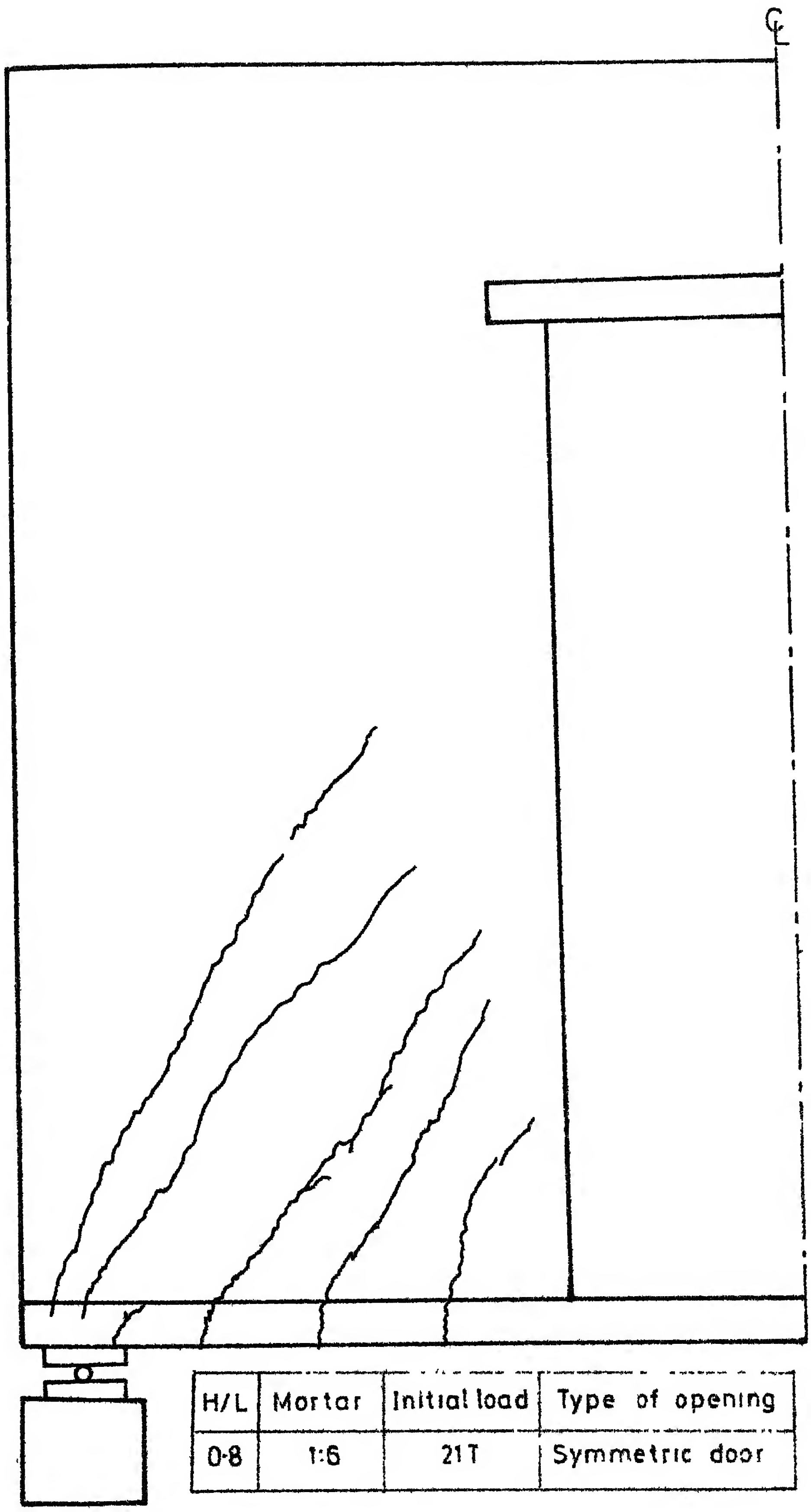

H/L	Mortar	Initial load	Type of opening
0·8	1:6	21T	Symmetric door

Fig.4·22 f Crack pattern at failure

H/L	Mortar	Initial load	Type of opening
0·8	1:6	15 T	Unsymmetric window

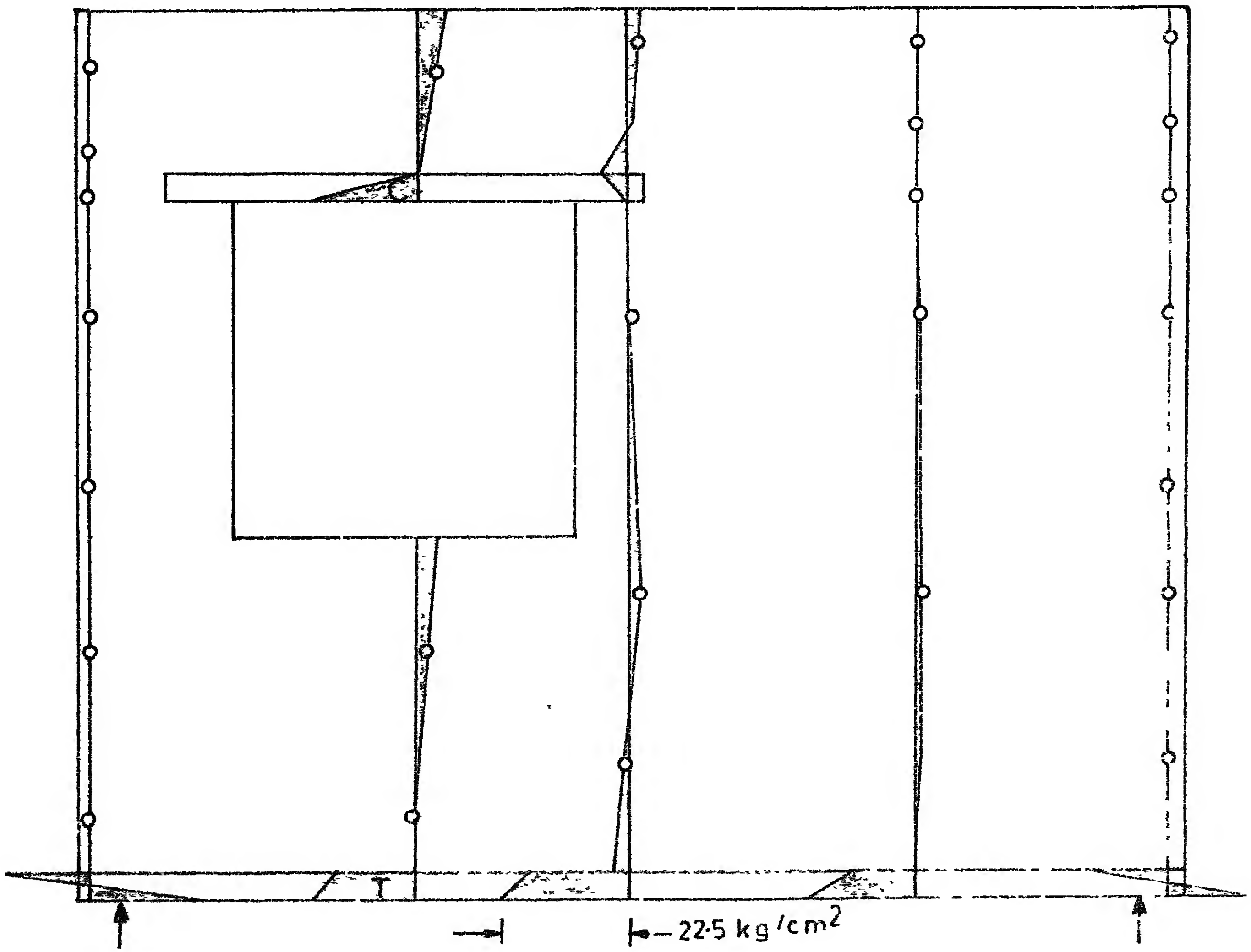

Fig. 4·23 a Longitudinal stress distribution at various cross section

H/L	Mortar	Initial load	Type of opening
0·8	1:6	15T	Unsymmetric window

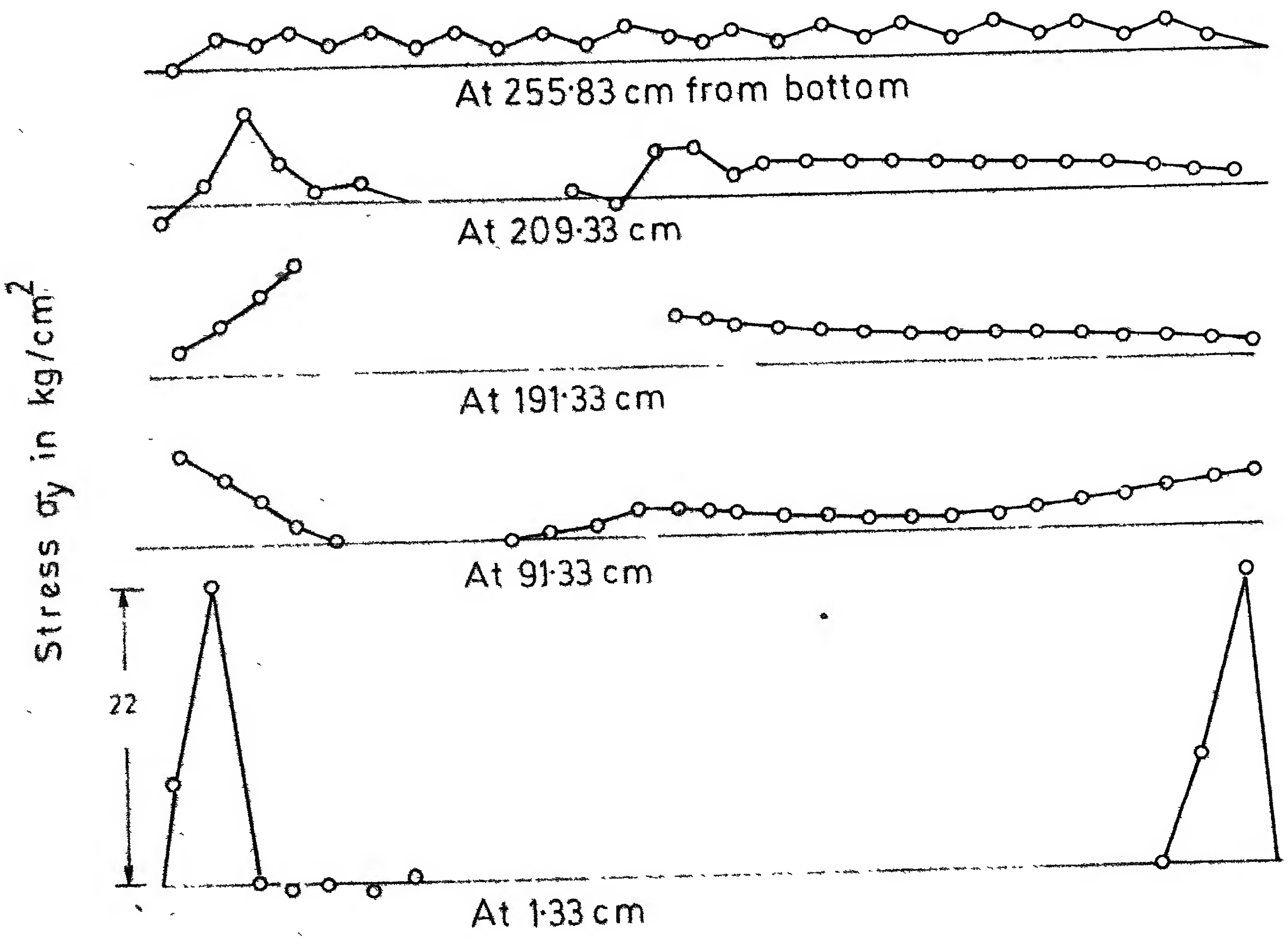

Fig.4·23 b Vertical stress σ_y distribution along span at various heights

H/L	Mortar	Initial load	Type of opening
0·8	1:6	21T	Symmetric door

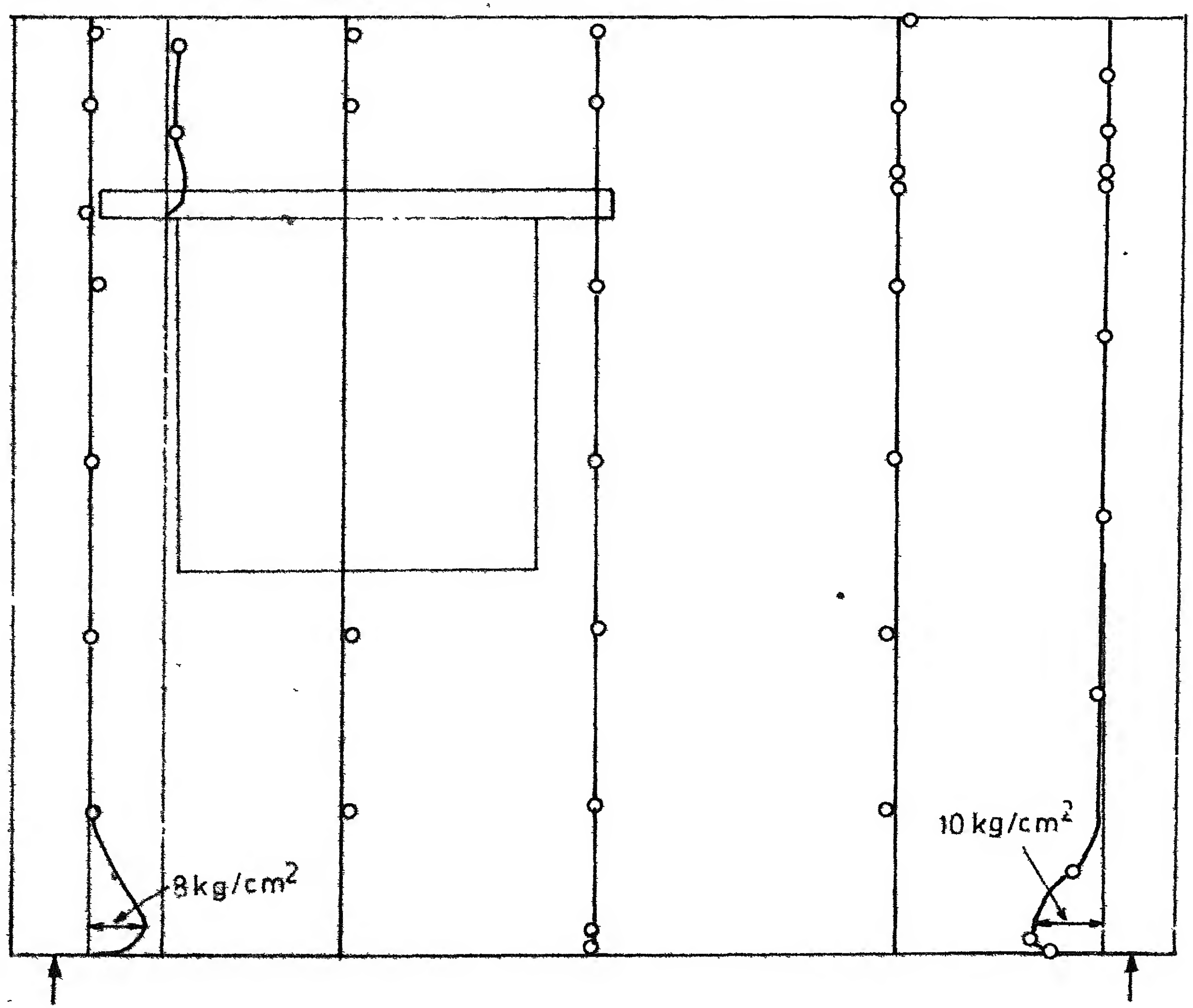

Fig. 4·23 c   Shear stress distribution at various cross sections

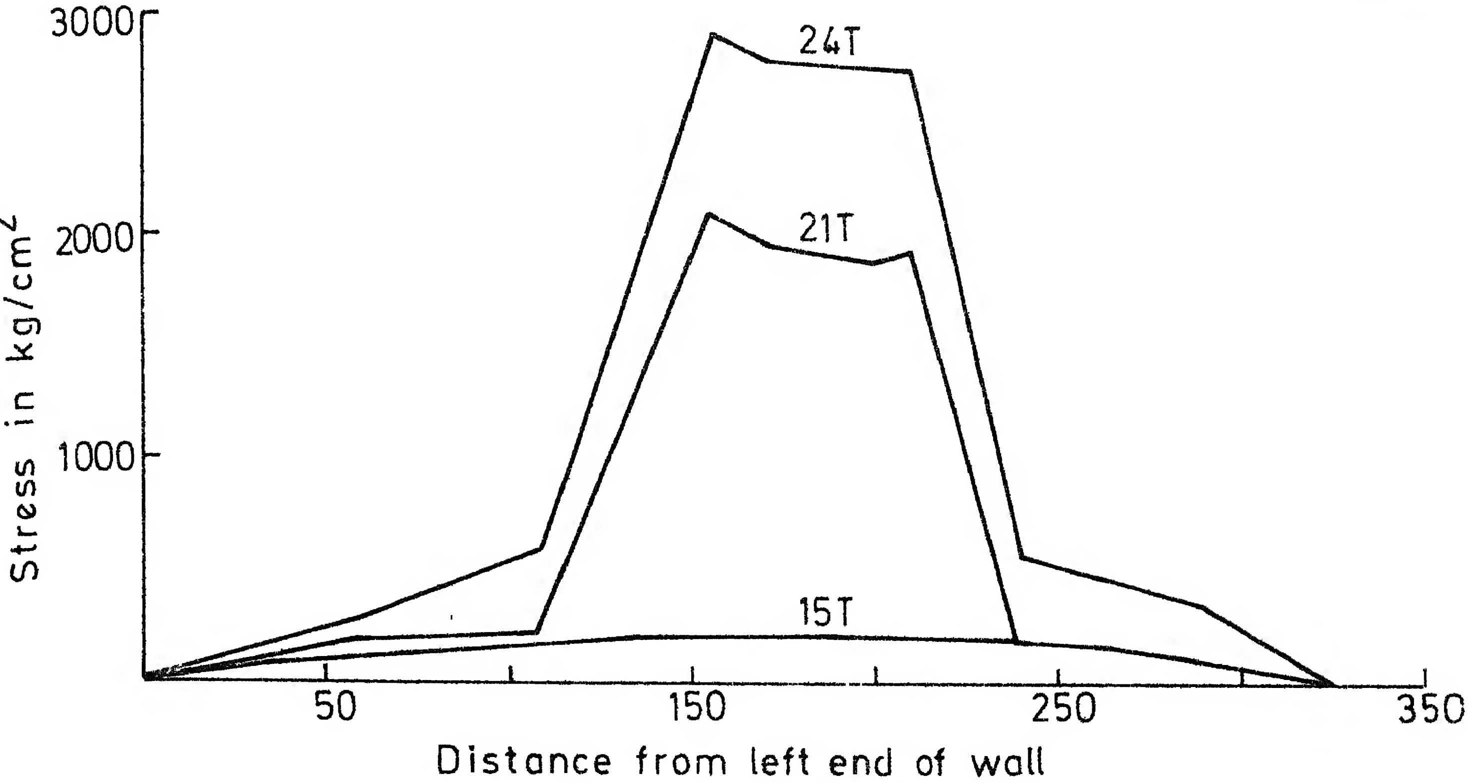

Fig. 4·23 d Variation of stress in bottom reinforcement along span at various loads

H/L	Mortar	Initial load	Type of opening
0·8	1·6	21 T	Symmetric door

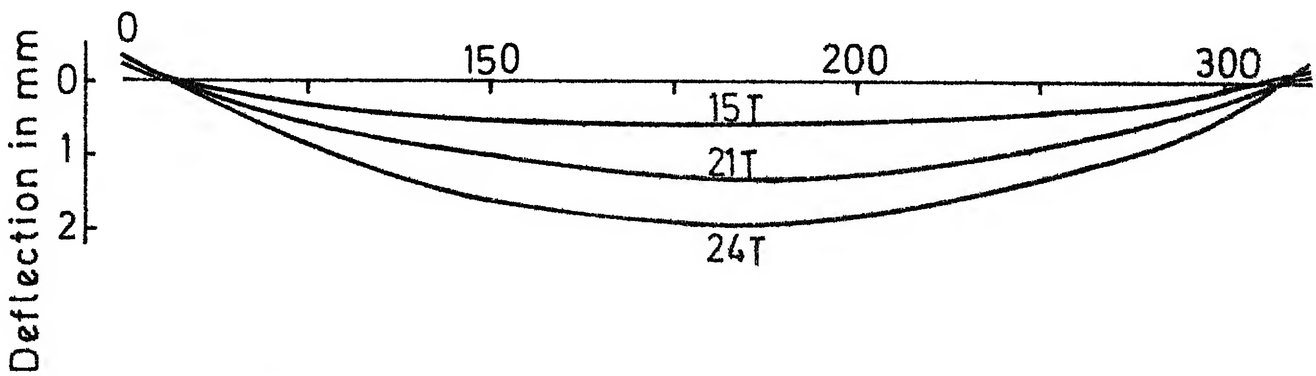

Fig. 4·23 e Vertical deflection of wall along span at various loads

H/L	Mortar	Initial load	Type of opening
0·8	1:6	21T	Symmetric door

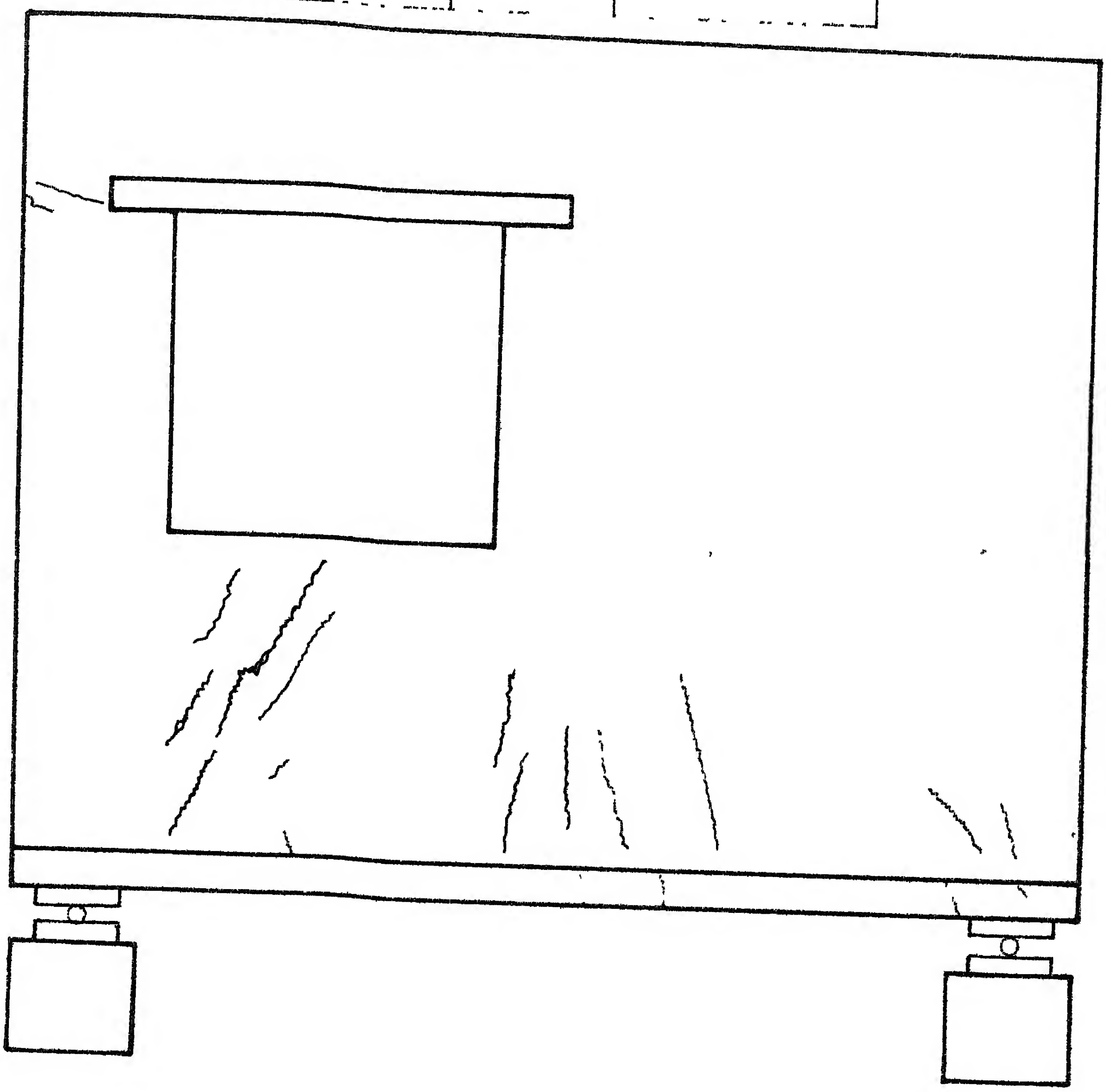

Fig.4·23f Crack pattern at failure

H/L	Mortar	Initial load	Type of opening
0·8	1:6	3T	Unsymmetric door

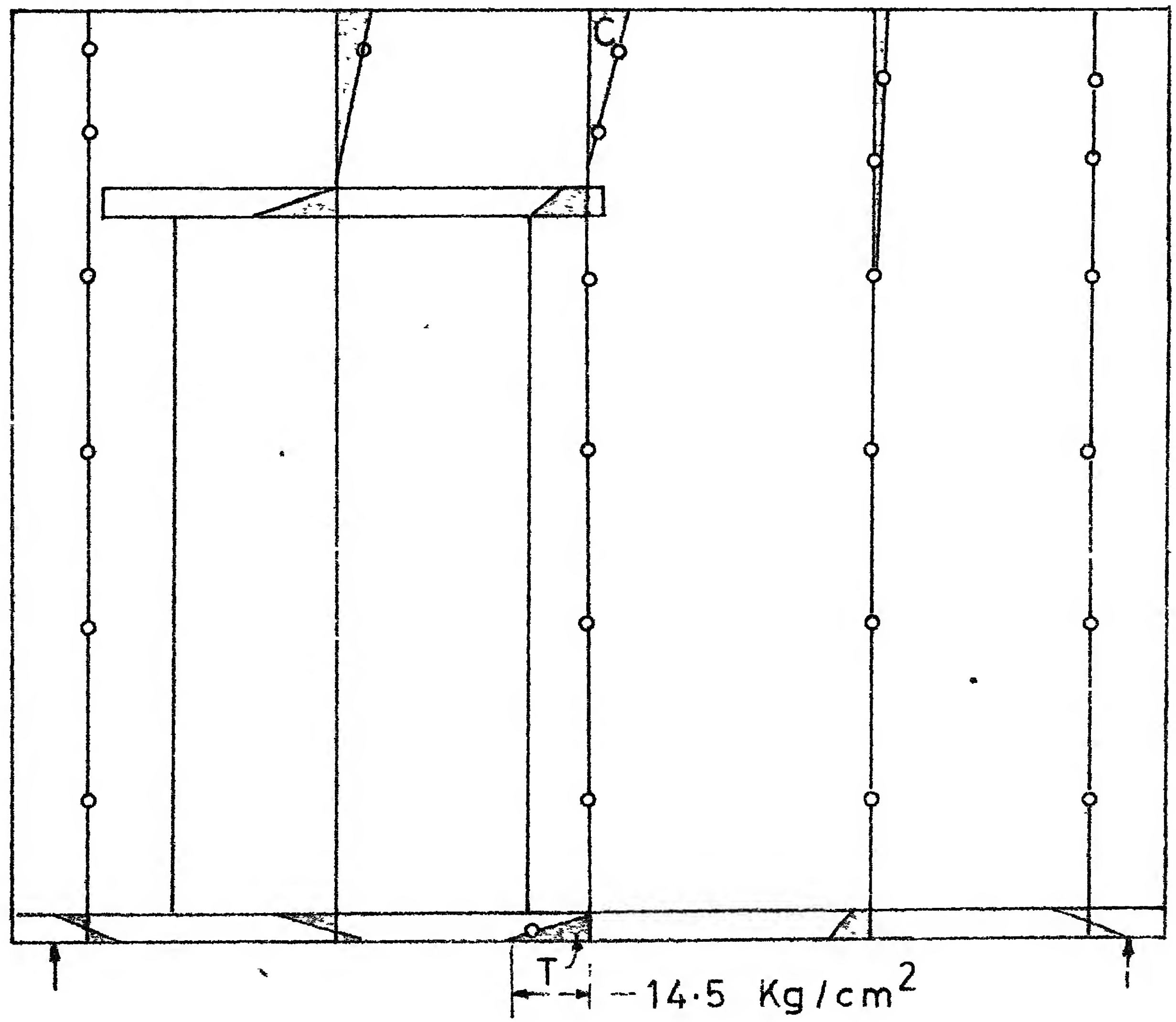

Fig.4·24 a Longitudinal stress distribution at various cross sections

H/L	Mortar	Initial load	Type of opening
0·8	1.6	3T	Unsymmetric door

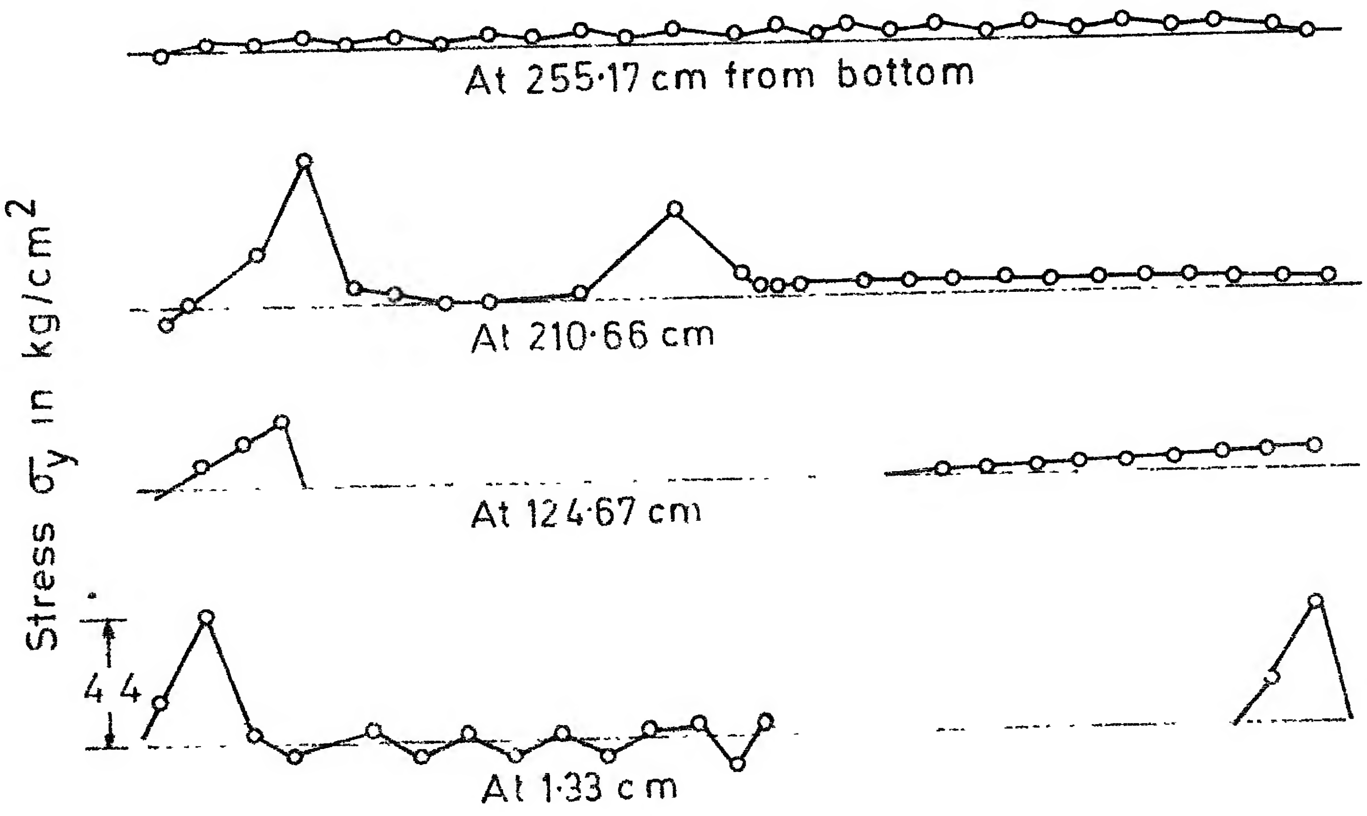

Fig. 4·24 b Vertical stress σ_y distribution along span at various heights

H/L	Mortar	Initial load	Type of opening
0·8	1:6	3 T	Unsymmetric door

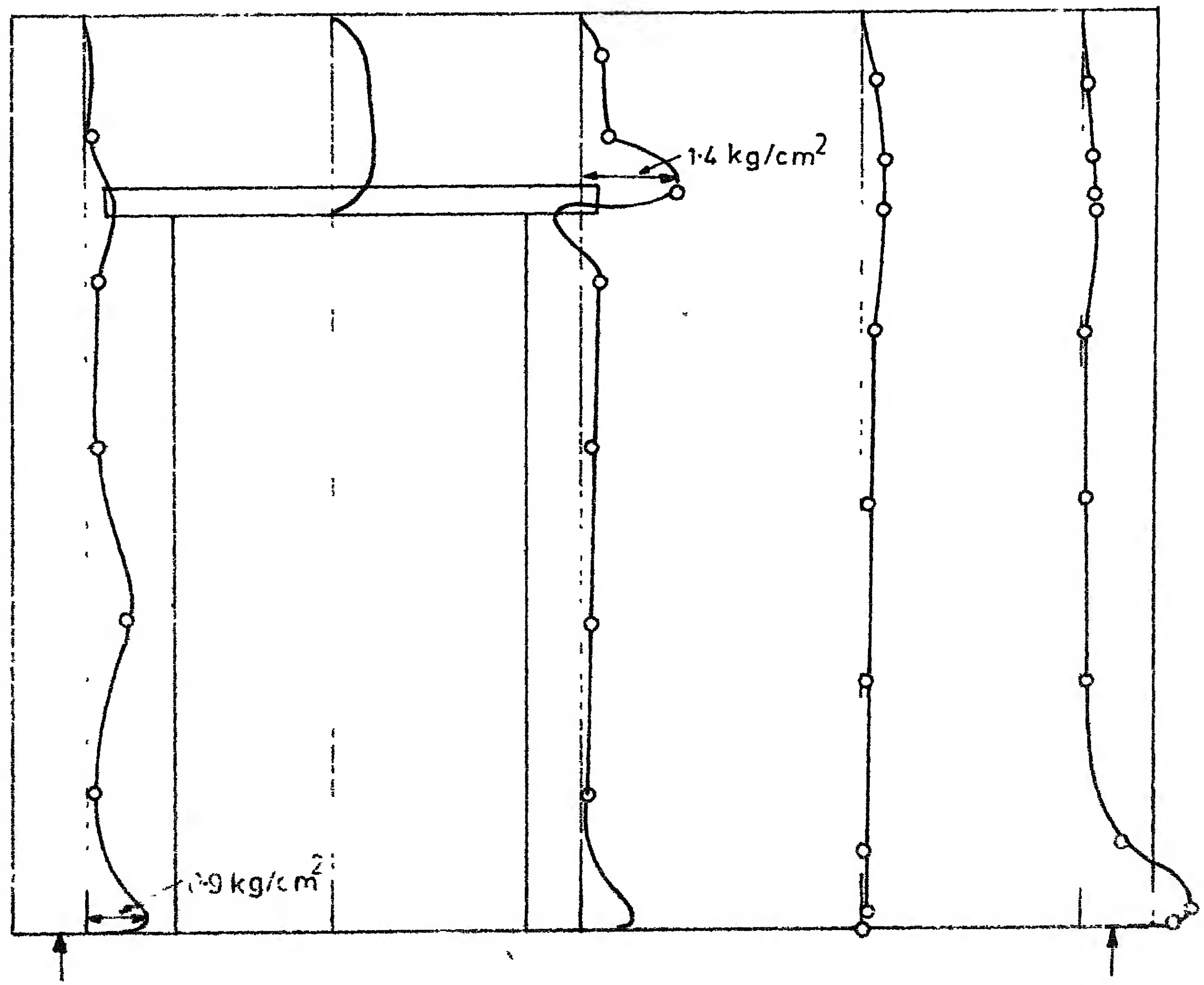

Fig.4.24 c Shear stress distribution at various cross section

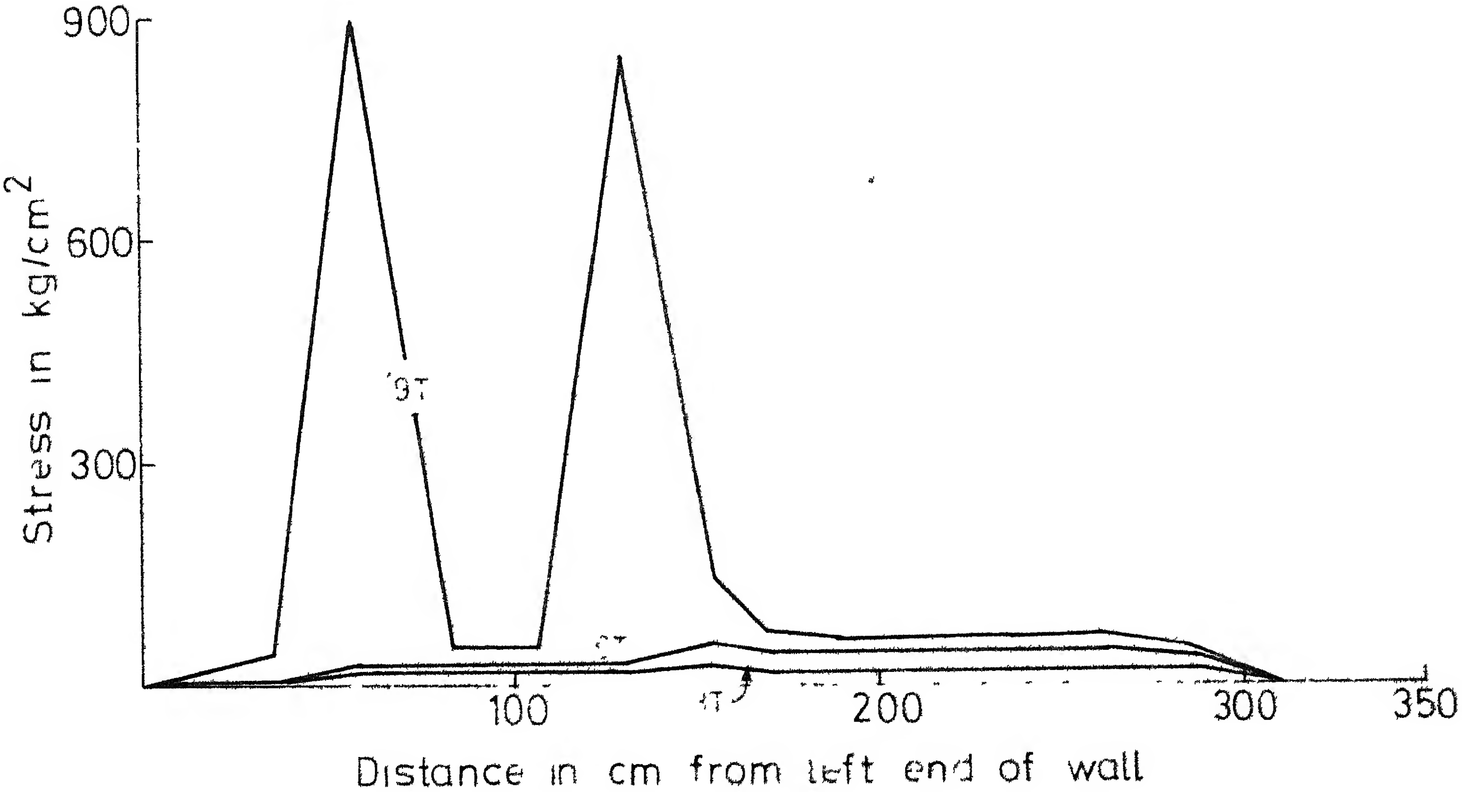

Fig.4·24 d Variation of stress in bottom reinforcement along span at various load

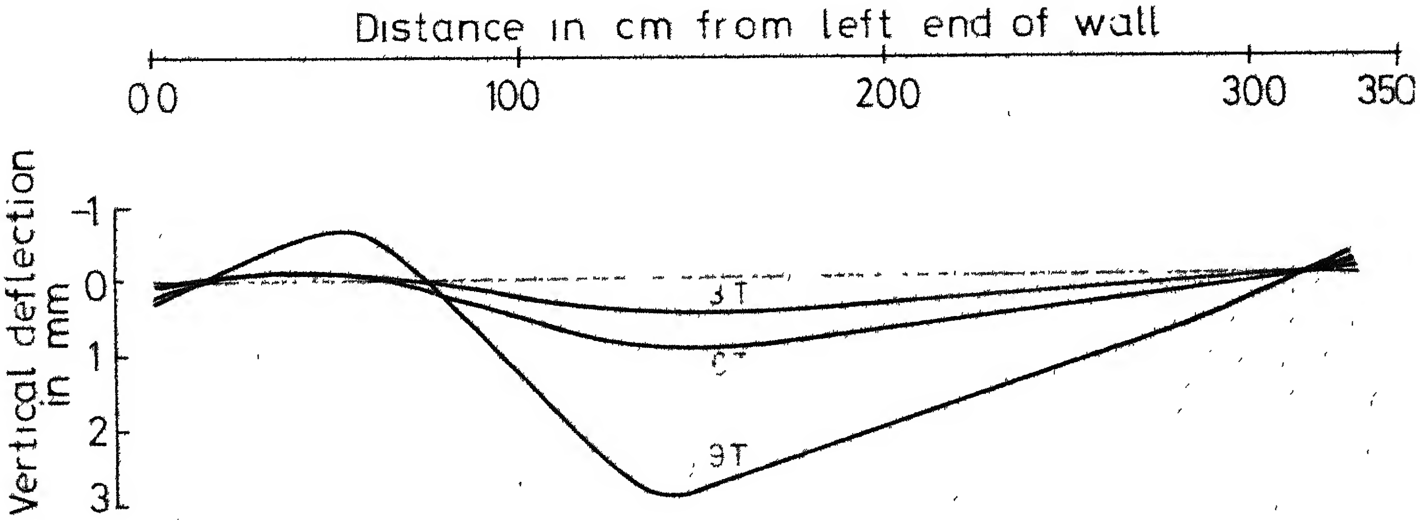

H/L	Mortar	Loading	Type of opening
0·8	1:6	Compressive	Unsymmetric door

Fig.4·24e Vertical deflection along span at various loads

H/L	Mortar	Initial load	Type of opening
0·8	1 6	3T	Unsymmetric door

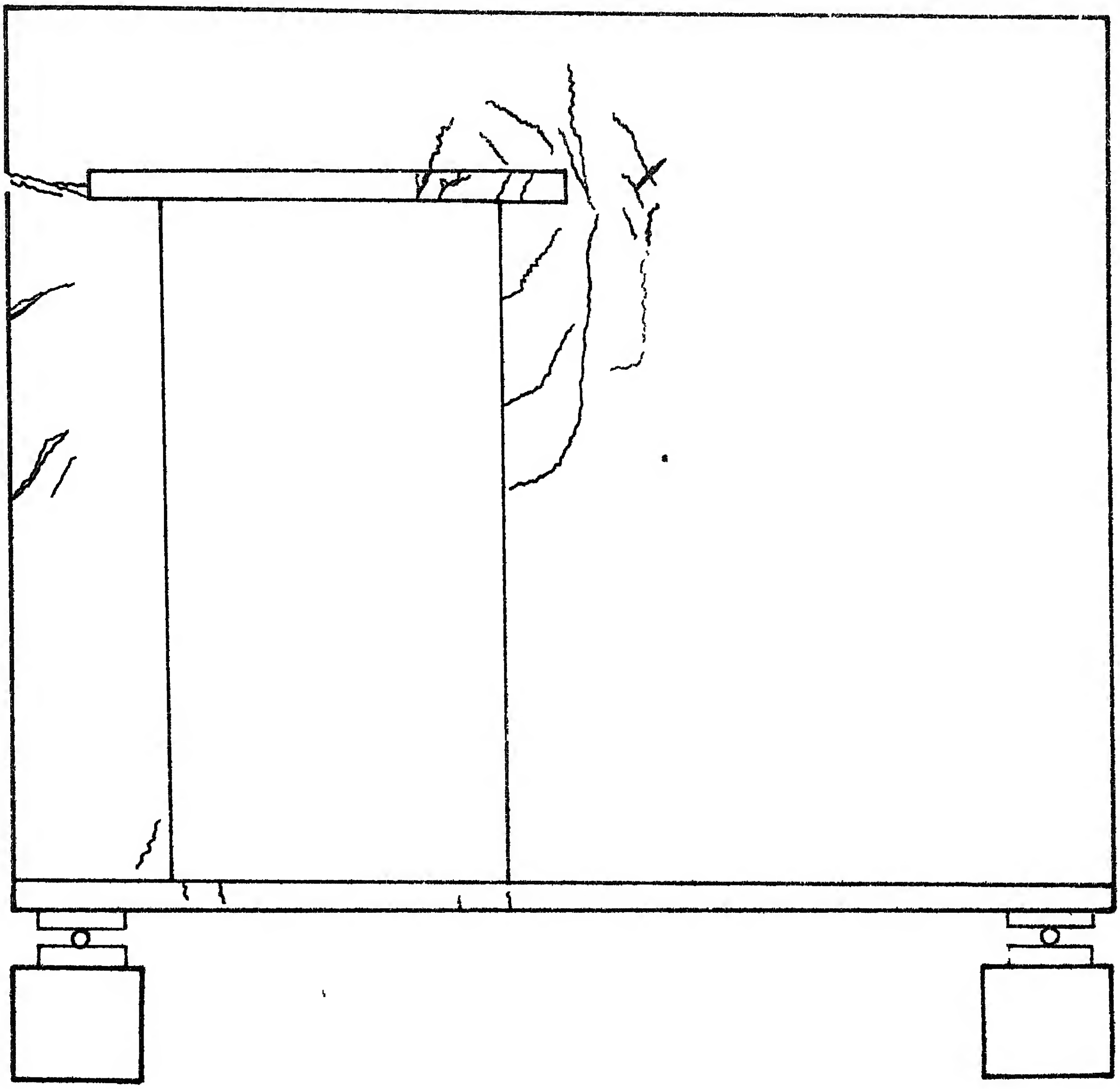

Fig.4·24 f Crack pattern at failure

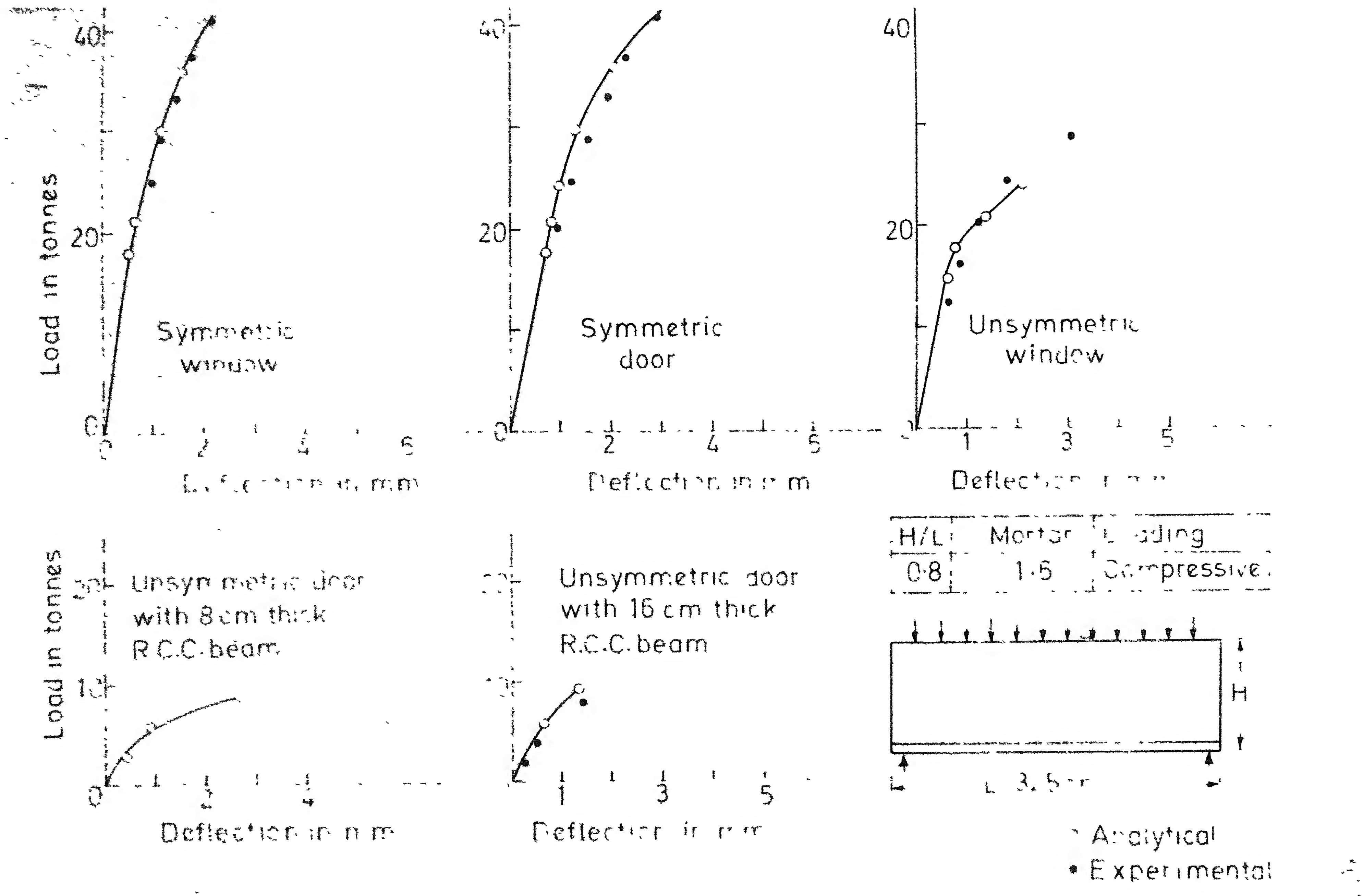

Fig.4.25 Load versus deflection curves

CHAPTER V

SUMMARY, CONCLUSIONS AND RECOMMENDATIONS

5.1 SUMMARY

Earlier investigators have established that brick masonry on reinforced concrete beams is not an overburden but behaves in a composite manner providing additional strength to the composite system through arching action. However benefit of such an interaction has been recommended only for composite construction of height to span ratio greater than 0.5 subject to compressive loading. This is probably because sufficient arching action does not come into play for height to span ratio below 0.5. Moreover, in this range the brickwork tries to slip over the reinforced concrete beam. Further more, it has been reported that such composite construction subject to tensile loading enjoys no benefit of composite action. It is obvious that under tensile loading, not only the advantage of arching action is absent but also the supporting reinforced concrete beam separates from the supported brickwork under tensile loading. The present effort demonstrates that such composite construction by use of single legged Z-shaped vertical connectors at equal spacing all along the length of the composite system behaves as a single composite structural element with much increased interaction under both compressive and tensile

loading. This has been established, in the present work, both by experimental studies and analytical verification.

The results from the present study lead to certain conclusions which are grouped in section 5.2. A design procedure is recommended for the design of such composite structural element in section 5.3. A set of recommendations to extend the scope of present study is presented in section 5.4. In any case the present work brings a consciousness that inorder to be able to make rational recommendations on the composite action of such elements extensive experimental and analytical work is warranted.

5.2 CONCLUSIONS

1. Single legged Z-shaped vertical connectors of plain reinforcing steel available in minimum size i.e. 6 mm diameter provided at a uniform spacing of one brick length make the brickwork and supporting R.C. beam to act as a single composite structural element.
2. Substantial interaction between the brickwork and the supporting R.C. beam in presence of single legged Z-shaped vertical connectors as described in (1) above exists. In other words, the composite structural element is much stronger and stiffer than the one without the vertical connectors. However,

the extent of this interaction depends upon various parameter e.g. the mortar strength, the height to span ratio and the type of loading.

3. Richer is the mortar mix used for the brickwork in the composite element,more is the interaction i.e. higher is the load carrying capacity and lower are the deflections.

4. Higher is the height to span ratio of the composite element more is the interaction i.e. higher is the load carrying capacity and lower are the deflections.

5. For composite element under compressive loading (load transferred at the top of brickwork) e.g. verandah beams, grade beams etc. use of 1:6 cement sand mortar mix gives a load factor of more than 2.0 and hence is recommended for height to span ratio of 0.33 or more. However, for height to span ratio below 0.33 use of richer mortar mix is recommended to achieve a load factor of 2.0 or above.

6. For composite element under tensile(load transferred directly to the supporting reinforced concrete) e.g. the multistorey framed buildings, use of 1:3 cement sand mortar mix is necessary irrespective of height to span ratio inorder to achieve a load factor of 2.0 or above.

7. Use of 6 mm diameter plain reinforcing steel vertical connectors is sufficient to achieve the desired interaction (load factor of 2.0 or above). Increasing the diameter of connectors does not help in increasing the load carrying capacity of the composite system under either compressive or tensile loading.

8. For composite element under compressive loading, the uniform spacing of the connectors at one brick length i.e. around 25 cms centre to centre is sufficient to achieve the desired interaction irrespective of mortar strength and height to span ratio.

9. For composite element under tensile loading, the uniform spacing of the connectors at one brick length is sufficient to achieve the desired interaction for height to span ratio of 0.33 or more. However, for height to span ratio below 0.33 which may not be frequently occurring in practice, closer spacing shall be necessary.

10. Normal size door and window openings considered in the present work symmetric about the vertical centre line of the composite element do not affect its load carrying capacity under compressive loading.

11. The load carrying capacity of a composite element having a symmetric door opening and subject to tensile loading is adverspely affected and use of thicker supporting reinforced concrete beam is necessary.

12. The load carrying capacity of a composite element having a symmetric window opening and subject to tensile loading is marginally affected. However, desired interaction is still available if the sill level is at a height equal to a third of span or more.

13. Unsymmetric window openings do affect the load carrying capacity of the composite element significantly under both types of loading. However, desired interaction is still available if the sill level is at a height equal to a third of the span or more for both types of loading. For purposes of design, the height upto the sill of window opening should only be considered for computing the height to span ratio of the composite system.

14. Unsymmetric door openings affect the load carrying capacity adversly. Experimental work shows that thicker supporting reinforced concrete beams are necessary if unsymmetric door openings are to be used in composite elements under compressive loading. The same obviously follows for the tensile loading.

15. The computer programme developed in the present work is suitable to predict the load response characteristics of composite element under compressive loading.

16. First crack load and the failure load analytically predicted by the use of finite element method for composite elements under compressive loading are conservative and hence can be safely used for design purposes.

5.3 DESIGN METHODOLOGY FOR COMPOSITE ELEMENT

Earlier investigators have recommended a suitable reduction factor in the design moments to design the supporting R.C. beam inorder to account for the benefit of interaction in the brickwork supported on R.C. beams. However, these recommendations vary markedly. The reason for these variations is the variation in mechanical properties of brickwork and the dimensions of supporting beam used by these investigators in their experimental work. In the present work, it has been shown that the thinnest possible supporting beam (thickness being just sufficient to provide suitable cover to bending reinforcement and hold the single legged Z-shaped connectors in position) interacting with the brick masonry over it in presence of vertical connectors behaves as a single composite structural element. Therefore, for the purposes of design

the composite system can be assumed as an under-reinforced R.B. (reinforced brickwork) beam provided the depth of brickwork is more than 20 percent of the span of the composite system. This limit gets fixed from the fact that a balanced R.B. section has a height to span ratio of approximately 0.2 for normal loading as considered in the present work. The depth of the composite system corresponds to the height of the composite element. In that event the parameters required to be fixed while designing are (1) bending reinforcement (2) spacing of 6 mm, dia single legged vertical connectors and (3) the mortar mix to be used for brickwork. The latter two are to be fixed from the conclusions summarised in the preceding section. The method for the determination of bending reinforcement follows the well known procedure of designing an under-reinforced section. However, the maximum value of the lever arm taken in the present work has been limited to 0.45 L where L is the span of the composite system.

5.4 PROPOSAL FOR FURTHER EXTENSION OF PRESENT WORK

Based on the knowledge gained during the present work, the following are the recommendations for further investigation.

1. Effect of the variation in the height of connectors should be studied experimentally as well as analytically for both type of loading conditions.

2. The bond slip between brick walls and supporting R.C. beams and between brick layers themselves has been noticed under tensile loading during the experimental work. Therefore, bond slip or linkage elements should be included in the finite-element model so as to predict correctly the response of composite system under tensile loading.

3. In the present work the load is either compressive or tensile. However, in real life e.g. for multi-storey framed construction, a combination of two types of independent loadings considered in the present work occur. Therefore, study should be undertaken by simultaneously applying in suitable combinations the load at the top of brickwork and at the level of R.C. beam at the first stage. Subsequently, even the self weight of the brickwork can be analytically modeled as a body force varying with height.

4. In real life situations composite elements shall not be simply supported. On the contrary it will be a composite infilled frame and should be studied as such. In the latter case the effect of unsymmetric door and window openings is not expected to be so adverse as observed in the present work.

5. Lateral loading to simulate the earthquake and wind load effects should be studied through experimental and analytical investigations on composite infilled frames.
6. The present and proposed studies should be repeated for other mortars e.g. lime surkhi mortar, lime sand cement mortar, pozzolana cement sand mortar etc. in varying thicknesses of brickwork.

REFERENCES

1. Pearson, Stang and Mc Burney, 'Shear Test on Reinforced Brick Masonry Beams', National Bureau of Standards, Research Paper No. 504, 1932.

2. Withey Mo, 'Tests on Brick Masonry Beams', ASTM Proceedings Vol.33, Part II, 1933.

3. Withey Mo, 'Test on Brick Masonry Columns', ASTM Proceedings Vol.34, Part II, 1938.

4. Thomos, F.G., 'The Strength of Brickwork', The Structural Engineer, Vol.33, No.2, Feb. 1953 .

5. Purshothaman, P., 'Experimental Investigation and Finite Element Simulation Studies on Behaviour of Walls on Beams Considering Material and Structural Nonhomogeneity', Ph.D. Thesis, Department of Civil Engineering, IIT Kanpur, May 1976.

6. SCPI, 'Recommended Practice for Engineered Brick Masonry', Structural Clay Products Institute, Mc Lean, Virginia, Nov. 1969 , pp. 246-254.

7. Wood, R.H., 'Studies in Composite Construction Part 1', National Building Studies, Research Paper No.13, HMSO, London , 1952 .

8. Rosenhaupt, S., 'Experimental Study of Masonry Walls on Beams', Journal of the Structural Division, ASCE, Vol.88, No. ST3 , June 1962 , pp.137-166.

9. Rosenhaupt, S., 'Stresses in Point Supported Composite Walls', Journal of American Concrete Institute, Vol.61 July 1964 , pp. 796-810.

10. Rosenhaupt, S., Beresford, F.D. and Blakey, R.A., 'Tests of a Post-Tensioned Concrete Masonry Wall', Journal of the American Concrete Institute, Vol.64 , Dec., 1967 , pp. 829-837.

11. Rosenhaupt, S., and Muller, G., 'Openings in Masonry Walls on Settling Supports', Journal of the Structural Division, ASCE, Vol.89, No. ST3, June 1963 , pp.107-132.

12. Rosenhaupt, S., and Sokal, Y., 'Masonry Walls on Continuous Beams', Journal of the Structural Division, ASCE, Vol.91, No. ST1, Feb. 1965 pp.,155-171.

13. Burhouse, P., 'Composite Action Between Brick Panel Walls and Their Supporting Beams', Proceedings of the Institution of Civil Engineers, London, Vol.43, June 1969, pp. 175-194.

14. Prasada Rao, N.V. and Mallick, S.K., 'Strength of Brick Masonry Walls, Supported on Reinforced Concrete Beams', Cement and Concrete, Vol.9 April-June, 1968, pp.14-27.

15. Ramesh, C.K., Dravid, P.S. and Anjaneyulu, E., 'A Study of Composite Action on Brick Panel Wall Supported on Reinforced Concrete', The Indian Concrete Journal, Vol.44, No. 10, Oct. 1970, pp. 442-448.

16. Smith B.Stafford, 'Contribution Towards the Design of Heavily Loaded masonry Walls on Reinforced Concrete Beams', Proceedings of North Amercian Masonry Conference University of Colo, Boulder, Aug. (14-16), 1978, Paper 85-14 pages.

17. K. Chandra Shekara, and K. Abraham Jacob, 'Photoelastic Analysis of Composite Action of Walls Supported on Beams', Building Environment, Vol.11, No.2, 1976, pp. 139-144.

18. Scordelis, A.C., 'Finite Element Analysis of Reinforced Concrete Structures', Proceedings of the Speciality Conference on Finite Element Method in Civil Engineering, McGill University, Montreal, Canada, June 1972, pp.71-113.

19. Ngo, D. and Scordelis, A.C., 'Finite Element Analysis of Reinforced Concrete Beams', Journal of American Concrete Institute, Vol.64, No.3, March 1967, pp.152-163.

20. Ngo, D., Scordelis, A.C. and Franklin, H.A., 'Finite Element Study of Reinforced Concrete Beams with Diagonal Tension Cracks',UC SESM Report No. 70-19, University of California, Berkeley, December 1970.

21. Nilson, A.H., 'Nonlinear Analysis of Reinforced Concrete by Finite Element Method', Journal of American Concrete Institute, Vol.65, No.9, September 1968, pp.757-766.

22. Rashid Y.R., 'Analysis of Prestressed Concrete Pressure Vessels', Nuclear Engineering and Design, Vol.7, No.4, April 1968, pp.334-344.

23. Franklin, H.A., 'Nonlinear Analysis of Reinforced Concrete Frames and Panels', Ph.D. Thesis, University of California, Berkeley, California, March 1970.

24. Zienkiewicz, O.C., Valliappan, S. and King, I.P., 'Stress Analysis of Rock as a 'No Tension Material', Geotechnique, Vol.18, March 1968, pp.56-66.

25. Valliappan, S. and Nath,P., 'Tensile Crack Propagation in Reinforced Concrete Beams-Finite Element Technique', International Conference on Shear, Torsion, and Bond in Reinforced and Prestressed Concrete, Coimbatore India, January 1969.

26. Zienkiewicz, O.C., Valliappan, S.and King,I.P.,'Elastic Plastic Solutions of Engineering Problems'Initial Stress'Finite Element Approach', International Journal for Numerical Methods in Engineering Vol.1, January 1969,pp.75-100.

27. Valliappan, S. and Doolan, T.F., 'Nonlinear Stress Analysis of Reinforced Concrete', Journal of the Structural Division, ASCE, Vol.98, No.ST4, April 1972, pp.885-898.

28. Mufti, A.A., Mirza, M.S., Mc Cutcheon, J.O. and Spokiwiski,R., 'A Study of Nonlinear Behaviour of Structural Concrete Elements', Proceedings of Speciality Conference on Finite Element Method in Civil Engineering, McGill University, Canada, June 1972, pp.762-802.

29. Suidan, M. and Schnobrich, W.C., 'Finite Element Analysis of Reinforced Concrete', Journal of Structural Division, ASCE, Vol.99, No.ST10, October 1973, pp.2109-2122.

30. Colville, J. and Abbasi, J., 'Plane Stress Reinforced Concrete Finite Elements', Journal of Structural Division, ASCE, Vol.100, No.ST5, May 1974, pp.1067-1083.

31. Houde, J., 'Study of Force Displacement Relations for the Finite Element Analysis of Reinforced Concrete', Ph.D. Thesis, McGill University, Montreal, Canada, December, 1973.

32. Mirza, M.S. and Mufti, A.A., 'Nonlinear Finite Element Analysis of Reinforced Concrete Structures', Proceedings of the International Conference on Finite Element Methods in Engineering, University of New South Wales, Kensington, Australia, August 1974, pp.403-417.

33. Nam, Chung-Hyum and Salmon, C.G., 'Finite Element Analysis of Concrete Beams', Journal of Structural Division, ASCE, Vol.100, No. ST12, December 1974, pp.2419-2432.

34. Majid, K.I. and Hashimi, K.A., 'Failure of Brittle Materials due to Crack Propagation', The Structural Engineer, Volume 54, Number 5, May 1976, pp.175-182.

35. Cedolin, L. and Dei Poli, S., 'Finite Element Studies of Shear Critical R.C.Beams', Journal of Engineering Mechanics Division, ASCE, Vol.103, No. EM3, June 1977, pp. 395-410.

36. Cedolin, L., Dei Poli, S. and Kapur, B.S., 'Finite Element Analysis of Reinforced Concrete Deep Beams', Estratto da Costruzioni in Cemento Armato, Studie Rendiconti, Volume 14, 1977.

37. Cedolin, L., Dei Poli, S.and Malerba, P.G., 'Finite Element Analysis of Prestressed Concrete Beams', Estratto da -- Costruzioni in Cemento Armato, Studie Rendiconti, Vol.14, 19

38. Paneerselvam, A., 'Nonlinear Finite Element Analysis of Reinforced Concrete Framed Structures', Ph.D. Thesis, Department of Civil Engineering, IIT Madras, India, 1977.

39. Agarwal, A.B., 'Nonlinear Analysis of Reinforced Concrete Planar Structures Subject to Monotonic, Reversed Cyclic and Dynamic Loads', Ph.D. Thesis, Department of Mechanica Engineering, University of New Brunswick, March 1977.

40. Darwin, D. and Pecknold, D.A., 'Nonlinear Biaxial Stress-Strain Law for Concrete', Journal of the Engineering Mechanics Division, ASCE, Vol.103, No. EM2, April 1977, pp. 229-241.

41. Jain, A.K. , 'Nonlinear Finite Element Analysis of R.C. Beams and Supporting Brick Panels', M.Tech. Thesis, Department of Civil Engineering, IIT Kanpur, March 1979.

42. Grimm, C.T., 'Strength and Related Properties of Brick Masonry', Journal of Structural Division, ASCE, Vol.101, No.ST1, January, 1975, pp.217-232.

43. Calcote, L.R., 'The Analysis of Laminated Composite Structures', Van Nostrand Reinhold Company, New York.

44. Lin, Chang-Shung and Scordelis, A.C., 'Nonlinear Analysis of R.C. Shells of General Form', Journal of the Structural Division, ASCE, No. ST3, March 1975, pp.523-538.

45. Popovics, S., 'A Review of Stress-Strain Relationships for Concrete', Journal of American Concrete Institute, Vol.67, No.3, March 1970, pp.243-248.

46. Kupfer, H., Hilsdorf, H.K. and Rusch, H., 'Behaviour of Concrete Under Biaxial Stresses', Journal of American Concrete Institute, Vol.66, No.8, August 1969 ,pp.656-666.

47. Liu, T.C.Y., Nilson, A.H., and Slate, F.O., 'Stress-strain Response and Fracture of Concrete in Uniaxial and Biaxial Compression', Journal of American Concrete Institute, Vol.69, No.5, May 1972, pp. 291-295.

48. Kupfer, H.B., and Gerstle, K.H., 'Behaviour of Concrete Under Biaxial Stresses', Journal of the Engineering Mechanics Division, ASCE, Vo.99, No.EM4, August 1973, pp.853-866.

49. Romstad, K.M., Taylor, M.A., and Herrmann, L.R., 'Numerical Biaxial Characterization for Concrete', Journal of the Engineering Mechanics Division, ASCE, Vol.100, No.EM5, October 1974, pp.935-948.

50. Rusch, H., 'Researches Towards a General Flexural Theory for Structural Concrete', Journal of American Concrete Institute, Vol.57, No.1, July 1960, pp.1-28.

51. Cook, R.D., 'Concepts and Applications of Finite Element Analysis', John Wiley and Sons, Inc., New York.

52. Wanchoo, M.K. and May, G.W., 'Cracking Analysis of Reinforced Concrete Plates', Journal of Structural Division, ASCE, Vol.101, No. ST1, January 1975, pp. 201-215.

53. Hand, F.R., Pecknold, D.A., and Schnobrich, W.C., 'A Layered Finite Element Nonlinear Analysis of Reinforced Concrete Plates and Shells', Structural Research Series No. 389, Civil Engineering Studies, University of Illinois, Urbana, Illinois, August 1972.

54. Wilson, E.L., Taylor, R.L., Doherty, W.P. and Ghaboussi, J., 'Incomplete Displacement Models', Numerical and Computer Methods in Structural Mechanics, Edited by Fenves, S.J., Robinson, A.R., Perrone, N. and Schnobrich, W.C., Academic Press, New York and London, 1973, pp.43-51.

55. Zienkiewicz, O.C., 'The Finite Element Method in Engineering Science', McGraw-Hill Publishing Company Limited, London, 1971.

56. Desai, C.S. and Abel, J.F., 'Introduction to the Finite Element Method-A Numerical Method for Engineering Analysis', Affiliated East-West Press Pvt. Ltd., New Delhi, 1977.

57. Rubinstein, M.F., 'Matrix Computer Analysis of Structures', Prentice-Hall, Inc., Canada, 1966.

58. Felippa, C.A., 'Refined Finite Element Analysis of Linear and Nonlinear Two-Dimensional Structures', Ph.D. Thesis, Civil Engineering, University of California, Berkeley, 1966.

APPENDIX

```
C     ****************************************************************
C            MAIN PROGRAME  FEACTS
C     ****************************************************************
      COMMON/AREA1/NNP,NEL,NOLD,NONBC,NMAT,NBODY,NSLC
      COMMON/AREA3/KODEL,LOC
      COMMON/AREA4/INOD,JNOD,KNOD,SURTRX,SURTRY,NODLOD,XLDIN,YLDIN,
     1MXINCR,MXITER
      COMMON/AREA8/NDF,IBAND,INCR,ITER
      COMMON/AREA9/Q,DQ,DP
      INTEGER KODEL(240),LOC(240,6),INOD(6),JNOD(6),KNOD(6),NODLOD(12)
     1,TITLE(10)
      REAL SURTRX(6,2),SURTRY(6,2), XLDIN(12,12),YLDIN(12,12),Q(800),
     1DQ(800), DP(800)
C     READ DATA FOR THE PROBLEM
      CALL DATAIN
C     COMPUTE MAXM NODAL DIFFERENCE FOR ELEMENTS AND SEMI BAND WIDTH
C     OF GLOBAL STIFFNESS MATRIX
      NDF=2*NNP
      MAXDIF=0
      DO20I=1,NEL
      IF (KODEL(I).EQ.3)GO TO 25
      DO 21 J=1,6
      DO 21 K=1,6
      IDIF=IABS(LOC(I,J)-LOC(I,K))
      IF(IDIF.GT.MAXDIF) MAXDIF=IDIF
21    CONTINUE
      GO TO 20
25    DO22J=1,3
      DO22K=1,3
      IDIF=IABS(LOC(I,J)-LOC(I,K))
      IF (IDIF.GT.MAXDIF)MAXDIF=IDIF
22    CONTINUE
20    CONTINUE
      IBAND=2*(MAXDIF+1)
      PRINT30,IBAND
30    FORMAT(/5X,'SEMI-BAND WIDTH OF GLOBAL STIFFNESS MATRIX=',I4)
      INCR=1
70    ITER=1
80    CALL AGSMAT
      CALL DSOLVE
      DO35I=1,NDF
      Q(I)=Q(I)+DQ(I)
35    CONTINUE
      DO40I=1,NDF
40    DP(I)=0.0
      CALL INSTMD(IFAIL,ICONVG)
      IF(IFAIL.EQ.1)GO TO 95
      IF(ICONVG.EQ.1) GO TO 85
      IF(ITER.GE.MXITER)GO TO 90
      ITER=ITER+1
      GO TO 80
85    IF(INCR.GE.MXINCR)GO TO 75
      INCR=INCR+1
      GO TO 70
75    PRINT76
76    FORMAT(//5X,'STRUCTURE HAS NOT FAILED WITHIN MAXIMUM INCREAMENTS
     1OF LOADS SPECIFIED'/5X,71(1H-))
      GO TO 100
90    PRINT91,INCR,ITER
91    FORMAT(//1X,'SOLUTION FOR THE LOAD INCREAMENT NO.',I3,'HAS NOT CON
     1VERGED WITHIN MAXIMUM NO. OF ITERATIONS(=',I3,' )ALLOWED FOR ANY
     2INCREAMENT OF LOAD'/1X,130(1H-)/3X,'THEREFORE STRUCTURE WILL BE
     3ASSUMEDTO HAVE FAILED'/3X,50(1H-)/)
      GO TO 100
95    PRINT96
96    FORMAT(/5X,'STRUCTURE HASFAILED DUE TO CRUSHING OF CONCRETE OR BR
     1ICK WORK '/5X,63(1H-)/)
100   PRINT101,INCR,ITER
101   FORMAT(/2X,'FINAL SOLUTION OF THE PROBLEM'/2X,30(1H-)/5X,'NO. OF L
     1OAD INCREAMENTSUSED TO REACH FINAL SOLUTION=',I3/5X,'NO. OF ITERAT
     2ION PERFORMED INLAST INCREAMENT OF LOAD='I3//2X,'TOTAL LOADS TO RE
     4ACH FINALSOLUTION'/2X,35(1H-))
      IF(NOLD.EQ.0)GO TO 105
      PRINT 102
102   FORMAT(/5X,'NODE NO.'3X,'TOTAL LOAD IN X-DIRECTION',3X,'TOTAL LOAD
     2IN Y-DIRECTION')
      DO103I=1,NOLD
      SUMX=0
      SUMY=0
      DO104J=1,INCR
      SUMX=SUMX+XLDIN(I,J)
      SUMY=SUMY+YLDIN(I,J)
104   CONTINUE
      PRINT106,NODLOD(I),SUMX,SUMY
106   FORMAT(/7X,I4,10X,E15.8,13X,E15.8)
103   CONTINUE
105   IF(NSLC.EQ.0)GO TO 115
      PRINT 107
107   FORMAT(/5X,'I-NODE',2X,'J-NODE',2X,4(3X,'TOTAL SURFACE TRACTION'
```

```
      1///2X,'IN X-DIRECTION ATNODEI',2X,'IN Y-DIRECTION AT NODE I'
      2,2X,'IN X-DIRECTION ATNODE J',2X,'IN Y-DIRECTION ATNODE J')
       DO112I=1,NSLC
       SUMX=0.0
       SUMY=0.0
       SUMXX=0.0
       SUMYY=0.0
       DO110J=1,INCR
       SUMX=SUMX+SURTRX(I,1)
       SUMY=SUMY+SURTRY(I,1)
       SUMXX=SUMXX+SURTRX(I,2)
       SUMYY=SUMYY+SURTRY(I,2)
110    CONTINUE
       PRINT108, INOD(I),KNOD(I),SUMX,SUMY,SUMXX,SUMYY
108    FORMAT(/6X,I4,3X,I4,8X,E15.8,10X,E15.8,10X,E15.8,10X,E15.8)
112    CONTINUE
115    IF((ICONVG.EQ.1).AND.(INCR.EQ.MXINCR)) GO TO 120
       PRINT116
116    FORMAT(//2X,'DISPLACEMENTS, STRAINS AND STRESSES AT FAILURE'/2X,
      145(1H-)/)
       CALL PRINTR
120    STOP
       END
C      *****************************************************************
C      *                 SUBROUTINE                 DATAIN             *
C      *****************************************************************
       SUBROUTINE DATAIN
       COMMON/AREA1/NNP,NEL,NOLD,NONBC,NMAT,NBODY,NSLC
       COMMON/AREA2/E,ANU,WTPUV
       COMMON/AREA3/KODEL,LOC
       COMMON/AREA4/INOD,JNOD,KNOD,SURTRX,SURTRY,NODLOD,XLDIN,YLDIN,
      1MXINCR,MXITER
       COMMON/AREA5/CX,CY
       COMMON/AREA6/YIELDS,YXBL,STENB1,YYBT,STENB2,YSHR,STENSN,ECU,FCP,
      1YSTC,DSTRN
       COMMON/AREA7/L1C,L2C,L3C,LBC
       COMMON/AREA12/ISUBRC,NSR,NSRB
       COMMON/AREA16/TH,ERPSUD,ERDISP
       COMMON/AREA18/MATCOD,NCODE
       INTEGER KODEL(240),LOC(240,6),MATCOD(3),INOD(6),JNOD(6),KNOD(6),
      1NODLOD(12),NCODE(400),ISUBRC(240,4)
       REAL E(3,2),ANU(3,2),WTPUV(3),SURTRX(6,2),SURTRY(6,2),XLDIN(12,12)
      1,YLDIN(12,12),CX(400),CY(400),DSTRN(3,1),TH(240),L1C(4),L2C(4),L3C
      2(4),LBC(4)
       READ10,ICODE, MORTAR, HLRATO
10     FORMAT(2I2,F6.3 )
       IF(ICODE.EQ.0)GO TO 110
       PRINT 20
20     FORMAT(//5X,'WALL LOADED AT TOP OF BRICK WORK'/5X,71(1H-))
       GO TO 40
110    PRINT 30
30     FORMAT(//5X,'WALL LOADED AT TOP OF THIN CONCRETE BEAM'/5X,71(1H-))
40     PRINT 120, MORTAR, HLRATO
120    FORMAT(/2X,'BRICK WALL IN 1:',I2,'CEMENT SAND MORTAR'/2X,
      1'HEIGHT TO SPAN RATIO=',F6.3)
       READ200,NSR,NSRB
       READ212,(L1C(I),L2C(I),L3C(I),I=1,NSR)
212    FORMAT(3F10.0)
       READ213,(LBC(I),I=1,NSRB)
213    FORMAT(F10.0)
       ERDISP=0.5E-6
       ERPSUD=1.0
       READ200,NNP,NEL,NOLD,NONBC,NMAT,NBODY,NSLC
200    FORMAT(16I5)
       PRINT205,NNP,NEL,NOLD,NONBC,NMAT,NBODY,NSLC
205    FORMAT(/5X,'TOTAL NO. OF NODES=',I5/5X,'TOTAL NO. OF ELEMENTS=',
      1I5/5X,'NO. OF NODES WHERE CONC. LOADS ARE PRESCRIBED=',I5/5X,'NO.
      2OF NODES WHERE DISPLACEMENTS AREPRESCRIBED=',I5/5X,'NO.OF DIFFEREN
      3T MATERIALS=',I5/5X,'BODY FORCE CODE(1=BODY FORCE IN Y-DIRECTION,
      40=NO BODY FORCE)=',I2/5X,'NO.OF SURFACE LOADING CARDS=',I4)
       READ200,MXINCR,MXITER
       READ200,(MATCOD(I),I=1,NMAT)

       PRINT210,(I,MATCOD(I),I=1,NMAT)
210    FORMAT(/5X,'CODE OF MATERIAL NO.',I2,'=',I2)
       PRINT211
211    FORMAT(/5X,'IFMATERIAL CODE IS=1,MATERIAL IS BRICK WORK'/24X,
      1'=2, MATERIAL IS CONCRETE'/24X,'=3,MATERIAL IS STEEL BAR')
       PRINT218
218    FORMAT(/2X,'MATERIALNO.',4X,'MASS DENSITY',4X,'MODULUS OF ELASTIC
      1ITYE1',2X,'POISSONS RATIOV1',2X,'MODULUS OF ELASTICITY E2',2X,
      2'POISSON,S RATIO V2')
       DO215I=1,NMAT
       IK=MATCOD(I)
       IF(IK.EQ.1)GO TO 216
       READ217,E(IK,1),ANU(IK,1),WTPUV(IK)
217    FORMAT(8F10.0)
       PRINT219,I,WTPUV(IK),E(IK,1),ANU(IK,1)
       GO TO 215
```

```
 216      READ217,E(IK,1),E(IK,2),ANU(IK,1),ANU(IK,2),WTPUV(IK)
          PRINT219,I,WTPUV(IK),E(IK,1),ANU(IK,1),E(IK,2),ANU(IK,2)
 219      FORMAT(/6X,I2,8X,E15.8,7X,E15.8,8X,E15.8,8X,E15.8,8X,E15.8)
 215      CONTINUE
          READ220,(NCODE(I),CX(I),CY(I),I=1,NNP)
 220      FORMAT(I5,2F10.0)
          PRINT221,(I,NCODE(I),CX(I),CY(I),I=1,NNP)
 221      FORMAT(/2(2X,'NODE NUMBER',2X,'CODE OF NODE',3X,'X-COORDINATE',8X,
         1'Y-COORDINATE')//(5X,I4,11X,I1,7X,E15.8,6X,E15.8,5X,I4,11X,I1,7X,
         2E15.8,4X,E15.8))
          READ222,(KODEL(I),(LOC(I,J),J=1,6),TH(I),I=1,NEL)
 222      FORMAT(7I5,F10.0)
          PRINT225,(I,KODEL(I),(LOC(I,J),J=1,6),TH(I),I=1,NEL)
 225      FORMAT(/2X,'GLOBAL NODE NO. OF ELEMENTS NODES'/5X,'ELEMENT NO.',2X
         1,'MATERIAL CODE',5X,'1',5X,'2',5X,'3',5X,'4',5X,'5',5X,'6',5X,
         2'THICKNESS OR AREA'/(6X,I4,12X,I2,10X,I3,3X,I3,3X,I3,3X,I3,3X,I3,
         33X,I3,8X,F8.3))
          IF(NSLC.EQ.0)GO TO 250
          READ235,(INOD(I),JNOD(I),KNOD(I),SURTRX(I,1),SURTRX(I,2),
         1SURTRY(I,1),SURTRY(I,2),I=1,NSLC)
 235      FORMAT(3I5,4F10.0)
          PRINT240,(INOD(I),JNOD(I),KNOD(I),SURTRX(I,1),SURTRX(I,2),
         1SURTRY(I,1),SURTRY(I,2),I=1,NSLC)
 240      FORMAT(/2X,'SURFACELOADING DATA'/5X,'I-NODE',2X,'J-NODE',2X,'K-NO
         1DE',10X,'SURTRX(I)',10X,'SURTRX(J)',10X,'SURTRY(I)',10X,'SURTRY(J)
         2'//(6X,I4,4X,I4,4X,I4,8X,E15.8,4X,E15.8,4X,E15.8,4X,E15.8))
 250      IF(NOLD.EQ.0)GO TO254
          PRINT246
 246      FORMAT(/2X,'NODE NO.',2X,'INCREAMENT NO.',3X,'LOAD IN X-DIRECTION'
         1,3X,'LOAD IN Y-DIRECTION')
          DO247I=1,NOLD
          READ245,NODLOD(I),(XLDIN(I,J),YLDIN(I,J),J=1,MXINCR)
 245      FORMAT(I5,(2F10.0))
          PRINT248,NODLOD(I),(J,XLDIN(I,J),YLDIN(I,J),J=1,MXINCR)
 248      FORMAT(/4X,I4,10X,I2,10X,E15.8,7X,E15.8,(/18X,I2,10X,E15.8,7X,
         1E15.8))
 247      CONTINUE
 254      DO255I=1,NMAT
          IF(MATCOD(I).EQ.1)GOTO260
          IF(MATCOD(I).EQ.2)GOTO270
          READ217,YIELDS
          PRINT280,YIELDS
 280      FORMAT(/5X,'YIELD STRESS IN STEEL=',E15.8)
          GOTO255
 260      READ217,YXBL, STENB1,YYBT,STENB2,YSHR,DTENSB
          PRINT265,YXBL,STENB1,YYBT,STENB2,YSHR
 265      FORMAT(/5X,'BRICK WORK PROPERTIES'/5X,21(1H-)//5X,'YIELD STRESS IN
         1X-DIRECTION=',E15.8,5X,'TENSILE STRENGTH IN X-DIRECTION',E15.8/5X,
         2'YIELD STRESS IN Y-DIRECTION=',E15.8,5X,'TENSILE STRENGTH IN Y-DIR
         3ECTION=',E15.8/5X,'YIELD STRESS IN SHEAR=',E15.8)
          GO TO 255
 270      READ217, FCP,STENSN,YSTC,ECU,DTENSC
          PRINT275,FCP,STENSN,YSTC,ECU
 275      FORMAT(/5X,'CONCRETE PROPERTIES'/5X,19(1H-)//5X,'YIELD STRESS=',
         1E15.8,5X,'TENSILE STRENGTH=',E15.8/5X,'YIELD STRAIN=',E15.8,5X,
         2'CRUSHING STRAIN=',E15.8)
 255      CONTINUE
          RETURN
          END
C         ****************************************************************
C         *              SUBROUTINE          AGSMAT                      *
C         ****************************************************************
          SUBROUTINE AGSMAT
          COMMON/AREA1/NNP,NEL,NOLD,NONBC,NMAT,NBODY,NSLC
          COMMON/AREA3/KODEL,LOC
          COMMON/AREA4/INOD,JNOD,KNOD,SURTRX,SURTRY,NODLOD,XLDIN,YLDIN,
         1MXINCR,MXITER
          COMMON/AREA5/CX,CY
          COMMON/AREA8/NDF,IBAND,INCR,ITER
          COMMON/AREA9/Q,DQ,DP
          COMMON/AREA11/KA,KG
          COMMON/AREA12/ISUBRC,NSR,NSRB
          COMMON/AREA13/LAMDA,B,AREA,BT
          COMMON/AREA14/AL,TM,TMT,N
          INTEGER KODEL(240),LOC(240,6),INOD(6),JNOD(6),KNOD(6),NODLOD(12)
         1,ISUBRC(240,4),N(12)
          REAL SURTRX(6,2),SURTRY(6,2), XLDIN(12,12),YLDIN(12,12),CX(400),
         1CY(400),Q(800),DQ(800),DP(800),KA(800,56),LAMDA(12,12),B(9,12),
         2BT(12,12),TM(3,6),TMT(6,3),KG(12,12)
          ITAPE1=21
          REWIND ITAPE1
          IF((INCR.EQ.1).AND.(ITER.EQ.1))GO TO 302
          GO TO 395
 302      CALL CIMAT
          DO301I=1,NEL
          DO301J=1,NSR
 301      ISUBRC(I,J)=0
          DO300I=1,NDF
          Q(I)=0.0
```

```
      DP(I)=0.0
      DO300J=1,IBAND
      KA(I,J)=0.0
300   CONTINUE
C     TRANSFORMATION MATRIX FOR NODAL-STRAIN-DISPLACEMENT MATRIX IN THE
C     CASE OF LINEAR-STRAIN-TRIANGLE
      DO305I=1,12
      DO305J=1,12
305   LAMDA(I,J)=0.0
      DO310I=1,6
      LAMDA(I,2*I-1)=1.0
      LAMDA(I+6,2*I)=1.0
310   CONTINUE
      DO315I=1,NEL
      L1=LOC(I,1)
      L2=LOC(I,2)
      L3=LOC(I,3)
      L4=LOC(I,4)
      L5=LOC(I,5)
      L6=LOC(I,6)
      IF(KODEL(I).EQ.3)GOTO316
      CALL ESMAT1(I,L1,L2,L3)
      WRITE(ITAPE1,*)((B(J,K),J=1,9),K=1,12),AREA
      GO TO 320
316   CALL ESMAT2(I,L1,L2,L3)
      WRITE(ITAPE1,*)AL,((TM(J,K),J=1,3),K=1,6)
C     ASSEMBLY OF GLOBAL STIFFNESS MATRIX
320   N(1)=L1*2-1
      N(2)=L1*2
      N(3)=L2*2-1
      N(4)=L2*2
      N(5)=L3*2-1
      N(6)=L3*2
      IF(KODEL(I).EQ.3)GO TO318
      N(7)=L4*2-1
      N(8)=L4*2
      N(9)=L5*2-1
      N(10)=L5*2
      N(11)=L6*2-1
      N(12)=L6*2
      IEMZ=12
      GOTO326
318   IEMZ=6
326   DO325J=1,IEMZ
      JJ=N(J)
      DO325K=1,IEMZ
      KK=N(K)-JJ+1
      IF(KK.LE.0)GOTO325
      IF(ABS(KG(J,K)).LT.1.0)KG(J,K)=0.0
      KA(JJ,KK)=KA(JJ,KK)+KG(J,K)
325   CONTINUE
315   CONTINUE
395   IF(ITER.NE.1)GO TO 390
C     ASSEMBLY OF LOAD VECTOR IN GLOBAL COORDINATE SYSTEM
C     ADD INCREAMENTS OF EXTERNALLY APPLIED CONCENTRATED LOADS TO DP
399   IF(NOLD.EQ.0)GOTO331
      DO330I=1,NOLD
      K=NODLOD(I)
      DP(2*K-1)=XLDIN(I,INCR)+DP(2*K-1)
      DP(2*K)=YLDIN(I,INCR)+DP(2*K)
330   CONTINUE
C     CONVERT LINEARLY VARYING SURFAC TRACTION TO STATIC EQUIVALENTS
C     AND ADD TO OVER ALL LOAD VECTOR DP
331   IF(NSLC.EQ.0)GOTO390
      DO 335L=1,NSLC
      I=INOD(L)
      J=JNOD(L)
      K=KNOD(L)
      II=2*I
      JJ=2*J
      KK=2*K
      DX=CX(K)-CX(I)
      DY=CY(K)-CY(I)
      AL=SQRT(DX**2+DY**2)
      PXI=SURTRX(L,1)*AL
      PXK=SURTRX(L,2)*AL
      PYI=SURTRY(L,1)*AL
      PYK=SURTRY(L,2)*AL
      DP(II-1)=DP(II-1)+PXI/6.0
      DP(JJ-1)=DP(JJ-1)+(PXI+PXK)/3.0
      DP(KK-1)=DP(KK-1)+PXK/6.0
      DP(II)=DP(II)+PYI/6.0
      DP(JJ)=DP(JJ)+(PYI+PYK)/3.0
      DP(KK)=DP(KK)+PYK/6.0
335   CONTINUE
390   CALL GEOMBC
      RETURN
      END
C     ********************************************************************
```

```
C     ******************************************************************
      SUBROUTINE INSTMD(IFAIL,ICONVG)
      COMMON/AREA1/NNP,NEL,NOLD,NONBC,NMAT,NBODY,NSLC
      COMMON/AREA2/E,ANU,WTPUV
      COMMON/AREA3/KODEL,LOC
      COMMON/AREA6/YIELDS,YXBL,STENB1,YYBT,STENB2,YSHR,STENSN,ECU,FCP,
     1YSTC,DSTRN
      COMMON/AREA7/L1C,L2C,L3C,LBC
      COMMON/AREA8/NDF,IBAND,INCR,ITER
      COMMON/AREA9/Q,DQ,DP
      COMMON/AREA12/ISUBRC,NSR,NSRB
      COMMON/AREA13/LAMDA,B,AREA,BT
      COMMON/AREA14/AL,TM,TMT,N
      COMMON/AREA15/TSIG,TSTR
      COMMON/AREA16/TH,ERPSUD,ERDISP
      COMMON/AREA17/CIB,CIC,CN,ANGLE
      COMMON/AREA19/ESX,ESY,ESXY,ESZ
      COMMON/AREA20/SIGX,SIGY,SIGXY,PSIG1,PSIG2,ANG
      INTEGER KODEL(240),LOC(240,6),ISUBRC(240,4),N(12),IY(4)
      REAL E(3,2),ANU(3,2),WTPUV(3),Q(800),DQ(800),DP(800),LAMDA(12,12),
     1B(9,12),BT(12,12),TM(3,6),TMT(6,3),TSIG(240,4,3),TSTR(240,4,3),
     2CIB(3,3),CIC(3,3),CN(3,3),ANGLE(240,4),TH(240),SQ(12,1),DSTRN(3,1)
     3,ESTRN(9,1 ),L1C(4),L2C(4),L3C(4),DSIG(3,1),INSIG(3,1),DPS(9,1),
     4SQL(3,1),INSIGM(4),LBC(4),SIGBAR(4,1),PLV(12,1),PLVL(3,1)
      ITAPE1=21
      REWIND ITAPE1
      IFAIL=0
      ICONVG=0
      IF((INCR.EQ.1).AND.(ITER.EQ.1))GOTO500
      GOTO506
  500 DO505J=1,NEL
      DO505K=1,NSR
      TSIG(J,K,1)=0.0
      TSIG(J,K,2)=0.0
      TSIG(J,K,3)=0.0
      TSTR(J,K,1)=0.0
      TSTR(J,K,2)=0.0
      TSTR(J,K,3)=0.0
  505 CONTINUE
  506 DO595I=1,NEL
      MC=KODEL(I)
      L1=LOC(I,1)
      L2=LOC(I,2)
      L3=LOC(I,3)
      L4=LOC(I,4)
      L5=LOC(I,5)
      L6=LOC(I,6)
      N(1)=L1*2-1
      N(2)=L1*2
      N(3)=L2*2-1
      N(4)=L2*2
      N(5)=L3*2-1
      N(6)=L3*2
      IF(MC.EQ.3)GOTO510
      N(7)=L4*2-1
      N(8)=L4*2
      N(9)=L5*2-1
      N(10)=L5*2
      N(11)=L6*2-1
      N(12)=L6*2
      JL=12
      GOTO512
  510 JL=6
C     CONDENCE ELEMENT NODALDISPLACEMENT FROM GLOBAL NODAL DISPLACEMENT
  512 DO515J=1,JL
      JJ=N(J)
      SQ(J,1)=DQ(JJ)
  515 CONTINUE
      IF(MC.EQ.3) GOTO520
C     COMPUTE ELEMENT STRAINS AT THE THREE CORNER  NODES OF TRIANGLE
      READ(ITAPE1,*)((B(J,K),J=1,9),K=1,12),AREA
      CALL MATMUL(B,SQ,ESTRN,9,12,1,9,12,9,1,9,1)
C     COMPUTE STRAINS AT THE CENTROID OF EACH SUBREGION OF ELEMENT
      DO518J=1,NSR
      DSTRN(1,1)=ESTRN(1,1)*L1C(J)+ESTRN(2,1)*L2C(J)+ESTRN(3,1)*L3C(J)
      DSTRN(2,1)=ESTRN(4,1)*L1C(J)+ESTRN(5,1)*L2C(J)+ESTRN(6,1)*L3C(J)
      DSTRN(3,1)=ESTRN(7,1)*L1C(J)+ESTRN(8,1)*L2C(J)+ESTRN(9,1)*L3C(J)
C     COMPUTE STRESSES ATTHE CENTROID OF EACH ELEMENT
      IF(MC.EQ.2)GOTO516
      CALL MATMUL(CIB,DSTRN,DSIG,3,3,1,3,3,3,1,3,1)
      GOTO517
  516 CALL MATMUL(CIC,DSTRN,DSIG,3,3,1,3,3,3,1,3,1)
C     CALCULATE TOTAL STRESSES AND STRAINS AT THE CENTROID OF SUBRFGION
  517 DO522K=1,3
      TSTR(I,J,K)=TSTR(I,J,K)+DSTRN(K,1)
      TSIG(I,J,K)=TSIG(I,J,K)+DSIG(K,1)
  522 CONTINUE
C     CALCULATE PRINCIPAL STRESSES AT THE CENTROID OF SUBREGION
```

```
      IPCDSR=ISUBRC(I,J)
      SIGX=TSIG(I,J,1)
      SIGY=TSIG(I,J,2)
      SIGXY=TSIG(I,J,3)
      CALL PSTRES
      IF(ISUBRC(I,J).EQ.0)ANGLE(I,J)=ANG
      IF(MC.EQ.1)GOTO525
C     CHECK FOR YIELDING OF CONCRETE
      IF((PSIG1.GT.0.0).OR.(PSIG2.GT.0.0))GOTO530
      IF(ISUBRC(I,J).EQ.1)GOTO532
      FYEL=SIGX**2+SIGY**2-SIGX*SIGY+3.0*(SIGXY**2)
      FYEL=SQRT(FYEL)-FCP
      IF(FYEL.GE.0.0)GOTO532
      IF(ISUBRC(I,J).NE.0)GOTO548
C
C     CALCULATE NEW CONSTITUTIVE MATRIX CN CORRESPONDING TO CURRENT
C     STATE OF STRESS
      CALL CNEW(I,J)
      ANGLE(I,J)=ANG
      GOTO535
532   CALL CYIELD(I,J)
      IF(ISUBRC(I,J).EQ.0)PRINT705,INCR,ITER,I,J ,ANG
705   FORMAT(1X,'LOAD INCREAMENT NO.=',I3,3X,'ITERATION NO.=',I3,3X,'ELE
     1MENT NO.=',I3,3X,'SUBREGION NO.=',I2,3X,'HAS YIELDED',3X,'ANGLE=',
     2E10.3)
      ISUBRC(I,J)=1
      ANGLE(I,J)=ANG
C     CHECK FOR CRUSHING OF CONCRETE
      ESX =TSTR(I,J,1)
      ESY =TSTR(I,J,2)
      ESXY=TSTR(I,J,3)
      ESZ=-ESX-ESY
      FCRUS=(ESX-ESY)**2+(ESY-ESZ)**2+(ESZ-ESX)**2+1.5*(ESXY**2)
      FCRUS=SQRT(2.0*FCRUS)/3.0-ECU
      IF(FCRUS.GT.0.0)GOTO534
        GO TO 535
534   ISUBRC(I,J)=4
      IFAIL=1
      PRINT710,INCR,ITER,I,J,ANG
710   FORMAT(1X,'LOAD INCREAMENT NO.=',I3,3X,'ITERATION NO.=',I3,3X,'
     1ELEMENT NO.=',I3,3X,'SUBREGION NO.=',I2,3X,'HAS CRUSHED',3X,'ANGLE
     2=',E10.3)
      CALL CYIELD(I,J)
      GOTO535
C     CHECK FOR CRACKING OF CONCRETE
530   ICRAC1=0
      ICRAC2=0
      IF(ISUBRC(I,J).EQ.3)GOTO548
      IF(PSIG1.LE.0.0) GO TO 545
      IF(PSIG1.GE.STENSN)ICRAC1=1
      IPRD = 1
      IF(ICRAC1.EQ.1) PRINT 715,J,I,IPRD,INCR,ITER,ANG
715   FORMAT(1X,'SUBREGION',I2,'OF ELEMENT NO.',I3,'HAS CRACKED IN',I2,
     1'PRINCIPAL DIRECTION AT LOAD INCREAMENT NO.',I3,'ITERATION NO.',I3
     2,2X,'ANGLE=',E10.3)
545   IF(PSIG2.LE.0.0)GOTO546
      IF(PSIG2.GE.STENSN)ICRAC2=1
      IPRD=2
      IF(ICRAC 2.EQ.1)PRINT715,J,I,IPRD,INCR,ITER,ANG
546   IF(ISUBRC(I,J).EQ.2)GOTO549
      IF((ICRAC 1.EQ.0).AND.(ICRAC 2.EQ.0))GOTO550
      IF((ICRAC 1.EQ.1).AND.(ICRAC 2.EQ.1))GOTO542
      ISUBRC(I,J)=2
      GOTO548
542   ISUBRC(I,J)=3
      GOTO548
549   IF(ICRAC1.EQ.1)ISUBRC(I,J)=3
548   CALL CCRAK (I,J)
      IF(IPCDSR.NE.0)GOTO536
      DSTRN(1,1)=TSTR(I,J,1)
      DSTRN(2,1)=TSTR(I,J,2)
      DSTRN(3,1)=TSTR(I,J,3)
      GOTO535
536   IF((IPCDSR.EQ.2).AND.(ISUBRC(I ,J).EQ.3))GOTO537
      GOTO535
537   INSIG(1,1)=TSIG(I,J,1)
      INSIG(2,1)=TSIG(I,J,2)
      INSIG(3,1)=TSIG(I,J,3)
      GOTO540
C     CALCULATE INITIAL STRESSES DUETO YIELDING OR CRUSHING OR DUE TO
C     NONLINEARITY OR DUE TO CRACKING OF CONCRETE
535   DO533K=1,3
      DO533L=1,3
      CN(K,L)=CIC(K,L)-CN(K,L)
533   CONTINUE
      CALL MATMUL(CN,DSTRN,INSIG,3,3,1,3,3,3,1,3,1)
      GOTO540
C     CHECK FOR YIELDING AND CRACKING OF BRICKWORK
525   IF(ISUBRC(I,J).EQ.1)GOTO652
```

```
      ICRAC2=0
      IF((PSIG1.LE.0.0).AND.(PSIG2.LT.0.0))GOTO560
      IF(ISUBRC(I,J).EQ.3)GOTO648
      IF(PSIG1.LE.0.0)GOTO650
      IF(PSIG1.GE.STENB1)ICRAC1=1
      IPRD=1
      IF(ICRAC1.EQ.1)PRINT715,J,I,IPRD,INCR,ITER,ANG
 650  IF(PSIG2.LE.0.0)GOTO651
      IF(PSIG2.GE.STENB2)ICRAC2=1
      IPRD=2
      IF(ICRAC2.EQ.1)PRINT715,J,I,IPRD,INCR,ITER,ANG
 651  IF(ISUBRC(I,J).NE.0)GOTO645
      IF((ICRAC1.EQ.0).AND.(ICRAC2.EQ.0))GOTO550
      IF((ICRAC1.EQ.1).AND.(ICRAC2.EQ.1))GOTO642
      ISUBRC(I,J)=2
      GOTO648
 642  ISUBRC(I,J)=3
      GOTO648
 645  IF(ICRAC1.EQ.1)ISUBRC(I,J)=3
 648  CALLCCRAK(I,J)
      IF(IPCDSR.NE.0)GOTO654
      DSTRN(1,1)=TSTR(I,J,1)
      DSTRN(2,1)=TSTR(I,J,2)
      DSTRN(3,1)=TSTR(I,J,3)
      GOTO665
 654  IF((IPCDSR.EQ.2).AND.(ISUBRC(I,J).EQ.3))GOTO657
      GOTO665
 657  INSIG(1,1)=TSIG(I,J,1)
      INSIG(2,1)=TSIG(I,J,2)
      INSIG(3,1)=TSIG(I,J,3)
      GOTO540
C     CHECK FOR YIELDING OF BRICK WORK
 560  RT=YYBT/YXBL
      SL=TSIG(I,J,1)/YXBL
      ST=TSIG(I,J,2)/YYBT
      SS=TSIG(I,J,3)/YSHR
      FYEL=SL**2-(SL*ST)/RT+ST**2+SS**2-1.0
      IF(FYEL.GT.0.0)GOTO910
      GOTO550
 910  SL=(TSIG(I,J,1)-DSIG(1,1))/YXBL
      ST=(TSIG(I,J,2)-DSIG(2,1))/YYBT
      SS=(TSIG(I,J,3)-DSIG(3,1))/YSHR
      FYEL1=SL**2-(SL*ST)/RT+ST**2+SS**2-1.0
      ESZ=(-FYEL1)/(FYEL-FYEL1)
      DO915K=1,3
      DO915L=1,3
 915  CN(K,L)=ESZ*CN(K,L)
      ISUBRC(I,J)=1
      PRINT705,INCR,ITER,I,J,ANG
      GOTO665
 652  CALL CYIELD(I,J)
      ISUBRC(I,J)=1
      PRINT705,INCR,ITER,I,J,ANG
      ANGLE(I,J)=ANG
 665  DO656K=1,3
      DO656L=1,3
 656  CN(K,L)=CIB(K,L)-CN(K,L)
      CALL MATMUL(CN,DSTRN,INSIG,3,3,1,3,3,3,1,3,1)
C     CORRECT STRESSES AT THE CENTROID OF EACH SUBREGION
 540  DO547K=1,3
 547  TSIG(I,J,K)=TSIG(I,J,K)-INSIG(K,1)
C     CALCULATION OF PSEUDO LOAD VECTOR DUE TO NONLINEARITY OF MATERIAL,
C     YIELDING OF MATERIAL,CRACKING OF MATERIAL AND CRUSHING OF MATERIAL
C     AREAOF THE SUB REGION
      ANSR=NSR
      AREAS=AREA/ANSR
      CT=TH(I)*AREAS
      DPS(1,1)=CT*INSIG(1,1)*L1C(J)
      DPS(2,1)=CT*INSIG(1,1)*L2C(J)
      DPS(3,1)=CT*INSIG(1,1)*L3C(J)
      DPS(4,1)=CT*INSIG(2,1)*L1C(J)
      DPS(5,1)=CT*INSIG(2,1)*L2C(J)
      DPS(6,1)=CT*INSIG(2,1)*L3C(J)
      DPS(7,1)=CT*INSIG(3,1)*L1C(J)
      DPS(8,1)=CT*INSIG(3,1)*L2C(J)
      DPS(9,1)=CT*INSIG(3,1)*L3C(J)
      DO552K=1,12
      DO552L=1,9
 552  BT(K,L)=B(L,K)
      CALL MATMUL(BT,DPS,PLV,12,9,1,12,12,9,1,12,1)
C     ASSEMBLE GLOBAL PSEUDO LOAD VECTOR
      DO555K=1,12
      L=N(K)
      DP(L)=DP(L)+PLV(K,1)
 555  CONTINUE
 550  CONTINUE
 518  CONTINUE
      GO TO 595
```

```
C     CHECK FOR YIELDING OF STEEL
  520 READ(ITAPE1,*) AL,((TM(K,L),K=1,3),L=1,6)
C     CALCULATE ELEMENTAL NODAL DISPLACEMENT IN LOCAL COORDINATE SYSTEM
      CALL MATMUL(TM,SQ,SQL,3,6,1,3,6,12,1,3,1)
C     FIND THE STRAINS AT THE MID POINT OF EACH SUB-BAR
      MC=KODEL(I)
      DO561K=1,NSRB
      ESTRN(K,1)=((-1.0+2.0*LBC(K))*SQL(1,1)+(1.0+2.0*LBC(K))*SQL(2,1)
     1+(-4.0*LBC(K))*SQL(3,1)) /AL
      SIGBAR(K,1)=E(MC,1)*ESTRN(K,1)
  561 CONTINUE
C     COMPUTE TOTAL STRAINS AND STRESS AT THE CENTROID OF EACH SUB-BAR
      DO562K=1,NSRB
      TSTR(I,K,1)=TSTR(I,K,1)+ESTRN(K,1)
      TSIG(I,K,1)=TSIG(I,K,1)+SIGBAR(K,1)
  562 CONTINUE
C     CHECK EACH SUB-REGION FOR YIELDING
      DO570K=1,NSRB
      IF(ABS(TSIG(I,K,1)).GT.YIELDS)GOTO569
      IY(K)=0
      GOTO570
  569 IY(K)=1
      IF(ISUBRC(I,K).EQ.0) PRINT701,INCR,ITER,I,K
  701 FORMAT(2X,'LOAD INCREAMENT NO.=',I3,3X,'ITERATION NO.=',I3,3X,
     1'BAR ELEMENT NO.=',I3,3X,'SUBREGION NO.=',I2,3X,'HAS YIELDED')
      ISUBRC(I,K)=1
  570 CONTINUE
      DO565J=1,3
  565 PLVL(J,1)=0.0
C     CALCULATE INITIAL STRESSES DUE TO YIELDING OF STEEL
      DO575K=1,NSRB
      INSIGM(K)=0.0
      IF(IY(K).EQ.0)GOTO575
      IF(TSIG(I,K,1).LT.0.0)GOTO574
      INSIGM(K)=(-YIELDS+TSIG(I,K,1))
      TSIG(I,K,1)=TSIG(I,K,1)-INSIGM(K)
      GOTO575
  574 INSIGM(K)=TSIG(I,K,1)+YIELDS
      TSIG(I,K,1)=TSIG(I,K,1)-INSIGM(K)
  575 CONTINUE
C     CALCULATE PSEUDO LOAD VECTOR DUE TO YIELDING OF STEEL
      IF(NSRB.EQ.1)GOTO579
      IF(IY(1).EQ.0)GOTO576
      CT=TH(I)*INSIGM(1)*0.5
      PLVL(1,1)=PLVL(1,1)-1.25*CT
      PLVL(2,1)=PLVL(2,1)-0.25*CT
      PLVL(3,1)=PLVL(3,1)+1.5*CT
  576 IF(IY(2).EQ.0)GOTO577
      CT=TH(I)*INSIGM(2)*0.5
      PLVL(1,1)=PLVL(1,1)-0.75*CT
      PLVL(2,1)=PLVL(2,1)+0.25*CT
      PLVL(3,1)=PLVL(3,1)+0.50*CT
  577 IF(IY(3).EQ.0)GO TO 578
      CT=TH(I)*INSIGM(3)*0.5
      PLVL(1,1)=PLVL(1,1)-0.25*CT
      PLVL(2,1)=PLVL(2,1)+0.75*CT
      PLVL(3,1)=PLVL(3,1)-0.50*CT
  578 IF(IY(4).EQ.0)GOTO580
      CT=TH(I)*INSIGM(4)*0.5
      PLVL(1,1)=PLVL(1,1)+0.25*CT
      PLVL(2,1)=PLVL(2,1)+1.25*CT
      PLVL(3,1)=PLVL(3,1)-1.50*CT
      GOTO580
  579 IF(IY(1).EQ.0)GOTO580
      CT=TH(I)*INSIGM(1)*0.5
      PLVL(1,1)=-2.0*CT
      PLVL(2,1)=2.0*CT
      PLVL(3,1)=0.0
  580 DO581K=1,NSRB
      IF(IY(K).NE.0)GOTO583
  581 CONTINUE
      GOTO595
C     TRANSFORM PSEUDO LOAD VECTOR FROM LOCAL COORDINATE SYSTEM TO
C     GLOBAL COORDINATE SYSTEM
  583 DO582K=1,6
      DO582L=1,3
  582 TMT(K,L)=TM(L,K)
      CALL MATMUL(TMT,PLVL,PLV,6,3,1,6,3,3,1,12,1)
C     ADD THIS PSEUDO LOAD VECTOR TO GLOBAL PSEUDO LOAD VECTOR
      DO585K=1,6
      L=N(K)
      DP(L)=DP(L)+PLV(K,1)
  585 CONTINUE
  595 CONTINUE
C     CHECK FOR CONVERGENCE
      ICONV=0
      ICOND=0
C     CHECK WHEATHER PSEUDO LOAD VECTOR,S ELEMENTS ARE LESS THAN SOME
C     SPECIFIED LIMIT
```

```
      DO586J=1,NDF
      IF(ABS(DP(J)).LE.ERPSUD)ICONV=ICONV+1
  586 CONTINUE
C     CHECK CONVERGENCE OF DISPLACEMENTS
      DO588J=1,NDF
      IF(ABS(DQ(J)/Q(J)).LE.ERDISP)ICOND=ICOND+1
  588 CONTINUE
      IF(ITER.EQ.1)GOTO590
      IF((ICONV.EQ.NDF).AND.(ICOND.EQ.NDF))GOTO600
      GOTO635
  590 IF(ICONV.EQ.NDF)GO TO 600
      GO TO 635
  600 ICONVG=1
      CALL PRINTR
  635 RETURN
      END
C     ****************************************************************
C     *            SUBROUTINE     PSTRESS                            *
C     ***************************** **********************************
      SUBROUTINE PSTRES
      COMMON/AREA20/SX,SY,TXY,SIG1,SIG2,ANG
      XPY=(SX+SY)*0.5
      XNY=(SX-SY)*0.5
      CT=SQRT(XNY**2+TXY**2)
      SIG1=XPY+CT
      SIG2=XPY-CT
      IF(CT.EQ.0.0)GOTO300
      ANG=(180.0/6.2831853)*ACOS(XNY/CT)
      IF(TXY.LT.0.0)ANG=180.0-ANG
      GOTO305
  300 ANG=0.0
  305 RETURN
      END
C     ****************************************************************
C     *            SUBROUTINE     MATMUL                             *
C     ****************************************************************
      SUBROUTINE MATMUL (ML,MR,PM,N,M,K,N1,M1,M2,K2,N3,K3)
      REAL ML(N1,M1),MR(M2,K2),PM(N3,K3)
      DO1210I=1,N
      DO1210J=1,K
      PM(I,J)=0.0
      DO1210L=1,M
      PM(I,J)=PM(I,J)+ML(I,L)*MR(L,J)
 1210 CONTINUE
      RETURN
      END
C     ****************************************************************
C     *          SUBROUTINE              ESMAT1                      *
C     ****************************************************************
      SUBROUTINE ESMAT1(I,L1,L2,L3)
      COMMON/AREA1/NNP,NEL,NOLD,NONBC,NMAT,NBODY,NSLC
      COMMON/AREA2/E,ANU,WTPUV
      COMMON/AREA5/CX,CY
      COMMON/AREA10/C,D
      COMMON/AREA11/KA,KG
      COMMON/AREA13/LAMDA,B,AREA,BT
      COMMON/AREA16/TH,ERPSUD,ERDISP
      REAL E(3,2),ANU(3,2),WTPUV(3),CX(400),CY(400),LAMDA(12,12),
     1B(9,12),BT(12,12),TH(240),C(9,9),D(9,9),KG(12,12),BU(3,6),BV(3,6),
     2KA(800,56)
       A1=CX(L3)-CX(L2)
       A2=CX(L1)-CX(L3)
       A3=CX(L2)-CX(L1)
       B1=CY(L2)-CY(L3)
       B2=CY(L3)-CY(L1)
       B3=CY(L1)-CY(L2)
       AREA=0.5*(A1*B3-A3*B1)
       CALL BMATRI(AREA,B1,B2,B3,BU)
       CALL BMATRI(AREA,A1,A2,A3,BV)
C      ASSEMBLY OF NODAL DISPLACEMENT MATRIX B
       DO100J=1,3
       DO100K=1,6
       B(J,K)=BU(J,K)
       B(J,K+6)=0.0
       B(J+3,K)=0.0
       B(J+3,K+6)=BV(J,K)
       B(J+6,K)=BV(J,K)
       B(J+6,K+6)=BU(J,K)
  100  CONTINUE
C      TRANSFORMATION OF B MATRIX
       CALL MATMUL(B,LAMDA,BT,9,12,12,9,12,12,12,12,12)
       DO102J=1,9
       DO102K=1,12
  102  B(J,K)=BT(J,K)
C      TRANSPOSE OF B MATRIX
       DO105J=1,9
       DO105K=1,12
       BT(K,J)=B(J,K)
  105  CONTINUE
```

```
C            STIFFNESS MATRIX IN GLOBAL COORDINATE
C     SYSTEM
      CALL DMATRI(AREA,I)
      CALL CMATRX(I)
      CALL MATMUL(BT,D,KG,12,9,9,12,12,9,9,12,12)
      DO110J=1,12
      DO110K=1,9
  110 BT(J,K)=KG(J,K)
      CALL MATMUL(BT,C,KG,12,9,9,12,12,9,9,12,12)
      DO115J=1,12
      DO115K=1,9
  115 BT(J,K)=KG(J,K)
      CALL MATMUL(BT,B,KG,12,9,12,12,12,9,12,12,12)
      RETURN
      END
C     ******************************************************************
C     *                    SUBROUTINE    ESMAT2                        *
C     ******************************************************************
      SUBROUTINE ESMAT2(I,L1,L2,L3)
      COMMON/AREA1/NNP,NEL,NOLD,NONBC,NMAT,NBODY,NSLC
      COMMON/AREA2/E,ANU,WTPUV
      COMMON/AREA3/KODEL,LOC
      COMMON/AREA5/CX,CY
      COMMON/AREA11/KA,KG
      COMMON/AREA14/AL,TM,TMT,N
      COMMON/AREA16/TH,ERPSUD,ERDISP
      INTEGER KODEL(240),LOC(240,6),N(12)
      REAL E(3,2),ANU(3,2),WTPUV(3),CX(400) ,CY(400),TM(3,6),TMT(6,3),
     1TH(240),KG(12,12),KA(800,56),KL(3,3)
      MC=KODEL(I)
      DX=CX(L2)-CX(L1)
      DY=CY(L2)-CY(L1)
      AL=SQRT(DX**2+DY**2)
C     CALCULATION OF TRANSFORMATION MATRIX
      COSA=DX/AL
      SINA=DY/AL
      DO400J=1,3
      DO400K=1,6
  400 TM(J,K)=0.0
      TM(1,1)=COSA
      TM(1,2)=SINA
      TM(2,3)=COSA
      TM(2,4)=SINA
      TM(3,5)=COSA
      TM(3,6)=SINA
C     TRASPOSE OF TRANSFORMATION MATRIX
      DO405J=1,3
      DO405K=1,6
  405 TMT(K,J)=TM(J,K)
C     ELEMENT STIFFNESS MATRIX OF BAR ELEMENT IN LOCAL COORDINATE SYSTEM
      CT=(TH(I)*E(MC,1))/(AL*3.0)
      KL(1,1)=7.0*CT
      KL(1,2)=CT
      KL(2,1)=KL(1,2)
      KL(1,3)=-8.0*CT
      KL(3,1)=KL(1,3)
      KL(2,2)=7.0*CT
      KL(2,3)=-8.0*CT
      KL(3,2)=KL(2,3)
      KL(3,3)=16.0*CT
C     TRANSFORMATION OF STIFFNESS MATRIX IN GLOBAL COORDINATE SYSTEM
      CALL MATMUL(TMT,KL,KG,6,3,3,6,3,3,3,12,12)
      DO410J=1,6
      DO410K=1,3
  410 TMT(J,K)=KG(J,K)
      CALL MATMUL(TMT,TM,KG,6,3,6,6,3,3,6,12,12)
      RETURN
      END
C     ******************************************************************
C     *                 SUBROUTINE              BMATRI
C     ******************************************************************
      SUBROUTINE BMATRI(AREA,A1,A2,A3,BM)
      DIMENSION BM(3,6)
      CT=0.5/AREA
      BM(1,1)=3.0*A1*CT
      BM(1,2)=-A2*CT
      BM(1,3)=-A3*CT
      BM(1,4)=4.0*A2*CT
      BM(1,5)=0.0
      BM(1,6)=4.0*A3*CT
      BM(2,1)=-A1*CT
      BM(2,2)=3.0*A2*CT
      BM(2,3)=-A3*CT
      BM(2,4)=4.0*A1*CT
      BM(2,5)=4.0*A3*CT
      BM(2,6)=0.0
      BM(3,1)=-A1*CT
      BM(3,2)=-A2*CT
```

```
         ICIC(3,3),CN(3,3),ANGLE(240,4)
          ALPHAB=1.0
          ALPHAC=0.4
          DO500K=1,3
          DO500L=1,3
 500      CN(K,L)=0.0
          IF(ISUBRC(I,J).EQ.3)GOTO599
          ANG=ANGLE(I,J)
          THEATA=(ANG*3.1415926)/180.0
          COSA=COS(THEATA)
          SINA=SIN(THEATA)
          MC=KODEL(I)
          IF(MC.EQ.2)GOTO550
C         TRANSFORM THE ELASTICITY MATRIX FROM GLOBAL COORDINATE SYSTEMTO
C         CRACKED DIRECTION
          TM(1,1)=COSA**2
          TM(1,2)=SINA**2
```

```
      TM(1,3)=-COSA*SINA
      TM(2,1)=TM(1,2)
      TM(2,2)=TM(1,1)
      TM(2,3)=-TM(1,3)
      TM(3,1)=-2.0*TM(1,3)
      TM(3,2)=-TM(3,1)
      TM(3,3)=TM(1,1)-TM(1,2)
C     TRANSPOSE OF TRANSFORMATION MATRIX
      DO505L=1,3
      DO505K=1,3
505   TMT(K,L)=TM(L,K)
      CALL MATMUL(TMT,CIB,PM,3,3,3,6,3,3,3,3,3)
      CALL MATMUL(PM,TM,CN,3,3,3,3,3,3,6,3,3)
```

```
      CN(1,1)=0.0
      CN(1,2)=0.0
      CN(1,3)=0.0
      CN(2,1)=0.0
      CN(3,1)=0.0
      CN(3,3)=ALPHAB*CN(3,3)
      GOTO560
550   CN(2,2)=E(MC,1)
      CN(3,3)=ALPHAC*(E(MC,1)/(1.0+ANU(MC,1)))*0.5
C     TRANSFORM ELASTICITY MATRIX FROM CRACKED SYSTEM TO GLOBAL
C     COORDINATE SYSTEM
560   TM(1,1)=COSA**2
      TM(1,2)=SINA**2
      TM(1,3)=COSA*SINA
      TM(2,1)=TM(1,2)
      TM(2,2)=TM(1,1)
      TM(2,3)=-TM(1,3)
      TM(3,1)=-2.0*TM(1,3)
      TM(3,2)=-TM(3,1)
      TM(3,3)=TM(1,1)-TM(1,2)
C     TRANSPOSE OF TRANSFORMATION MATRIX
      DO540L=1,3
      DO540K=1,3
540   TMT(K,L)=TM(L,K)
      CALL MATMUL(TMT,CN,PM,3,3,3,6,3,3,3,3,3)
      CALL MATMUL(PM,TM,CN,3,3,3,3,3,3,6,3,3)
599   RETURN
      END
C     ****************************************************************
C                SUBROUTINE         CIMAT                            *
C     ****************************************************************
      SUBROUTINE CIMAT
      COMMON/AREA1/NNP,NEL,NOLD,NONBC,NMAT,NBODY,NSLC
      COMMON/AREA2/E,ANU,WTPUV
      COMMON/AREA17/CIB,CIC,CN,ANGLE
      COMMON/AREA18/MATCOD,NCODE
      INTEGER MATCOD(3),NCODE(400)
      REALE(3,2),ANU(3,2),WTPUV(3),CIB(3,3),CIC(3,3),CN(3,3),
     1ANGLE(240,4)
      DO700I=1,NMAT
      MC=MATCOD(I)
      IF(MC.EQ.3)GOTO700
      IF(MC.EQ.1)GOTO705
      CT=E(MC,1)/(1.0-ANU(MC,1)**2)
      CIC(1,1)=CT
      CIC(1,2)=ANU(MC,1)*CT
      CIC(1,3)=0.0
      CIC(2,1)=CIC(1,2)
      CIC(2,2)=CT
      CIC(2,3)=0.0
      CIC(3,1)=0.0
      CIC(3,2)=0.0
      CIC(3,3)=0.5*(1.0-ANU(MC,1))*CT
      GOTO700
705   CT=1.0/(1.0-ANU(MC,1)*ANU(MC,2))
      G=0.25*CT*(E(MC,1)+E(MC,2)-2.0*SQRT(ANU(MC,1)*ANU(MC,2)*E(MC,1)*
     1E(MC,2)))
      CIB(1,1)=CT*E(MC,1)
      CIB(1,2)=CT*E(MC,1)*ANU(MC,2)
      CIB(1,3)=0.0
      CIB(2,1)=CIB(1,2)
      CIB(2,2)=CT*E(MC,2)
      CIB(2,3)=0.0
      CIB(3,1)=0.0
      CIB(3,2)=0.0
      CIB(3,3)=G
700   CONTINUE
      RETURN
      END
C     ****************************************************************
C     *                    SUBROUTINE     CNEW                        *
C     ****************************************************************
      SUBROUTINE CNEW(I,J)
      COMMON/AREA2/E,ANU,WTPUV
      COMMON/AREA3/KODEL,LOC
      COMMON/AREA6/YIELDS,YXBL,STENB1,YYBT,STENB2,YSHR,STENSN,ECU,FCP,
     1YSTC,DSTRN
      COMMON/AREA15/TSIG,TSTR
      COMMON/AREA17/CIB,CIC,CN,ANGLE
      COMMON/AREA19/EX,EY,EXY,EZ
      INTEGER KODEL(240),LOC(240,6)
      REAL E(3,2),ANU(3,2),WTPUV(3),DSTRN(3,1),TSIG(240,4,3),TSTR(240,4,
     13),CIB(3,3),CIC(3,3),CN(3,3),ANGLE(240,4)
      MC=KODEL(I)
      EX=TSTR(I,J,1)
      EY=TSTR(I,J,2)
      EXY=TSTR(I,J,3)
      V=ANU(MC,1)
C     CALCULATE EQUIVALENT STRAIN
```

```
      EZ=-(V*(EX+EY))/(1.0-V)
      ES=((EX-EY)**2+(EY-EZ)**2+(EZ-EX)**2+1.5*(EXY**2))
      ES=(SQRT(ES/2.0))/(1.0+V)
      EX =TSTR(I,J,1)-DSTRN(1,1)
      EY =TSTR(I,J,2)-DSTRN(2,1)
      EXY=TSTR(I,J,3)-DSTRN(3,1)
      EZ=-(V*(EX+EY))/(1.0-V)
      ES1=((EX-EY)**2+(EY-EZ)**2+(EZ-EX)**2+1.5*(EXY**2))
      ES1=SQRT(ES1/2.0)/(1.0+V)
      ESAV=0.5*(ES+ES1)
      EMN=FCP*1000.0*(1.0-500.0*ESAV)
      EZ=EMN/(1.0-V**2)
      CN(1,1)=EZ
      CN(1,2)=V*EZ
      CN(1,3)=0.0
      CN(2,1)=CN(1,2)
      CN(2,2)=EZ
      CN(2,3)=0.0
      CN(3,1)=0.0
      CN(3,2)=0.0
      CN(3,3)=0.5*(1.0-V)*EZ
      RETURN
      END
C     ***************************************************************
C     *     SUBROUTINE         CYIELD                               *
C     ***************************************************************
      SUBROUTINE CYIELD(I,J)
      COMMON/AREA2/E,ANU,WTPUV
      COMMON/AREA3/KODEL,LOC
      COMMON/AREA6/YIELDS,YXBL,STENB1,YYBT,STENB2,YSHR,STENSN,ECU,FCP,
     1YSTC,DSTRN
      COMMON/AREA12/ISUBRC,NSR,NSRB
      COMMON/AREA15/TSIG,TSTR
      COMMON/AREA17/CIB,CIC,CN,ANGLE
      COMMON/AREA19/EX,EY,EXY,EZ
      INTEGER KODEL(240),LOC(240,6),ISUBRC(240,4)
      REAL E(3,2),ANU(3,2),WTPUV(3),DSTRN(3,1),TSIG(240,4,3),TSTR(240,4,
     13),CIB(3,3),CIC(3,3),CN(3,3),ANGLE(240,4)
      DO650K=1,3
      DO650L=1,3
  650 CN(K,L)=0.0
      IF(KODEL(I).EQ.1)GOTO690
      AM=0.0
      IF(ISUBRC(I,J).NE.0)GOTO690
      MC=KODEL(I)
      EX=TSTR(I,J,1)-DSTRN(1,1)
      EY=TSTR(I,J,2)-DSTRN(2,1)
      EXY=TSTR(I,J,3)-DSTRN(3,1)
      V=ANU(MC,1)
      EZ=-(V*(EX+EY))/(1.0-V)
      ES1=((EX-EY)**2+(EY-EZ)**2+(EZ-EX)**2+1.5*(EXY**2))
      ES1=SQRT(ES1/2.0)/(1.0+V)
      EX=TSTR(I,J,1)
      EY=TSTR(I,J,2)
      EXY=TSTR(I,J,3)
      EZ=-(V*(EX+EY))/(1.0-V)
      ES2=((EX-EY)**2+(EY-EZ)**2+(EZ-EX)**2+1.5*(EXY**2))
      ES2=SQRT(ES2/2.0)/(1.0+V)
      AM=(YSTC-ES1)/(ES2-ES1)
      DO655K=1,3
      DO655L=1,3
  655 CN(K,L)=CIC(K,L)*AM
  690 RETURN
      END
C     ***************************************************************
C     *               SUBROUTINE         GEOMBC
C     ***************************************************************
      SUBROUTINE GEOMBC
      COMMON/AREA1/NNP,NEL,NOLD,NONBC ,NMAT,NBODY,NSLC
      COMMON/AREA8/NDF,IBAND,INCR,ITER
      COMMON/AREA9/Q,DQ,DP
      COMMON/AREA11/KA,KG
      COMMON/AREA18/MATCOD,NCODE
      INTEGER MATCOD(3),NCODE(400)
      REAL KA(800,56),KG(12,12),Q(800),DQ(800),DP(800)
      IF((INCR.EQ.1).AND.(ITER.EQ.1))GOTO400
      GOTO450
C     APPLY DISPLACEMENT BOUNDRY CONDITIONS IN STIFFNESS MATRIX
  400 DO405I=1,NNP
      IF(NCODE(I).EQ.0)GOTO405
      IF(NCODE(I).EQ.2)GOTO410
      KA(2*I-1,1)=KA(2*I-1,1)*0.1E15
      IF(NCODE(I).EQ.1)GOTO405
  410 KA(2*I,1)=KA(2*I,1)*0.1E15
  405 CONTINUE
C     APPLY DISPLACEMENT BOUNDRY CONDITIONS IN LOAD VECTOR
  450 DO420I=1,NNP
      IF(NCODE(I).EQ.0)GOTO420
      IF(NCODE(I).EQ.2)GOTO425
```

```
      DP(2*I-1)=0.0
      IF(NCODE(I).EQ.1)GOTO420
425   DP(2*I)=0.0
420   CONTINUE
      RETURN
      END
C     ****************************************************************
C     *     SUBROUTUNE         PRINTR                                *
C     ****************************************************************
      SUBROUTINE PRINTR
      COMMON/AREA1/NNP,NEL,NOLD,NONBC ,NMAT,NBODY,NSLC
      COMMON/AREA3/KODEL,LOC
      COMMON/AREA8/NDF,IBAND,INCR,ITER
      COMMON/AREA9/Q,DQ,DP
      COMMON/AREA12/ISUBRC,NSR,NSRB
      COMMON/AREA15/TSIG,TSTR
      COMMON/AREA18/MATCOD,NCODE
      COMMON/AREA20/SIGX,SIGY,SIGXY,PSIG1,PSIG2,ANG
      INTEGER MATCOD(3),NCODE(400),KODEL(240),LOC(240,6),ISUBRC(240,4)
      REAL Q(800),DQ(800),DP(800),TSIG(240,4,3),TSTR(240,4,3)
      PRINT4000
4000  FORMAT(/1X,131(1H-))
      PRINT4005,INCR,ITER
4005  FORMAT(/5X,'INCREAMENT NO.=',I3/5X,17(1H-)/22X,'ITERATION NO.=',I3
     1/22X,18(1H-))
      PRINT4010,(I,Q(2*I-1),Q(2*I),DP(2*I-1),DP(2*I),I=1,NNP)
4010  FORMAT(/2X,'NODAL DISPLACEMENT OF THE STRUCTURE AND PSEUDO LOADVE
     1CTOR IN GLOBAL COORDINATE SYSTEM'/2X,87(1H-)//2X,'NODE NUMBER',8X,
     2'U=X-DISPLACEMENT',8X,'V=Y-DISPLACEMENT',5X,'PSEUDO LOAD IN X-DIRE
     3CTION',5X,'PSEUDO LOAD IN Y-DIRECTION'/,(5X,I4,12X,E15.8,9X,E15.8,
     412X,E15.8,16X,E15.8))
      PRINT4015
4015  FORMAT(//2X,'STRAINS AT THE CENTROID OF EACH SUBREGION OF ATRIANGU
     1LAR ELEMENT'/2X,66(1H-)//5X,'ELEMENT NO.',3X,'SUBREGION NO.',8X,
     2'STRAIN EX',12X,'STRAIN EY',12X,'STRAIN EXY')
      DO4020I=1,NEL
      IF(KODEL(I).EQ.3)GOTO4020
      PRINT4025,I,(J,TSTR(I,J,1),TSTR(I,J,2),TSTR(I,J,3),J=1,NSR)
4025  FORMAT(/8X,I4,12X,I2,13X,E15.8,6X,E15.8,6X,E15.8/(24X,I2,13X,
     1E15.8,6X,E15.8,6X,E15.8))
4020  IF(INCR.GE.3)GO TO 4035
      PRINT4030
4030  FORMAT(//2X,'STRESSES AT THE CENTROID OF EACH SUBREGTON OF A TRIAN
     1GULAR ELEMENT'/2X,67(1H-)/1X,'ELEMENT',2X,'SUBREGION',2X,'SUBREGIO
     3ION' ,4X,'STRESS SIGMAX',4X,'STRESS SIGMAY',4X,'STRESS SIGMAXY ',3
     3X,'STRESS SIGMA1',4X,'STRESS SIGMA2',6X,'ANGLE PHI'/3X,'NO.',6X,
     4'NO.',4X,'CONDITION'/22X,'CODE')
      DO4035I=1,NEL
      IF(KODEL(I).EQ.3)GOTO4035
      PRINT4070
4070  FORMAT(/)
      DO4036J=1,NSR
      SIGX=TSIG(I,J,1)
      SIGY=TSIG(I,J,2)
      SIGXY=TSIG(I,J,3)
      CALL PSTRES
      PRINT4040,I,J,ISUBRC(I,J),SIGX,SIGY,SIGXY,PSIG1,PSIG2,ANG

4040  FORMAT(2X,I4,6X,I2,9X,I1,6X,E15.8,2X,E15.8,2X,E15.8,2X,E15.8,2X,
     1E15.8,2X,E15.8)
4036  CONTINUE
4035  CONTINUE
C     STRESSES AND STRAINS AT THE CENTROID OF EACH SUB-BAR
      DO4045I=1,NMAT
      IF(MATCOD(I).EQ.3)GOTO4050
4045  CONTINUE
      GOTO4095
4050  PRINT4055
4055  FORMAT(//2X,'STRAINS AND STRESSES AT THE MIDPOINT OF EACH SUB-BAR
     1OF A BAR ELEMENT'/2X,70(1H-)//5X,'ELEMENT NO.',2X,'SUBREGION NO.',
     22X,'SUBREGION CONDITION CODE',3X,' AXIALSTRAINEX',5X,'AXIAL STRESS
     3SIGMAX')
      DO4060I=1,NEL
      IF(KODEL(I).NE.3)GOTO4060
      PRINT4065,I,(J,ISUBRC(I,J),TSTR(I,J,1),TSIG(I,J,1),J=1,NSRB)
4065  FORMAT(/8X,I4,10X,I2,17X,I1,14X,E15.8,7X,E15.8/(22X,I2,17X,I1,14X,
     1E15.8,7X,E15.8))
4060  CONTINUE
4095  PRINT4000
      RETURN
      END
C     ****************************************************************
C     *              SUBROUTINE    DSOLV
C     ****************************************************************
      SUBROUTINE DSOLVE
      COMMON/AREA8/N,IBW,INCR,ITER
      COMMON/AREA9/Q,X,B
      COMMON/AREA11/A,KG
      REAL Q(800),B(800),X(800),A(800,56),KG(12,12)
```

```
      GOTO10
5     DO100I=1,N
      IP=N-I+1
      IF(IBW.LT.IP)IP=IBW
      DO150J=1,IP
      IQ=IBW-J
      IF(I-1.LT.IQ)IQ=I-1
      SUM=A(I,J)
      IF(IQ.EQ.0)GOTO110
      DO115K=1,IQ
      IK=I-K
      JK=J+K
      SUM=SUM-A(IK,K+1)*A(IK,JK)
115   CONTINUE
110   IF(J.NE.1)GOTO120
      IF(SUM.LE.0.0)GOTO125
      A(I,J)=SQRT(SUM)
      GOTO150
120   A(I,J)=SUM/A(I,1)
150   CONTINUE
100   CONTINUE
10    DO155I=1,N
      J=I-IBW+1
      IF(I+1.LE.IBW)J=1
      SUM=B(I)
      IM1=I-1
      IF(IM1.EQ.0)GOTO160
      DO165K=J,IM1
      IK=I-K+1
      SUM=SUM-A(K,IK)*X(K)
165   CONTINUE
160   X(I)=SUM/A(I,1)
155   CONTINUE
      DO170I=1,N
      IR=N+1-I
      J=IR+IBW-1
      IF(J.GT.N)J=N
      SUM=X(IR)
      IM1=IR+1
      IF(IM1.GT.N)GOTO175
      DO180K=IM1,J
      IK=K-IR+1
      SUM=SUM-A(IR,IK)*X(K)
180   CONTINUE
175   X(IR)=SUM/A(IR,1)
170   CONTINUE
      RETURN
125   PRINT126,SUM
126   FORMAT(/2X,'MATRIX IS NOT POSSITIVE DEFINITE'//2X,'SUM=',E15.8)
      STOP
      END
```